Acta morphologica et anthropologica 28 (1–2)

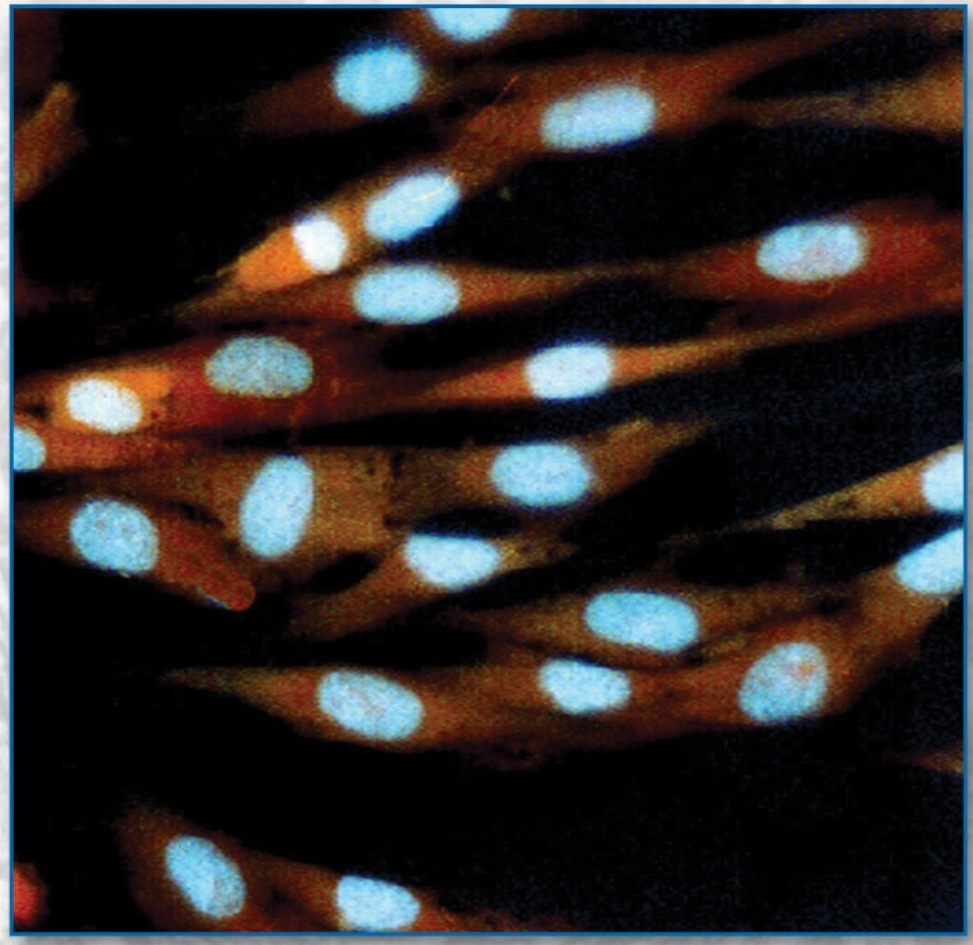

Prof. Marin Drinov Publishing House
of Bulgarian Academy of Sciences

ISSN 1311-8773 (print)
ISSN 2535-0811 (online)

Acta morphologica et anthropologica

28
(1-2)

28 (1-2) ● Sofia ● 2021
Institute of Experimental Morphology, Pathology and Anthropology with Museum
Bulgarian Anatomical Society

Contents

MORPHOLOGY 28 (1)

Original Articles

Review Articles

ANTHROPOLOGY AND ANATOMY 28 (2)

Original Articles

Institute of Experimental Morphology, Pathology and Anthropology with Museum
Bulgarian Anatomical Society

Acta morphologica et anthropologica, 28 (1-2)
Sofia ● 2021

MORPHOLOGY 28 (1)

Original Articles

Folia of Human Cerebellum: Structure and Variations

Nataliia Maryenko, Oleksandr Stepanenko*

Department of Histology, Cytology and Embryology, Kharkiv National Medical University, Kharkiv, Ukraine

* Corresponding author e-mail: maryenko.n@gmail.com

The aim of the study was to describe possible variations in size and shape of folia of human cerebellum to determine morphological and morphometric characteristics of normal cerebellar folia. Cadaveric material (cerebella of 50 people) was studied. It was shown that cerebellar folia aren't uniform in size and shape. We developed the original classification of cerebellar folia. The folia were divided into 3 types according to folium height (small, medium and large) and width (small, medium and large). 9 anatomical variants of cerebellar folia were described in accordance with the shape and ratio of height and width of the folia. Different cerebellar lobules and branches have different folial variants, but all described folial types and variants may be found in a single cerebellum. The results of the study may be helpful to distinguish normal and abnormal cerebellar folia to diagnose cerebellar malformations in clinical neuroimaging and morphological studies of cerebellum.

Key words: brain, cerebellum, vermis, folium, variations

Introduction

Human cerebellum has the most geometrically complex shape and spatial configuration among the various structures of the central nervous system. Cerebellar cortex forms a three-dimensional convoluted foliated structure, duplicating external contour of white matter [7, 13].

Cerebellar folium is the smallest recognizable fold of the cerebellar cortex (gyrus), located on the plate of white matter. Some folia have their own white matter (core of the folium) departing from the underlying white matter of the cerebellar branches.

Cerebellar folium has the crown (apex) and walls (lateral surfaces). Adjacent folia are separated by fissures. The bottoms of separating fissures have their own cortex (interfolial) and are also called "fundi". The folial cortex has some structural features in different parts of folia: the granular layer has greater volume and thickness in the folial crown, Purkinje cell density is greater in folial crowns than in walls and fundi [13].

Cerebellar folium is considered by some scientists as a distinct structural, connectional and functional entity and independent working module (unit) of cerebellum, which has common afferent and common efferent pathways [13].

Morphological changes of cerebellar folia (changes in size, structure and spatial organization) are found in many neurodegenerative diseases, cerebellar dysplasia and hypoplasia [4, 10] and are used as basic parameters in classifications of cerebellar malformations [4, 9]. There are some studies describing pathological changes in cerebellar folia and cortex as neuroimaging findings: disorganization and malorientation of the folia, abnormal folial pattern, decrease in folium size (cerebellar microgyria), absence of folia (cerebellar agiriya) etc. [3, 4, 9, 10, 11, 12]. Thus, detailed information about shape and size of normal cerebellar folia is needed to distinguish normal and abnormal cerebellar folia to diagnose cerebellar malformations using neuroimaging methods. Welker described the structure of cerebellar folia [13]. But we didn't find any information about size and variability of folia of human cerebellum. That's why in this study we aimed to describe possible variations in size and shape of folia of human cerebellum to determine morphological and morphometric characteristics of normal cerebellar folia.

Material and Methods

The study was performed on cadaveric material. Cerebella of 50 people (20-88 years old) who died of causes unrelated to central nervous system pathology were studied. Causes of death of people included in the study are given in **Table 1.**

Table 1. Causes of death of people included in the study

Cause of death	Acute heart failure	Malignant tumors (except brain tumors)	Pneumonia	External or internal bleeding	Asphyxia	Total
N	25	14	5	3	3	50

Cerebella were obtained during the forensic autopsies and were fixed during one month in 10% formalin solution. Macrophotographs of midsagittal sections of cerebella (**Fig. 1**) were investigated. Possible variations in the size, shape of the folia of cerebellar vermis were described.

Histological sections of individual cerebellar vermal lobules were prepared and used for morphometric study of cerebellar folia (**Fig. 2**). Hematoxylin and eosin staining was used.

The morphometric study was performed using the computer program "Image Tool". The height, the width, the length of the ganglionic layer (Purkinje cell layer), the number of Purkinje cells, the average distance between the centers of the Purkinje cells and the Purkinje cells density were measured and calculated on each individual folium.

Fig. 1. Midsagittal section of human cerebellum vermis, folia of lobules IX and X. Scale bar 1 cm.

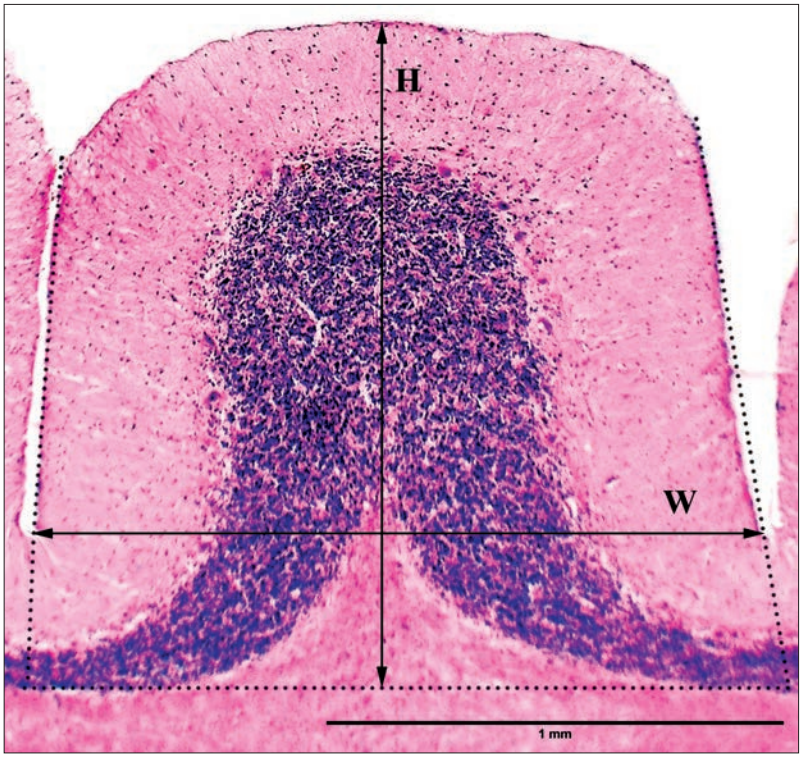

Fig. 2. Cerebellar folium (hematoxylin and eosin staining), H – folium height, W – folium width. Scale bar 1 mm.

The folium height was measured as a distance between the apical point of the folium and the line, which connects basal (the deepest) points of the granular layer of the fundi – interfolial fissures (basal line). The folium width was measured as a maximal distance between the lateral surfaces of the folium. The folium height was perpendicular (or close to perpendicular) to the basal line and to the folium width in folia with simple shape. The morphometric parameters (height and width) and features of the shape of folia were used to describe folial types and variants to develop classification of cerebellar folia.

Statistical data processing was performed using Microsoft Excel 2010. The relative prevalence of different folial types and variants was calculated as a ratio between the number of folia which were classified as belonging to different types or variants and the general number of folia. The following values of morphometric parameters of cerebellar folia were calculated: the sample mean (M) and the standard error of the mean (m), standard deviation (σ), the minimum (min) and the maximum (max) values. These parameters were calculated for all folia and individually for different variants of folia (M±m). The normality of distribution was verified using the Kolmogorov–Smirnov KS test: the empirical distribution function of the sample was compared to normal distribution function with the same values of the sample mean and standard deviation. The significance of statistical difference between the values of morphometric parameters of different folial variants was assessed using Kruskal–Wallis test and post hoc Dunn's test for multiple comparisons. The significance level for all results was accepted as $p<0.05$ (the differences between groups (folial variants) and the differences between distributions (empirical and normal) were considered as significant).

Results

The morphometric parameters and the shapes of cerebellar folia are quite diverse. We measured and calculated the average morphometric parameters of cerebellar folia in general in our previous studies [8] and used those average values to develop the original classification of cerebellar folia in the present study. The values of folium height and folium width were normally distributed ($p>0.95$). Thus, the values of the sample mean and standard deviation were eligible to be used to develop the classification of the folia. We divided folia into groups (types) in accordance with the sample mean values of the folia height and width (M) and standard deviation of those values (σ) (**Table 2**). Height and width of the folia were classified as medium if value of size parameter was ranged between M-σ and M+σ; small – up to M-σ; large – more than M+σ. The mean value of folium height was 1727.94±55.94 μm (min – 324 μm, max – 5286 μm, standard deviation – 842.82 μm). The folia were divided into three types according to the height: small (height up to 884 μm), medium (height 885-2571 μm), and large (height 5286 μm and more). The mean value of folium width was 1794.94±58.10 μm (min – 828 μm, max – 3893 μm, standard deviation – 436.78 μm). The folia were also divided into similar types according to the width: small (width up to 1357 μm), medium (width 1358-2231 μm), and large (width 2232 μm and more). These types of folia may be combined in different ways and have different prevalence. The folial types (described according to height and width) are combined independently of each other, all possible combinations were found.

Table 2. The prevalence of combinations of different folial types

Height of folium	Width of folium			Total
	Small	Medium	Large	
Small	2.10%	9.01%	3.04%	14.15%
Medium	11.01%	48.22%	8.70%	67.93%
Large	1.47%	13.52%	2.94%	17.92%
Total	14.57%	70.75%	14.68%	100%

However, in addition to morphometric parameters, folia have shape features that have a significant impact on their structure. We described 9 anatomical variants of cerebellar folia, taking into account the morphometric characteristics (height, width and their ratio) and the shape of folia (**Table 3**, **Fig. 3**).

Table 3. Classification of cerebellar folia

Folium variant	Ratio "height / width"		Height	Width
	Min	Max		
1st	0.25	0.489	small	large
	0.25	0.489	small	medium
	0.25	0.489	medium	large
	except		*medium*	*medium*
2nd	0.25	0.75	medium	medium
	0.49	0.75	small	small
	0.49	0.75	small	medium
	except		*medium*	*large*
3rd	0.49	0.75	medium	large
4th	0.751	1.249	small	medium
			medium	medium
			medium	large
			large	large
5th	1.25	1.799	medium	medium
			medium	small
			large	medium
6th	1.8	2.78	medium	small
			large	medium
			large	small

Folium variant	Ratio “height / width”		Height	Width
	Min	Max		
7th	0.49	1.249	The folia have the isthmus (basal narrowing or neck) in the basal part	
8th	1.25	1.799		
9th	1.8	3.77		

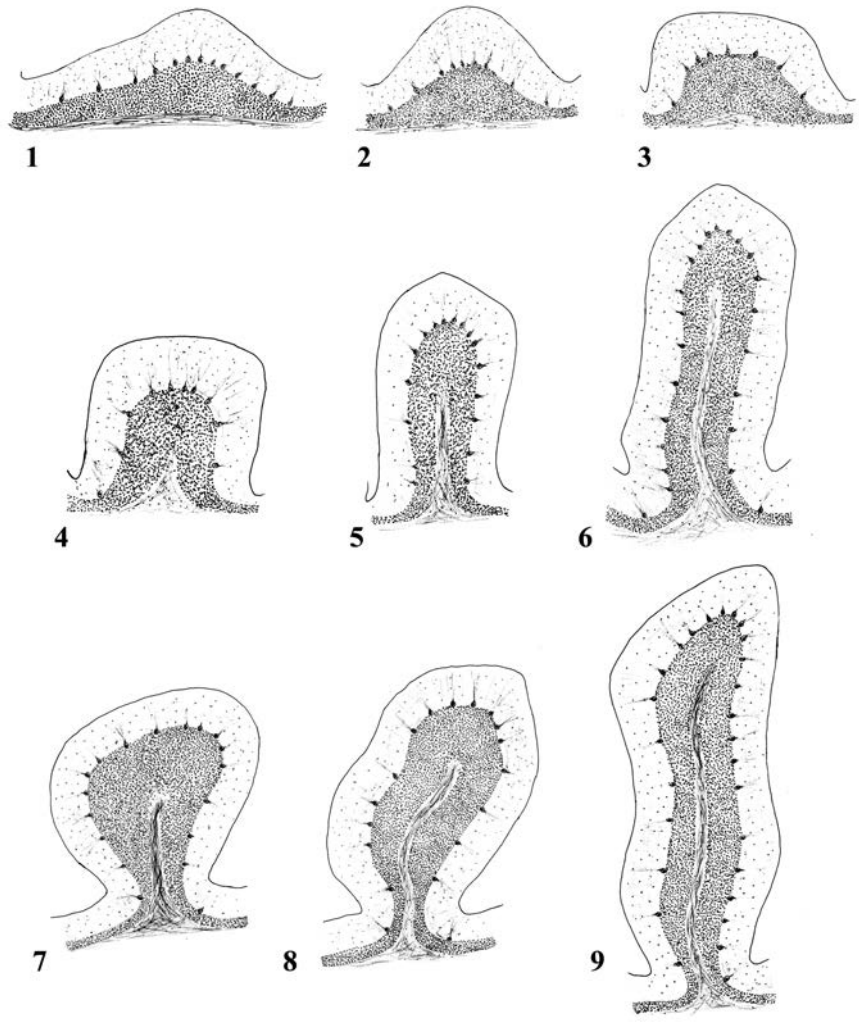

Fig. 3. Anatomical variants of cerebellar folia (author’s drawing)

The 1st variant: the folia have the shape of a low wave, have rounded or flattened crown (top) and don't have their own white matter. The shape of those folia may be asymmetrical. The folia are located on the inner surfaces of the white matter branches near their base (often) or on the outer surfaces of the white matter branches between large long folia (rarely).

The 2nd variant: the folia are small, have triangle-like or crescent-like (demilune-like) shape and have rounded or pointed crown. White matter also has triangle-like or crescent-like shape. Sometimes folia don't have their own white matter. The folia are located between large folia (often) or are located on the inner surfaces of the white matter branches (rarely).

The 3rd variant: the folia have the semicircle-like or rectangle-like shape. The folia often don't have their own white matter. The folia are located on small white matter branches (often) or on the main trunk of white matter, forming the lobule (less often).

The 4th variant: the folia have the square-like or semicircle-like shape; the crown is rounded or rectangular. The shape of white matter is triangle-like (often) or crescent-like (rarely). Sometimes the folia don't have their own white matter. The folia are located on the inner surfaces of the white matter branches (often) or on the outer surfaces of branches and the main trunk of white matter (less often).

The 5th variant: the folia have the elongated rectangle-like shape; the crown is rounded or rectangular. The white matter has the shape of the elongated plate (simple branch). The folia are located on the outer surfaces of the main trunk and secondary branches of the cerebellar white matter.

The 6th variant: the folia have the shape of a tall rectangle; the crown is round or rectangular. The white matter has the branch-like shape. The folia are located on the main trunk of the lobules (often) or on the outer surfaces of the branches (less often).

The folia of *7th, 8th and 9th variants* have the isthmus in the basal part (basal narrowing or neck) which is a distinctive feature of the shape.

The 7th variant: the folia have rounded goblet-like shape and have the isthmus in the basal part. The crown is rounded, pointed or flattened. The white matter has the branch-like shape. The folia are located on the apical points of branches and form the visible surface of cerebellum (often) or are located on the main trunk of lobules (less often).

The 8th variant: the folia have elongated goblet-like or leaf-like shape and have the isthmus in the basal part. The apex is pointed or rounded. The white matter has the branch-like shape. The folia may be apical and form the visible surface of cerebellum or are located on the main trunk of lobules (more often).

The 9th variant: the folia are the longest among all variants, have the isthmus in the basal part. The folium shape is leaf-like or sword-like: the apex is pointed or rounded (rarely), sometimes flattened. The white matter has the branch-like shape. The folia are located on the common trunk of the lobules VI-VII, on the main trunks of lobules VIII and IX (often), less often on the main trunks of lobules II, III and X.

The variants of cerebellar folia shape have different values of morphometric parameters (**Table 4**). The sample mean values of height, width, length of ganglionic layer and number of Purkinje cells in different folial variants were significantly different ($p<0.05$). The sample mean values of the average distance between the centers of Purkinje cells and the Purkinje cells density in different folial variants were not significantly different ($p>0.05$).

Table 4. The morphometric parameters of different variants of cerebellar folia, *M±m*

Parameters		Folium variant								
		1st	**2nd**	**3rd**	**4th**	**5th**	**6th**	**7th**	**8th**	**9th**
Height, μm	*M*	838.8	1026.5	1358.1	1396.7	1961.9	2784.0	1993.8	2613.2	3437.3
	m	70.2	78.5	266.3	106.8	314.2	718.8	157.6	201.6	459.3
Width, μm	*M*	2225.2	1730.7	2178.9	1502.2	1372.0	1281.9	1996.1	1759.1	1583.6
	m	182.2	132.4	427.3	114.9	219.7	331.0	157.8	135.7	211.6
Ratio "height/ width", μm	*M*	0.385	0.599	0.627	0.937	1.431	2.182	1.011	1.486	2.204
	m	0.03	0.05	0.12	0.07	0.23	0.56	0.08	0.11	0.29
Length of ganglionic layer, μm	*M*	2683.4	2441.0	3569.4	3048.5	4121.1	5666.1	4729.1	5717.9	7286.9
	m	221.3	186.7	700.0	233.1	659.9	1463.0	373.9	441.2	973.8
Number of Purkinje cells	*M*	11.24	10.49	14.12	13.52	15.74	22.93	19.39	23.47	30.16
	m	0.92	0.80	2.77	1.03	2.52	5.92	1.53	1.81	4.03
Average distance between the centers of the Purkinje cells, μm	*M*	249.22	282.60	302.82	255.80	345.69	263.06	289.04	280.82	252.90
	m	24.15	21.61	59.39	19.56	55.35	67.92	22.85	21.67	33.80
Purkinje cells density, cells per mm	*M*	4.14	4.33	3.98	4.42	3.80	4.04	4.09	4.07	4.16
	m	0.34	0.33	0.78	0.34	0.61	1.04	0.32	0.31	0.56

The described folial variants have different prevalence, which reflects the distribution of the folia in different phylogenetic regions of cerebellum – Upper Paleocerebellum (lobules I-V), Neocerebellum (lobules VI-VII), Lower Paleocerebellum (lobules VIII-X) and Archicerebellum (lobule X) (**Table 5**). Different cerebellar lobules and branches have different prevalence of folial variants, but all described folial types and variants may be found in a single cerebellum. Thus, the differences in size and shape of cerebellar folia aren't the direct signs of cerebellar malformations. Distribution and grouping of folia with different shape and size into lobules would be expected to reflect functional features of various cerebellar regions.

Table 5. The prevalence of different variants of the folia in different phylogenetic regions of human cerebellum

Folium variant	Localization of the folia (phylogenetic regions of cerebellum)				Total
	Upper Paleocerebellum (lobules I-V)	Neocerebellum (lobules VI-VII)	Lower Paleocerebellum (lobules VIII-X)	Archeo-cerebellum (lobule X)	
1st	5.97%	3.98%	4.93%	0.42%	15.30%
2nd	7.97%	4.51%	5.14%	0.31%	17.93%
3rd	1.47%	0.84%	0.42%	0%	2.73%
4th	8.39%	5.14%	3.67%	0.84%	18.04%
5th	1.68%	0.94%	1.15%	0.31%	4.08%
6th	0.31%	0.51%	0.42%	0.42%	1.66%
7th	7.65%	4.30%	3.98%	0.84%	16.77%
8th	6.18%	4.72%	5.66%	1.05%	17.61%
9th	1.26%	1.26%	2.94%	0.42%	5.88%
Total	40.88%	26.20%	28.31%	4.61%	100.00%

Discussion

In this study we described variations in size and shape of cerebellar folia. Differences in folial shape and size reflect anatomical variability of human cerebellum. Larsell and Jansen [7] and Bispo et al. [2] described some anatomical variations of individual lobules of cerebellar vermis; it was shown that vermal lobules are varying in size and shape.

But we didn't find the information about anatomical variability of folia of human cerebellum. Variations in the size of folia of the avian cerebellum were described by Iwaniuk et al. [5]. The length of the Purkinje cell layer (ganglionic layer) of each cerebellar folium was measured as well as in the present study. Additionally, we measured and calculated some other parameters: height, width of folia and their ratio, the number of Purkinje cells, the average distance between the centers of the Purkinje cells and the Purkinje cells density in individual folia.

The distance between Purkinje cells and the Purkinje cells density were determined by other researches [1, 6]. These values particularly coincide with our data. The distance between 2 Purkinje cells was ranged between 82.6-346.6 μm (mean 179.3±18.4 μm) [6]; in our study the mean value was ranged between 249.22-345.69 μm in different folial variants. The mean value of the Purkinje cells density in the control group was 3.46 cells/mm [1]; in our study it was ranged between 3.80-4.42 cells/mm in different folial variants. These parameters were previously determined only in the cerebellar cortex in general; we determined them in the individual folia and in the folia with different shape and size for the first time.

Thus, the obtained values of morphometric parameters of folia of human cerebellum, the original classification of folial variants with variant descriptions may be considered as quantitative and qualitative parameters of normal cerebellar folia.

Conclusions

It was shown that folia of human cerebellum aren't uniform in size and shape. Size and shape of all normal cerebellar folia would be expected to correspond to one of the folial variants which were described in the present study. The results of the study may be helpful to distinguish normal and abnormal cerebellar folia to diagnose cerebellar malformations in clinical neuroimaging and in morphological studies of cerebellum.

References

1. **Axelrad, J. E., E. D. Louis, L. S. Honig, I. Flores, G. W. Ross, R. Pahwa, K. E. Lyons, P. L. Faust, J.P. Vonsattel.** Reduced Purkinje cell number in essential tremor: a postmortem study. – *Arch. Neurol*., **65**(1), 2008, 101-107.
2. **Bispo, R., A. Ramalho, L. Gusmão, A. Cavalcante, A. Rocha, C. Sousa-Rodrigues.** Cerebellar vermis: Topography and variations. – *Int. J. Morphol*., **28**(2), 2010, 439-443.
3. **Chatur, C., A. Balani, R. Vadapalli, M. G. Murthy.** Isolated unilateral cerebellar hemispheric dysplasia: A rare entity. – *Can. J. Neurol. Sci*., **46**(6), 2019, 760-761.
4. **Demaerel, P.** Abnormalities of cerebellar foliation and fissuration: classification, neurogenetics and clinicoradiological correlations. – *Neuroradiology,* **44**, 2002, 639-646.
5. **Iwaniuk, A. N., P. L. Hurd, D. R. Wylie.** Comparative morphology of the avian cerebellum: II. Size of folia. – *Brain Behav Evol*., **69**(3), 2007, 196-219.
6. **Kalanjati, V. P., A. K. Dewi, M. W. A. Santoso.** Quantitative study on human cerebellar cortex from anatomy cadaver preparations. – *Int. J. Morphol*., **35**(1), 2017, 167-171.
7. **Larsell, O., J. Jansen**. **Adult Human Cerebellum.** – In: *The comparative anatomy and histology of the cerebellum. The human cerebellum, cerebellar connections, and the cerebellar cortex* (Ed. J. Jansen). Minneapolis, The University of Minnesota Press, 1972, 36-64.
8. **Maryenko, N. I., O. Yu. Stepanenko**. Folium as a structural unit of the human cerebellum. – *Ukr. ž. med. biol. sportu*, **5**(1), 2020, 56–61. [in Ukrainian]
9. **Patel, S., A. J. Barkovich.** Analysis and classification of cerebellar malformations. – *Am J Neuroradiol*., **23**(7), 2002, 1074-1087.
10. **Poretti, A., E. Boltshauser, D. Doherty.** Cerebellar hypoplasia: Differential diagnosis and diagnostic approach. – *Am. J. Med. Genet. Part. C Semin. Med. Genet*., **166**, 2014, 211-226.
11. **Sasaki, M., H. Oikawa, S. Ehara, Y. Tamakawa, S. Takahashi, H. Tohgi.** Disorganised unilateral cerebellar folia: a mild form of cerebellar cortical dysplasia? – *Neuroradiology*, **43**(2), 2001, 151-155.
12. **Soto-Ares, G., C. Delmaire, B. Deries, L. Vallee, J. P. Pruvo.** Cerebellar cortical dysplasia: MR findings in a complex entity. – *Am. J. Neuroradiol*., **21**(8), 2000, 1511-1519.
13. **Welker, W. I.** The significance of foliation and fissuration of cerebellar cortex. The cerebellar folium as a fundamental unit of sensorimotor integration. – *Arch. Ital. Biol*., **128**(2-4), 1990, 87-109.

Institute of Experimental Morphology, Pathology and Anthropology with Museum
Bulgarian Anatomical Society

Acta morphologica et anthropologica, 28 (1-2)
Sofia ● 2021

Cotinus coggygria Non-Volatile Fraction Affects the Survival of Human Cultured Cells

Ivan Iliev[1], Ivaylo Ivanov[2], Katerina Todorova[1], Donka Tasheva[3], Mashenka Dimitrova[1]*

[1] *Institute of Experimental Morphology, Pathology and Anthropology with Museum, Bulgarian Academy of Sciences*
[2] *Department of Bioorganic Chemistry and Biochemistry, MedicalUniversity – Sofia*
[3] *Faculty of Chemistry and Pharmacy, Sofia University "St. Kl. Ohridski"*

***** Corresponding author e-mail: mashadim@abv.bg

Ethyl acetate extract from *Cotinus coggygria* (smoke tree) leaves contains non-volatile components, some of which are potent inhibitors of prolyl oligopeptidase (POP) and fibroblast activation protein α (FAP). Those enzymes are known to participate in tumorigenesis and tumor growth. Effects of the above extract on several human cultured cells, originating from the most common and aggressive cancers were examined using the Neutral Red Uptake Test. The IC_{50} values were determined and selectivity indices (SI) versus non-tumorigenic cell lines MCF-10A and BJ were calculated. According to the results, *C. coggygria* extract has a highly selective effect on HeLa cells and can be considered as a potential therapeutic agent in cervical carcinoma. Additionally, it is shown that the simultaneous suppression of POP and FAP has a pronounced impact on the cell proliferation of both tumor and normal human cells at concentrations > 12 μg/ml, which proves the enzymes' role in the control of cell proliferation.

Key words: Cotinus coggygria, prolyl oligopeptidase, fibroblast activation protein α, human cultured cells, cell survival

Introduction

Cotinus coggygria (smoke tree) is a flowering plant from the family *Anacardiaceae*, also known as smoke bush, Venetian sumach, or dyer's sumach. Extracts from both aerial and underground parts of the plant are used as antiseptic, anti-inflammatory and hepatoprotective agents [6]. Alcoholic extracts contain considerable amount of polyphenols, fusetin and other ingredients with a pronounced antitumor activity (see e.g [2]). Our previous study showed that the ethyl acetate extract of smoke tree leaves inhibits fibroblast activation protein α (FAP, EC 3.4.21.B28) – a protease involved in the development of a large number of solid tumors [3]. On the other hand, FAP has similar substrates to another serine protease – prolyl oligopeptidase (POP). Thus, a possibility exists that POP can also

be suppressed by the above extract. POP (EC 3.4.21.26) is a cytosolic peptidase of S9 family, hydrolysing peptide bonds at the C-terminus of proline from short peptides (up to 30 amino acids). In actively proliferating cells, the enzyme localizes in the nucleus, where, by a yet unknown mechanism, it is involved in the stimulation of cell division and cell differentiation [7]. Increased levels of POP have been found in a variety of solid tumors [5]. It is believed that the administration of POP inhibitors may result in a suppression of cell proliferation and restriction of tumor growth [4].

The aim of the present study is to assess the effect(s) of ethyl acetate extract of *Cotinus coggygria* leaves on the activity of POP as well as on the cell viability and proliferative activity of human tumor and non-tumorigenic cultured cells.

Materials and Methods

Ethyl acetate extract of Cotinus coggygria leaves. This extract was obtained exactly as described previously [3]. In brief, crude ethanol extract of *C. coggygria* leaves (Vemo 99 Ltd, Sofia, Bulgaria) was suspended in dist. water and acidified to pH 3.0 with 6N hydrochloric acid. The mixture was extracted with ethyl acetate, filtered, washed with brine and dried over sodium sulfate. Then, diisopropyl ether was added in drops and the formed dark yellow solid was filtered and dried.

POP inhibition by the C. coggygria extract. POP inhibition properties of the above extract (1 to 10 μg/ml) were tested on recombinant human POP (R&D Systems through Biomedica, Bulgaria) in phosphate buffered saline (PBS, pH 7.4) with the addition of 1 mM EDTA, 5 mM dithiotreitol (DTT) and 80 μM fluorogenic substrate Z-glycyl-prolyl-methylcoumaryl amide (Z-Gly-Pro-MCA, Bachem, Switzerland) at 37ºC. Enzyme assays were carried out in 96-well plates on Varioscan Fluorescence spectrofluorimeter at 360 nm excitation and 460 nm emission every 3 min. The program EnzFilter V2 was used for data processing.

Cell culturing and treatment. For the experiments, the following human cell lines were used: **MCF-10A** (immortalized normal epithelial cells of mammary gland), **BJ** (activated normal skin fibroblasts), **MCF-7** (luminal type A breast carcinoma), **MD-MBA-231** (triple negative breast carcinoma), **A549** (lung alveolar adenocarcinoma), **HeLa** (cervical cancer), **HT-29** (colorectal adenocarcinoma), **H1299** (non-small cell lung carcinoma cells), **HepG2** (hepatocellular carcinoma) and **PC3** (prostate adenocarcinoma). They were cultured in Dulbecco's Modified Eagle's medium – high glucose (DMEM 4,5 g/l glucose), supplied with 10 % fetal bovine serum and antibiotics in usual concentrations in a humidified atmosphere with 5 % CO_2 at 37.5ºC. In the case of MCF-10A cells, epidermal growth factor, insulin and cholera toxin were added in concentrations corresponding to the cell bank instructions. Cells were plated at a density of 2×10^3 in 100 μl culture medium in 96-well flat-bottomed microplates and allowed to adhere for 24 h before treatment with *C. coggygria* extract. The extract was dissolved in DMSO and diluted with culture medium. A concentration range from 0.75 to 100μg/ml was applied for 48 h. After treatment with Neutral Red for 3 h, washing and application of the ethanol/acetic acid solution (NR Desorb) (after [10]), the absorption was measured on ELISA microplate reader (TECAN, SunriseTM, Grödig/ Salzburg, Austria) at a wavelength of 540 nm. GraphPad Prizm5 software was used for the processing of the results. All experiments were performed in triplicate.

Results and Discussion

In a recent paper, we showed that ethyl acetate extract of *C. coggygria* leaves possesses one or more components inhibiting FAP with an IC_{50} value of 3.7 μg/ml [3]. However, FAP and POP are both serine-type post-proline specific endopeptidases with similar substrate specificity. Thus, it is reasonable to suggest that the extract can inhibit POP, too. Our present study shows an inhibition of human recombinant POP by IC_{50}= 0.12μg/ml, i.e. the extract is 30 times more effective inhibitor of POP than of FAP.

POP is widely expressed in human organs and tissues with the highest levels in brain, testis and kidney [8]**.** Physiological functions of the enzyme include processing of neuropeptides, signal transduction, control of protein secretion, etc. It is shown to be involved in cell division and differentiation and in the nervous system – in learning and memory (reviewed in [1]). POP expression is elevated in many types of carcinomas, suggesting it may promote cancer development and growth [5]. Furthermore, it was shown that treatment with the inhibitor J94 (inhibits both POP and FAP) suppressed growth of human colon cancer xenograft tumors in mice by >90% [4]. Recent studies of Perez et al. [9] using the POP inhibitor Y-29794 demonstrate a lowered survival of *in vivo* tumor growth of triple-negative breast cancer, implanted in mice. Thus, POP inhibitors are recognized as potential therapeutics in cancer. That is why we decided to test the impact of *C. coggygria* ethyl acetate extract on the survival/proliferation of human tumor cells of different origin.

In the Atlas ARCHS4 of tissue expression of a number of genes, POP's expression (https://maayanlab.cloud/archs4/gene/PREPL#tissueexpression) and this one of the FAP (https://maayanlab.cloud/archs4/gene/FAP#tissueexpressionexpressions) in the most commonly used cell lines are presented in provisional units from zero to fourteen. According to this database, POP is expressed in all the cells, studied here, in large quantities from 9 to 12. It has the lowest amount in H1299 (9.5) and highest in HeLa cells (11.8). Effects *of C. coggygria* ethyl acetate extract on the proliferative activity of human tumor cells are illustrated in **Fig. 1** and **Fig. 2**. Low extract concentrations (up to 12 μg/ml) showed a minimal or no effect. In HT-29, HepG2 and PC3 cells at concentrations about 1.5 – 3.0 μg/ml a statistically significant pro-proliferative activity was observed (**Fig. 2**). It should be noted, that cells of none or reverse effect have a zero or close to zero FAP expression. The most powerful anti-proliferative activity was observed in HeLa cells which expresses FAP by 5.9 provisional units. In view of the above findings, it might be suggested that the proliferative activity of tumor cells depends on both enzymes but most of all, on the tissue origin. Results for the non-tumorigenic MCF-10A and BJ cells were given in our previous paper [3]. In the present study, we repeated the experiment to obtain very close results for the two cell lines. In Table 1, IC_{50} and SI values for the cells are presented. Since IC_{50} for the two "normal" cell lines are very close, SI indices calculated versus MCF-10A and BJ are almost equal. From these results, it becomes clear that SI is very promising only for HeLa cells (SI > 11). A moderately good selectivity was obtained also for HepG2 cells (SI around 2.5).

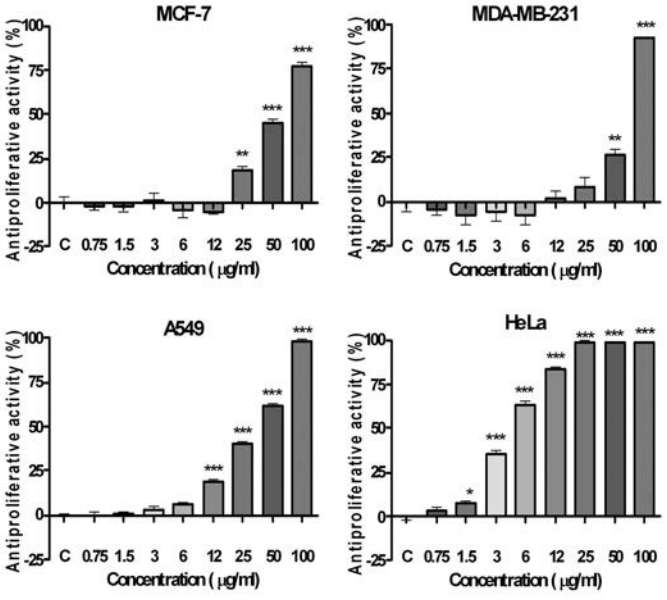

Fig. 1. Effect of C. coggygria ethyl acetate extract on the proliferative activity of the cells MCF-7, MDA-MB-231, A549 and HeLa. The effect in not-treated control cells was accepted to be zero (C). Each value is a mean of three independent experiments.

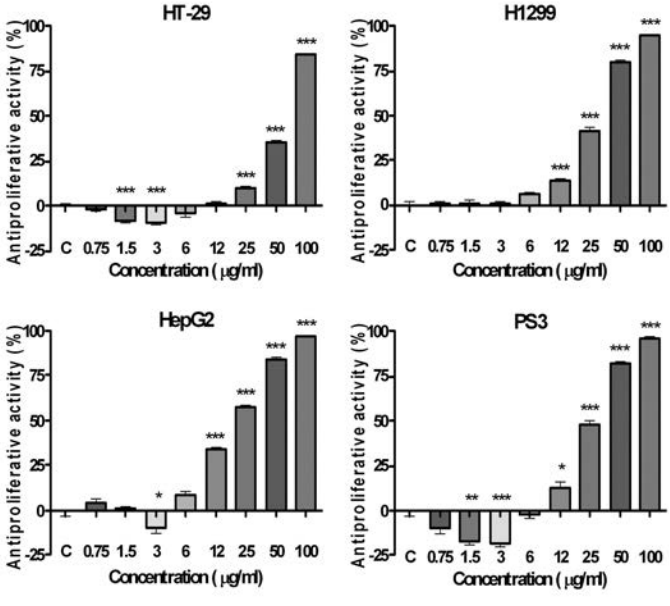

Fig. 2. Effect of C. coggygria ethyl acetate extract on the proliferative activity of the cells HT-29, H1299, HepG2 and PC3. The effect in not-treated control cells was accepted to be zero (C). Each value is a mean of three independent experiments.

Table 1. IC_{50} and SI values of different cultured cells after application of *C. coggygria* ethyl acetate extract.

Cell line	IC_{50} [μg/ml] mean ± SD	SI versus MCF-10A	SI versus BJ
MCF-10A	50,79 ± 4,645	1,00	1,05
BJ	53,34 ± 4,64	0,95	1,00
MCF-7	57,32 ± 4,702	0,89	0,93
MDA-MB-231	67,63 ± 3,67	0,75	0,79
A549	36,25 ± 3,47	1,40	1,47
HeLa	4,53 ± 0,36	11,2	11,78
HT-29	65,24 ± 2,92	0,78	0,82
H1299	30,32 ± 2,48	1,68	1,76
HepG2	21,03 ± 1,71	2,42	2,54
PC3	26,64 ± 3,5	1,91	2,00

Conclusions

According to the results presented here, *C. coggygria* extract has a highly selective effect on HeLa cells and can be considered as a potential therapeutic agent in cervical carcinoma. Additionally, it is shown that the simultaneous suppression of POP and FAP has a pronounced impact on the cell proliferation of both tumor and normal human cells at concentrations > 12 μg/ml, which proves the enzymes' role in the control of cell proliferation.

Acknowledgement. This work is financially supported by the National Science Fund of the Bulgarian Ministry of Education and Science, Grant No KP-06-N31/1.

References

1. **Garcıa-Horsman, J. A., P. T. Mannisto, J. I. Venalainen**. On the role of prolyl oligopeptidase in health and disease. – *Neuropeptides*, **41**, 2007, 1-24.
2. **Gospodinova, Z., N. Bózsity, M. Nikolova, M. Krasteva, I. Zupkó.** Antiproliferative properties against human breast, cervical and ovarian cancer cell lines, and antioxidant capacity of leaf aqueous ethanolic extract from *Cotinus coggygria* Scop. – *Acta Medica Bulgarica*, **XLIV**, 2017, 20-25.
3. **Iliev, I., I. Ivanov, K. Todorova, M. Dimitrova.** Effects of a *Cotinus coggygria* ethyl acetate extract on two human normal cell lines. – *Acta morphol. anthropol.*, **27**(3-4), 2020, 25-29.
4. **Jackson, K. W., V. J. Christiansen, V. R. Yadav, R. Silasi-Mansat.** Suppression of tumor growth in mice by rationally designed pseudopeptide inhibitors of fibroblast activation protein and prolyl oligopeptidase. – *Neoplasia*, **17**(1), 2015, 43-54.
5. **Larrinaga, G., I. Perez, L. Blanco, J. I. López, L. Andrés, C. Etxezarraga, F. Santaolalla, A. Varonaq J. Irazusta.** Increased prolyl endopeptidase activity in human neoplasia. – *Regulatory Peptides*, **163**, 2010, 102-106.
6. **Matić, S., S. Stanić, M. Mihailović, D. Bogojević.***Cotinus coggygria* Scop.: An overview of its chemical constituents, pharmacological and toxicological potential. – *Saudi Journal of Biological Sciences*, **23**, 2016, 452-461.
7. **Myöhänen, T. T., J. I. Venäläinen, J. A. García-Hornsman, Piltonen M., P. T. Männistö.** Distribution of prolyl oligopeptidase in the mouse whole-body sections and peripheral tissues. – *Histochem. Cell Biol.*, **130**, 2008, 993-1003.

8. **Myohanen, T. T., E. Pyykko, P. T. Mannisto, O. Carpen.** Distribution of prolyl oligopeptidase in human peripheral tissues and in ovarian and colorectal tumors. – *J. Histochem. Cytochem.*, **60**, 2012, 706-715.
9. **Perez, R. E., S. Calhoun, D. Shim, V. V. Levenson, L. Duan, C. G. Maki.** Prolyl endopeptidase inhibitor Y-29794 blocks the IRS1-AKT-mTORC1 pathway and inhibits survival and *in vivo* tumor growth of triple-negative breast cancer. – *Cancer Biol. Ther.*,**21**(11), 2020, 1033-1040.
10. **Repetto, G., A. del Peso, J. L. Zurita.** Neutral red uptake assay for the estimation of cell viability/ cytotoxicity. – *Nature Protocols*, **3**, 2008, 1125-1131.

Institute of Experimental Morphology, Pathology and Anthropology with Museum
Bulgarian Anatomical Society

Acta morphologica et anthropologica, 28 (1-2)
Sofia ● 2021

Morphological Characteristics of Rabbit Cornea in Norm and Wound Healing Cytoarchitecture

Katerina Todorova[1], Alexander Angelov[2]*

[1] *Institute of Experimental Morphology, Pathology and Anthropology with Museum, Bulgarian Academy of Sciences*
[2] *CEO Resbiomed - Company For Clinical Research & Medical Director Resbiomed - Sofia Eye Clinic*

* Corresponding author: email: katerinagencheva@yahoo.com

Cornea is an avascular structure with an important role in vision, which could be impaired by different conditions. The most suitable animal model in ophthalmology research, comparable to human, is the rabbit model. Data on the morphology of rabbit cornea are capable to predict or to be used for comparison of the fundamental processes in corneal wound healing. In this study the morphological aspects of corneal postoperative wound healing processes were assessed in comparison with the normal histology of corneal layers in rabbits. Our findings demonstrated that the corneal wound healing was between the phases of proliferation and maturation-tissue regeneration restored the integrity for three months but lamellar organization and remodeling still were not completed. Strong postoperative keratitis was observed in one case and structure similar to the human pre-Descemet's layer was noticed.

Key words: morphology of rabbit cornea, wound healing, tissue regeneration

Introduction

Cornea is an avascular part of the fibrous tunic (corneoscleral layer) – the outermost layer of the eye with an important role in focusing vision. It provides also transparency, refractivity and light transition into the retina - the innermost layer of the eye and gives mechanical strength of the eye. These functions could be deteriorated by corneal infections and injuries resulting into inflammation and ulcers, keratoconus, Fuchs endothelial corneal dystrophy, pterygium, etc. Such problems are found in animals, as well as in humans and have a high social and economic impact for the last, especially if the disease ends in blindness. Some superficial injuries can be treated by PRK (photorefractive keratectomy) or LASIK (laser assisted in situ keratomileusis) but often a corneal transplantation is recommended – penetrating or endothelial keratoplasty, or deep anterior lamellar keratoplasty. In such cases the usage of donor tissues from a human or xenotransplantation from a pig, because of similarities in biomechanical properties of human and pig corneas [13], is needed. The cornea is an immunologically privileged site and incidences for tissue rejection of corneal allografts or xenografts are less common than in other tissues requiring passage

through immunological barriers. However, there are many incidents of unsuccessful operations and along with the factor of cadaveric donation the demand for substitutes and new materials for medical implants in ophthalmology is determined. These facts require strict analysis in real situation – testing on living organisms, as this is the most suitable form of prediction of medicine or medical devices' behavior in humans. Usually, the ophthalmic surgery encounters difficulties due to micro-volumes of the work and challenges connected with the integration of different biomaterials with host tissues and preserving the corneal transparency, biomaterial degradation or aggressive wound healing response, which can even worsen the vision. Rapid restoration of corneal integrity after defects is a crucial factor for intraocular inflammation prevention and avoidance of permanent blindness. To study and evaluate the safety and biocompatibility of materials, the researcher has to be familiar with the histoarchitecture and morphological specificity of vision organs in norm and in pathology. Particularly, the corneal wound healing consists of complex events, involving different cell types and biochemical conditions demanding an understanding of the anatomical and physiological characteristics of the cornea and its multilayered structure. The establishment of the morphological characteristics of these specific cellular and subcellular structures in norm and during healing could be a helpful paraclinical tool in ophthalmology. The corneal histological structure is well-known [21], but as a surface structure it is in a constant state of morphological reconstruction due to epithelial regeneration or dynamic healing processes after physical or chemical injuries. In 1989 studies on cell kinetics indicated the presence on the ocular surface of proliferative cell compartments of stem cells and transitional amplifying cells [12]. Since then, the scientific research in the direction of transplantology and tissue-repair by stem cells usage in regenerative ophthalmology has developed rapidly. The most appropriate model, in research concerning ophthalmology comparable to human, is the rabbit model – *(Oryctolagus cuniculus)* and particularly the New Zealand White [26]. Rabbits are suitable specifically with their relatively large eyes and similarities with some anatomical features in humans – eyeball size, its internal structure and optical system, biomechanical and biochemical features, as well as conjunctiva cavity volume [27] and for age-related changes studies. Along with the comparable with human eye structures exist differences in some segment, for example: larger anterior segment, resulting in iris bulging and curvature of the anterior chamber [26], non-uniform changes in human and rabbit lens dimensions after excision, despite their similar size in eye [25], capacity to resist blinking due to lipids in their tears, produced by Hardarian gland, absent in primates [15], differences in the lamina cribrosa and its vascular supply, prelaminar optic nerve head and a retinal ganglion cell layer [2], partially myelinated by oligodendrocytes retina [19]. In the study of Ojeda et al. [18] was found that all epithelial cells exhibited microplicae regardless of their location and the stromal lamellae organisation and keratocytes in both species are not functionally homogeneous. Differences were also found: in the collagen fiber patterns of the epithelial basement membranes and the surface of keratocytes located near Descemet's membrane – in humans exhibited small fenestrations, which were absent in rabbits. In brief, histological investigations of rabbit cornea can be used for comparison of the fundamental processes in corneal wound healing on the basis of the known similarities and differences in both species.

This study aimed to investigate and highlight some morphological aspects of corneal postoperative wound healing process and cell interplay and to compare them with the normal histology of corneal layers in rabbits.

Materials and Methods

In vivo study: White New Zealand male rabbits (n=6), 6-7 months of age and mean body weight of 3,5 kg were divided into 2 groups as follow: 1st group – the control intact animals (n=2, 4 intact corneas); 2nd group (n=4, 4 intact corneas of the left eyes and 4 corneas of the right eyes with surgically made incisions – modified micropocket assay) and screened for corneal regeneration. After a postoperative period of three months, rabbits were sacrificed with an intravenous injection of 5-6 ml Euthanasin "N", Vetprom and Magnesium sulphate 5 mg/kg body mass and the corneas were excised. Several criteria for corneal healing or inflammation, visible with naked eye or after histological procedure were evaluated: signs for corneal layers regeneration and lack of ulceration or inflammation of the cornea (keratitis) and the adjacent sclera (signaling for uveitis). Macroscopically were evaluated: signs of inflammation (eye redness, pain, light sensitivity, signs for decreased vision and visible neovascularization, optical transparency; histologically – endothelial decompensation (dystrophy), fibrosis, stromal vascularization, keratoconus, interstitial keratitis, etc. *Surgery techniques*: According to Chan et al. [6] the rabbit cornea has uniform thickness of 407 +/- 20 μ, with an average thickness variation of only 7μ. In other study, it was found that the corneal thickness increased gradually from the center to the periphery of the 6 mm measured and the center corneal thickness of the right eyes was 387 ± 19.8 μ, while of the left – 384 ± 20.2 μ [24]. Based on these data, in our study a small perforation in the central cornea (debt 200μ) was made on the right eye through the anterior corneal stromal layer. The procedure was done under standard general ketamine/xylazine anesthesia with starting points of 10 mg/3 mg/kg. After the operation, both eyes of each rabbit from 2nd group were treated 21 days (three weeks × 4-3-2 times daily) with TobraDexEye Drops (tobramycin and dexamethasone, 3 mg/1 mg/ml), Alconand Crystal Vision Eye Drops (INN hydroxypropylmethylcellulose), Antibiotic-Razgrad AD. The left corneas were left intact but treated with both types of eye drops for comparison. *Histopathology: hematoxylin-eosin (H&E) staining.* After surgical excision tissue samples from the central corneas were routinely fixed in 10% buffered formalin, rinsed in water, dehydrated in graded ethanol, cleared in xylene, embedded in paraffin and subjected to histopathological H&E processing and evaluation by light microscope Leica DM 5000B, Wetzlar, Germany. *DAPI nuclear staining.*The materials fixed and embedded in paraffin were cut to 3-5 μm thick tissue sections, dewaxed in xylene and were DAPI [4,6-Diamidino-2-phenylindole, dihydrochloride] (10 mM solution in water, Abcam) stained and examined under UV light (359 nm excitation and 461 nm emission) by fluorescent microscope Leica DM 5000B, Wetzlar, Germany.

All the experiments with animals were carried out in the Institute of Experimental Morphology, Pathology and Anthropology with Museum, Bulgarian Academy of Sciences (Permit number: 11 30 127) in accordance with the national Regulation № 20/01.11.2012 regarding laboratory animals and animal welfare and European legislation. The medical procedures were strictly guided by the Directive 2010/63/EU of the European Parliament and of the Council of 22 September 2010 on the protection of animals used for scientific purposes and approved by the Ethics Committee in IEMPAM-BAS.

Results

During the experiment daily checks of the health status of all rabbits and observations of both eyes were made. Visible changes during the period of daily treatment with eye drops were not noticed. One week after the end of the eye drop course one of the rabbits from the second group showed clinical manifestation of eye irritation and inflammation, perhaps connected with external contamination of the cornea. In the end of the experiment in the control group histological observations of rabbit corneas revealed standard histoarchitecture composed of a stratified non-keratinized squamous epithelial layer, Bowman acellular collagenous layer beneath the epithelial basement membrane; a stromal layer with regular collagen organization, evenly interspersed with keratocytes, Descemet's basement membrane and endothelial cell monolayer of polygonal cells (**Fig. 1D**). On day 90 after the operation, in 3 of the rabbits from the second group, the histological aspects of corneal healing revealed wound regeneration processes at the site of the operative area on the right corneas with some individual differences observed (**Fig. 1A, B, C**). All layers of the cornea comprised of: epithelium layers, Bowman's layer, anterior and posterior collagen stroma, Descemet's membrane and the endothelium were present as in cornea of the rabbits from the control group described above. In these rabbits epithelial events involving the superficial squamous cells, central suprabasal cells and especially the single layer of inner columnar basal cells generating the other two types and populating the defect were observed microscopically. In the central corneal region, corresponding to the operative defect, were noticed focal proliferations, reattachment and differentiation of the epithelium forming more layers, compared to control left eye, perhaps due to initiated migration of epithelial cells as well from the periphery, but also from the columnar basal cell layer, leading to complete regeneration and covering of the corneal defect. Thus were formed prominent islets of epithelium, alternating with focal thinnings, similar to mid-stage keratoconus, but lack of the other main keratoconus characteristics was found. The stroma consisted of well-arranged collagenous fibers forming lamellae with parallel distributions, but in some regions were perpendicular to each other, following the curves of the anterior stroma and epithelium. Slight focal noncellular edema was present in some collagenous lamellae (**Fig. 1C**). Stromal resynthesys and reorganization phase was still present. Endothelial or Descemet's membrane damage was not observed. Inflammatory cell response, intrastromal neovasculature or other signs of chronic ocular inflammation were not seen in three of the rabbits from the second group at the end of the third month. Also lack of ulcerations, hyalinization, keratocyte loss, necrosis, stromal calcification after topical steroid therapy (as the described calcareous degeneration of the corneal stroma by Schlötzer-Schrehardt et al. [20]) was found. In one of the rabbits from the second group clinical signs for eye irritation were evident and the microscopic description confirmed acute inflammation and keratitis (**Fig. 2**). Distinct hyperplasia of the stratified squamous corneal epithelium lining was observed, along with histopathological signs of corneal fibrosis, strong neovascularization in the stroma, abundant inflammatory cell infiltrates in the upper lamellar layers. Keratocytes' homogeneity and intensity presented significant differences of populating the stromal lamellae, compared to the controls. Obvious stratification and drainage of the lamellae were found, different from fixation artifacts. In the same individual irregular Bowman's layer with taperings or tearings was noticed and moreover – a clearly visible layer – thin, acellular composed of collagen fibers was observed, resembling the pre-Descemet's layer – Dua's layer found in humans (**Fig. 3**), but

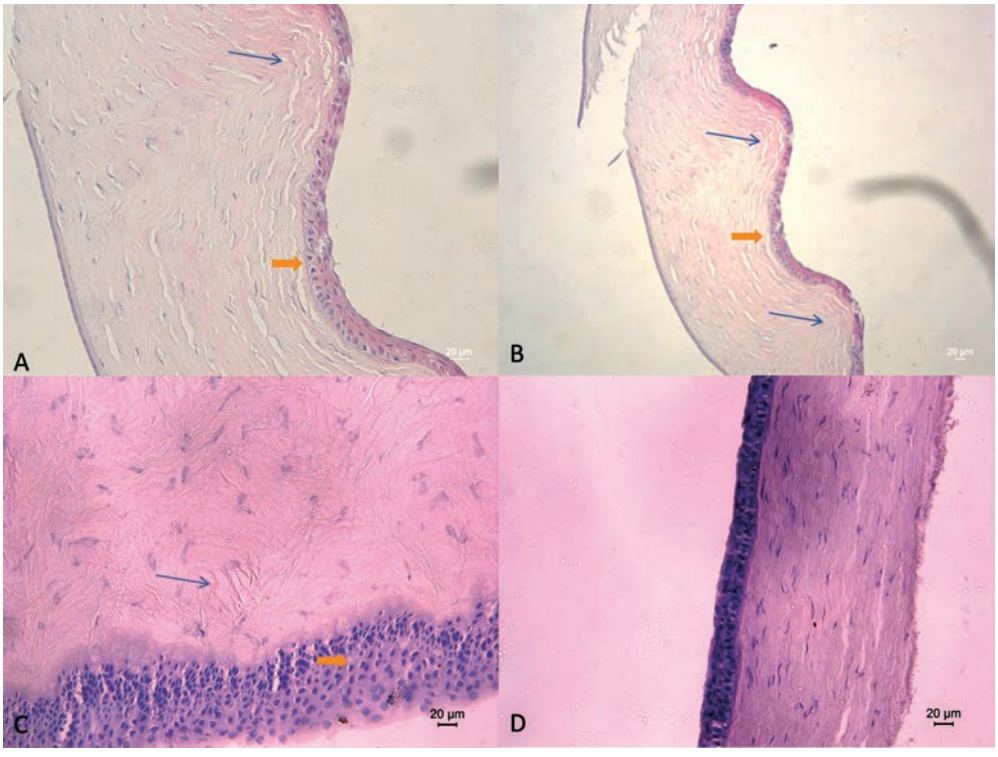

Fig. 1. Central region of rabbit cornea at the site of the operation: two individuals from the second group (A, B-one specimen; C – second specimen): obvious epithelial layer thickening (short orange arrow) and changed partial corneal thickness, irregular Bowman's layer and anterior stroma curves with changed lamellae organization towards perpendicular (long narrow blue arrow), A, B – enlargement of basal epithelium, C – changed inner basal cell layer of columnar cells connected with regeneration and slight lamellar edema; D – control cornea from an animal from the first group. H&E. Scale bar=20µm.

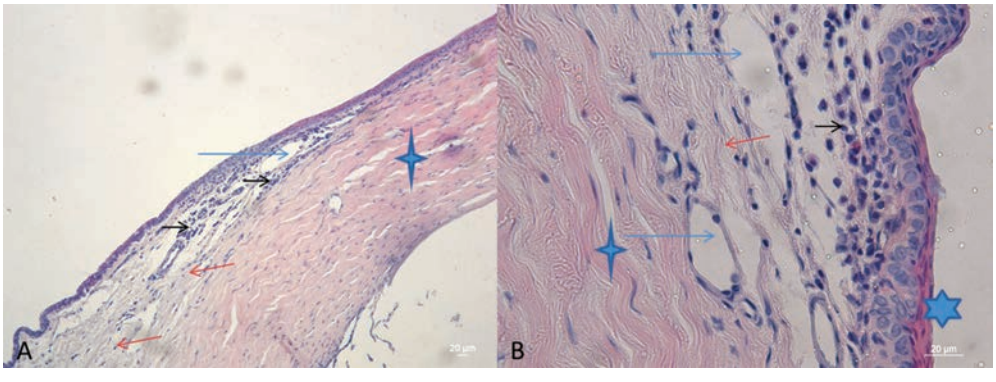

Fig. 2. Keratitis in rabbit: Inflammatory cells in the basal epithelium and Bowman's layer (small black arrow, pointing to the right), fibrosis (longer orange arrow, pointing to the left) and neovasculature (the longest blue arrow, pointing to the right) in stroma (four – point star), enlarged basal cells and epithelial squamous hyperplasia (six – point star). H&E. Scale bar=20µm.

thinner, which has to be studied in detail in separate study. DAPI staining revealed a similar picture reaffirming the multiplying of epithelial layers in operated eyes with a focus on the inner basal cell that changed their placement and nuclear morphology from elongated nuclei, but preserved uniform distribution of chromatin without signs of apoptosis and pyknosis (**Fig. 4**). Also, lack of inflammatory stromal response was confirmed in the three healthy animals with even distribution of keratocytes on the collagen lamellae.

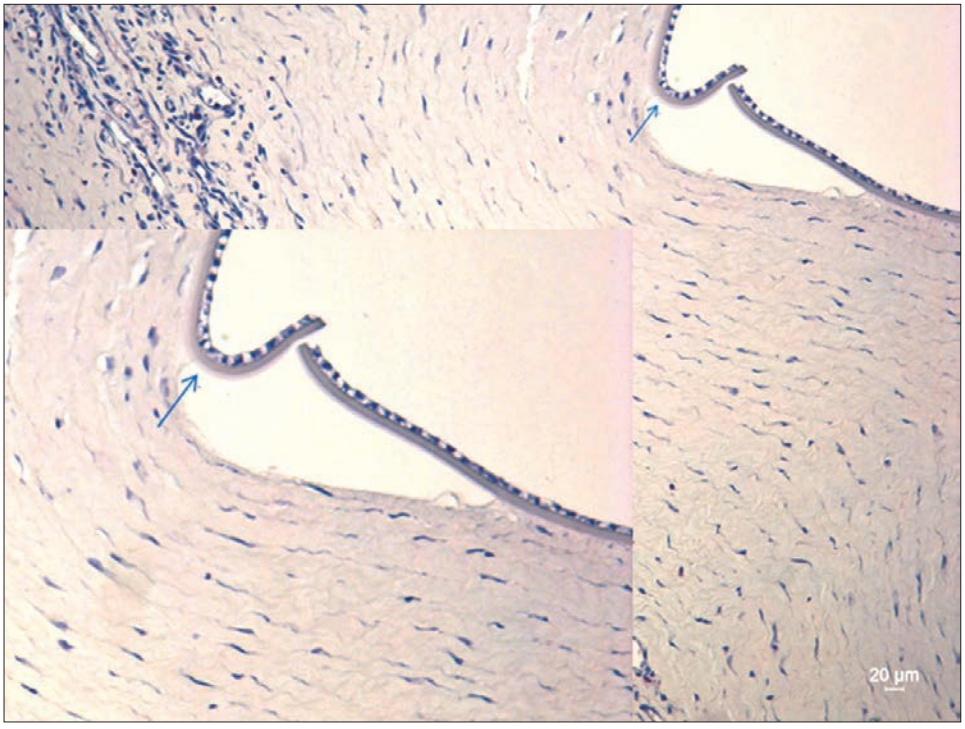

Fig. 3. Rabbit cornea-acellular layer (blue arrow) resembling the pre-Descemet's layer – Dua's layer in humans, <10µm. H&E. Scale bar=20µm.

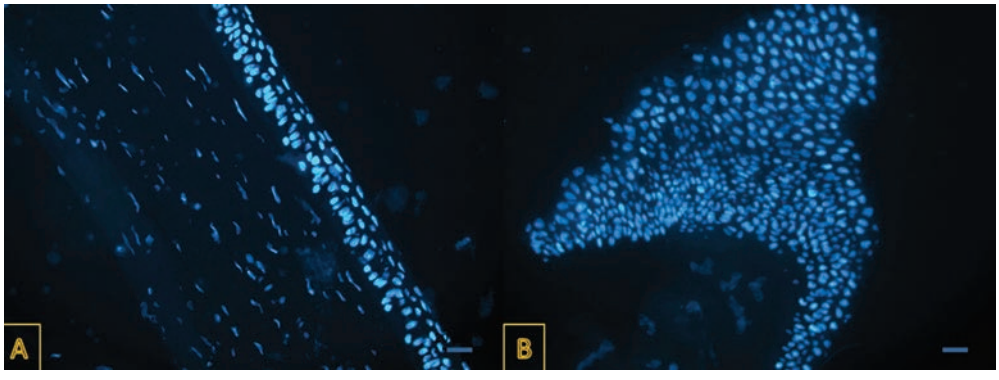

Fig. 4. Central region of rabbit cornea at the site of the operation: A-control, B-obvious epithelial layer thickening and changed nuclear morphology of inner columnar epithelium. DAPI. Scale bar=20µm.

Discussion

Wound healing of cornea is a similar process to skin wound healing, where the inflammatory processes are fundamental responses [16]. Our histopathological findings on 90 day confirmed postinflammatory phases and corneal repair in 3 of the operated animals and demonstrated that the corneal tissue regeneration restored the integrity but was still under maintenance and maturation. This complex process, orchestrated by growth factors that largely overlaps skin repair, was described in other studies [1, 4, 14]. The corneal immune system is an important factor in wound healing and regeneration along with corneal angiogenic privileges essential for homeostasis and functiontionality. Cornea is perceived as a privileged place in this regard, but when the stimulus is strong enough, a network of signals is triggered and an immune response and blood supply is released. Our observations provided insight into the cellular events in corneal wound healing and also revealed strong corneal inflammatory reactions in one case. The incidentally made observation in our study – notable inflammatory process and well developed new vascularization in rabbit stroma, indicated the principal opportunity and capacity of the cornea to react as a consequence of immune cell function against antigens and to rule the outcome of the healing response. This confirms the possibilities for easy rejection of graft transplants or frustration of other surgical invasions, essential in ophthalmology. The epithelium normally is constantly renewing itself at every 7–10 days [4]. In our study we visualized in healing corneas adhesion and migration of superficial epithelial cells and observe the advanced formation of multilayered cell stratum covering the defects. In this population cell-related and protein-related events are involved. As it was elucidated, stem cells migrate from the limbal palisades towards the corneal center and differentiate to transient amplifying cells and basal cells to replenish the epithelium [8, 17], but except this vertical movement from deep layers to superficial layers, a centripetal migration takes place [17]. Protein-related events include the extracellular matrix and basement membrane proteins promoting the chemotactic and haptotactic migration of cells, especially fibronectin, laminin, and type IV collagen with major role as reported by Cameron et al. [5].The stroma represents tightly-packed collagen fibers organized in lamellae and arranged in right angles relative to the fibers in neighboring layers [10] and sparsely-spread resting keratocytes, secreting the collagen and proteoglycans components of the matrix. Keratocytes are the cells activated and involved in corneal repair after injury and are quickly replenished. In our case at the site of injury they restored to some extend the histoarchitecture after 3 months with the presence of occasional focuses of noncellular edema, connected with extacellular matrix transformation and not fully completed lamellar organization. This result is comparable to the reported reestablishment for at least one year of the lamellar organization of the stromal collagen across the site of the incision [9], but this remodeling process and restoration to perfect transparency can take also years [7]. In this study, the endothelium had not been directly surgically manipulated or ruptured. The endothelial capacity to preserve the barrier function and to resume the draining activity towards excessive fluids during wound healing was observed. The corneal layer of endothelium consists of a single layer of hexagonal-shaped cells which ensure corneal dehydration at about 78% and preserve from swelling in norm. These cells are situated on a basal Descemet's membrane, composed of collagen [3, 10]. Here we found focal microedema in the anterior stroma, connected with extracellular matrix events, while in the posterior near

the endothelium it was insignificant, testifying preserved postoperative desiccating functionality. In contrast, in one of the cases, we observed interlamellar edema and a lot of new intrastromal blood and lymph vessels as clinicopathological correlation during inflammation. In this particular case was found keratitis supposed to be a residual effect of external contamination. Normally, the corneal vessels are found in the limbus region, but are nonspecific for the central cornea. Only severe inflammatory conditions can result in a massive upregulation of proangiogenic growth factors overwhelming the antiangiogenic mechanisms, resulting in stromal vessels ingrowth to the center [4]. Neovasculature was accompanied by an abundance of incoming inflammatory elements, anterior and posterior corneal stromal differences in keratocyte populations and the development of fibrous tissue and disorganized lamellae in the process of restoration of the stromal defect. In this case could be seen injury responses in eye, which determine an exacerbation of the normal physiological processes, influenced by extracellular matrix proteins and growth factors, as was previously described [22]. Moreover, we observed visible layer, resembling the pre-Descemet's layer - Dua's layer discoved in 2013 by the team of Harminder S. Dua [11]. It was announced that the new layer in the human cornea supports the endothelium thus having many surgical and clinical implications. In literature such layer was not indicated in rabbit cornea, which provoked our interest in the direction of tracking more deeply the existence and histological specifics, if this layer is proved in future studies.

Conclusion

The involvement mainly of corneal epithelium, stroma and endothelium formed a complex and dynamic cascade of microevents restoring the entirety of eye cornea, but also depending on the type and strength of the injury process. Histological diversity from the intact cornea prolongs months after the invasion and could be aggravated in certain postoperative situations.

References

1. **Ahmadi, A. J., F. A. Jakobiec**. Corneal wound healing: Cytokines and extracellular matrix proteins. – *Int. Ophthalmol. Clin.*, **42**, 2002, 13-22.
2. **Albrecht, M. C**. Comparative anatomy of the optic nerve head and inner retina in non-primate animal models used for glaucoma research. – *Open Ophthalmol. J.*, **2**, 2008, 94-101.
3. **Bourne, W. M**. Biology of the corneal endothelium in health and disease. – *Eye*, **17**, 2003, 912-918.
4. **Bukowiecki, A., D. Hos, C. Cursiefen, S. A. Eming**. Wound-healing studies in cornea and skin: parallels, differences and opportunities. – *Int. J. Mol. Sci*., **18**(6), 2017, 1257.
5. **Cameron, J. D., S. T. Hagen, R. R. Waterfield, L. T. Furcht**. Effects of matrix proteins on rabbit corneal epithelial cell adhesion and migration. – *Curr. Eye Res.*, **7**(3), 1988, Published online: 02 Jul 2009, 293-301.
6. **Chan, T, S. Payor, B. A. Holden**. Corneal thickness profiles in rabbits using an ultrasonic pachometer. – *Investig. Ophthalmol. Vis. Sci*., **24**, 1983, 1408-1410.
7. **Cintron, C., H. I. Covington, C. L. Kublin**. Morphologic analyses of proteoglycans in rabbit corneal scars. – *Investig. Ophthalmol. Vis. Sci*., **31**, 1990, 1789-1798.
8. **Davanger, M., A. Evensen**. Role of the pericorneal papillary structure in renewal of corneal epithelium. – *Nature*, **229**, 1971, 560-561.
9. **Davison, P. F., E. J. Galbavy**. Connective tissue remodeling in corneal and scleral wounds. – *Invest. Ophthalmol. Vis. Sci*., **27**(10), 1986, 1478-1484.

10. **DelMonte, D. W., T. Kim T**. Anatomy and physiology of the cornea. – *J. Cataract Refract. Surg*., **37**, 2011, 588-598.
11. **Dua, H. S., L. A. Faraj, D. G. Said, T. Gray, J. Lowe**. Human corneal anatomy redefined: a novel pre-Descemet's layer (Dua's layer). – *Ophthalmology,* **120**(9), 2013, 1778-1785.
12. **Hall, P. A., F. M. Watt.** Stem cells: the generation and maintenance of cellular diversity. – *Development*, **106**(4), 1989, 619-633.
13. **Hara, H., D. K. Cooper**. Xenotransplantation – the future of corneal transplantation? – *Cornea*, **30**(4), 2011, 371-138.
14. **Imanishi, J., K. Kamiyama, I. Iguchi, M. Kita, C. Sotozono, S. Kinoshita**. Growth factors: Importance in wound healing and maintenance of transparency of the cornea. – *Prog. Retin. Eye Res*., **19**, 2000, 113–129.
15. **Korb, D. R., J. V. Greiner, T. Glonek, A. Whalen, S. L. Hearn, J. E. Esway, C. D. Leahy**. Human and rabbit lipid layer and interference pattern observations. – In: *Lacrimal gland, tear film, and dry eye syndromes* 2, Boston, MA, Springer, 1998, 305-308.
16. **Lucas, T., A. Waisman, R. Ranjan, J. Roes, T. Krieg, W. Müller, A. Roers, S. A. Eming**. Differential roles of macrophages in diverse phases of skin repair. – *J. Immunol*., **184**, 2010, 3964-3977.
17. **Nowell, C. S., F. Radtke**. Corneal epithelial stem cells and their niche at a glance. – *J. Cell Sci*., **130**, 2017, 1021–1025.
18. **Ojeda, J. L., J. A. Ventosa, S. Piedra**. The three-dimensional microanatomy of the rabbit and human cornea. A chemical and mechanical microdissection-SEM approach. – *J. Anat*., **199**(5), 2001, 567-576.
19. **Quesada, A., Y. Aguilera, R. Caparros, F.A Prada, C. Santano, R. López-López, C. Prada**. Myelin oligodendrocyte-specific protein is expressed in Muller cells of myelinated vertebrate retinas. – *J. Neurosci. Res.,* **89**, 2011, 674-688.
20. **Schlötzer-Schrehardt, U., Z. Zagórski, L. M. Holbach, C. Hofmann-Rummelt, G. O. H. Naumann**. Corneal stromal calcification after topical steroid-phosphate therapy. – *Arch. Ophthalmol*., **117**(10), 1999, 1414-1418.
21. **Sridhar, M. S.** Anatomy of cornea and ocular surface. - *Indian J. Ophthalmol*., **66**(2), 2018, 190-194
22. **Thoft, R. A., J. Friend.** The X, Y, Z hypothesis of corneal epithelial maintenance. – *Invest. Ophthalmol. Vis. Sci*., **24**(10), 1983, 1442-1443.
23. **Thomasy, S. M., V. K. Raghunathan, M. Winkler, Ch. M. Reilly, A. R. Sadeli, P. Russell, J. V. Jester, Ch. J. Murphy.** Elastic modulus and collagen organization of the rabbit cornea: epithelium to endothelium. – *Acta Biomater*., **10**(2), 2014, 785-791.
24. **Wang, X., Q. Wu.** Normal corneal thickness measurements in pigmented rabbits using spectral-domain anterior segment optical coherence tomography. – *Vet. Ophthalmol*., **16**(2), 2013, 130-134.
25. **Werner, L, J. Chew, N. Mamalis**. Experimental evaluation of ophthalmic devices and solutions using rabbit models. – *Veter. Ophthalmol.,* **9**, 2006, 281-291.
26. **Zernii, E., V. E. Baksheeva, E. N. Iomdina, O. A. Averina, S. E. Permyakov, P. P. Philippov, A. A. Zamyatnin, I. I. Senin.** Rabbit models of ocular diseases: new relevance for classical approaches. – *CNS Neurol. Disord. Drug Targets* (*formerly Current Drug Targets-CNS & Neurological Disorders*), **15**(3), 2016, 267-291.
27. **York, M., W. Steiling**. A critical review of the assessment of eye irritation potential using the Draize rabbit eye test. – *J. Appl. Toxicol*., **18**, 1998, 233-240.

Institute of Experimental Morphology, Pathology and Anthropology with Museum
Bulgarian Anatomical Society

Acta morphologica et anthropologica, 28 (1-2)
Sofia ● 2021

Structure and Innervation of the Pulmonary Neuroepithelial Bodies in Rats

Nikola Stamenov[1], Nikolai Lazarov[1,2]*

[1] *Department of Anatomy and Histology, Medical University of Sofia, Sofia, Bulgaria*
[2] *Institute of Neurobiology, Bulgarian Academy of Sciences, Sofia, Bulgaria*

***** Corresponding author e-mail: nstamenov@medfac.mu-sofia.bg

Neuroepithelial bodies (NEBs) are highly specialized clusters of cells spread in the epithelium of intrapulmonary airways. The present study aimed at the visualization and morphological description of the pulmonary NEBs. For this purpose, we used tissue slices from the lungs of 1-month-old Wistar rats stained either routinely with hematoxylin and eosin (H&E) or with the vital dye neutral red. In addition, we processed them by the histochemical NADPH-diaphorase (NADPH-d) technique to get insight on their complex innervation. The H&E staining revealed the neuroendocrine cells as visible clusters of clear cells with lucid cytoplasm. Neutral red staining visualized the NEBs as pinkish red cell clusters protruding in the airway lumen. The varicose nerve fibers innervating the neuroendocrine cells were NADPH-d-reactive. Our results show that NEBs possess distinct morphological characteristics of sensory structures which have to be further investigated neurochemically with specific markers.

Key words: neuroepithelial bodies, H&E stain, neutral red, NADPH-diaphorase, lungs, rat

Introduction

Neuroepithelial bodies (NEBs) are polymodal sensors dispersed throughout the epithelium of the intrapulmonary airways [4]. They are formed by up to 25 neuroendocrine cells with elongated shape and a cytoplasm with an abundant number of vesicles containing a variety of bioactive substances [1, 4, 5]. They include typical neurotransmitters, like acetylcholine and serotonin, and also local regulatory peptides like bombesin, calcitonin, somatostatin, etc. [4]. NEBs are dually innervated by vagal and spinal primary afferents and by postganglionic fibers from sympathetic and parasympathetic ganglia [2, 3].

Materials and Methods

For the present study we used three 1-month-old Wistar rats. The animals were bred and provided by the vivarium of the Medical University of Sofia. The experiments were performed in agreement with the European Communities Council Directive 2010/63/EU for the protection of animals used for scientific purposes and approved by the

Research Ethics Commission of the Medical University of Sofia. The rats were deeply anesthetized with an intraperitoneal injection of sodium pentobarbital (70 mg/kg) and then transcardially perfused with cold 4% paraformaldehyde. After lung removal, we prepared 6 μm thick paraffin sections and routinely stained them with H&E following a basic protocol that included dewaxing, dehydration in increasing concentrations of ethanols, staining with hematoxylin, differentiation with 0.3% acid alcohol, rinsing, staining with eosin, dehydration in ascending ethanol solutions, clearing in xylene and coverslipping in Entellan (Merck). For the staining with neutral red, the deparaffinized sections of the lungs were rehydrated and then were stained with neutral red dye for 3-4 min until desired intensity was obtained. Thereafter, they were dehydratated, cleared in xylene and coverslipped.

In addition, we prepared 20 μm thick frozen sections from the lungs with freezing microtome and processed them with the NADPH-d technique according to Scherer-Singler et al. (1983). Briefly, the sections were incubated for 30-60 min at 37ºC in a staining solution consisting of 1 mg/ml β-NADPH, 0.25 mg/ml nitroblue tetrazolium (both from Sigma), and 0.3% Triton X-100 dissolved in Tris-buffered saline (TBS), pH 7.4. After incubation, the sections were rinsed in TBS, washed in distilled water (3 × 15 min) and coverslipped in glycerol jelly. For control purposes, sections were treated in the same way with omission of the substrate from the incubation medium. No specific reactivity was observed in any of the control sections under these conditions.

Results

The H&E staining revealed the NEBs as clearly visible clusters of oval cells with lucid cytoplasm protruding into the lumen of the intrapulmonary airways (**Fig. 1**). With the neutral red staining we were able to detect the NEBs in the mucosa of the terminal bronchioles and in the alveoli as well. The NEBs were observed as intensively stained red clusters of cells (**Fig. 2**) and the apical compartments of the neuroendocrine cells protruded into the airways lumen (**Fig. 3**). After applying the NADPH-diaphorase technique we observed the presence of varicose neve fibers in the NEBs reaching and terminating on the neuroendocrine cells of the NEBs (**Fig. 4**).

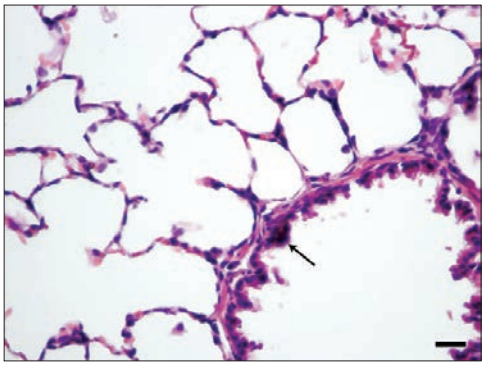

Fig. 1. Cross-section of a terminal bronchiole depicting a group of oval cells with abundant eosinophilic cytoplasm that are protruding to the airway lumen (arrow). Scale bar = 50 μm.

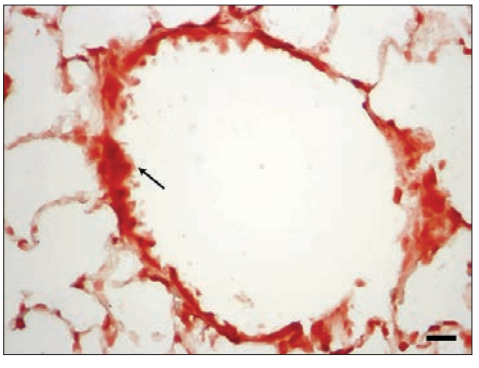

Fig. 2. A cross-sectional view of a terminal bronchiole showing a few red clusters of neuroendocrine cells forming the NEB (arrow). Scale bar = 50 μm.

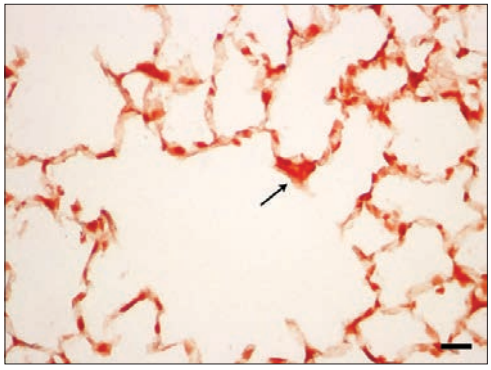

Fig. 3. A group of intensely stained neuroendocrine cells (arrow) protruding into the alveolar cavity. Scale bar = 50 μm.

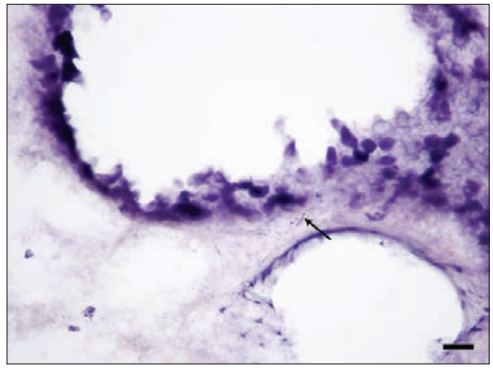

Fig. 4. NADPH-diaphorase staining demonstrating a varicose nerve fiber (arrow) innervating a protruding-like structure of weakly-stained neuroendocrine cells resembling the NEB. Scale bar = 50 μm.

Discussion

Our results support the general structural patterns of the typical sensory receptors such as the NEBs. In particular, following routine histological stainings we were able to observe clusters of neuroepithelial cells. With the NADPH-d staining we found that these cells are contacted by terminals of afferent nerve fibers. Such a location, morphology and complex innervation of the NEBs support their role as peripheral sensory receptors [3]. The peculiar positioning of NEBs within the lumen of the intrapulmonary airways implies their oxygen sensing role, which is mainly registred at the neonatal stages of the development of the lungs [5]. In adults, NEBs are considered to be important mechanical and chemical receptors which detect changes in the local chemical composition of the extracellular fluid [6].

In conclusion, NEBs possess an intricate internal structure and distinct morphological characteristics of typical sensory receptors in the lungs. Their visualization with routine histological methods is possible yet limited due to their small number and size. Moreover, NEBs could be visualized by NADPH-diaphorase technique, that makes it possible to observe the nerve fibers contacting the basal pole of neuroendocrine cells. Nonetheless, because of the lack of studies on the neurochemical patterns of NEBs under hypertensive conditions, further immunohistochemical experiments with specific markers are needed to clarify their chemical nature.

References

1. **Adriaensen, D., I. Brouns, J. Van Genechten, JP. Timmermans.** Functional morphology of pulmonary neuroepithelial bodies: extremely complex airway receptors. – *Anat. Rec. A Discov. Mol. Cell Evol. Biol.,* **270**, 2003, 25-40.
2. **Adriaensen, D., I. Brouns, I. Pintelon, I. De Proost, J. P. Timmermans.** Evidence for a role of neuroepithelial bodies as complex airway sensors: comparison with smooth muscle-associated airway receptors. – *J. Appl. Physiol. (1985),* **101**, 2006, 960-970.

3. **Brouns, I., J. Van Genechten, H. Hayashi, M. Gajda, T. Gomi, G. Burnstock, J. P. Timmermans, D. Adriaensen.** Dual sensory innervation of pulmonary neuroepithelial bodies. – *Am. J. Respir. Cell Mol. Biol.,* **28**, 2003, 275-285.
4. **Cutz, E., J. Pan, H. Yeger, N. J. Domnik, J. T. Fisher.** Recent advances and contraversies on the role of pulmonary neuroepithelial bodies as airway sensors. – *Semin. Cell. Dev. Biol.,* **24**, 2013, 40-50.
5. **Linnoila, R. I.** Functional facets of the pulmonary neuroendocrine system. – *Lab. Invest.,* **86**, 2006, 425-444.
6. **Scherer-Singler, U., S. R. Vincent , H. Kimura , E. G. McGeer.** Demonstration of a unique population of neurons with NADPH-diaphorase histochemistry. – *J. Neurosci. Methods*, **9**, 1983, 229-234.
7. **Verckist, L., R. Lembrechts, S. Thys, I. Pintelon, J. P. Timmermans, I. Brouns, D. Adriaensen.** Selective gene expression analysis of the neuroepithelial body microenvironment in postnatal lungs with special interest for potential stem cell characteristics. – *Respir. Res.*, **18**, 2017, 87.

Institute of Experimental Morphology, Pathology and Anthropology with Museum
Bulgarian Anatomical Society

Acta morphologica et anthropologica, 28 (1-2)
Sofia ● 2021

Adrenal Glands Histological Structure in Brown Bear (Ursus arctos, Linnaeus, 1758)

Emil Sapundzhiev[1], Mihail Chervenkov[1], Georgi Popov[1], Katerina Todorova[2]*

[1] Faculty of Veterinary Medicine, University of Forestry, Sofia, Bulgaria
[2] Institute of Experimental Morphology, Pathology and Anthropology with Museum, Bulgarian Academy of Sciences

* Corresponding author e-mail address: emisapun@yahoo.com

The adrenal glands exhibit species specific differences in the outer layer of the glandular parenchyma cortex where in ruminants, some laboratory animals and human the cells form glomeruli, but in carnivores, horse and pig they are arranged in arches. The purpose of this study was to examine histologically adrenal gland of a deceased adult male Brown bear during summer time and to compare its morphology with those of other domesticated animals and human. In our study we found endocrine cell clusters in the capsule of the gland which was described only in horse adrenal gland. We also established that in outer cortical zone of the adrenal glands parenchyma the cells form arches which resembled the shape and the height of the dog's glands. The remaining inner cortical zones and the medulla were situated similarly to those of the bovine, horse, pig, dog and human adrenal glands and did not show structural peculiarities.

Key words: adrenal glands, histology, bear

Introduction

The Brown bear (*Ursus arctos*, Linnaeus, 1758, subspecies *Ursus arctos arctos* distributed in Europe) belongs to class Mammalia, order Carnivora, family Ursidae, and it was classified as caniforms, or doglike carnivores [5, 7, 9]. According to the taxonomy the scientific name Ursus arctos of the Brown bear, comes from the Latin term "ursus" meaning bear, and from the Greek term for bear Άρκτος (arctos) [20]. As a wild animal it consumes a great variety of foods and fish preferentially, but also supplements its diet with fruits, vegetables and mushrooms to 90% which is the cause bears to be classified as omnivorous animals [7, 19].

The Brown bear was subjected to various genetic and ecological studies of its origin and behavior [5, 8, 12, 17, 19, 20]. In our country there are little scientific reports that are related to clinical cases and bear raising or medical treatment and legislation [1, 6, 12, 13, 16]. Furthermore, there are less morphological investigations focusing

on the specific bear organs. Therefore, after investigation of the bear stomach in our previous studies [18], we continued our research on adrenal glands morphology.

The adrenal glands are paired organs and according position of the body they are situated in the cranial topographic area of kidneys in most mammals, but in human they are in suprarenal site [9, 14]. Histologically the glandular parenchyma is composed of an outer part – cortex, derived from intermediate mesoderm and an inner or central part – medulla, derived from neural crest ectoderm. A solid capsule of a dense irregular fibrous connective tissue envelops the organ. Delicate trabeculae of loose connective tissue arising from the capsule and bringing blood vessels and preganglionic sympathetic axons, sparse the parenchyma and also form fragile membrane-like coat between cortex and medulla. The adrenal cortex architecture shows three zones which the outermost is *zona glomerulosa* (syn. *arcuata*), then the consecutive is *zona fasciculata* and the innermost is *zona reticularis*. The first zona constitutes the outer cortex and the latter two zones form the inner cortex. In some animals like uniungulates, carnivores, but usually not in ruminants, between the outer and the inner cortex exists a narrow band of polymorphic undifferentiated cells forming additional the *zona intermedia* [2, 3, 4, 10, 11, 15].

The purpose of this study was to examine histologically adrenal glands of the brown bear (*Ursus arctos*, Linnaeus, 1758) and to compare its morphology with those of other domesticated mammalian species – cattle, pig, horse, dog and comparatively with human.

Materials and Methods

The examined animal was a 32 years old, male Brown bear (*Ursus arctos*, Linnaeus, 1758) with body weight of approximately 160 kg, deceased at the The Dancing Bears Park near by Belica town, Bulgaria. The bear was autopsied at the Faculty of Veterinary medicine, University of Forestry, Sofia in summer 2019 and samples from the internal organs were collected for examination. The death was caused by a trauma received as a result of a tragic accident. The animal had no anamnestic data of other chronic illness or pathology.

Histological sections of bear adrenal gland with 7-8 μm thickness were prepared using the conventional method of formalin fixed paraffin embedded tissue [18]. After staining with hematoxylin and eosin, the slides were observed, examined and measured under light microscope Olympus, Cx 21FS1, (China) in form of optical and computerized system and finally recorded with photocamera Olympus C5050 (Japan).

Results and Discussion

Starting the investigation of the bear adrenal glands' structure, firstly the capsule was measured. Its thickness was 300±10 μm, consisted of dense irregular connective tissue layer, where clusters of endocrine polymorphic cells were found (**Fig. 1**). The same morphological characteristic was only described in the horse adrenal gland capsule [3]. The capsule of the bear adrenal gland was found to be the thickest of all investigated animal species glands and also the man.

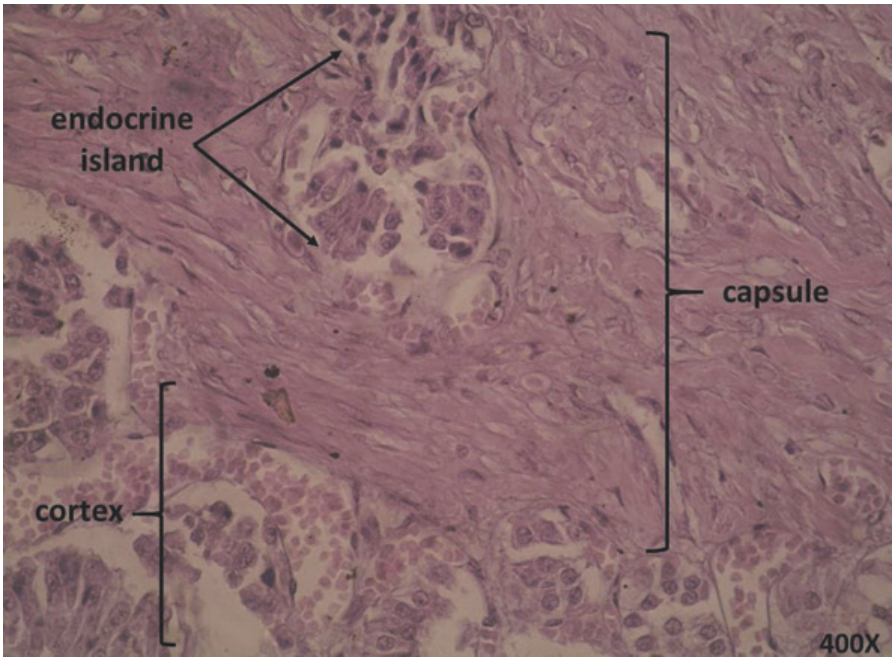

Fig. 1. Adrenal gland periphery, *Ursus arctos*. H&E.

Our study demonstrated that in the brown bear as an omnivorous animal, the outer cortical zone (za) of the adrenal gland represented arcuate type and the curves had similar shape and height as in the dog (**Fig. 2**). Arranged as arches of columnar cells, the arcuate zone (za) is the source of mineralocorticoids (aldosterone and corticosterone). The observed endocrinocytes were bipolar cells with lipid droplets at both poles. Arising from zona intermedia, the arcuate cells are differentiated and, in turn, undergo apoptosis [2, 9]. In comparison the arches are best presented in horse's, then in dog's and least demonstrated in pig's adrenal glands (**Fig. 3**).

The cells found in the fasciculate zone (zf), which produce glucocorticoids (cortisol and cortisone) were spherical, separated by sinusoids and bundled as fascicles. The reticular zone (zr) was constructed by polyhedral cells, excreting androgens, arranged in frame of anastomosing cords and plates, splitted up by large sinusoids. The intermediate zone (zi) which is established in horse adrenal gland in the examined samples from brown bear was not apparent and non-differentiated polymorphic cells were not observed.

For the purposes of comparison, bovine and human adrenal glands were also examined (**Fig. 4**). In the outer cortex *zona glomerulosa* was visible and cells arranged in convoluted and globular formations were easily differentiated. The inner cortex, which consists of two zones- fasciculate and reticular respectively, the community of cells had typical histological organization in bundles and network respectively, as described by other authors [3, 4, 11, 15].

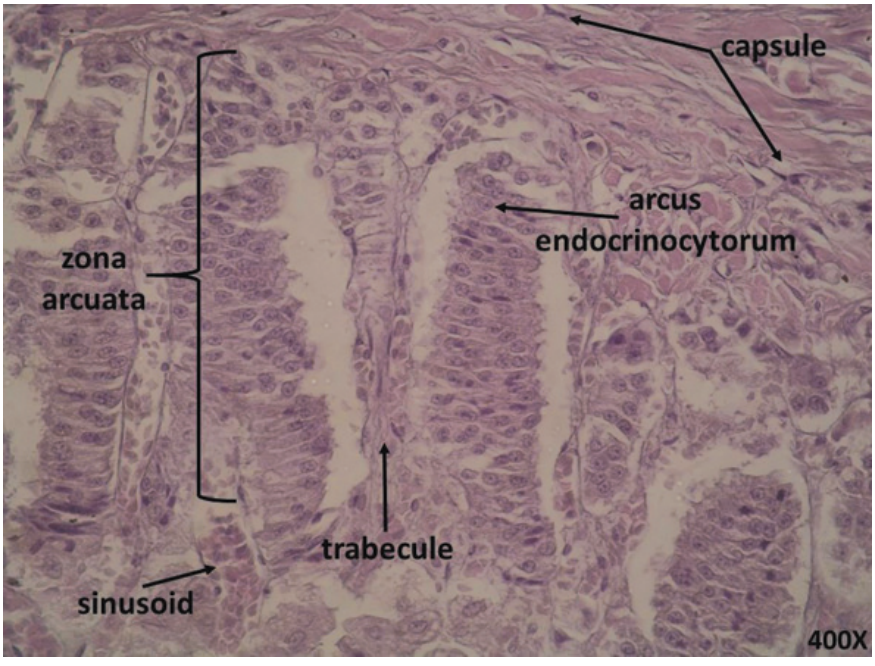

Fig. 2. Outer cortex of adrenal gland, *Ursus arctos*. H&E.

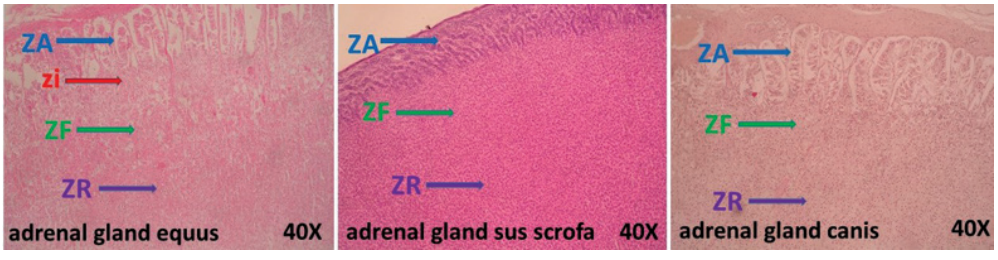

Fig. 3. Cortical zones of adrenal glands in domesticated animal species. H&E.

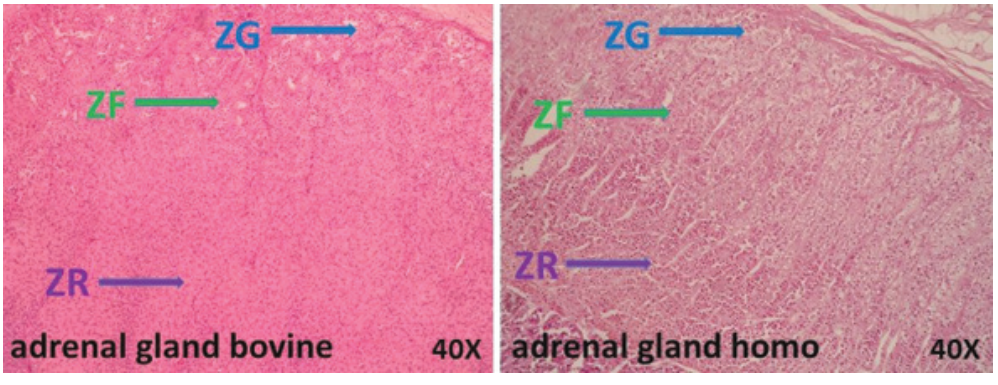

Fig. 4. Cortical zone of adrenal glands in large ruminant and human. H&E.

As norm, the medullary endocrinocytes (neuroendocrinocytes or chromaffin cells, secreting catecholamines) are derived from the embryonic ectodermal neural crests and are modified sympathetic neurons which lack axonal projections [2, 3, 4, 10, 15].

In our samples (**Fig. 5**) from brown bear's adrenal glands medulla were observed cells with classic characteristics of neuroendocrine cells too and granules were situated in poles. The endocrine cells were organized in the form of clusters (cl) separated by sinusoids (si), which were filled with blood cells. Some of the neuroendocrine cells in the parenchyma demonstrated lipid vacuolization (lv). Cells were of two types according to their specificity synthesizing epinephrine (adrenalin) or norepinephrine (noradrenalin). The epinephrocytes (epn) were larger and eosinophilic lighter rounded cells with euchromatic nucleus, while the norepinephrocytes (nep) observed were columnar cells with reddish darker cytoplasm and heterochromatic ellipsoidal nucleus.

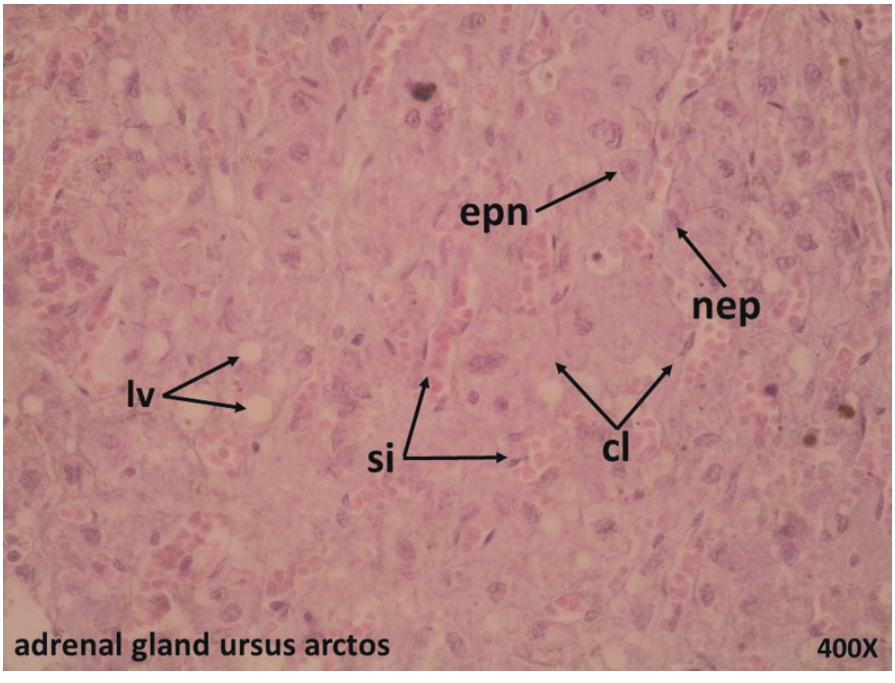

Fig. 5. Medulla of adrenal gland, *Ursus arctos*. H&E.

Conclusion

The adrenal glands in brown bear, as omnivorous mammal, have specificity in histological structure and differ from that one in human. The organ capsule was the thickest of all compared glands and presence of clusters of endocrine cells in it showed similar organization as in the horse. The arcuate zone in the outer parenchymal cortex and the alignment of endocrine cells, forming the curves was closer to dog's glandular histoarchitecture. The rest of the parenchymal zones of the cortex and the medulla were identical to those of the bovine, horse, pig, dog and human adrenal glands and did not show morphological peculiarities in their structural arrangement.

Acknowledgement: The financial support by the National Program of Ministry of Education and Science for Young Scientists and Postdoctoral investigators 2018-2020 is acknowledged.

References

1. **Aminkov, B., P. Nanev, K. Aminkov.** Radiographic findings in joint disease in three brown bears. – *J. Tradition and Modernity in Veterinary Medicine*, **3,** (4), 2018, 3-6.
2. **Aughey E., F. L. Frye.** Endocrine system. – In: *Comparative veterinary histology with clinical correlates.* (Ed. J. Northcott) Manson Publishing/The Veterinary Press, 2001, 149-166.
3. **Bacha, W. Jr., L. M. Wood.** Endocrine system. – In: *Color atlas of veterinary histology.* (Eds. W. Jr. Bacha, L. M. Wood), PA, USA, Williams & Wilkins Scientific Publishers, 1990, 177-188.
4. **Eurell, J. A. C.** Suprarenal gland. – In: *Veterinary histology* (Ed. C. C. Cann, S. S. Hunsberger, N. Giandomenico), Jackson, Wyoming Teton New Media, 2004, 34-35.
5. **Frackowiak, W.** Diet and food habits of the BrownBear (Ursus arctos L.) in the Polish eastern Carpathians. – *Journal Wild life Research,* **2,** 1997, 2,154-160.
6. **Georgiev, G. I.** Characteristic features of the skeleton in different animals **–** In:*Veterinary osteology***.** (Ed. M. Stefanova), Sofia, D. V. Disign, 2015, 144-184.
7. **Gómez, C. F. L.** Diet of bears according to carnivorous, omnivorous species. – *AlimentacionDe,* https://alimentacionde.com/reino-animal/alimentacion-de-los-osos-segun-especies/ December 07, 2020. [in Spanish]
8. **Gunchev R.** In*: Mechkata*. Nasluka Publishing, 1994, 1-77. [in Bulgarian]
9. **Hopson J. L., N. K. Wessells.** Animals: The great consumers (Ch. 24) and hormonal controls (Ch. 35) – In: *Essentials of biology* (Ed. E. Borve) McGraw-Hill Publishing Company, USA, 1990, 409-648.
10. **Hullinger, R., Q. M. Andrisani.** Endocrine system. – In: *Dellmann's textbook of veterinary histology – VI.* (Eds. H. D. Dellmann, J. A. Eurell), Ames, Iowa, USA, Blackwell Publishing, 2006, 298-319.
11. **International Committee on Veterinary Histological Nomenclature, Gent,** Systema endocrinum – *In: Nomina histologica veterinaria. splanchnologia,* 2017, 45-47.
12. **Kostov, Y., V. Alexandrova.** How to recognize (decode) animal language. – *Bulgarian Journal of Agricultural Science*, **15,** 5, 2009, 475-477.
13. **Kostov, I., Z. Shindarska, H. Neshovska.** Analysis of the implementation. of the European and national legislation in the feed manufacturing. – *International Journal of Veterinary Sciences and Animal Husbandry,* **5,** 2020, 4, 97-100.
14. **Kovachev, G., G. Georgiev, A. Vodenicharov.** Endocrine glands – In: *Anatomy of domestic animals. III,* (Ed. A. Vodenicharov), Stara Zagora, KOTA, 2019, 203-210. [in Bulgarian]
15 .**Krystev, H., S. Vitanov**. Systema endocrinum. – In: *Citologia i histologia* (Ed. G. Kondov), Sofia, Zemizdat Scientific Publishers, 1993, 347-355. [in Bulgarian]
16. **Manov, V., B. Aminkov, J. Ananiev, A. Kril, B. Nikolov, K. Aminkov.** Clinical case: neuroendocrine tumor and closed pneumothorax at dancing brown eurasian bear (Ursus arctos). – *Suppl. Proc. Sci. Conf. Tradition and Modernity in Veterinary Medicine*, 2013, 134-145. [in Bulgarian]
17. **McLellan, B. N., M. F. Proctor, D. Huber, S. Michel.** Ursus arctos (amended version of 2017 assessment). – *The IUCN Red List of Threatened Species* 2017,e.T41688A121229971.https://dx.doi.org/10.2305/IUCN.UK.
18. **Sapundzhiev, E., M. Chervenkov, Y. Iliev, S. Mustafa, M. Dimitrova.** Morphofunctional investigation of brown bear (Ursus arctus) stomach. – *Tradition and Modernity in Vet. Medicine,* **3,** 2, (5), 2018, 50-54.
19. **Vlachos, Ch., D. Bakaloudis, K. Dimitriou, D. Chouvardas.** Seasonal food habits of the European Brown bear (Ursus arctos) in the Pindos Mountains, Western Greece. – *Folia Zoologica - Praha*, **41,** 2000, 19-25.
20. **Wallace, Robert A.** The bear. In: *Biology: The world of life, 7th edition*. (Ed. G. P. Sanders), Menlo Park, CA Addison-Wesley Educational Publishers, Inc., 1997, 1-576.

Institute of Experimental Morphology, Pathology and Anthropology with Museum
Bulgarian Anatomical Society

Acta morphologica et anthropologica, 28 (1-2)
Sofia ● 2021

Urticarial Dermatitis – a Define Clinical Entity or a Predilection Histological Marker?

*Valentina Broshtilova[1,2], Mary Gantcheva[3,4]**

[1] *Department of Dermatology and Venereology, Military Medical Academy, Sofia, Bulgaria*
[2] *Department of Infectious diseases, Parasitology and Dermatovenereology, Medical University "Prof. Dr. Paraskev Stoyanov", Varna, Bulgaria*
[3] *Institute of Experimental Morphology, Pathology and Anthropology with Museum, Bulgarian Academy of Science, Sofia, Bulgaria*
[4] *Acibadem City Clinic, Mladost, Sofia, Bulgaria*

* Corresponding author e-mail: mary_gant@yahoo.com

Urticarial dermatitis is introduced as a descriptive term to correlate a specific dermal hypersensitivity reaction pattern to urticarial papules and plaques, appearing in the context of a large spectrum of inflammatory skin conditions. Despite the unspecific clinical features, urticarial dermatitis is considered distinctive pathological finding, which should be considered in all cases with a long history of refractory itch in elderly patients. Herein, we present a 73-year-old patient with a long-lasting disseminated urticarial rash, which revealed the histology features of urticarial dermatitis. The diagnosis of bullous pemphigoid was established upon direct immunofluorescence finding.

Key words: urticarial dermatitis, dermal hypersensitivity

Introduction

Excoriated urticarial papules and plaques that last more than 24 hours with the histological picture of perivascular round cell inflammatory inflammation with plenty of eosinophils in the upper dermis, are designated as urticarial dermatitis (UD) by Kossard et al. in 2006 [8]. Although the term totally corresponds to the histopathology findings of dermal hypersensitivity reaction, it requires a close clinico-pathological correlation with intensively pruritic urticarial lesions, which show pityriasiform desquamation and persist longer than 24 hours [4]. This clinical presentation is not considered specific to a certain nosology and is most commonly associated with eczema or drug-induced dermatosis [3].

Herein, we present a 73-year-old man with a history of extremely itchy urticarial papules and plaques that stay longer than 24 hours and resorb with postlesional hyperpigmented macules. The lack of pathognomic clinical signs in association with

persistent pruritus and strictly dermal histological changes coin the diagnosis of UD.

Case report

A 73-year-old Caucasian man with a 5-year history of severely itchy erythematous papules, plaques and patches disseminated on the trunk and extremities, is presented. The patient had no personal or family history of atopy or any other dermatological condition. He was treated for parasitic infestation with no therapeutic result. He claimed to have no effect on topical corticosteroids, peroral antihistamines and leukotriene antagonists. Physical examination revealed good general health with no concomitant diseases and medications. Multiple erythematous urticarial papules and plaques, excoriations and eczematous lesions were disseminated on the lateral aspects of the trunk and dorsal extremities. Elevated dermographism was demonstrated. The clinical suspicion encompassed chronic contact eczema, autoimmune bullous dermatosis, spontaneous urticaria, unrecognized drug eruption, and viral exanthema. Since the erythematous wheals lasted more than 24 hours, all urticarial-like dermatoses such as urticaria-vasculitis and Schnitzer syndrome, were also considered. Histological analysis showed intact epidermis with slight papillary edema, mild perivascular lymphocytic infiltrate with many interstitial eosinophils in the superficial dermis (**Fig. 1, Fig. 2**).

The eczematous skin lesions in association with dermal hypersensitization and the lack of epidermal histopathological changes constellated UD. In order to further verify the underlying dermatological condition a direct immunofluorescence was performed, which showed linear IgG and C3 (**Fig. 3**) deposits on the dermal-epidermal junction. The patient was recognized as an urticarial, pre-bullous form of pemphigoid and put on pathogenetic therapy. Full remission was achieved a month later.

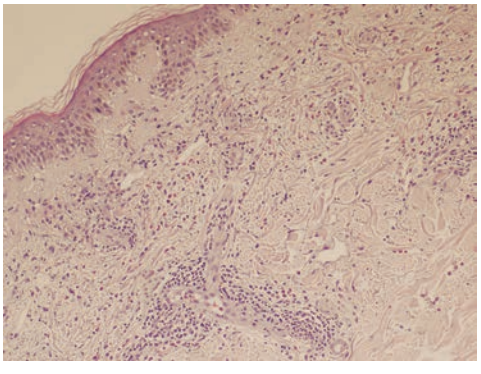

Fig. 1. Hyperkeratosis, intact epidermis, mild perivascular lymphocytic infiltrate and abundance of eosinophils in the interstitium of the papillary dermis (hematoxylin and eosin staining × 200).

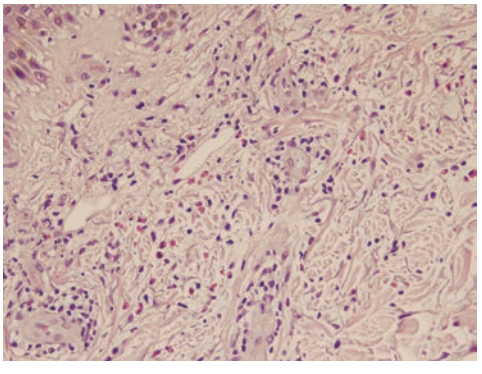

Fig. 2. Edematous papillary dermis with a lot of eosinophils gathered around the dilated capillary loops and intermixed with lymphocytes along the collagen bundles in the upper dermal segment (hematoxylin and eosin staining, × 400).

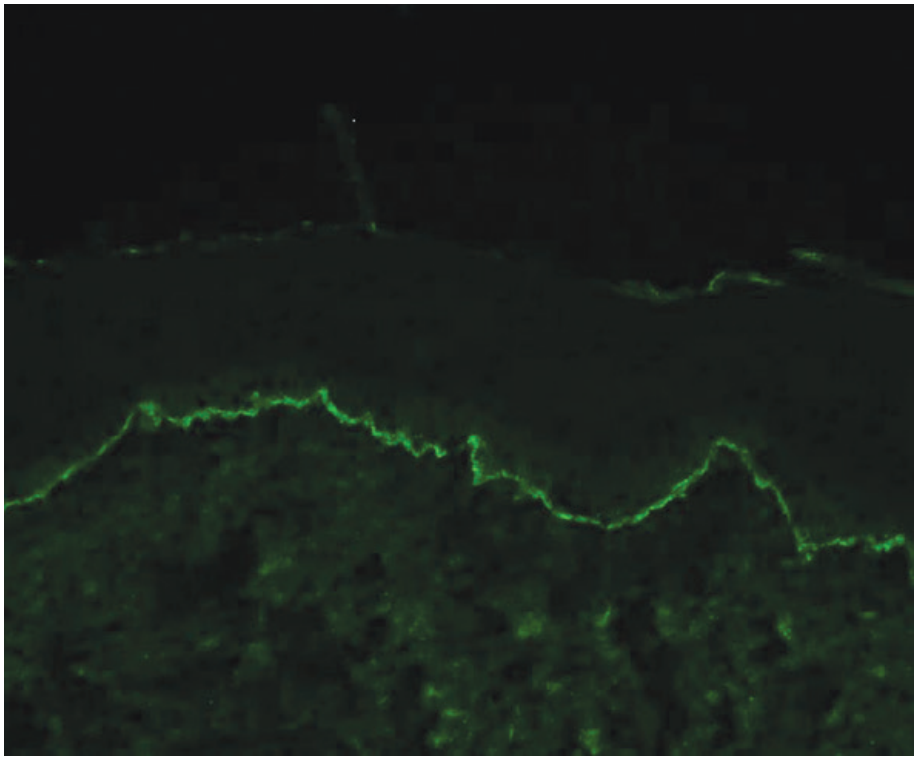

Fig. 3. Linear C3 deposits on the dermal-epidermal junction (direct immunofluorescence, × 100)

Discussion

UD is a term, introduced to encompass a group of skin diseases that have similar clinical and histological features. The original description classified most of these cases as drug-induced or eczematous, while later studies demonstrated more idiopathic origin [5]. The clinical presentation is polymorphous, interacting specific urticarial lesions with lichenifications and excoriations, typical for eczema. These second type of skin changes may result from diffuse xerosis, which usually affects the predilected age group of elderly patients, who are commonly co-morbid and take a lot of concomitant medications and home remedies to relief itch. Dermographism is more common in chronic urticaria and drug-induced dermatoses, however, it may sometimes correspond to blistering dermatoses, as in our case.

Some histopathological clues may facilitate the clinical diagnosis, especially in the initial stages of the disease. It has been well-documented that mild spongiosis and horizontal parakeratosis is more suggestive of contact dermatitis. Tortuous capillaries in the subepidermalspace and lymphocytic exocytosis constitute viral infection, while papillary edema is more common in chronic urticaria and drug reactions [8]. Dermal fibrosis and eosinophilic exocytosis is seen in subacute prurigo. It is always advisable to conduct a direct immunofluorescence study to rule out a pre-bullous stage of subepidermal autoimmune bullous dermatosis.

The pathogenesis of UD is not clearly understood. A dominant T helper inflammatory profile is suspected to enhance production of IL-4 and especially IL-5, which activate eosinophil synthesis and tissue infiltration [9]. Some physical triggers such as mechanical friction and solar exposition can serve as inductors, too. Recent studies demonstrated that nerve fibers often penetrate into the epidermis of patients with atopic dermatitis, thus stimulating IL-13 production from keratinocytes to induce metalloproteinase-9 and degrade collagen type IV [7]. In contrast, basal membrane in UD is intact and shows no changes on special stains, indicating that only the dermal hypersensitivity inflammatory pattern plays a causative role in itch induction.

No specific therapeutic options for UD exist. Since the exact etiology and pathogenetic pathway is obscure, only symptomatic treatment is introduced. Topical corticosteroids, calcineurin inhibitors and emollients together with itch-relieving agents (antihistamines, gabapentin) and phototherapy modalities are partially effective [1]. Anecdotal reports reveal good results by pathogenetic immunosuppressive therapy with azathioprine, cyclosporine, mycophenolate mofetil, hydroxyurea, and dapsone [2, 6].

UD manifests with clinical features of a broad spectrum of skin diseases triggered by a similarpatho-physiological mechanism. A thorough work-up and often a long-term follow-up is needed to establish the final diagnosis since the skin changes can mimic a plethora of dermatological conditions, which only feature dermal hypersensitivity reaction pattern. UD is considered a descriptive term to embrace various clinical scenarios that often require more sophisticated laboratory investigations and an extensive monitoring of the patients.

References

1. **Banan, P., G. Butler, J. Wu.** Retrospective chart review in a cohort of patients with urticarial dermatitis. – *Australas J. Dermatol*., **55**, 2014, 137-139.
2. **Chaptini, C., S.Sidhu.** Mycophenolate mofetil as a treatment of urticarial dermatitis. – *Australas J. Dermatol*., **55**, 2014, 275-278.
3. **Fung, M.** The clinical and histopathological spectrum of "dermal hypersensitivity reactions" – a nonspecific diagnosis that is not very useful in clinical practice, and a concept of "a dermal hypersensitivity reaction pattern". – *J. Am. Acad. Dermatol.,* **47**, 2002, 898-907.
4. **García del Pozo, M., I. Poveda, P. Álvarez, J. Silvestre.** Urticarial dermatitis. A cutaneous reaction pattern. – *Actas Dermosifiliograf*, **109**, 2018, 929-932.
5. **Hannon, G., D. Wetter, L. Gibson**. Urticarial dermatitis: Clinical features, diagnostic evaluation, and etiological associations in a series of 146 patients at Mayo Clinic (2006-2012). – *J. Am. Acad. Dermatol*., **70**, 2014, 263-268.
6. **Kim, J., K. Lim, H. Kim, H. Ko, M. Kim, B. Kim**. Urticarial dermatitis: Clinical characteristics of Itch and therapeutic response to cyclosporine. – *Annal. Dermatol.,* **29**, 2017, 143.
7. **Kim, T., H. Park, Y. Won, H. Choi, K. Jeong, J. Sung, M. Shin.** Basement membrane status is intact in urticarial dermatitis vs. adult-onset atopic dermatitis. – *Annal. Dermatol*., **30**, 2018, 258.
8. **Kossard, S., I. Hamann, B. Wilkinson**. Defining urticarial dermatitis. A subset of dermal hypersensitivity pattern. – *Arch. Dermatol*., **142**, 2006, 29-34.
9. **Thepen, T., E. Langeveld-Wildschut, I. Bihari, D. van Wichen, F. van Reijsen, G. Mudde, C. BruijnzeeI-Koomen**. Biphasic response against aeroallergen in atopic dermatitis showing a switch from an initial TH2 response to a TH1 response in situ: An immunocytochemical study. – *J. Allergy Clin. Immunol*., **97**, 1996, 828-837.

Institute of Experimental Morphology, Pathology and Anthropology with Museum
Bulgarian Anatomical Society

Acta morphologica et anthropologica, 28 (1-2)
Sofia ● 2021

Eosinophilic Metaplasia in Benign Breast Epithelium: a Case Report

Desislava Bozhkova[1,2]

[1] *Department of General and Clinical Pathology, Medical University – Plovdiv, Bulgaria*
2 Department of General and Clinical Pathology, University Hospital Kaspela, Plovdiv, Bulgaria

***** Corresponding author e-mail: desislava_lapteva@abv.bg

The aim is to present an extremely rare epithelial lesion of the breast with detailed description of its immunophenotype. A 73-year-old woman with invasive ductal carcinoma with conventional intralobular hyperplasia without atypia demonstrated a massive diffuse, PAS-D positive, granular eosinophilic transformation of the cell cytoplasm. The lesion was assessed as eosinophilic (acinar) metaplasia and showed a phenotype, proving its mammary origin. In addition, the eosinophilic and granular cytoplasm was MUC1 positive, similar to prostatic eosinophilic metaplasia. The data in the literature were compared with the presented unique finding in diagnostic and differential diagnostic aspects.

Key words: breast, eosinophilic metaplasia, acinar metaplasia, MUC1.

Introduction

Metaplasia is a process, representing the transformation of one tissue into another, related to the first (initial) one [10]. Such conversion is possible only between tissues originating from a single embryonic layer. Metaplasia is a sign of tissue adaptation towards changed conditions or requirements to them.

Only a few cases of eosinophilic metaplasia (EM) in the breast have been described in the English literature so far [1]. The authors call them Paneth cell like changes or acinar cell differentiation (metaplasia) and are found mainly in tumor mammary epithelium [1,6]. From the described in the literature cases, only one concerns intraductal hyperplasia without atypia in which granular eosinophilic transformation of the cellular cytoplasm is observed. In this case, both extensive expression of lysozyme and the presence of multiple zymogenic granules ultrastructurally confirm the acinar cell-like phenotype [6].

A case of EM in a non-tumor mammary parenchyma, adjacent to ductal carcinoma is presented.

Case report

Surgical specimen from partial right mastectomy of 73 year-old woman was observed. Histological investigation showed an invasive ductal carcinoma (NOS) with size of 8 mm, grade II according to Elston & Ellis grading system, pT1b, negative sentinel lymph nodes (TNM 2017). It is combined with ductal carcinoma *in situ* in the right breast with size of 8 mm, with low grade. As an accompanying lesion in both breasts, a fibrocystic mastopathy with and without atypia was also observed.

EM was found in foci of fibrocystic mastopathy without atypia. It was presented by well-defined benign lobules, adjacent to the tumor parenchyma. Hyperplastic benign lobular epithelium was polygonal in shape and with abundant cytoplasm, filled with eosinophilic cytoplasmic granules (**Fig. 1**). The granules were round in shape, measuring 2 to 5μm and filled the entire cellular cytoplasm (**Fig. 2**). The nuclei were centrally located, with no evidence of cellular atypism, with small, non-prominating nucleoli and without mitoses (**Fig. 2**). Eosinophilic secretion was observed in the lumens of the acini (**Figs. 1 and 2**).

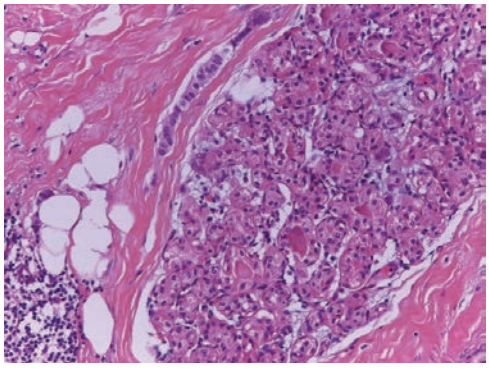

Fig. 1. EM in benign hyperplastic mammary lobule in the context of chronic inflammation (at the bottom left) and carcinoma (at the top left – lymphatic tumor embolus). HES, 200.

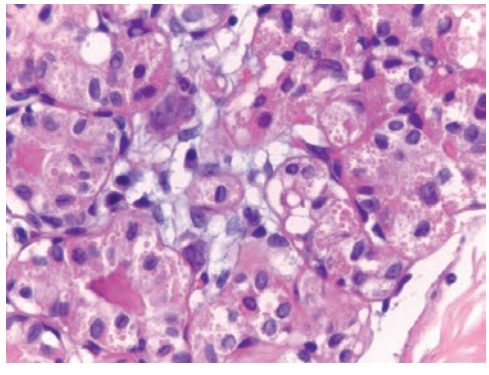

Fig. 2. EM in benign hyperplastic mammary lobule on higher microscopic magnification. HES, ×630.

Histochemically, with staining of periodic acid-Schiff reaction (PAS) and PAS-D – periodic acid-Schiff reaction with diastase, the granules showed a non-constant weak positive reaction (**Fig. 3**).

Immunihistochemically, the granules were GATA-3, estrogen and progesteron receptors (ER and PR) positive (**Figs. 4-6**). They were also cytokeratin 7 positive and Her2 negative (data not shown). Eosinophilic cytoplasmic granules were positive for epithelial membrane antigen (EMA or MUC1) (**Fig. 7**). The surrounding context was of chronic inflammation (**Fig. 1**).

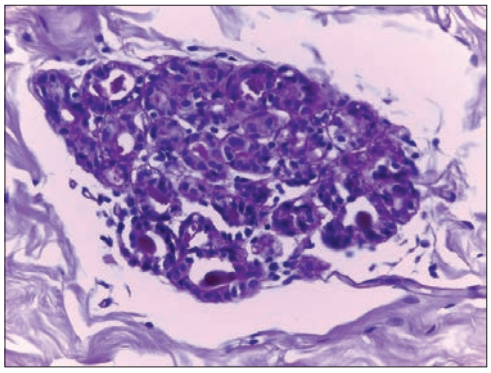

Fig. 3. Weak to moderate PAS-D positivity of EM. PAS-D, ×400.

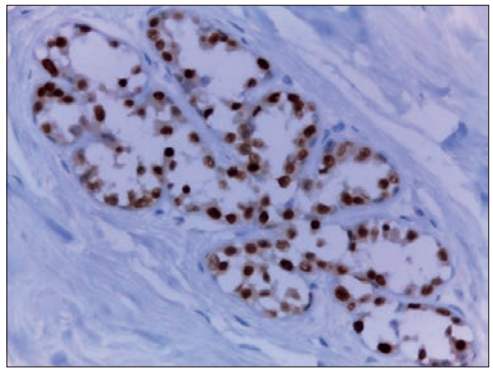

Fig. 4. Pronounced nuclear immunostaining of EM-epithelium for GATA3 in favor of mammary phenotype. Immunohistochemistry, GATA3, ×400.

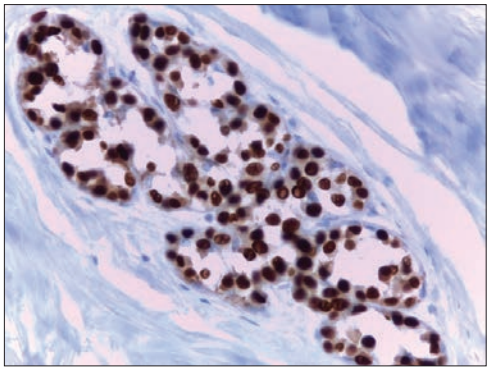

Fig. 5. Pronounced nuclear immunostaining of EM-epithelium for ER in favor of mammary phenotype. Immunohistochemistry, ER, ×400.

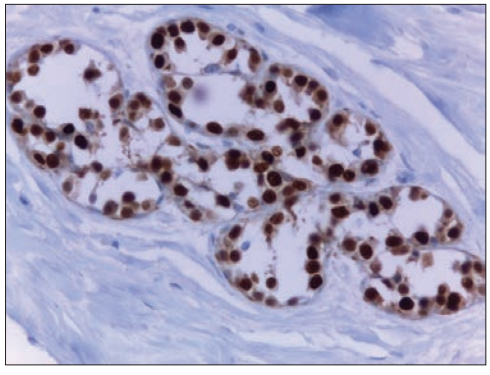

Fig. 6. Pronounced nuclear immunostaining of EM-epithelium for PR in favor of mammary phenotype. Immunohistochemistry, PR, ×400.

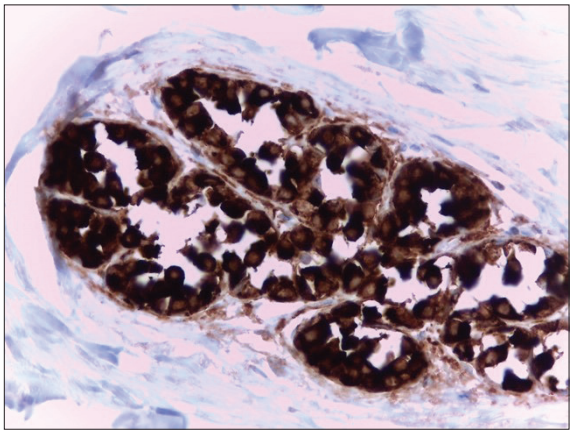

Fig. 7. Pronounced cytoplasm immunostaining of EM-epithelium for MUC1. Immunohistochemistry, MUC1, ×400.

Discussion

EM represents the presence of different in size, intensivelly eosinophilic intracytoplasmic granules in benign epithelium [7]. The process is described in a number of glandular organs and mucus membranes – uterine endometrium [12], prostate [1,14] and breast [6]. EM is a phenomenon in which the glandular epithelium is replaced by another similar type of epithelium, which is either not found or is very rarely observed in normal glands. From all organs, the process in the prostate gland has been studied in most details. In this organ, EM is represented by secretory cytoplasmic granules with both exocrine and lysosomal character [7]. These granules have different size and mainly ductal localization [9]. Eosinophilic cytoplasmic granules in prostatic EM express MUC1, which can serve as a reliable immunohistochemical marker for the EM phenotype [8]. From a general pathological point of view, prostate EM is an indirect (phenotypic type) metaplasia [7]. EM in the prostate is accompanied by banal or granulomatous chronic inflammation [3] and prostate adenocarcinoma [4].

It is well known that breast and salivary gland tissues share embryologic similarities. Similar to the salivary glands, the breast has modified sweat or apocrine glands, and some tumors arising in the breast are subject of development of salivary type tumors, such as pleomorphic adenoma, adenoid cystic carcinoma, adenomyoepithelioma and acinar cell carcinoma (ACC) [5]. Matoso et al. emphasized that breast tumors with salivary gland differentiation originate from a malignant transformation of terminal duct-lobular units with metaplastic changes. Furthermore, the immunohistochemical profile of the tumor is identical to the salivary ACC. The significance of acinar cell differentiation in breast carcinomas is not clear [11].

Most of the described cases with such changes were of acinar cell carcinoma or lesions, associated with micronodular adenosis. ACC of the breast with features of acinar-type differentiation was first described by F. Roncaroli et al. in 1996 as the breast counterpart of identical tumors of the parotid gland [13]. This carcinoma shows diffuse infiltrative growth pattern of small glandular structures and is composed of cells with a coarse glanular or clear cytoplasm resembling acinar cells of the salivary glands or Paneth cells. Histologically small acinar or glandular structures mixed with solid nests are seen. Most of the tumor is comprised of monotonous round cells with a finely granular, weakly eosinophilic or clear vacuolated cytoplasm resembling acinar cells of the salivary glands. Morphologically distinct cells show dark eosinophilic granules, resembling Paneth cells. The lumen of some small acinar or glandular structures contains red colloid-like material and microcalcifications. Other solid nests, similar to *in situ* carcinoma and invasive ductal carcinoma are focally observed. These large solid tumor nests revealed central comedo-like necrosis, reminiscent of ductal carcinoma *in situ* and were originally interpreted as an "ordinary" invasive ductal carcinoma (similar to another case of invasive ductal breast carcinoma with acinar cell metaplasia descriped in the literature), but these cells are cytologically and immunohistochemically closely similar to typical acinar cells [13]. Peridic acid-Schiff (PAS) stain demonstrates strong staining of cytoplasmic granules with diastase resistance. Immunohistochemically, both the glandular and solid tumor cell populations are strongly positive for lysozyme, a-1-antitrypsin an MUC1. Intense expression with E-cadherin and focal cytoplasmic positive reaction for S-100 protein are demonstrated. Chromogranin is also expressed focally in the areas of the granular acinar cells. Focal neoplastic cells are weakly positive for cytokeratin 7, compared to a strongly

positive reaction in normal ducts and lobules. The other areas are negative for estrogen receptor, progesterone receptors, GCDFP 15, cytokeratin 20, MUC2, MUC5A, MUC6, neuron specific enolase, CD68, smooth muscle actin, and human epidermal growth factor receptor-2 (HER2 / neu) [1, 13].

Electron microscopy, performed on formalin-fixed tissue, demonstrates numerous variable sized electron dense granules in the cytoplasm, which are consistent with zymogenic granules [1,13].

Damiani et al. investigated acinar cell differentiation in salivary gland tumors and defined the presence of zymogen-type granules. Zymogen is only one of the components in ACC, as amylaze, lysozyme and a1-antichymotrypsin are also constituents of salivary gland acinar cells. They found amylaze expression in all breast tumors, as well as in all cases of ACC of the studied parotid glands. Amylaze expression was negative in "ordinary" breast carcinomas. [2].

In the presented case EM was localized in hyperplastic benign mammary epithelium and the results showed that similar to the prostate EM [8], EM in benign mammary epithelium was PAS-D+/MUC1+. In adition, in the presented case, the immunihistochemical study showed an organ-specific mammary phenotype: GATA3+/ck7+/RO+/RP+/Her2-. Cytoplasmic granules in EM are negative with PS-100 staining [14], while in apocrine metaplasia a moderate staining is observed [1]. Immunohistochemical staining with GCFP15 is found in areas with apocrine metaplasia [1]. These results can also be used in the differential diagnosis with salivary-gland type differentiation in the conventional ductal hyperplasia or malignancy of the breast.

Conclusion

Similarly to prostate and endometrium, EM in the breast can be observed in benign hyperplastic and neoplastic epithelium, where they may be associated with other types of epithelial metaplasias [1, 4, 5]. The presented observation is the first detailed immunohistochemical study of the phenotype of EM in benign mammary epithelium. EM in the breast may be part of a benign hyperplastic lesion and accompany mammary carcinoma.

References

1. **Chang, E. D., E. J. Lee, A. W. Lee, J. S. Kim, C. S. Kang.** Primary acinic cell carcinoma of the breast: a case report with an immunohistochemical and ultrastructural studies. – *J. Breast Cancer*, **14**, 2011, 160-164.
2. **Damiani, S., G. Pasquinelli, J. Lamovec, J. L. Peterse, V. Eusebi**. Acinic cell carcinoma of the breast: an immunohistochemical and ultrastructural study. – *Virchows Arch*., **437**, 2000, 74-81.
3. **Dikov, D. I., M. S. Koleva, J. F. Boivin, T. Lisner, V. T. Belovezhdov, V. Sarafian.** Histopathology of nonspecific granulomatous prostatitis with special reference to eosinophilic epithelial metaplasia: Pathophysiologic, diagnostic and differential diagnostic correlations. – *Indian J. Pathol. Microbiol.*, **63**(Supplement), 2020, S34-S40.
4. **Dikov, D. I., M. S. Koleva, Z. K. Peshev, V. T. Belovezhdov.** Nonspecific granulomatous prostatitis in association with eosinophilic epithelial metaplasia and prostatic adenocarcinoma. – *Indian J. Pathol. Microbiol.,* **60**, 2017, 409-411.

5. **Foschini, M. P., T. Krausz.** Salivary gland-type tumors of the breast: a spectrum of benign and malignant tumors including "triple negative carcinomas" of low malignant potential. – *Semin. Diagn. Pathol.,* **27**, 2010, 77-90.
6. **Kinkor, Z., A. Skálová.** Acinic cell-like differentiation in invasive ductal carcinoma and in ductal hyperplasia of the breast-report of two cases. – *Cesk Patol.*, **41**, 2005, 29-33.
7. **Koleva, M.** Eosinophilic metaplasia in prostatic epithelium: main characteristics, morphology, morphogenesis. *PhD thesis*, Medical University-Plovdiv, 2020, 7-80 pp.
8. **Koleva, M, D. Dikov, V. Belovejdov, V. Sarafian**. Expression of MUC1 in eosinophilic metaplasia of the prostate. – *Prostate,* **79**, 2019, 622-627.
9. **Koleva, M. S., D. I. Dikov, V. T. Belovezhdov, V. Sarafian**. Eosinophilic metaplasia in transurethral resection of the prostate. – *Indian J. Pathol. Microbiol.,* **63**, 2020, 423-426.
10. **Lugo, M., P. B. Putong**. Metaplasia. An overview. – *Arch. Pathol. Lab. Med*., **108**, 1984, 185-189.
11. **Matoso, A., S. E. Easley, D. R. Gnepp, S. Mangray**. Salivary gland acinar-like differentiation of the breast. – *Histopathology,* **54**, 2009, 262-263.
12. **Moritani, S., R. Kushima, S. Ichihara, H. Okabe, T. Hattori, T. K. Kobayashi, S. G. Silverberg.** Eosinophilic cell change of the endometrium: a possible relationship to mucinous differentiation. – *Mod. Pathol.,* **18**, 2005, 1243-1248.
13. **Roncaroli, F., J. Lamovec, A. Zidar, V. Eusebi**. Acinic cell-like carcinoma of the breast. – *Virchows Arch.,* **429**, 1996, 69-74.
14. **Weaver, M., F. Abdul-Karim, J. Srigley, D. Bostwick, J. Ro, A. Ayala**. Paneth cell-like change of the prostate gland. A histological, immunohistochemical, and electron microscopy study. – *Am. J. Surg. Pathol.,* **16**, 1992, 62-68.

Institute of Experimental Morphology, Pathology and Anthropology with Museum
Bulgarian Anatomical Society

Acta morphologica et anthropologica, 28 (1-2)
Sofia ● 2021

Unusual Cause of Death in a Patient with COVID-19

Natasha Davceva[1,2,3], Ana Ivceva[1], Katerina Tosevska-Trajkovska[4], Jasar Dzengis[5]

[1] *Institute of Forensic Medicine and Criminalistcs, Faculty of Medicine, University "Ss Cyril and Methodius" Skopje, Republic of North Macedonia*
[2] *Faculty of Medical Sciences, University Goce Delcev Stip, Republic of North Macedonia*
[3] *Faculty of Medicine, University of Maribor, Republic of Slovenia.*
[4] *Institute of Medical and Experimental Biochemistry, Faculty of Medicine, University "Ss Cyril and Methodius" Skopje, Republic of North Macedonia;*
[5] *Acibadem Sistina hospital Skopje; Faculty of Medical Sciences, University Goce Delcev Stip, Republic of North Macedonia.*

* Corresponding author e-mail: drdavcevamk@yahoo.com

This is a case presentation of a patient with confirmed coronavirus disease (COVID-19) who ended his life with suicide by hanging. We are presenting the history of the disease, a clinical feature, the onset of the psychiatric symptoms and finally the pathological feature. Aims are: to perceive, in which phase of the disease occurred the psychiatric symptoms and eventually their connection with some morphological feature of the brain; to evaluate the changes of the primary disease to internal organs and finally, the ethical aspect i.e. how are these patients protected by the health care system. Results: patient committed suicide on the 12th day of the disease and around the 21st day after the infection, looking by its serum antibodies. On lungs dominated the picture of acute restrictive pulmonary disease and ARDS (acute respiratory distress syndrome) with strong inflammatory answer. A psychiatric disorder occurred with the epilog of double suicide attempt, of which the second one was successful.

Key words: COVID-19, suicide, psychiatric disorder, ARDS

Introduction

Of imminent importance and the main aim of this report is to present, in which phase of the disease occurred the onset of the psychiatric symptoms, in a person with no previous history of psychiatric illness, and if there has been found some morphological feature of the brain, underlining these symptoms. A wide discussion exists between medical professionals about that, if COVID-19 is causing some neurological and psychiatric disturbances, which are actually connected with some morphological manifestation of the disease on the CNS (central nervous system) [8, 9].

The second aim of this paper comes out by the fact that, the patient didn't die due to COVID-19 itself, but died of a violent death, which in turn has been found as a

special challenge during the examination of the internal organs. We expected to see the typical pathological feature of a developed COVID-19 disease, often described before [3, 5, 8,14] with no feature characteristic for the terminally ill patients, which more or less can mask and mimic the feature of the primary disease.

Finally, one of the important aspects of this paper is the ethical one. Are COVID patients protected enough by the health care system, having in regard the pretty diverse and still very unknown, in fact not explored enough yet, clinical manifestation of this disease.

Material and Methods

Presentation of the case

By the order of the public prosecutor, a body of a 39 years old man has been admitted to the Institute of forensic medicine for forensic autopsy, because of the obviously violent death i.e. suicide by hanging. During the collection of the data before the autopsy, we realized that the deceased was confirmed COVID-19 patient, who was receiving medical treatment for the disease. In fact, as shown by the records, death by suicide occurred 12 days since the beginning of the illness.

History of the illness

Day 1 (12 days before death). The illness has started with mild to moderate symptoms: raised temperature to 38°C, feeling of exhaustion and muscle pain. After two to three days he was advised by his family doctor to make PCR COVID-test.

Day 5 Patient had problems to schedule for a PCR-test in his own city (he was living in the capital city), so he decided to make test in the city about 40 km far from the capital. He signed the statement that from the moment of giving material for testing, he is going to be in self-isolation.

Day 7 Still waiting for the result from the SARS CoV-2 molecular biology testing, the patient decided to visit the City hospital, one of the three centers for COVID-19 in the capital city. By that time, he developed respiratory symptoms, difficulty breathing, feeling of chest pressure and also loosing of the sense for smell and taste.

During his first admission to the City-hospital in the early hours of the day 7, patient has not been hospitalized, even the fact that he had positive radiological feature (bilateral pulmonary inhomogeneous consolidations in middle and basal parties, phrenic-costal sinuses free of liquid) and the CRP (C-reactive protein) of 97,5, the body temperature of 37,4ºC and saturation O_2 of 96%. With the prescribed therapy (paracetamol, azythromycin, anticoagulants, vitamin C and probiotics) he was released for home treatment.

Meanwhile, he received positive result for SARS CoV-2, when, by the words of his wife, parallel to his breathing symptoms, he started to develop psychiatric symptoms like feeling very much scared, restless and with difficulty sleeping.

In the late hours on the day 7, the patient attempted his first suicide, by injecting himself subcutaneously a poison (some grass drying substance used in the agriculture), for what he has been admitted to the toxicology clinic, from where was readmitted to the COVID centre, and then was released home with an advice to consult the toxicology

clinic if symptoms of intoxication occur. This moment, by the records, saturation O_2 was 95%, body temperature was 38ºC and blood pressure was 110/70.

Day 11 With the ambulance the patient has been urgently admitted to the COVID center because of developing symptoms of extreme psychomotor tension, anxiousness, sleeplessness and black thoughts. A psychiatric therapy has been prescribed (amp. Diazepam 10 mg for acute treatment and then: risperidone, escitalopram, biperidone and zolpidem) and the patient has been released at home again.

Day 12 In the early morning hours, several hours after his last visit to the hospital, the patient committed a suicide by hanging.

Results

Autopsy finding

On autopsy we found a body of a 39 years old male, with regular osteomuscular constitution.

During the external examination dominated a feature of an asphyxiation death: subconjuctival hemorrhages, cyanosis, and the hanging mark in the neck region.

During the examination of the internal organs, some specific signs of inflammation of the pharynx, larynx and trachea haven't been found except some petechial hemorrhages of the tracheal mucosa (**Fig. 1a**).

The lung finding was rich. Lungs have been voluminous, heavy and full of liquid, especially in the down and back parts and with compensatory hyperinflation in the upper parts. The lung tissue has been found as colorful, consolidated, and solid by its consistence. In the basal parts there have been zones of whitish color and like rubbery consistence and a lot of spot bleedings on the cut surface (**Fig. 1b, c**). Effusion of liquid hasn't been found in the pleural and pericardial cavity, but a fibrin adhesion has been found on the pleura of the left lung and on the epicardium.

No specific feature on the other internal organs, except the dark-colored kidneys and congestion of the internal organs as non-specific but typical signs of asphyxiation.

Hanging has been established as a cause of death.

Fig. 1a

Fig. 1b

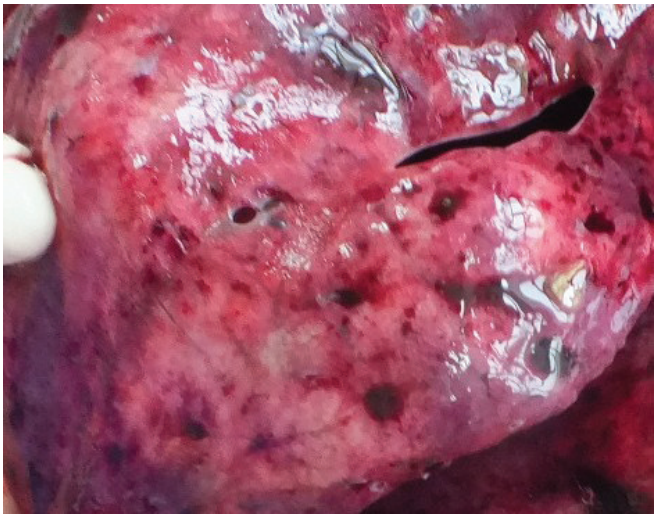

Fig. 1c

Fig. 1. Findings of the examination of internal organs: **a.** spot bleedings of the tracheal mucosa; **b.** the appearance of lungs (voluminous, heavy and full of liquid); **c.** on cut surface tissue was colorful, consolidated, and solid by its consistence, with zones of whitish color and a lot of spot bleedings between.

Histopathology

A significant pathohistological feature has been found on lungs presented as diffuse alveolar damage. There have been found zones of the consolidation of the lung tissue and next to them zones of hyperinflation, probably compensatory (**Fig. 2a**). It has been found the exudative phase of ARDS (acute respiratory distress syndrome), with diffuse alveolar damage, edema and cellular infiltration with leukocytes, lymphocytes and also desquamated pneumocytes (**Fig. 2b**). Also, the presence of the pulmonary micro

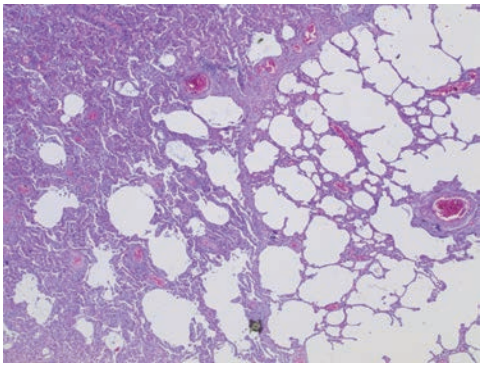

Fig. 2a

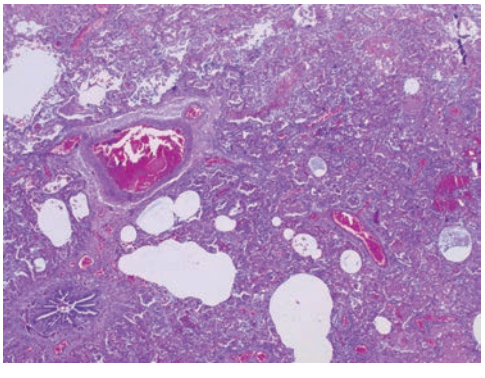

Fig. 2b

thrombi inside the blood vessels has been documented (**Fig. 2c**). Additionally, in some parts were seen signs of a transition to proliferative phase with the pneumocytes type 2 hyperplasia and zones of the organization (**Fig. 2d**).

No specific feature has been found to the other organs. Special attention has been paid to the brain tissue, where some signs of hypoxia have been found, but very unsure if they were result of the primary COVID disease or of the asphyxiation that has been found as the cause of death.

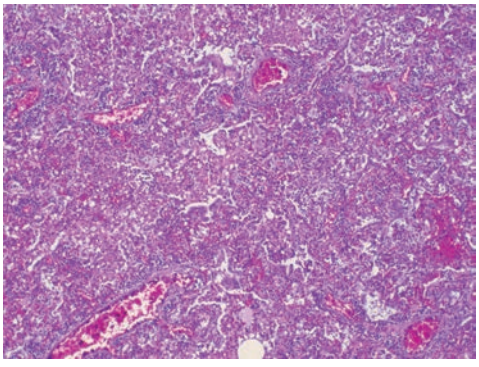

Fig. 2c

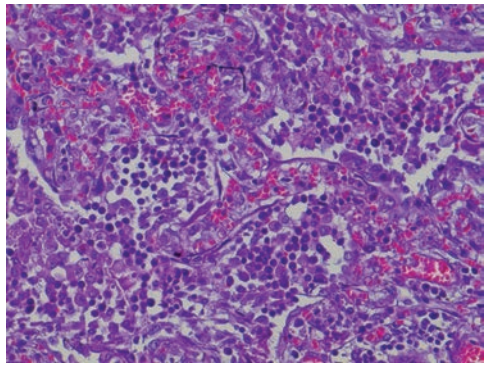

Fig. 2d

Fig. 2. Histopathology of lungs presented as diffuse alveolar damage: **a.** consolidation zones of the lung tissue and next to them zones of hyperinflation, probably compensatory; **b.** exudative phase of ARDS, with diffuse alveolar damage, edema and cellular infiltration with leukocytes, lymphocytes and also desquamated pneumocytes; **c**. the presence of the pulmonary microthrombi inside the blood vessels; **d.** in some parts were seen signs of a transition to proliferative phase with the pneumocytes type 2 hyperplasia and zones of the organization.

Laboratory findings

Intravital laboratory findings (received by medical records)

Day 7 laboratory results: CRP of 97,5; LDH (lactate dehydrogenase) of 267; CK (creatine kinase) of 246; ACT (aspartat transaminase) of 40; d-dimers of 21; mild leukocytosis of 12,8 with the domination of the granulocyte fraction.

Radiology finding: inhomogeneous bilateral consolidations in the middle and basal parts, phrenicocostal sinuses have been free of liquid.

Postmortem laboratory findings

By applying molecular diagnostics on the pharyngeal and tracheal swabs, a presence of SARS Cov2 has been confirmed.

Additionally, detection of the anti-COVID antibodies has been undertaken. A positive result has been received for IgM antibodies with value of 30 AU/ml (referent value <1.00 AU/ml), and the positive result for IgG antibodies, with the value of 47,5 AU/ml (referent value <1.00 AU/ml).

Detection of the antiCOVID IgM antibodies has been expected which has been proof of the developed and lasting COVID-19 disease, fully coinciding with the data received that the death occurred on the 12th day of the disease. The presence of the

antiCOVID IgG antibodies undoubtedly has shown that the infection existed at least a week longer than the onset of the symptoms.

Postmortem biochemical analyses have shown a moderately raised values of myoglobin and the serum troponin, as well as the enzymes Alcaline phosphatase, AST (aspartat aminotransferase), CK (creatin kinase), and more significantly raised values of the LDH (lactate dehydrogenase), GAMA (glutamil transpeptidase) and ALT (alanine aminotransferase). Erythrocytes have been found $3{,}11\times10^{12}$/L, hemoglobin of 92g/L; leukocytosis of $14{,}9\times10^{9}$/L with the lymphocyte fraction of $6{,}3\times10^{9}$/L; as well as mildly raised thrombocytes of 594×10^{9}/L.

Toxicology analysis has shown benzodiazepines in the blood with therapeutically values.

Discussion

Coronavirus disease 2019 (COVID-19) first occurred in China by the end of 2019, but very fast has spread over the planet. The first confirmed case in USA has been on January 20, 2020 [3]. The first case in Republic of North Macedonia has been confirmed in the middle of February 2020. Until recently it has been a relatively new and unexplored disease with very diverse clinical picture. Some author concluded that severe COVID-19 form is a consequence of immune-mediated, rather than pathogen-mediated organ injury [2]. That is why, autopsies are essential to understand all the organ alterations in COVID-19 [2, 5, 14].

This disease is represented by two phases. For the first phase of the disease are typical symptoms very much like influenza syndrome: muscle pain, headache and fatigue. In mild cases the disease stops here. If condition continues more than 7 days, then a second pulmonary phase sets in. Careful medical records and autopsy reports published worldwide have shown that coronavirus 2 (SARS-CoV-2) is actually organotropic to many other organs than lungs [4, 8, 10], especially involving the thrombotic system and causing a kind of coagulopathy [1].

In the case presented here, a 39 years old man committed suicide by hanging on the 12th day of the COVID-19 disease, which is the second pulmonary phase of the disease and at least 21 days after the contact with the coronavirus 2 (SARS-CoV-2), as shown by the anti- SARS-CoV-2 antibodies found in his blood. The clinical course of the disease developed as typical acute restrictive lung disease i.e. a virus pneumonia, as in detail described in the classic pathology books [7] with strong inflammatory answer, as seen by the laboratory indicators (CRP, LDH, transaminaze enzymes, etc.)

Psychiatric symptoms first occurred on the seventh day of the disease and have been strongly related with the receiving of the positive PCR (polymerase chain reaction) molecular testing results. Actually, on that day the patient has been admitted to the hospital and there is a medical record that then he had oxygen saturation of 96%. Unfortunately, we don't have the exact recording of the oxygen saturation in the next 4 days (from the seventh to twelfth day, when he committed suicide), because the patient hasn't been hospitalized.

That is the reason why, our analysis has been directed toward the possible changes and conditions that eventually can be considered as a morphological substrate for the occurring of the psychiatric symptoms, and the hypoxia as the most probable among

them. A question arose: can the hypoxia of the brain be the pathological substrate for the onset of the psychiatric symptoms in COVID-19 patients?

During the 2020 there have been a lot of reports about the connection between COVID-19 and neurologic and also neuropsychiatric complications [9]: encephalopathy, meningo-encephalitis, ischemic stroke, acute necrotizing encephalopathy and Guillain-Barre syndrome (GBS).

Collecting the data from the 24 medical institutions in United Kingdom, in a study [8] has been described a wide range of the neurological complication in COVID-19 patients. A total of 43 patients have been analyzed where five major categories of neurological conditions have been described: 1. Encephalopathy (n = 10) with delirium/psychosis and no distinct MRI or CSF abnormalities; 2. Inflammatory CNS syndromes (n = 12) including encephalitis; 3. Ischemic strokes (n = 8) associated with a pro-thrombotic state; 4. Peripheral neurological disorders (n = 8), and five patients with miscellaneous neurological complication who did not fit these categories. As a possible mechanisms have been described: the direct viral neuronal injury; a secondary hyperinflammation syndrome; postinfectious inflammatory or immune-mediated disorders; and also the effects of a severe systemic disorder with the neurological consequences of sepsis, hyperpyrexia, hypoxia, hypercoagulability and critical illness. Those conditions occurred in the period from 6 days before and up to 27 days following the onset of the COVID-19 symptoms.

Upon that, the previous mentioned study shows that hypoxia of the brain can be found as a serious factor for the occurring of the neurological and the psychiatric disturbances. Examining the brain in the presented case some signs of hypoxia have been seen, but not clear if they are result of the primary disease or of the asphyxiation. The degree of the neurological disturbance often is not correlated with the severity of the primary COVID disease and also the neurological symptoms can be found as a first presentation of the COVID disease [6, 8]. Hence, it is a kind of challenge early recognizing and managing of the neurological and psychiatric disturbances in the COVID-19 disease.

Based of the aforementioned, if we look back to the medical history of the presented case, in fact the patient has asked for a psychiatric support twice: first time, indirectly by his first attempt for suicide, and second time, four days later he and his family directly asked for it. Unfortunately, the patient has been released home only with the prescribed antipsychotic therapy. This event shows that, regarding the COVID-19 patients, medical professionals must be aware about the neurological and psychiatric manifestation of the disease, as well as the possible consequences of it.

The second important aspect of this case report is to perceive the pathological feature of the lungs in a confirmed COVID-19 patient, who actually didn't die of the disease itself but of a violent death. The clinical data along with the pathological findings were pointing to the acute restrictive lung disease which started as an atypical viral pneumonia and then progressed to diffuse alveolar damage, known as ARDS (acute respiratory distress syndrome).

The concept of the primary atypical pneumonia has been presented since 1938 and described as non-productive pneumonia, with minimal physical and rich radiology findings, with predominantly good prognosis and bad outcome only in immunosuppressed organisms [7]. The bad outcome actually means the development toward the diffuse alveolar damage and ARDS.

Acute respiratory distress syndrome (ARDS) is a clinical syndrome defined in 1994 by the American-European Consensus Conference (AECC) which is characterized by: 1. acute respiratory distress, 2. decreased arterial oxygen pressure and 3. the development of diffuse pulmonary infiltrates on radiographs [7, 11, 12, 13]. By the Berlin Definition [11] there are proposed three categories of ARDS upon the severity: mild, moderate and severe, with strict parameters given. Diffuse alveolar damage is the morphologic counterpart of ARDS [7]. It is characterized by diffuse injury of the alveolar epithelial and capillary endothelial cells, accompanied with the pulmonary edema.

In the pathogenesis of ARDS, no matter of the initiating agent (chemical, physical or viral), there is a sequence of the events: 1. endothelial and epithelial damage; 2. the cellular reaction by neutrophiles and macrophages; 3. releasing of the TNF-alpha (tumor necrotizing factor alpha) and activating of the complement with subsequent production and release of the cytokines, powerful mediators, proteases etc. which all further damage the endothelium and increase vascular permeability. These all cause the changes of the first or exudative phase of ARDS: interstitial and intraalveolar edema and hemorrhage, necrosis of the epithelial cells and forming of the typical hyaline membranes underlining the alveolar walls which sufficiently compromise the oxygenation. 72 hours after the process begins, a disseminated intravascular coagulation may become evident and complicate the clinical picture [7]. The next two phases in the morphology of ARDS are the proliferative phase characterized by the proliferation of the type II pneumocytes and fibroblasts, and finally the fibrotic phase with the progressive fibrosis involving the interstitial and alveolar spaces, leading to diffuse interstitial fibrosis (honeycomb lungs) [7].

In the presented case were found changes of the exudative and proliferative phase of ARDS. Having in regard that the mortality rate of ARDS nowadays is beneath 50% [13], comparing with the past when it was almost 100%, we can assume that if patient overcomes the exudative phase, there are good chances of survival. Implying that to the presented case, there are good chances that the person could have overcome the COVID-19 disease, but unfortunately he died of suicide. Here lies the obligation for the medical professionals to recognize the neurological and psychiatric disturbances as part of the diverse clinical picture of COVID-19, in order to provide a complete health care for the patient.

Conclusion

This case presentation shows that the psychiatric and neurological disturbances can be significant part of the clinical picture of the COVID-19 disease and they are not necessarily correlated with the severity of the primary disease. Medical professionals must be aware of these manifestations of the COVID-19 disease, because sometimes they can be more fatal than the lung disease itself. High degree of caution and care are important in these cases.

Having in regard the diverse and still not enough explored clinical manifestation of the COVID-19, besides treating the pneumonia and coagulopathy in these patients, attention to the psychiatric status of the patient must be paid, in order to enable him/her a complete health care protection.

References

1. **Campbell, C., R. Kahwash.** Microvascular thrombi in COVID-19. Expert Analysis. – *American College of Cardiology*. January 25th 2021. https://www.acc.org/latest-in-cardiology/articles/2021/01/25/14/28/microvascular-thrombi-in-covid-19
2. **Dorward, D. A., C. D. Russell, I. H. Um, M. Elshani, S. D. Armstrong, R. Penrice-Randal, T. Millar, C. E. B. Lerpiniere, G. Tagliavini, C. S. Hartley, N. P. Randle, N. N. Gachanja, P. Potey, A. M. Anderson, V.L. Campbell, A. J. D. BChir, W. Al. Qsous, R. BouHaidar, J. K. Baillie, K. Dhaliwai, W. A. Wallace, C. Bellamy, S. Prost, C. Smith, J. A. Hiscox, D. J. Harrison, C. D. Lucas**. Tissue specific immunopathology in fatal COVID-19. – *Am. J. Respir. Crit Care Med.*, **203**(2), 2021, 192-201.
3. **Fox, S. E., A. Akmatbekov, J. L. Harbert, G. Li, J. Q. Brown, R. S. V. Heide.** Pulmonary and cardiac pathology in African American patients with COVID-19: an autopsy series from New Orleans. – *Lancet Respir. Med*., **8**, 2020, 681-686.
4. **Guo, T., F. Yongzhen, M. Chen, W. Xiaoyian, L. Zhang, J. Wan, X. Wang, Z. Lu.** Cardiovascular implications of fatal outcomes of patients with Coronavirus disease 2019 (COVID-19). – *JAMA Cardiol*., **5**(7), 2020, 811-818.
5. **Hanley, B., S. B. Lucas, E. Youd, B. Swift, M. Osborn.** Autopsy in suspected COVID-19 cases. – *J. Clin. Pathol.*, **73**, 2020, 239-242.
6. **Helms, J., S. Kremer, H. Merdji, R. Clere-Jehl, M. Schenck, C. Kummerlen, O. Collange, C. Boulay, S. Fafi-Kremer, M. Ohana, M. Anheim.** Neurologic features in severe SARS-CoV-2 infection. – *N. Engl. J. Med.*, **382**, 2020, 2268-2270.
7. **Kumar, V., R. S. Cotran, S. L. Robbins.** Acute restrictive lung diseases. Chapter 13. – In: *Basic Pathology – Sixth edition*, W. B. Saunders company, USA, 1997, 405-407.
8. **Mushumba, H., C. Edler, A.S. Schroeder, A. Fitzek, A. Ron.** An autopsy study of SARS-CoV-2-related deaths examined at the Hamburg Institute of legal medicine between March 20th and August 15th 2020. *DGRM 2020 Congresbook*. Lucern.
9. **Paterson, W. R., L. R. Brown, L. Benjamin, R. Nortley, S. Wiethoff, T. Bharucha, D. L. Jayaseelan, G. Kumur, R. E. Raftopoulos, L. Zambreanu, V. Vivekanandam, A. Khoo, R. Geraldes, K. Chinthapalli, E. Boyd, H. Tuzlali, G. Price, G. Christofi, J. Morrow, P. McNamara, B. McLoughlin, S. T. Lim, P. R. Mehta, V. Levee, S. Keddie, W. Yong, S. A. Trip, A. J. M. Foulkes, G. Hotton, T. D. Miller, A. D. Everitt, C. Carswell, N. W. S. Davies, M. Yoong, D. Attwell, J. Sreedharan, E. Silber, J. M. Schott, A. Chandratheva, R. J. Perry, R. Simister, A. Checkley, N. Longley, S. F. Farmer, F. Carletti, C. Houlihan, M. Thom, M. P. Lunn, J. Spillane, R. Howard, A. Vincent, D. J. Werring, C. Hoskote, H. R. Jager, H. Manji, M. S. Zandi.** The emerging spectrum of COVID-19 neurology: clinical, radiological and laboratory findings. – *BRAIN*, **143**, 2020, 3104-3120.
10. **Puelles, V. G., M. Lütgehetmann, M. T. Lindenmeyer, J. P Sperhake, M. N. Wong, L. Allweiss, S. Chilla, A. Heinemann, N. Wanner, S. Liu, F. Braun, S. Lu, S. Pfefferle, A. S. Schröder, C. Edler, O. Gross, M. Glatzel, D. Wichmann, Th. Wiech, S. Kluge, K. Pueschel, M. Aepfelbacher, T. B. Huber.** Multiorgan and renal tropism of SARS-CoV-2. – *N. Engl. J. Med.*, **383**, 2020, 590-592.
11. **Ranieri, V. M., G. D. Rubenfeld, B. Taylor Thompson, N.D. Ferguson, E. Caldwell, E. Fan, L. Camporota, A. S. Slutsky.** Acute Respiratory Distress Syndrome: the Berlin definition. – *JAMA*, **307**(23), 2012, 3072542-3072544.
12. **Schmitt, W., E. Marchiori.** Covid-19: Round and oval areas of ground-glass opacity. - *Pulmonology,* 2020. doi: 10.1016/l.pulmoe.2020.04.001.
13. **Thompson, T., B. R. C. Chambers, K. D. Liu.** Acute Respiratory Distress Syndrome. – *N. Engl. J. Med.*, 377-6, 2017, 562-572.
14. **Tzankov, A.** Lessons learned from autopsies of COVID-19: deadly disease courses due to (micro-) angiopathy and thrombosis. – *DGRM 2020 Congressbook.* Lucern.

Institute of Experimental Morphology, Pathology and Anthropology with Museum
Bulgarian Anatomical Society

Acta morphologica et anthropologica, 28 (1-2)
Sofia ● 2021

Review Articles

Microscopic Changes in the Hypertensive Heart and Kidney – Structural Alterations, Role of Mast Cells and Fibroblast Growth Factor-2

Dimo Dimitrov, Alexandar Iliev, Georgi Kotov, Nikola Stamenov, Stancho Stanchev, Boycho Landzhov*

Department of Anatomy, Histology and Embryology, Medical University of Sofia, Bulgaria

* Corresponding author e-mail: dralexiliev@abv.bg

Hypertension is among the disorders with the highest impact on human health and healthcare systems around the world. It is responsible for various pathological conditions, which lead to a shortened life expectancy. There are multiple studies on the effects of prolonged hypertension on the heart and kidneys. While much is known about the structural and functional changes occurring in the left ventricle, data exploring the alterations in the right ventricle are quite scarce. In this review article, we report on the structural alterations in both ventricles and in the kidney. We also present newly emerging evidence on the role of mast cells and fibroblast growth factor-2 in hypertension-induced fibrosis in the heart and kidney. The aim of this review is to look at some recent scientific data and point out the role of often overlooked aspects of hypertensive heart and kidney damage, which may well turn out to have a pivotal role in the better understanding and treatment of these conditions.

Key words: Mast cells, fibroblast growth factor-2 (FGF-2), heart, kidney, hypertension, spontaneously hypertensive rats (SHR)

Introduction

Hypertension is a worldwide disease, which is recognised as an important risk factor for premature death. Prolonged and untreated hypertension is a major reason for the development of inevitable structural alterations in many organs and systems, which are collectively described by the term ‘target organ damage’. The most commonly affected organs are heart, kidneys and brain, and the most common hypertension-related disorders include coronary heart disease (CHD), end-stage renal disease (ESRD) and stroke, respectively. Elevated blood pressure leads to an increased hemodynamic stress

on the myocardium, thus causing myocardial remodelling first evident by changes in the myocytes at the ultrastructural level. Historically, those changes have been well evaluated for the left ventricle (LV), but changes in the right ventricle (RV) have often been overlooked. An increasing number of recent studies have been assessing the pathological changes and dysfunction of the RV and their relation to the LV. In the kidney, hypertensive damage is related to renal fibrosis in both the medulla and cortex caused by expansion of extracellular molecules. Scientific evidence demonstrates that changes in the interstitial tissue correlate better with renal function than changes in the glomeruli [35]. Recent reports have indicated that damage found in these target organs is associated with the pathological function of mast cells, well beyond their previously explored role in allergic and anaphylactic reaction, as well as signal molecules expressed by them, such as fibroblast growth factor-2.

Herein, we report on the structural alterations in both ventricles and in the kidney. We also present newly emerging evidence on the role of mast cells and fibroblast growth factor-2 in hypertension-induced fibrosis in the heart and kidney. The aim of this review is to look at some recent scientific data and point out the role of often overlooked aspects of hypertensive heart and kidney damage, which may well turn out to have a pivotal role in the better understanding and treatment of these conditions.

Structural changes in the hypertensive heart

It is a well known fact that prolonged hypertension leads to microstructural and functional changes in the heart. The spontaneously hypertensive rat (SHR) is an often used model of hypertensive target organ damage. Blood pressure in this animal reaches systolic values of 180-200 mmHg as early as 4-6 weeks of age, with subsequent alterations observed in their heart, kidneys and other target organs [18,27,29]. These changes have been shown to correlate with changes observed in human organs. Therefore, it should be noted that a significant number of studies focusing on the structural aspects of hypertensive damage are based on this animal model.

CHD and its complications are responsible for a considerable burden on healthcare systems around the world. Hypertension is among the leading factors for the development of CHD. The chronic increase in hemodynamic stress causes myocardial remodelling and is associated with alterations at the ultrastructural level. A study by Iliev et al. showed similar ultrastructural changes in both the LV and RV [10]. The progression of hypertensive heart damage is accompanied by cardiomyocytic hypertrophy, hypertrophy and hyperplasia of the cardiomyocytic nuclei and multiple invaginations of the nuclear membrane. Alterations in the strict arrangement of the myofibrils, with occurrence of disorganised filamentous structures adjacent to the myofibrils are also observed. In addition, it is noted that mitochondria become swollen, with appearance of amorphous matrix and disintegration of the cristae. These changes take place along with an increased collagen deposition in the interstitial space, as evidenced by the presence of multiple fibroblasts and the development of endo- and perimysial fibrosis [10].

Structural changes in the hypertensive kidney

Many cases of newly diagnosed ESRD are due to hypertension-induced damage and the structural changes in the kidney associated with it. The relationship between hypertension and ESRD is pathologically referred to as hypertensive nephrosclerosis.

Alterations occur in both the interstitium and parenchyma. They include changes such as glomerulosclerosis, thickening of the glomerular basement membrane, tubular atrophy of distal and proximal segments, hyaline and fibrinoid arteriosclerosis and proliferation of the intimal smooth muscle cells of the interlobar arteries [32,34]. Glomerular injury can be classified in two types: solidification and obsolescence, each presenting with a definitive ultrastructural picture. The alterations, in the solidification type, are represented by collapse of the glomerulus and intracapsular fibrosis. Distinctive changes in the obsolescence type include expansion of the matrix and enlargement of the glomeruli tuft [34]. Interstitial fibrosis can be observed throughout the kidney structure – periglomerular, peritubular, periarteriolar fibrosis. It is associated with expansion of the extracellular matrix [32].

The role of mast cells and FGF-2 in the hypertensive heart

Another interesting finding in the hypertensive heart is the presence of mast cells. Mast cells are well known mononuclear cells, which participate in the innate immune response of the body. They take part in the regulation of multiple physiological functions and also play a main role in pathological conditions such as allergies, anaphylactic shock, etc. There are two types of mast cells, which have been described in rats. These are mucosal mast cells (MMCs) and connective tissue mast cells (CTMCs). Both types differ in lifespan, localization and dependence on T cells [8]. MMCs are found in the intestinal and respiratory mucosa. CTMCs are found around blood vessels and nerve endings. MMCs are T-cell induced and T-cell dependent, while CTMCs are T-cell independent [8]. MMCs contain chymase in their granules, while CTMCs contain chymase, tryptase and carboxypeptidase [16].

The presence of CTMCs has been described in the LV of the heart [19,26]. Recent studies have demonstrated the role of these cardiac mast cells in the pathogenesis of myocardial remodelling in the LV [11,17,19]. In particular, the essence of the mediators contained in mast cell granules – namely chymase, tryptase, histamine, fibroblast growth factor-2 (FGF-2), transforming growth factor-beta (TGF-beta) – have been discussed. These mediators initiate the activation and proliferation of fibroblasts, the differentiation of myofibroblasts and collagen synthesis [17,19]. Mast cell granules also contain tumour necrosis factor-alpha (TNF-alpha), which is responsible for promotion of apoptosis of the cardiomyocytes, hypertrophy, inflammation and increase in the expression of matrix metalloproteinase-9. In addition, the stem cell factor (SCF) and its receptor on the mast cell membrane c-kit (also known as CD117), have been shown to have a role in the survival, proliferation, differentiation and maturation of mast cells. SCF, in particular, is important for the interaction between fibroblasts and mast cells [2,3]. Interestingly, mast cells can produce SCF themselves, which may signify possible autoregulation [3]. Anti-inflammatory cytokines, such as interleukin-10 (IL-10) and interleukin-33 (IL-33) produced by mast cells are another factor demonstrating their complex role in heart remodelling [15,17]. Mast cells are involved in both myocardial remodelling after myocardial infarction and in heart failure, and fibrotic remodelling caused by hypertension and myocarditis [20].

An interesting recent finding by Iliev et al. is the presence of mast cells not only in the LV, but also in the RV of SHR [10]. Moreover, a comprehensive study by Kotov et al. discovered that a statistically significant increase in the number of mast cells takes

places as hypertensive heart damage progresses. The authors also used a semi-quantitative analysis to evaluate FGF-2 immunoreactivity in the myocardium of the LV and RV, and demonstrated an increase in the expression of this growth factor in both ventricles as hypertension progressed [15]. The same study reported a positive correlation between the number of mast cells, the expression of FGF-2 and the extent of interstitial fibrosis in both ventricles [15]. These findings further solidify the data from previous studies on the connection between mast cells and interstitial fibrosis [12,21]. The information above can be demonstrated by the following cascade: increase in mast cells → increased synthesis of FGF-2 by mast cells → increased collagen production and interstitial fibrosis → further stimulation of mast cells by fibroblasts through the SCF-c-kit pathway [15]. Perhaps contrastingly, Widiapradja et al. observed that what increases is not the actual number of mast cells, but rather the percentage of mature mast cell, showing the need for more studies in the area so it can be fully understood [43].

The role of mast cells and FGF-2 in the hypertensive kidney

Another target organ which is impacted by the prolonged elevation of blood pressure is the kidney. With time, hypertension leads to renal injury and changes in the structure of the kidney, which ultimately causes ESRD. Morphological changes affect both the renal parenchyma and interstitium and include glomerulosclerosis, arteriolar sclerosis, tubular atrophy, infiltration of inflammatory cells and expansion of the extracellular matrix [23]. An interesting fact demonstrated by numerous studies is that changes in the interstitium rather than these in the glomeruli are more indicative of the extent of kidney damage and correlate better with renal function [30,40]. A recent research by Stanchev et al. showed that it is the various cellular interactions which lead to the above-described changes rather than a simple accumulation of molecules in the interstitium [37].

Similar to the heart, more recent data have focused on the role of mast cells and FGF-2 in the development of interstitial changes in the kidney [28,33]. Researchers observed that renal damage, regardless of its pathological origin, is accompanied by an increase in the number of mast cells in the kidneys, as well as SCF levels. Furthermore, the number of mast cells also increases with the extent of kidney damage [41,42]. In number of pathological conditions mast cells localise in the interstitium around vessels and tubules but are not found in the glomeruli [42]. A recent work by Stanchev et al. found a similar picture in the kidneys of SHR – namely, the lack of mast cells in the renal corpuscles [33]. As previously mentioned, FGF-2 is an important growth factor released by mast cells, which leads to proliferation of mesangial cells, glomerular and tubular epithelial cells, vascular endothelial cells and vascular smooth muscles. In their study, Stanchev et al. observed a positive correlation between the immunoreactivity of FGF-2, the number of mast cells and the degree of tubulointerstitial changes [33]. While FGF-2 levels in the corpuscles were minimal, other studies have described positive expression of FGF-2 in the layers of the Bowman's capsule and the glomerular mesangium [5,38].

Renal fibrosis is a complex process. A balance exists between collagen synthesis and collagen degradation. Many studies revealed the close relationship between mast cells and fibroblasts [24,39]. Stanchev et al. found a possible correlation between mast cells and the extent of renal fibrosis – there was a higher number of mast cells in SHR with more advanced hypertension-induced renal fibrosis [33]. Significant evidence points to the fact that tryptase secreted by mast cells serves as a mitogen for fibroblasts responsible for collagen synthesis [7,14,33]. Myofibroblasts are another key element in

the development of renal fibrosis. It has been reported that they can serve as an indicator of the extent of renal extracellular expansion. Fibroblasts stimulated by mast cells can differentiate into myofibroblasts [6,22]. Mast cell-fibroblasts relationship, however, is a two-way relationship, with the latter capable of influencing mast cell differentiation and activation by producing SCF. It should nevertheless be noted that other studies have presented contradictory data. Kim et al. observed a decrease in collagen type I expression induced by mast cells [13], while Miyazawa et al. concluded that mast cells exhibit a renoprotective effect [24].

In line with the above data, it would be worth noting that the expression of various collagen types in the kidney changes in response to hypertension. Collagen types I, III and V are commonly expressed in the renal interstitium, while only type V is expressed in the glomeruli. Prolonged hypertension leads to glomerular injury and subsequent glomerulosclerosis. These processes are associated with an increased expression of collagen types I and III [35]. A research by Stanchev et al. also observed an increase in the expression of collagen type V in the parietal and visceral layer of the glomerular capsule of SHR, which suggests a possible role in the process of renal fibrosis [35]. While only collagen type V is expressed in healthy kidney glomeruli, in the process of glomerulosclerosis deposition of types I and III is noted in the glomerular capillary tufts [1,35]. Finally, the study of Farris et al. revealed a likely key role of myofibroblasts in renal fibrosis, revealing thus another aspect of the complex mechanism behind hypertension-induced kidney damage [4].

Conclusion

Hypertension-induced changes in target organs such as the heart and kidney are associated with multiple alterations at the ultrastructural level and are initiated and maintained by complex mechanisms. Notably, in contrast to earlier understanding, the RV of the heart appears to be affected in a similar manner to the LV, albeit to a lesser degree. Recent evidence suggests that mast cells and substances produced by them, in particular FGF-2, are implicated in the development of interstitial fibrosis in the heart and kidney in response to elevated blood pressure. The positive correlations between the number of mast cells, the expression of FGF-2 and the extent of cardiac fibrosis are a reliable foundation for future research. Similar correlations show that the higher number of mast cells and the stronger expression of FGF-2 are associated with more pronounced renal alterations as evidenced by changes in the respective markers of renal damage and fibrosis, further supporting the shared mechanism of hypertension-induced heart and kidney damage.

Acknowledgements: This work is supported by the Bulgarian Ministry of Education and Science under the National Program for Research ‘Young Scientists and Postdoctoral Students’.

References

1. **Alexakis, C., P. Maxwell, G. Bou-Gharios.** Organ-specific collagen expression: implications for renal disease. – *Nephron Exp. Nephrol.,* **102**, 2006, e71-e75.

2. **Bagher, M., A. K. Larsson-Callerfelt, O. Rosmark, O. Hallgren, L. Bjermer, G.Westergren-Thorsson.** Mast cells and mast cell tryptase enhance migration of human lung fibroblasts through protease-activated receptor 2. – *Cell Commun. Signal,* **16**, 2018, 59.
3. **Bradding, P., G. Pejler.** The controversial role of mast cells in fibrosis. – *Immunol. Rev.,* **282**, 2018, 198-231.
4. **Farris, A. B., R. B. Colvin.** Renal interstitial fibrosis: mechanisms and evaluation. – *Curr. Opin. Nephrol. Hypertens.,* **21**, 2012, 289–300.
5. **Floege, J., E. Eng, V. Lindner, C. E. Alpers, B. A. Young, M. A. Reidy, R. J. Johnson.** Rat glomerular mesangial cells synthesize basic fibroblast growth factor. Release, upregulated synthesis, and mitogenicity in mesangial proliferative glomerulonephritis. – *J. Clin. Invest.,* **90**, 1992, 2362-2369.
6. **Gailit, J., M. J. Marchese, R. R. Kew, B. L. Gruber.** The differentiation and function of myofibroblasts is regulated by mast cell mediators. – *J. Invest. Dermatol.,* **117**, 2001, 1113–1119.
7. **Garbuzenko, E., A. Nagler, D. Pickholtz, P. Gillery, R. Reich, F. X. Maquart, F. Levi-Schaffer.** Human mast cells stimulate fibroblast proliferation, collagen synthesis and lattice contraction: a direct role for mast cells in skin fibrosis. – *Clin. Exp. Allergy,* **32**, 2002, 237-246.
8. **Gurish, M. F., K. F. Austen.** Developmental origin and functional specialization of mast cell subsets. – *Immunity,* **37**, 2012, 25-33.
9. **Iliev, A. A., G. N. Kotov, B. V. Landzhov, L. S. Jelev, V. K. Kirkov, D. V. Hinova-Palova.** A comparative morphometric study of the myocardium during the post- natal development in normotensive and spontaneously hypertensive rats. – *Folia Morphol. (Warsz),* **77**, 2018, 253-265.
10. **Iliev, A., G. Kotov, I. N. Dimitrova, B. Landzhov.** Hypertension-induced changes in the rat myocardium during the development of cardiac hypertrophy – a comparison between the left and the right ventricle. – *Acta Histochem.,* **121**, 2018, 16-28.
11. **Janicki, J. S., G. L. Brower, S. P. Levick.** The emerging prominence of the cardiac mast cell as a potent mediator of adverse myocardial remodelling. – *Methods Mol. Biol.,* **1220**, 2015, 121-139.
12. **Juliano, G. R., M. F. Skaf, L. S. Ramalho, G. R. Juliano, B. G. S. Torquato, M. S. Oliveira, F. A. Oliveira, A. P. Espíndula, C. L. Cavellani, V. P. A. Teixeira, M. L. D. F. Ferraz.** Analysis of mast cells and myocardial fibrosis in autopsied patients with hypertensive heart disease. – *Rev. Port.Cardiol.,* **39**, 2020, 89-96.
13. **Kim, D. H., S. O. Moon, Y. J. Jung, A. S. Lee, K. P. Kang, T. H. Lee, S. Lee, O. H. Chai, C. H. Song, K. Y. Jang, M. J. Sung, X. Zhang, S. K. Park, W. Kim.** Mast cells decrease renal fibrosis in unilateral ureteral obstruction. – *Kidney Int.,* **75**, 2009, 1031-1038.
14. **Kondo, S., S. Kagami, H. Kido, F. Strutz, G. A. Müller, Y. Kuroda.** Role of mast cell tryptase in renal interstitial fibrosis. – *J. Am. Soc. Nephrol.,* **12**, 2001, 1668-1676.
15. **Kotov, G., B. Landzhov, N. Stamenov, S. Stanchev, A. Iliev.** Changes in the number of mast cells, expression of fibroblast growth factor-2 and extent of interstitial fibrosis in established and advanced hypertensive heart disease. – *Ann. Anat.,* **232**, 2020, 151564.
16. **Kurashima, Y., H. Kiyono.** New era for mucosal mast cells: their roles in inflammation, allergic immune responses and adjuvant development. – *Exp. Mol. Med.,* **46**, 2014, e83.
17. **Legere, S. A., I. D. Haidl, J. F. Légaré, J. S. Marshall.** Mast cells in cardiac fibrosis: new insights suggest opportunities for intervention. – *Front. Immunol.*, **10**, 2019, 580.
18. **Leong, X. F., C. Y. Ng, K. Jaarin.** Animal models in cardiovascular research: hypertension and atherosclerosis. – *Biomed. Res. Int.,* **2015**, 2015, 528757.
19. **Levick, S. P., A. Widiapradja.** Mast cells: key contributors to cardiac fibrosis. – *Int. J. Mol. Sci.,* **19**, 2018, 231.
20. **Levick, S. P., G. C. Meléndez, E. Plante, J. L. McLarty, G. L. Brower, J. S. Janicki.** Cardiac mast cells: the centrepiece in adverse myocardial remodelling. – *Cardiovasc. Res.*, **89**, 2011, 12-19.
21. **Liu, T., D. Song, J. Dong, P. Zhu, J. Liu, W. Liu, X. Ma, L. Zhao, S. Ling.** Current understanding of the pathophysiology of myocardial fibrosis and its quantitative assessment in heart failure. – *Front. Physiol.,* **8**, 2017, 238.
22. **Meran, S., R. Steadman.** Fibroblasts and myofibroblasts in renal fibrosis. – *Int. J. Exp. Pathol.,* **92**, 2011, 158-167.
23. **Meyrier, A.** Nephrosclerosis: update on a centenarian. – *Nephrol. Dial. Transplant*., **30**, 2015, 1833-1841.
24. **Miyazawa, S., O. Hotta, N. Doi, Y. Natori, K. Nishikawa, Y. Natori.** Role of mast cells in the development of renal fibrosis: use of mast cell-deficient rats. – *Kidney Int.,* **65**, 2004, 2228-2237.
25. **Mukai, K., M. Tsai, H. Saito, S. J. Galli.** Mast cells as sources of cytokines,chemokines, and growth factors. – *Immunol. Rev.*, **282**, 2018, 121-150.

26. **Ngkelo, A., A. Richart, J. A. Kirk, P. Bonnin, J. Vilar, M. Lemitre, P. Marck, M. Branchereau, S. Le Gall, N. Renault, C. Guerin, M. J. Ranek, A. Kervadec, L. Danelli, G. Gautier, U. Blank, P. Launay, E. Camerer, P. Bruneval, P. Menasche, C. Heymes, E. Luche, L. Casteilla, B. Cousin, H. R. Rodewald, D. A. Kass, J. S. Silvestre.** Mast cells regulate myofilament calcium sensitization and heart function after myocardial infarction. – *J. Exp. Med.*, **213**, 2016, 1353-1374.
27. **Okoshi, M. P., K. Okoshi, L. S. Matsubara, M. D. Pai-Silva, A. L. Gut, C. R. Padovani, V. D. Pai, A. C. Cicogna.** Myocardial remodelling and dysfunction are induced bychronic food restriction in spontaneously hypertensive rats. – *Nutr. Res.*, **26,** 2006, 567-572.
28. **Owens, E. P., D. A. Vesey, A. J. Kassianos, H. Healy, W. E. Hoy, G. C. Gobe.** Biomarkers and the role of mast cells as facilitators of inflammation and fibrosis in chronic kidney disease. – *Transl. Androl. Urol.,* **8**, 2019, S175-S183.
29. **Pagan, L. U., R. L. Damatto, M. D. Cezar, A. R. Lima, C. Bonomo, D. H. Campos, M. J. Gomes, P. F. Martinez, S. A. Oliveira, R. Gimenes, C. M. Rosa, D. M. Guizoni, Y. C. Moukbel, A. C. Cicogna, M. P. Okoshi, K.Okoshi.** Long-term low intensity physical exercise attenuates heart failure development in aging spontaneously hypertensive rats. – *Cell. Physiol. Biochem.*, **36**, 2015, 61-74.
30. **Rodriguez-Iturbe, B., R. J. Johnson, J. Herrera-Acosta.** Tubulointerstitial damageand progression of renal failure. – *Kidney Int.*, **99**, 2005, S82-S86.
31. **Savova, K., P. Yordanova, D. Dimitrov, S. Tsenov, D. Trendafilov, B. Georgieva.** Light microscopic morphological characteristics and data on the ultrastructure of the cardiomyocytes. – *Acad. Anat. Int.*, **3**, 2017, 4-8.
32. **Stanchev, S., A. Iliev, G. Kotov, L. Malinova, B. Landzhov.** A comparative morphometric study of the superficial and juxtamedullary nephrons during the postnatal development in spontaneously hypertensive rats. – *Arch Anat. Physiol.,* **3**, 2018, 001-004.
33. **Stanchev, S., B. Landzhov, G. Kotov, N. Stamenov, T. Dikov, A. Iliev.** The potential role of mast cells and fibroblast growth factor-2 in the development of hypertension-induced renal damage. – *Acta Histochem.,* **122**, 2020, 151599.
34. **Stanchev, S. S., A. A. Iliev, L. G. Malinova, B. V. Landzhov, G. N. Kotov, D. V.Hinova-Palova.** Light microscopic study of renal morphological alterations in spontaneously hypertensive rats. – *J. Biomed. Clin. Res.*, **10**, 2017, 18-24.
35. **Stanchev, S., A. Iliev, B. Landzhov.** Comparative Immunohistochemical Study on Collagen Types in Kidney during Aging and Hypertension. –*Acta morphol. anthropol.*, **26**, 2019, 38-45.
36. **Stanchev, S., A. Iliev, L. Malinova, B. Landzhov, W. Ovtscharoff.** Light microscopic and ultrastrucural kidney changes in spontaneously hypertensive rats. – *C. R. Acad. Bulg. Sci.,* **73**, 2020, 1449-1455.
37. **Stanchev., S., N. Stamenov, V. Kirkov, E. Dzhambazova, D. Nikolov, A. Paloff.** Differential collagen expression in kidney and heart during hypertension. – *Bratisl. Lek. Listy.,* **121**, 2020, 73-78.
38. **Takeuchi, A., N. Yoshizawa, M. Yamamoto, Y. Sawasaki, T. Oda, A. Senoo, H. Niwa, Y. Fuse.** Basic fibroblast growth factor promotes proliferation of rat glomerular visceral epithelial cells in vitro. – *Am. J. Pathol.,* **141**, 1992, 107-116.
39. **Veerappan, A., N. J. O'Connor, J. Brazin, A. C. Reid, A. Jung, D. McGee, B. Summer, D. Branch-Eliman, B. Stiles, S. Worgall, R. J. Kaner, R. B.Silver.** Mast cells: a pivotal role in pulmonary fibrosis. – *DNA Cell Biol.,* **32**, 2013, 206-218.
40. **Vleming, L. J., J. W. de Fijter, R. G. Westendorp, M. R. Daha, J. A. Bruijn, L. A. van Es.** Histomorphometric correlates of renal failure in IgA nephropathy. – *Clin. Nephrol.,* **49**, 1998, 337-344.
41. **Wasse, H., N. Naqvi, A. Husain.** Impact of mast cell chymase on renal disease progression. – *Curr. Hypertens. Rev.*, **8**, 2012, 15-23.
42. **Welker, P., S. Krämer, D. A. Groneberg, H. H. Neumayer, S. Bachmann, K. Amann, H. Peters.** Increased mast cell number in human hypertensive nephropathy. – *Am. J. Physiol. Renal Physiol*., **295**, 2008, F1103-F1109.
43. **Widiapradja, A., E. J. Manteufel, H. M. Dehlin, J. Pena, P. H. Goldspink, A. Sharma, L. L. Kolb, J. D. Imig, J. S. Janicki, B. Lu, S. P. Levick.** Regulation of cardiacmast cell maturation and function by the Neurokinin-1 receptor in the fibroticheart. – *Sci. Rep.,* **9**, 2019, 11004.

Institute of Experimental Morphology, Pathology and Anthropology with Museum
Bulgarian Anatomical Society

Acta morphologica et anthropologica, 28 (1-2)
Sofia ● 2021

Toxic Effects of Heavy Metals (Mercury and Arsenic) on the Male Fertility

Iliana Ilieva[1], Iskra Sainova[1], Kristina Yosifcheva[2]*

[1] *Dept. Experimental Morphology, Institute of Experimental Morphology, Pathology and Anthropology with Museum, Bulgarian Academy of Sciences*
[2] *Dept. Laboratory of Heavy Metal, University Hospital "St. Ivan Rilski"*

* Corresponding author e-mail: iilieva@abv.bg

Heavy metals are proving to be an important factor in determining male infertility. The accumulation of lead, cadmium, mercury, arsenic, bismuth and other elements, even in low concentrations, induces strong toxic effects in the reproductive tract. The current review focuses on the naturel toxicants mercury (Hg) and arsenic (As) as the main pollutants of the environment, and their effects on the function of the male gonads and spermatogenesis, as well as the related reproductive consequences as poor sperm quality and male infertility. Massive degeneration of germ cells and alterations in the levels of testosterone are also reported. Generally, it has been accepted that heavy metals affect the oxidative stress.

Key words: arsenic, mercury, heavy metals, testis, male reproductive system, male fertility

Introduction

Most of the heavy metals are able to form toxic diluted compounds in the living organisms, (including humans), but also in the environment. The professional exposition of these elements could be available in many fields of the industry, and it could lead to significantly increased pathogenicity and mortality. It has been suggested that the risk is usually connected with both increased concentrations and exposition duration. Each one of them could be harmful to the organism, if it is applied in a high dose or when the normal mechanisms of its elimination and/or metabolism are disrupted. The intoxications (acute or chronic) with metal ions are usually due to the impossibility for regeneration of the normal functions in the injured tissues of the organism.

It has generally been accepted that the exposure on the influence of heavy metals causes abnormalities in the male reproductive tract [34, 59, 65]. According to many literature data, even low doses of cadmium (Cd), mercury (Hg), arsenic (As) and lead (Pb) could lead to appearance of such effects [11, 53, 62]. For instance, exposure to Cd could lead to decreased semen quality and to damages in the sperm DNA. Pb could reduce male fertility by decreasing sperm count and motility, but also by causing abnormal

morphology and by affecting many functional parameters. Hg could be connected with sperm abnormality in humans. As could impair the development of the reproductive organs and steroidogenesis, but also to reduce the sperm quality. Generally, it has been accepted that heavy metals affect the mechanisms, related to the oxidative stress (OS) [25, 28]. The environmental tools of Hg and As could be natural and/or anthropogenic (by human activities). The application of As and Hg as pesticides, herbicides, fungicides and rodenticides is also an important factor for contamination [27, 41]. Besides the professional exposure, other important sources of heavy metals are harmful food habits and the consumption of contaminated marine organisms/seafood [38].

The main routes of non-occupational Hg exposure include dental amalgams, pharmaceutical applications, cosmetics, but also Hg vapor exposure from flooring in homes and schools [3, 6]. The organic Hg or methylmercury (MeHg) is found in water sediments, where microorganisms methylate inorganic mercury converting it to MeHg. This compound is persistent and it can accumulate in the food chain with predator species, such as fish and raptors, having the highest levels of Hg [33]. The reference intake levels for MeHg exposures range from 0.7 to 2 μg per kilogram (μg/kg) body weight per week. Levels of MeHg in the blood are related to fish consumption. The Hg concentration in approximately 98% of all urine samples from people without known exposure to Hg is less than 5 μg/l. Mild proteinuria may occur in the most sensitive adults at urine values of 50–100 μg/l following chronic occupational exposures. A positive point in Hg vapor poisoning is that most of the toxic effects usually disappear within a few months after cessation of exposure. Mercury blood levels higher than 200 μg/l may be associated with healthy effects in adults, but a concentration of 40-50 μg/l in a pregnant woman could be associated with a toxic risk for the fetus. Total blood Hg includes inorganic and organic forms, while urinary or plasma levels reflect inorganic Hg exposure. Blood levels of mercury higher than 5.8 μg/l are accepted as toxic. Mercury is suspected to have a negative impact on male fertility [61].

Chronic use of As may cause severe health-destructive effects including lung disease, reproductive problems, vascular disease and gangrene [12]. In absorption in the human body (by breath, digestive tract and skin), As passes into the blood, 95-99% of which accumulates in erythrocytes in the form of stable compounds with hemoglobin, and it is thus transported to the tissues and organs in the organism. The body releases through urine about 70% of the absorbed As as reference values of As in urine in humans show 10–30 μg/l and 0.5-1.5 μg/l in the blood, respectively. The average daily human intake of As is about 20 μg, while the lowest fatal dose is estimated to be in the range of 70-180 mg. Arsenic is categorized by the IARC (International Agency for Research on Cancer) as a human carcinogen (group 1), associated with increased risks of various cancers, as well as with numerous other non-cancer illnesses including cardiovascular diseases, diabetes, reproductive and developmental problems, but also neurological and cognitive problems [4, 30].

According to the Panel on Contaminants, the toxic tolerable weekly intake (PTWI) of 15 μg/kg body weight as determined by the Joint FAO/WHO Expert Committee on Food Additives (JECFA) is not applicable due to uncertainty regarding the dose-response relationship and because of the established much lower doses of As to cause lung and urinary tract cancer. The degree of impact of As on the living organisms depends on its form (organic or inorganic), as well as its valency/oxidation degree. About the inorganic As, it is not considered necessary to determine a dose of permissible daily or weekly

intake without having a significant healthy risk [14]. Diagnosis is by testing the urine, blood, or hair [48]. Arsenic acts by changing the functioning of around 200 enzymes [48]. The toxicity of the inorganic compounds of As has been found as higher than that of the organic ones. Furthermore, the tri-valent As ion (As^{3+}) in the chemical compounds is more toxic than the five-valent (As^{5+}) [57]. The high toxicity of the inorganic forms of As induced severe reproductive impairments in both men and women. It could cause miscarriages, stillbirths, or premature births. Also, women who work or live near industrial activity with As or As-compounds have a higher-than-normal miscarriage rate, and newborns are underweight because of the inorganic arsenic ingested, passing through the placenta. Similar teratogenic effects have been demonstrated in rodents (rats and mice) too. In the study of rats exposed to As in an amount of 0.24 mg per day for 28 days, ovarian and uterine compressed and inhibition of enzymes responsible for the normal course of individual stages of reproductive development has been observed. Regarding the organic forms of As, no negative reproductive effects have been identified so far.

The current review focuses on the toxic metals Hg and As as the main pollutants of the environment. In this regard, we discuss their effects on male gonadal function and spermatogenesis, as well as related reproductive effects such as poor sperm quality and male infertility.

Testicular and hormonal effects of heavy metals

Chronic intoxication with Hg and As (and/or their compounds) also affects the endocrine glands, including the testes and spermatogenesis. Similarly to Pb and Cd, the exposure to Hg can develop a pathological affect on the male reproductive organs [42] and to influence negatively the criteria of male reproductive health/fertility [54, 61]. Mercury has also been proved to pass through the blood-testis barrier (BTB) and to accumulate in Sertoli and Leydig cells [17], in the testes of experimental animals. In experimental *in vitro* incubation of rat Sertoli cells with 31 mM (6.22 mg/L) of inorganic Hg, lower levels of cell-produced inhibin B have been established [37]. Treatment of rats with inorganic (50 or 100 mg/kg) or organic Hg (MeHg) (5 or 10 mg/g) for 90 days has induced disintegration of the Leydig cells and inhibited the activity of 3b-hydroxysteroid dehydrogenase (3-b-HSD), an enzyme critical for testosterone (TE) production, and decreased TE levels respectively [58]. The treatment of mice (aged 12 weeks) with inorganic Hg at a dose of 4 mg kg^{-1}/dg body weight for 12 weeks by gavage caused a decrease in the epididymal sperm number and testicular weight [42]. According to another study, also showing a declined number of rat epididymal sperm after incubation with inorganic Hg, a dose-dependent decrease in motility has also been noted [47].

Increased Hg levels in patients with infertility and subfertility than fertile men have been assessed [13], as observed and tubular atrophy or/and Sertoli-cell-only syndrome (SCOS) in infertile patients exposed to mercury [29]. In one case (25-year-old male with infertility), bilateral testicular biopsy has revealed marked interstitial lymphatic infiltration and about 33% of the tubules analyzed showed SCOS) and tubular atrophy. Fewer than 4% of the tubules showed qualitatively intact spermatogenesis. Furthermore, autometallographic (AMG) analysis of the biopsy material yielded silver-enhanced Hg grains, primarily in the interstitial Leydig cells, but sections from a control patient not exposed to this element have devoid of Hg grains [29].

Arsenic, like other toxicogens, has been shown to impair the development of the reproductive organs, to inhibit steroidogenesis and to reduce sperm quality, which can lead to male infertility [23, 61]. However, a general view of As-induced male reproductive toxicity still lacks, and the underlying mechanisms remain largely unclear. Data on the harmful effects of As on the male reproductive health criteria are mainly from studies with experimental animals. The substantial amounts of arsenic detected in testes, epididymus, seminal vesicle, and ventral prostate suggest a possible direct effect on testicular tissue. In an experimental model of mice treated with drinking water containing 533.9 mmol/L arsenite (the form of arsenic that is normally found in drinking water) for 35 days, the As levels increased of about 10-fold in the testes (0.52 to 5.26 mg/kg), approximately twice in the epididymis (2.70 to 4.70 mg/kg) and relatively less in the seminal vesicles, but no signs of toxicity were found [43]. However, mice injected subcutaneously with 3 mg/kg arsenic trioxide accumulated As in the testes and plasma and exhibited inhibition of spermatogenesis. The results of different studies show that most likely adverse effects of arsenic exposure are due to large individual variability in As metabolism affecting both retention and distribution of As metabolites [43].

According to a recent study on the general influence of As exposure on the proteome and metabolome in rat testis, significant changes in all of the identified proteins (total 70, up- and down-regulated) and metabolites (total 13, increased and decreased) have been established, compared with the controls [23]. For instance, elevated expression levels of glutathione peroxidase 4 (GPx4), 11β–hydroxysteroid dehydrogenase (HSD11B1), nuclear autoantigenic sperm protein (NASP), and calcium-binding and spermatid-specific protein 1 (CABS1) have been established, which have suggested impaired spermatogenesis (with damage of germ cells morphology and functions) after As exposure. Overexpression of protein GPx4 has been proposed to cause spermatogenic defects, including primary spermatocyte apoptosis, loss of haploid cells and seminiferous epithelium disorganization [44]. Testicular NASP was demonstrated to be involved in cell cycle progression in male germ cells (probably through an interaction with the Cdc2/cyclin B and Hsp70-2 complex) [51] and its overexpression has been observed during androgen receptor blockade when the process of meiosis of spermatocytes could be inhibited [52]. CABS1 is a calcium-binding protein that is involved in the extremely complex structural rearrangements occurring in haploid germ cells (with specific expression in the elongated spermatids) during spermiogenesis. The depletion of scaffolding factor B1 (SAFB1), transcriptional intermediary factor 1β (TIF1β), retinol-binding protein 1 (RBP1), DnaJ homolog subfamily A member 1 (DNAJA1), Y-box binding protein 3 (YBX3) and allopregnanolone in As-treated rats have been suggested as connected with abnormal spermatogenesis in the testis due to germ cell deficiency and low testosterone levels [23]. SAFB1 contains a transcriptional repression domain and can bind certain hormone receptors and repress their activity. Arsenic-induced inhibition of SAFB1 similar to male SAFB1 null mice may lead to infertility due to increased germ cell apoptosis, Leydig cell hyperplasia, and low TE levels, which may be due to decreased circulating insulin-like growth factor 1 (IGF1), and loss of SAFB1-mediated suppression of hormone receptors [24]. TIF1β is a transcriptional co-repressor known to play key roles in spermatogenesis and early embryonic development. This factor is preferentially associated with heterochromatin structures in the Sertoli cells and round spermatids, as well as with the formation of meiotic chromosomes [60]. Its absence has been observed to lead to a clear defect in spermatogenesis, associated

with failure to spermatids release and testicular degeneration [21]. RBP1 is a specific plasma transport protein (mainly localized in the SCs) that delivers retinol (Vit. A) in the seminiferous tubules required for the maintenance of normal spermatogenesis in the mammalian testis. The continuous deficiency of RBP1 and retinol, respectively, could lead to spermatogenic arrest at preleptotene spermatocytes, followed by extensive loss of germinal epithelium in rats [42]. DNAJA1 works similarly as a co-chaperone of Hsp70 in protein folding and mitochondrial protein import. Its loss could cause severe defects in the SCs, increased androgen receptor (AR) levels and disrupted Sertoli-germ cell contacts, which proves the critical role of this protein in the spermatogenesis through AR-mediated signaling in the Sertoli cells [55**]**. The necessity of protein YBX3 for the activation of protamine 2 transcription in post-meiotic male germ cells has been suggested, and thus, a relationship between its loss and decreased protamine 2 transcription [64]. It has further been proposed that As mainly impaired spermatogenesis and fertilization via aberrant modulation of the described male reproduction-related proteins and metabolites, which could be mediated by the ERK/AKT/NF-κB-dependent signaling pathway [23]. Also, As levels in the serum and testis of rats in the treated experimental groups were significantly higher than those in the control, and a dose-dependent increase has been assessed. In the serum, As concentration ranged from 0.18 to 0.67μg/mL, while in the testes - from 0.35 to 1.74μg/g, respectively. These results suggest a possibility for passing of As through the BTB, which could lead to its accumulation in the rat testes, and subsequently, to a variety of adverse effects on male reproduction [23]. However, no significant effects of the As exposure on the body weight (BW), testis weight (TW) and testicular coefficient (TW/BW) of rats have been established. The described data are important for clarification in some cases of idiopathic male infertility.

Spermatogenesis-related hormonal disruptions

Androgen hormones play a complex and important role in the regulation of spermatogenesis and maturation of male germ cells. The results of experimental studies in rats show many locations where the effects of heavy metals are involved in the dynamics of male sex hormones, mainly in the hypothalamic-pituitary-testicular axis [63].

In the pituitary gland is also possible to be accumulated Hg following exposure to Hg vapour. However, as a Hg exposure giving rise to a mean urinary Hg level of 37 μg/g of creatinine, there was no association between Hg exposure and serum levels of prolactin, thyroid-stimulating hormone, luthenizing hormone (LH) and foliculle-stimulating hormone (FSH) [16]. Decreased TE levels have also been reported in other experiments with rats. Impaired spermatogenesis and decreased TE levels were observed in 7-week-old rats treated with MeHg-chloride by subcutaneous injection at a daily dose of 10 mg/kg for 8 days [22]. Decreased TE levels were reported in animals with mean blood Hg levels of 30.8 ng/ml [39], and in other cases (among 3-month-old rats) observed OS and significant variations of the TE levels with blood mercury concentrations of 94.3 and 176.5 ng/ml [7].

Human studies on the toxic effects of Hg on male reproductive hormones are few and contradictory. A limitation of most epidemiological studies is the small sample size [1]. However, in one large epidemiological study (529 adult men from Greenland, Poland, and Ukraine) about hazardous effects of environmental Hg exposure on the human semen quality and male reproductive hormones, a significant positive

association between blood Hg levels (average whole blood concentration 9.2 ng/ml) with the serum concentrations of inhibin B among the Greenlandic Inuit men has been proved. The authors found that inhibin B serum levels increased with increasing Hg exposure among the Inuit. Usually, the high serum concentrations of inhibin B reflect high activity of the Sertoli cells and high sperm counts, and thus the direction of the association between blood Hg and inhibin B odds with the alleged toxic effects of Hg [36]. In this regard, an *in vitro* study of immature rat Sertoli cells has shown markedly decreased inhibin B levels after Hg exposure at levels far below those causing cellular toxicity [37]. The diet among Greenlandic Inuit is mainly based on seafood and fish that contain polyunsaturated fatty acids (PUFAs), but also accumulates Hg along the aquatic food chain. Authors have reported that levels of omega-3 PUFAs in human sperm are positively correlated with semen characteristics [2], and their positive association between Hg and inhibin B among Greenlandic Inuit may be due to their higher consumption of PUFAs through diet [36]. However, in this study the influence of low Hg levels on the reproduction-related hormones has been evaluated.

Arsenic is an electrophilic element and can bind to the electron-rich sulfhydril groups in proteins and may thus directly modulate the activities of key enzymes involved in TE production. The activity of 17β-HSD, an enzyme involved in TE metabolism, has been established to be decreased from 3.28 units to 1.50 units [8]. Plasma and testicular TE levels decreased by 38.2% and 59.4%, respectively, and plasma LH level decreased by 51.6%. Decreased expression and activities of 3β-HSD and 17β-HSD have been established in rodents administered to low levels of As (20–40 mg/L drinking water) [8, 10]. Several studies have suggested as major targets of As influence the hypothalamus and brain, which could cause hormone dysregulation and decreased sperm concentrations [26]. According to another report, the increasing arsenic level was associated with increased odds for low LH levels, after adjusting for age, BMI and current smoking [35].

In experiments with rats, As has been found to affect the levels of various proteins in the testicular tissue, which play an important role in the synthesis of TE and, accordingly, for the normal course of spermatogenesis. For example, arsenic-induced inhibition of SAFB1 may defect the activity of certain hormone receptors [24]. Corticosteroid 11β-dehydrogenase isozyme 1 (HSD11B1) is an enzyme (located exclusively in Leydig cells in rat testes), generating cortisol by catalyzation of the conversion of inactive cortisone to biologically-active cortisol and involved in this way in the TE production [51] allopregnanolone is the metabolite of progesterone by the actions of enzymes 5α-reductase and 3α-HSD [50]. The As-induced decrease of allopregnanolone levels is associated with the reduction of progesterone - a key intermediate metabolite in TE biosynthesis pathway levels, which would lead to impaired TE synthesis and spermatogenesis, but also to abnormal functions of other biologically-active proteins, described above. Thus, indirect inhibition on the TE synthesis, which then impaired spermatogenesis and produced low-quality sperm in rats, has been proposed on the influence of As [23].

By taking in consideration the ethical limitations, many of the described studies on the reproductive organs have been performed on experimental animals (mainly rodents), where large doses of Hg and As ions have been applied to reveal their influence on cellular and tissue levels. However, the used experimental animal models substantially differ from human occupational and environmental exposure conditions (including that through smoking).

Influence of heavy metals on sperm quality and male fertility

Similarly to other spermato-toxicants, Hg derivatives are also the cause of oligozoospermia, and chronic poisoning with them causes infertility in men. Some studies have reported that high, even low doses of mercury exposure harm men's reproductive health [1, 11, 54]. In most of these studies, the increased blood Hg levels in men were associated with a diet or consumption of more seafood than in people with lower Hg levels [61]. However, human studies are few and contradictory, probably due to different interpretations of the results, which did not always take into account the possibility of exposure to other substances (contaminants) in the food, environment or lifestyle, as well as the small number of men participating in the study. In most of the cases, seminal fluid Hg concentrations are correlated with abnormal sperm morphology and motility [11, 15]. In *in vitro* studies have been demonstrated changes in many bio-physiological parameters of human sperm after treatment with Hg (concentrations from 10.0 to 160.4 mg/L), inducing membrane lipid peroxidation and DNA breaks, decreased sperm motility, viability and lowered rate of the acrosome reaction leading to sperm dysfunction [1]. A large-scale study with subfertile men (111 men from Hong Kong) has shown a correlation of the seminal fluid Hg concentrations (mean level 22.1 ± 2.0 nmol/L) with abnormal sperm morphology, particularly with defects in the head and midpiece, as well as with abnormal sperm motility [11]. Straightline velocity (VSL), linearity (LIN) of the motion path, and amplitude of lateral head displacement (ALH) were reduced, whereas average path velocity (VAP) was increased, depicting that sperm motion lost forward progression and became violently erratic in the presence of higher semen Hg concentrations. Besides, these authors have shared that the men with significantly higher blood Hg concentrations than those in semen (41.4 ± 1.7 nmol/L versus 22.1 ± 2.0 nmol/L) have shown the presence of a functionally-active blood-testis barrier to Hg, but no correlation of the overall percentage of motile spermatozoa and sperm concentration with blood Hg concentrations [11]. In one case with a young man with unexplained infertility, with assessed chronic Hg intoxication (with high blood and urine levels), semen analysis has been connected with severe oligoasthenoteratospermia (or azoospermia) with elevated serum FSH [29]. Thus, Hg may behave as a spermatotoxicant and to impair fertility potential both *in vivo* and in IVF programs, because fertility potential has been shown to be related to sperm morphology and motion [15]. In other small investigations, performed by Swedish, Michigan (USA) and Singapore scientists, no associations between blood or semen MeHg levels and sperm concentration (or total sperm count), motility, chromatin integrity or on the proportion of Y-chromosome bearing sperm [9, 46, 49], and/or significant alterations in reproductive hormone levels [35], have been found, except a study of infertility patients in Singapore [9]. Other case-patients, characterized with high total blood Hg concentrations (14.4 ng/L), have had lower sperm number, as well as percentages of morphologically normal sperm and motile sperm, compared to men, characterized with lower levels (6.3 ng/L) of the same element [31]. The authors, however, have noted no statistically significant differences in sperm parameters probably due to the small number of participants [31]. Taken together, these findings suggest that probably men with somewhat higher blood Hg concentrations (above 8 mg/L) were more likely to have reduced sperm parameters than men with a lower concentration of the element [36]. Many studies with different animal models (mice, rats, monkeys) have also confirmed the toxic effects of Hg on the reproductive system, with adverse effects on seminal parameters (decreased sperm motility, viability and induced DNA breaks in the

spermatozoa) after Hg exposure [7, 22, 42]. Another experiment has shown a decreased sperm number in the rat epididymis after incubation with inorganic Hg, as well as their decreased motility, in a dose-dependent manner [47]. Adult monkeys treated with MeHg orally at doses 50 or 70 mg/kg/day for 20 weeks had a decreased motility and swimming speed sperm (in a dose-dependent fashion) and increased abnormal sperm tail morphology (probably associated with interference in the dynein/microtubule sliding assembly). The percent total tail defects increased significantly in the MeHg treated groups compared to controls (approximately 16% vs. approximately 33% for both treated groups) [36].

According to most of the epidemiological reports, As exposure has also been associated with genotoxicity, increased risk of prostate carcinogenesis, reduced sperm quality, and lead to adverse birth outcomes [5, 62]. Sperm nuclear chromatin showed large amounts of thiol-rich protamines, but their flagellums are also rich in thiol bonds. These groups provide binding sites for As in the sperm nucleus or flagellum, impairing their structure and function. Just a few experimental animal studies available have found the harmful effects of As on parameters of male reproductive health [10, 23, 30]. Significantly reduced sperm motility, sperm viability, and total epididymal sperm counts, as well as the increased percent of germ cells with morphological abnormalities, have been observed in mice, experimentally treated with As [10, 43]. Elevated levels of GPx4, HSD11B1, NASP, and CABS1 lead to produced low-quality sperm, that sperm number and motility have been reduced in As-treated rats [23]. Furthermore the As-induced repression of other proteins such as VDAC3 (voltage-dependent anion channel protein 3), PRKACA (cAMP-dependent protein kinase catalytic subunit alpha), and GPD2 (glycerol-3-phosphate dehydrogenase 2), as well as the aberrant increase of L-tyrosine, may disrupt the extent of protein tyrosine phosphorylation required for sperm capacitation, which then results in fertilization failure and male infertility. Tyrosine phosphorylation of proteins is one of the most common mechanisms, through which several signal transduction pathways in the spermatozoa are adjusted. This mechanism regulates various sperm functions, such as motility, hyperactivation, capacitation, acrosome reaction, and fertilization [27]. It has also been suggested that As could negatively affect the fertilization process by inhibiting the binding and fusion of spermatozoa with the ovum. In this regard, 6 proteins (down-regulated) and 1 metabolite with an elevated level have been studied, which inhibited the fertilization process in arsenic-exposed rats [23]. Besides, decreased expression levels of SPACA1 (sperm acrosome membrane-associated protein 1), ACE (angiotensin-converting enzyme), and SMCP (sperm mitochondrial-associated cysteine-rich protein) in the testis under the influence of As, hinder sperm fertility, has been assessed in the rat. Disruption of SPACA1 levels has also been found to lead to abnormal formation of the sperm head (or globozoospermia), leading to male infertility in mice [18]. Also, antibodies against recombinant SPACA1 inhibit both the binding and the fusion of sperm to zona-free eggs [20]. A germinal ACE knockout in mice has caused a defect in zona pellucida of the oocyte [19]. Li *et al.* reported that the absence of gACE expression is responsible for fertilization failure [32]. Sperm mitochondrial-associated cysteine-rich protein (SMCP) is a constituent of the keratinous capsule surrounding sperm mitochondria that enhances sperm motility. The deletion of SMCP has been found to impair sperm motility, resulting in male germ cells that fail to migrate in the female reproductive tract and to penetrate the egg membranes during fertilization [40]. On the other hand, a possible mechanism for decreased sperm motility might be associated with the direct binding of arsenic to sperm [56].

The studies investigating the effects of As (in natural or low-level exposure) on human male reproductive outcomes are relatively few. Recently, a few epidemiologic studies showed that As-exposure significantly lower sperm quality and causes infertility, as well as erectile dysfunction in men [35]. Another cross-sectional investigation of men attending infertility clinics in Michigan, USA, has indicated a significantly increased risk for low sperm motility in exposure to environmental levels of As (after adjusting for smoking and age) [35]. The odds ratio for low sperm motility with the highest As quartile was 3.80 (1.38–10.4). Arsenic was also a significant risk factor for low semen volume in a multi-metal model. However, the molecular mechanisms underlying As-induced male reproductive dysfunctions are still poorly understood.

Conclusion

As and Hg injure the reproductive system by mechanisms, associated with hormonal regulation and function, binding to sperm and regulation of steroidogenesis, as well as direct effects of testicular component cells. The toxic effects are influenced by the sources, forms and routes, but also by the doses and periods of exposure of these elements. However, the reproductive and developmental toxicity of Hg and As is poorly understood and the molecular mechanisms of the induced reproductive toxicity remains unclear. As-induced dysregulation of series of differential proteins and metabolites (specifically related to male reproduction) could lead to impaired spermatogenesis and sperm function, and/or to male infertility. Arsenic also influences the hypothalamus and brain, which could cause hormone dysregulation and may thus directly modulate the activities of key enzymes involved in TE production. Mercury also induces massive degeneration of germ cells and alterations in the levels of the testosterone. The wide specter of harmful effects in the different tissues and organs is probably due to the activated production of reactive oxygen species and OS, in result of the exposure on high Hg and As levels, together with the influence of other heavy metals.

References

1. **Arabi, M., M. S. Heydarnejad.** *In vitro* mercury exposure on spermatozoa from normospermic individuals. – *Pak. J. Biol. Sci*., **10**, 2007, 2448-2453.
2. **Attaman, J. A., T. L. Toth, J. Furtado, H. Campos, R. Hauser, J. E. Chavarro**. Dietary fat and semen quality amongmen attending a fertility clinic. – *Human Reproduction*, **27**(5), 2012, 1466-1474.
3. **ATSDR.** Toxicological profile for mercury [Update]. Ed. Agency for Toxic Substances and Disease Registry. US Department of Health and Human Services. Public Health Service, Atlanta, GA, USA, 1999.
4. **ATSDR.** Arsenic toxicity case study: What are the physiologic effects of arsenic exposure? Ed. Agency for Toxic Substances and Disease Registry. Environmental Medicine & Environmental Health Education – CSEM, Atlanta, GA, USA, 2013.
5. **Bardach, A., A. Ciapponi, N. Soto, M. R. Chaparro, M. Calderon, A. Briatore, N. Cadoppi, R. Tassara, M. I. Litter.** Epidemiology of chronic disease related to arsenic in Argentina: A systematic review. – *Sci. Total Environ*., **538**, 2015, 802-816.
6. **Beaulieu, H. J., S. Beaulieu, C. Brown.** Phenyl mercuric acetate (PMA): mercury-bearing flexible gymnasium floors in schools – evaluation of hazards and controlled abatement. – *J. Occup. Environ. Hyg*., **5**, 2008, 360-366.

7. **Boujbiha, M. A., K. Hamden, F. Guermazi, A. Bouslama, A. Omezzine, A. Kammound, A. E. Feki.** Testicular toxicity in mercuric chloride treated rats: association with oxidative stress. – *Reprod. Toxicol*., **28**, 2009, 81–89.
8. **Chang, S. I., B. Jin, P. Youn, C. Park, J. D. Park, D. Y. Ryu.** Arsenic-induced toxicity and the protective role of ascorbic acid in mouse testis. – *Toxicol. Appl. Pharmacol*., **218**, 2007, 196-203.
9. **Chia, S. E., C. N. Ong, S. T. Lee, F. H. Tsakok.** Blood concentrations of lead, cadmium, mercury, zinc, and copper and human semen parameters. – *Arch. Androl*., **29**, 1992, 177-183.
10. **Chiou, T. J., S. T. Chu, W. F. Tzeng, Y. C. Huang, C. J. Liao.** Arsenic trioxide impairs spermatogenesis via reducing gene expression levels in testosterone synthesis pathway. – *Chem. Res. Toxicol*., **21**, 2008, 1562-1569.
11. **Choy, C. M., Q. S. Yeung, C. M. Briton-Jones, C. K. Cheung, C. W. Lam, C. J. Haines.** Relationship between semen parameters and mercury concentrations in blood and in seminal fluid from subfertile males in Hong Kong. – *Fertil. Steril*., **78**(2), 2002; 426-428.
12. **Das, H. K., A. Mitra, P. K. Sengupta, A. Hossain, F. Islam, G. H. Rabbani**. Arsenic concentrations in rice, vegetables, and fish in Bangladesh: A preliminary study. – *Environment International*, **30**(3), 2004, 383-387.
13. **Dickman, M. D., K. M. Leung.** Mercury and organochlorine exposure from fish consumption in Hong Kong. – *Chemosphere*, **37**, 1998, 991-1015.
14. **EFSA.** Panel on Contaminants in the Food Chain (CONTAM). Scientific opinion on arsenic in food. – *EFSA Journal* (European Food Safety Authority), **7**(10), 2009, 1351.
15. **Eggert-Kruse, W., H. Schwarz, G. Rohr, T. Demirakca, W. Tilgen, B. Runnebaum.** Sperm morphology assessment using strict criteria and male fertility under *in vivo* conditions of conception. – *Hum. Reprod*., **11**(1), 1996, 139-146.
16. **Erfurth, E. M., A. Schutz, A. Nilsson, L. Barregard, S. Skerfving.** Normal pituitary hormone response to thyrotropin and gonadotropin releasing hormones in subjects exposed to elemental mercury vapour. – *British journal of industrial medicine*, **47**, 1990, 639-644.
17. **Ernst, E., B. Moller-Madsen, G. Danscher.** Ultrastructural demonstration of mercury in Sertoli and Leydig cells of the rat following methyl mercuric chloride or mercuric chloride treatment. – *Reprod. Toxicol*., **5**, 1991, 205-209.
18. **Fujihara, Y., Y. Satouh, N. Inoue, A. Isotani, M. Ikawa, M. Okabe**. SPACA1-deficient male mice are infertile with abnormally shaped sperm heads reminiscent of globozoospermia. – *Development,* **139,** 2012, 3583-3589.
19. **Hagaman, J. R., J.S. Moyer, E.S. Bachman, M. Sibony, P.L. Magyar, J. E. Welch, O. Smithies, J. H. Krege, D.A. O'Brien**. Angiotensin-converting enzyme and male fertility. *Proc. Natl. Acad. Sci., USA*, **95**(5), 1998, 2552-2557.
20. **Hao, Z., M. J. Wolkowicz, J. Shetty, K. Klotz, L. Bolling, B. Sen, V. A. Westbrook, S. Coonrod, C. J. Flickinger, J. C. Herr.** SAMP32, a testis-specific, isoantigenic sperm acrosomal membrane-associated protein. – *Biol. Reprod.*, **66**(3), 2002, 735-744.
21. **Herzog, M., O. Wendling, F. Guillou P. Chambon, M. Mark, R. Losson, Florence Cammas.** TIF1β association with HP1 is essential for post-gastrulation development, but not for Sertoli cell functions during spermatogenesis. – *Dev. Biol*., **350**, 2011, 548-558.
22. **Homma-Takeda, S., Y. Kugenuma, T. Iwamuro, Y. Kumagai, N. Shimojo.** Impairment of spermatogenesis in rats by methylmercury: involvement of stage- and cell-specific germ cell apoptosis. – *Toxicology*, **169**, 2001, 25-35.
23. **Huang, Q., L. Luo, A. Alamdar, J. Zhang, L. Liu, M. Tian, S. A. Musstjab, A. S. Eqani, H. Shen.** Integrated proteomics and metabolomics analysis of rat testis: Mechanism of arsenic-induced male reproductive toxicity. – *Scientific Reports*, **6**, 32518, 2016, 1-12.
24. **Ivanova, M., K. M. Dobrzycka, S. Jiang, K. Michaelis, R. Meyer, K. Kang, B. Adkins, O. A. Barski, S. Zubairy, J. Divisova, A. V. Lee, S. Oesterreich.** Scaffold attachment factor B1 functions in development, growth, and reproduction. - *Mol. Cell. Biol.*, **25**, 2005, 2995–3006.
25. **Jan, A. T., M. Azam, K. Siddiqui, A. Ali, I. Choi, Q. M. Haq**. Heavy metals and human health: mechanistic insight into toxicity and counter defense system of antioxidants. – *Int J Mol Sci*., **16**(12), 2015, 29592-29630
26. **Jana, K., S. Jana, P. K. Samanta.** Effects of chronic exposure to sodium arsenite on hypothalamo-pituitary-testicular activities in adult rats: possible an estrogenic mode of action. – *Reprod. Biol. Endocrinol*., **4**, 2006, 9.

27. **Järup, L.** Hazards of heavy metal contamination. British Medical Bulletin, **68**(1), 2003, 167-182.
28. **Jomova, K., D. Vondrakova, M. Lawson, M. Valko**. Metals, oxidative stress and neurodegenerative disorders. – *Mol Cell Biochem*., **345**(1-2), 2010, 91-104.
29. **Keck, C., G. Bramkamp, E. Ernst, C. Müller, S. Kliesch, E. Nieschlag**. Autometallographic detection of mercury in testicular tissue of an infertile man exposed to mercury vapor. – *Reprod Toxicol.,* **7**(5), 1993, 35-40.
30. **Kim, Y-J., J-M. Kim**. Arsenic Toxicity in Male Reproduction and Development. Dev. Reprod., **19**(4), 2015, 167-180.
31. **Leung, T. Y., C. M. Choy, S. F. Yim, C. W. Lam, C. J. Haines**. Whole blood mercury concentrations in sub-fertile men in Hong Kong. – *Aust. N. Z. J. Obstet. Gynaecol*., **41**, 2001, 75-77.
32. **Li, L. J., F. B. Zhang, S. Y. Liu, Y. H. Tian, F. Le, L. Y. Wang, H. Y. Lou, X. R. Xu, H. F. Huang, F. Jin.** Human sperm devoid of germinal angiotensin-converting enzyme is responsible for total fertilization failure and lower fertilization rates by conventional *in vitro* fertilization. – *Biol. Reprod.*, **90,** 2014, 125.
33. **Mahaffey, K. R., R. P. Clickner, C. C. Bodurow.** Blood organic mercury and dietary mercury intake: national health and nutrition examination survey, 1999 and 2000. – *Environ. Health Perspect*, **112**, 2004, 562-570.
34. **Mehrpour, O., P. Karrari, N. Zamani, A. M. Tsatsak, M. Abdollahi**. Occupational exposure to pesticides and consequences on male semen and fertility: a review. – Toxicol Lett. 2014;230(2):146-156
35. **Meeker, J. D., M. Rossano, B. M. Protas, V. Padmanahban, M. P. Diamond, E. Puscheck, D. Daly, N. Paneth, J. J. Wirth.** Environmental exposure to metal and male reproductive hormones: circulating testosterone is inversely associated with blood molybdenum. – *Fertil. Steril*., **93**, 2008, 130-140.
36. **Mocevic, E., I. O. Specht, J. L. Marott, A. Giwercman, B. A. G. Jönsson, G. Toft, T. Lundh, J. P. Bonde.** Environmental mercury exposure, semen quality and reproductive hormones in Greenlandic Inuit and European men: a cross-sectional study. – *Asian J. Androl.*, **15**, 2013, 97-104.
37. **Monsees, T. K., M. Franz, S. Gebhardt, U. Winterstein, W. B. Schill, J. Hayatpour**. Sertoli cells as a target for reproductive hazards. – *Andrologia*, **32**(4-5), 2000, 239-246.
38. **Morais, S., F. G. Costa, M. D. Pereira**. Heavy metals and human health. – *Environment Health*, **10**, 2012, 227-246.
39. **Moussa, H., L. Hachfi, M. Trimeche, M. F. Najjar, R. Sakly**. Accumulation of mercury and its effects on testicular functions in rats intoxicated orally by methylmercury. – *Andrologia*, **43,** 2011, 23-27.
40. **Nayernia, K.**, **I. M. Adham, E. Burkhardt-Göttges, J. Neesen, M. Rieche, S. Wolf, U. Sancken, K. Kleene, W. Engel.** Asthenozoospermia in mice with a targeted deletion of the sperm mitochondria-associated cysteine-rich protein (Smcp) gene. – *Mol. Cell. Biol.*, **22**, 2002, 3046-3052.
41. **Nickson, R., J. McArthur, W. Burgess, K. M. Ahmed, P. Ravenscroft, M. Rahman**. Arsenic poisoning of Bangladesh groundwater. Nature 395(6700), 1998, 338.
42. **Orisakwe, O. E., O. J. Afonne, E. Nwobodo, L. Asomugha, C. E. Dioka.** Low-dose mercury induces testicular damage protected by zinc in mice. – *Eur. J. Obstet. Gynecol. Reprod. Biol*., **95**, 2001, 92-96.
43. **Pant, N., R. Kumar, R. C. Murthy, S. P. Srivastava.** Male reproductive effect of arsenic in mice. – *Biometals*, **14**, 2001, 113–117.
44. **Puglisi, R., A. Bevilacqua, G. Carlomagno, A. Lenzi, L. Gandini, M. Stefanini, F. Mangia, C. Boitani.** Mice overexpressing the mitochondrial phospholipid hydroperoxide glutathione peroxidase in male germ cells show abnormal spermatogenesis and reduced fertility. – *Endocrinology,* **148**, 2007, 4302-4309.
45. **Rajan, N., W. K. Sung, D. S. Goodman.** Localization of cellular retinol-binding protein mRNA in rat testis and epididymis and its stage-dependent expression during the cycle of the seminiferous epithelium. – *Biol. Reprod.*, **43**, 1990, 835-842.
46. **Ramamoorthi, R. V., M. G. Rossano, N. Paneth, J. C. Gardiner, M. P. Diamond, E. Puscheck, D. C. Daly, R. C. Potter, J. J. Wirth.** An application of multivariate ranks to assess effects from combining factors: metal exposures and semen analysis outcomes. – Stat. Med., **27**, 2008, 3503-3514.

47. **Rao, M. V., B. Gangadharan.** Antioxidative potential of melatonin against mercury induced intoxication in spermatozoa *in vitro*. – *Toxicol. In Vitro*, **22**, 2008, 935-942.
48. **Ratnaike**, **R. N**. Acute and chronic arsenic toxicity. – *Postgraduate Medical Journal,* **79** (933), 2003, 391-396.
49. **Rignell-Hydbom, A., A. Axmon, T. Lundh, B. A. Jonsson, T. Tiido, M. Spano.** Dietary exposure to methyl mercury and PCB and the associations with semen parameters among Swedish fishermen. – *Environ. Health*, **6**, 2007, 14.
50. **Santoru, F., R. Berretti, A. Locci, P. Porcu, A. Concas.** Decreased allopregnanolone induced by hormonal contraceptives is associated with a reduction in social behavior and sexual motivation in female rats. – *Psychopharmacology*, **231**, 2014, 3351-3364.
51. **Sharp, V., L. M. Thurston, R. C. Fowkes, A. E. Michael.** 11β-Hydroxysteroid dehydrogenase enzymes in the testis and male reproductive tract of the boar (*Sus scrofa domestica*) indicate local roles for glucocorticoids in male reproductive physiology. – *Reproduction*, **134**, 2007, 473-482.
52. **Stanton, P. G., P. Sluka, C. F. H. Foo, A. N. Stephens, A. I. Smith, R. I. McLachlan, L. O'Donnell.** Proteomic changes in rat spermatogenesis in response to *in vivo* androgen manipulation impact on meiotic cells. – *PLoS One*, **7**, 2012, e41718.
53. **Taha, E. A., S. K. Sayed, N. M. Ghandour, A. M. Mahran, M. A. Saleh, M. M. Amin, R. Shamloul**. Correlation between seminal lead and cadmium and seminal parameters in idiopathic oligoasthenozoospermic males. – *Cent Eur J Urol*., **66**, 2013, 84.
54. **Tan, S. W., J. C. Meiller, K. R. Mahaffey.** The endocrine effects of mercury in humans and wildlife. – *Crit. Rev. Toxicol*., **39**, 2009, 228-269.
55. **Terada, K., K. Yomogida, T. Imai, H. Kiyonari, N. Takeda, T. Kadomatsu, M. Yano, S. Aizawa, M. Mori.** A type I DnaJ homolog, DjA1, regulates androgen receptor signaling and spermatogenesis. – *EMBO J*., **24**, 2005, 611-622.
56. **Uckun, F. M., X. P. Liu, O. J. D'Cruz.** Human sperm immobilizing activity of aminophenyl arsenic acid and its N-substituted quinazoline, pyrimidine, and purine derivatives: Protective effect of glutathione. – *Reprod. Toxicol*., **16**, 2002, 57-64.
57. **Ueki, K., T. Kondo, Y. H. Tseng, C. R. Kahn.** Central role of suppressors of cytokine signaling proteins in hepatic steatosis, insulin resistance, and the metabolic syndrome in the mouse. – *Proc. Natl. Acad. Sci. USA*, **101** (28), 2004, 10422-10427.
58. **Vachhrajani, K. D., A. R. Chowdhury.** Distribution of mercury and evaluation of testicular steroidogenesis in mercuric chloride and methylmercury administered rats. – *Indian J. Exp. Biol*., **28**, 1990, 746-751.
59. **Vallascas, E., A. De Micco, F. Deiana, S. Banni, E. Sanna**. Adipose tissue: another target organ for lead accumulation? A study on Sardinian children (Italy). – *Am. J. Hum. Biol*., **25**(6), 2013, 789-794.
60. **Weber, P., F. Cammas, C. Gerard, D. Metzger, P. Chambon, R. Losson, M. Mark.** Germ cell expression of the transcriptional co-repressor TIF1beta is required for the maintenance of spermatogenesis in the mouse. – *Development*, **129**, 2002, 2329-2337.
61. **Wirth, J. J., R. Mijal.** Adverse effects of low level heavy metal exposure on male reproductive function. – *Systems Biology in Reproductive Medicine,* **56**(2), 2010, 147-167.
62. **Xu, D. X., H. M. Shen, Q. X. Zhu, L. Chua, Q. N. Wang, S. E. Chia, C. N. Ong**. The associations among semen quality, oxidative DNA damage in human spermatozoa and concentrations of cadmium, lead and selenium in seminal plasma. – *Mutat. Res/Gen. Tox. En*., **534**(1-2), 2003, 155-163.
63. **Xu, W., H. Bao, F. Liu, L. Liu, Y-G. Zhu, J. She, S. Dong, M. Cai, L. Li, C. Li, H. Shen.** Environmental exposure to arsenic may reduce human semen quality: associations derived from a Chinese crosssectional study. – *Environ. Health,* **11**, 2012, 46.
64. **Yiu, G. K., N. B. Hecht.** Novel testis-specific protein-DNA interactions activate transcription of the mouse protamine 2 gene during spermatogenesis. – *J. Biol. Chem*., **272**, 1997, 26926-26933.
65. **Zhang, Z. H., H. B. Zhu, L. L. Li, Y. Yu, H. G. Zhang, R. Z. Liu**. Decline of semen quality and increase of leukocytes with cigarette smoking in infertile men. – *Iranian J. Reprod. Med*., **11**(7), 2013, 589.

Institute of Experimental Morphology, Pathology and Anthropology with Museum
Bulgarian Anatomical Society

Acta morphologica et anthropologica, 28 (1-2)
Sofia ● 2021

Relationship Between Ganglioside Metabolism and the Development of Metabolic Syndrome and its Complications

Vera Kolyovska, Iskra Sainova*

Institute of Experimental Morphology, Pathology and Anthropology with Museum, Bulgarian Academy of Sciences, Sofia

* Corresponding author e-mail: verakol@abv.bg

Gangliosides are important biological molecules, performing functions as key regulators of many physiological processes on cellular, tissue, organ and organism level. These substances have shown a large structural heterogeneity, mainly in result from differences in number, identity, linkage and anomeric configuration of the carbohydrate residues, as well as from some structural differences. Relationship between the values of different gangliosides, the titers of specific auto-antibodies to each one ganglioside and the pathology of multi-factor socially important diseases and disorders has been underlined. These bio-molecules, as well as the interactions with their participation, or even lack of gangliosides in separate cases, are underlining the final clinical picture. Based on the deviation levels of ganglioside GM3 in some abnormalities of the glucose and lipid metabolism, the serum levels of GM3 are characterized as a marker for the severity of metabolic syndrome.

Key words: gangliosides, cascade regulatory pathways, socially important diseases and disorders, metabolic syndrome.

Introduction

Gangliosides are complex acidic glycosphingolipids, containing one or more sugar residues, attached to a sphingolipid moiety, usually to a ceramide, but in rare cases also to a sphingoid base [13]. A large structural heterogeneity has been found to result from differences in number, identity, linkage and anomeric configuration of the carbohydrate residues, as well as from some structural differences, particularly within the hydrophobic part. These molecules have been characterized as key regulators of many physiological processes on cellular, tissue, organ and organism level. Although the structures of gangliosides have been assigned to only a few series with a common carbohydrate core, their structural variety and the complex pattern are challenges for their elucidation and quantification by mass spectrometric techniques [8]. The alterations in the metabolism of gangliosides have been determined as one of the earliest changes, associated with the diabetic pathology [9, 13, 43]. Besides in free form, each ganglioside has been found to exist in various bounded forms with different bio-molecules, depending of the

respective functions, in which it participates [4, 7, 25-27, 52, 59]. In addition, cross-reactions of specific antibodies to each ganglioside with other biological molecules have also been suggested. Furthermore, these studies show a possibility for production of immunoglobulins/antibodies by non-lymphoid types of cells, tissues and organs [18, 37]. The control of the activity of the so produced antibodies is very important. Namely gangliosides have been proved also as small molecules, which provide such control.

Gangliosides, Obesity and Metabolic Syndrome. Ganglioside GM3 has been found to function as a physiological regulatory factor of the balance between homeostatic and pathological states in adipocytes by modulating insulin signaling in lipid rafts [35]. In order to counteract obesity-related metabolic disorders, the importance of therapies targeting GM3 biosynthesis has been highlighted [26]. The role of this ganglioside in mediation of obesity-induced perturbations in metabolic function, including impaired insulin action, has been particularly underlined. A probability of development of insulin resistance in increased levels of GM3 in the visceral adipose tissue of obese humans has been proposed [58]. In this connection, therapeutic strategies, aimed at targeting biosynthesis of this ganglioside for counteraction to obesity-induced metabolic perturbations, as well as of other manifestations of the metabolic syndrome, have been suggested. Several candidate-proteins, which may be involved in the generation of NeuGc (N-glycolyl) GM3 have been revealed, particularly GM3 synthase and subunit B of respiratory complex II (SDHB) [5]. Significant changes in quantity and quality of gangliosides (particularly GM3) in each stage of differentiation of mouse C2C12 myoblasts have been found [15]. According to other studies, induced down-regulation of enzyme NEU3 sialidase in the same mouse cells has totally inhibited the capability of these cells to differentiate by increasing the GM3 level above a critical point [2, 19]. The authors have also proposed that influence on the functions of epidermal growth factor receptor (EGFR) could probably lead to activated responsiveness of the myoblasts to apoptotic stimuli. GM3, as well as the enzymes, involved in its metabolism, have been characterized as the best "candidates", correlating with a number of metabolic disease risk factors as autotaxin, LDL-c and homeostatic model assessment insulin resistance [6, 55]. These data have been supported by the established metabolic abnormalities in *Rhesus macaques*, subjected to high-fat and high-fructose Western-style diet [6]. Based on the deviation levels of GM3 in some abnormalities of the glucose and lipid metabolism, the serum levels of GM3 are characterized as a marker for the severity of metabolic syndrome [44]. In this aspect, the role of GM3 as a negative regulator of insulin signaling has confirmed it as a potential therapeutic target in type II *Diabetes mellitus* [60]. The role of GM3 in mediating obesity-induced perturbations in metabolic function, including impaired insulin action has been proved [26].

***Gangliosides and Diabetes*.** The synthesis of gangliosides has been suggested as an important pathway for glucose utilization in early stages of some diabetic complications as diabetic nephropathy [38]. These molecules have also been proved as mediators of the insulin resistance. Reports about correlation of alterations in their levels, types, distribution and metabolism with diabetes, including its autoimmune form, have also been obtained [28, 31, 32, 54]. In this way, gangliosides have been suggested as antigens, playing a role of targets for specific auto-antibodies in diabetic patients [14]. a-Series gangliosides are mediators of the effects of advanced glycation end products (AGEs). Their participation in some pathological and degenerative consequences of

diabetes, as diabetic retinopathy and diabetic nephropathy, has been suggested [28]. AGEs have also been proposed to be involved in the micro-vascular alterations in some diabetic complications as diabetic retinopathy [36]. In non-obese diabetic (NOD) mice increased titers of the islet cell antibodies (ICA) have been observed, and the distribution of beta-cells has been found as associated with a significant decrease in the amounts of gangliosides GM1 and GM2 in their pancreas, unlike of C57BL/10 mice [11]. Significant correlation of the increased production of plasma ceramides with the decline in insulin sensitivity has been established [6]. In this aspect, particularly the increased values of ganglioside GM3 have been supposed to participate in the development of the insulin resistance and in this way – in the pathogenesis of diabetes [20, 23, 26, 51]. Affected serum GM3 levels have been established in abnormalities in the glucose and lipid metabolism [45]. Additionally, the depletion of the same ganglioside, as well as of enzymes, responsible for its synthesis, has been found to protect against different pathological and degenerative consequences of diabetes [30, 41, 57]. In this relation, GM3 has been determined as a pathophysiological mediator in the development of diabetic nephropathy [38, 56]. On the other hand, ganglioside GM1 has been determined as an attractive target for detection, prevention and treatment of insulin resistance, of subsequent diabetes development, as well as of related complications, probably by abundant activity of this ganglioside on the surface of endothelial cells [44, 66]. In this regard, a possibility for improvement of both insulin sensitivity and glucose homeostasis by glycosphingolipid synthesis inhibition has been suggested as a novel therapeutic approach for the treatment of type 2 diabetes [67]. Based on the deviation levels of GM3 in some abnormalities of the glucose and lipid metabolism, the serum levels of GM3 are characterized as a marker for the severity of metabolic syndrome [45]. Additionally, the role of GM1 in the activation of mediated by NO vasodilatation has been proved [13]. Taking in consideration the established nature of tyrosine kinase substrate p58/p53 and the insulin receptor as components of central nervous system (CNS) synapses, a role of the insulin signaling at these synapses has been proved [1]. Increased risk for development of type 2 diabetes in patients with *Alzheimer's* disease has also been assessed, caused by general mechanism, underlining loss of β-cells and brain cells, respectively [21].

Gangliosides and Neurodegenerative Complications. The influence of gangliosides, but also the correlation of their levels, distribution and metabolism, on the development, structure and functions of the neural system and brain, have been proved [10, 61]. Due to their amphiphilic nature, gangliosides have been found localized to the cellular membranes, and many of their functions in health and disease have been established to result from both membrane reorganization and lipid interaction with proteins within the membrane structures [10]. The injuries in the levels, synthesis, degradation and metabolism of gangliosides have been proved as main signs of the early development of the neuro-degenerative diseases and disorders, as well as for understanding of the pathological mechanisms, underlining these processes [3, 17, 59]. Brain ganglioside content and composition, but also the metabolism of these bio-molecules, have been found to be altered in *Alzheimer's* disease. Changes in the neuron membrane physico-chemical properties have been proposed as a consequence of primary pathology, which might also be involved in the early pathogenesis of this neuro-degenerative disorder through documented effects on proteolytic processing and amyloid aggregation of

amyloid-precursor protein (APP). In *Parkinson's* and *Huntington's* diseases, significant alterations in the levels, distribution and metabolic pathways of gangliosides have also been established [10]. These results could be confirmed by data for the proved role of ganglioside GM1 in the promotion of neurite outgrowth signal [19, 59, 64]. Binding of GM1 to laminin-1 leads to activation of NGF-TrkA signaling pathway. This mechanism has been supposed as underlining the processes, described above. The role of auto-antibodies to gangliosides in the development of many neuropathies has also been proved [27, 54]. Furthermore, most of the anti-ganglioside antibodies have shown anti-sulfatide reactivity distinct from the other known antibodies, which has been proposed as one of the factors in demyelinating neuropathies development [29]. The appearance of anti-sulfatide, but also of anti-GM1 and anti-GM2 IgM auto-antibodies have been associated with immune-mediated neuropathies in younger age [24]. In many cases, the role of GM1 in modulation of Trk and Erk kinases phosphorylation and activity in the brain has been established [12, 33]. Namely the proved tight association of GM1 with Trk has determined this ganglioside as a specific endogenous activator of the neuronal growth factor (NGF) receptor function [34]. A novel mechanism of neuronal apoptosis, mediated by GM1 accumulation has also been proposed [53]. Participation of ganglioside GM3 as a mediator in the neuronal cell death has also been proved [50].

Gangliosides and Vascular Complications. Gangliosides have been established to be primarily but not exclusively, localized in the outer leaflets of plasma membranes of the cells, and they have been characterized as integral components of cell surface microdomains with sphingomyelin and cholesterol, from which they participate in cell-to-cell recognition, adhesion and signal transduction [62]. In many cases, alterations in the levels of this ganglioside GM3, as well as in its metabolism, have been associated with obesity, type 2 diabetes, metabolic syndrome, atherosclerosis and hypertension [54]. A correlation of the increased cellular levels of GM3 in monocytes and lymphocytes in atherosclerosis with cell activation, facilitating their adhesion to endothelial cells and penetration into the *tunica intima*, has been suggested [16]. In this connection, GM3 has been suggested to be significantly correlated with the thickness of *tunica intima* and *tunica media*, which is often used for detection of atherosclerotic disease, as well as with many connected with the same disorder risk factors as LDL and insulin resistance [55]. Biologically-relevant GM1 concentrations have been found to lead to submicron-sized domains in a cholesterol-rich liquid-ordered phase [65]. Eventual existence of small ganglioside-rich microdomain within a larger ordered domain in both natural and model membranes has been proposed [62, 63].

Gangliosides and Cholestatic Complications. Most of the normal serum gangliosides have been found to be synthesized in the liver [46, 48]. However, this anatomic organ has also been characterized as the main source of elevated levels of serum gangliosides in many liver diseases and disorders [46, 47]. Changes in the synthesis and/or distribution of gangliosides within the hepatocytes have been established due to estrogen-induced cholestasis, probably as a consequence of oxidative stress, but also the detergent properties of highly-concentrated bile acids [40, 49]. In this way, the authors have proposed a general mechanism of hepatoprotection by the gangliosides. These data have been confirmed by the observed significant changes in the distribution and synthesis of liver gangliosides, accompanying the cholestasis, in particular its obstructive form. Similar effects have been observed in the livers

of rats with experimentally-induced diabetes by treatment with Streptozotocin [43]. Also, changes in the molecular sub-species of ganglioside GM3 in human liver during the aging have been noted [39, 42]. Enhanced production of ganglioside GM1 at the sinusoidal membrane has been proposed to be due to re-distribution of cellular GM1 at limited biosynthesis and thus, could be responsible for protection of hepatocytes against harmful effects of bile acids, accumulated during the process of cholestasis [22]. In liver diseases deviations in the total concentration, pattern and distribution of serum gangliosides to different lipoprotein classes have been supposed [46]. These changes are probably due to qualitative and quantitative alterations in biosynthesis of gangliosides and secretion into the circulation (in cirrhosis), and lipoprotein metabolism alterations following cholestasis.

Conclusion

Gangliosides perform important role as key regulators in many physiological processes on cellular, tissue, organ and organism level. Disbalance in their values, as well as of different molecules, participating in their metabolism by cascade regulatory pathways, has been implicated in the pathology of multi-factor socially important diseases and disorders. On the other hand, the deviations, connected with the type, values and distribution of respective ganglioside and/or of various molecules, participating in its metabolism, could lead to development of various diseases and disorders. These molecules and the interactions between them or even lack of gangliosides in separate cases could lead to the final clinical picture. In this way, monitoring of the quantity and quality changes of gangliosides could be usable for determination the eventual risk for the metabolic syndrome development and expression.

References

1. **Abbott, M.-A., D. G. Wells, J. R. Fallon**. The insulin receptor tyrosine kinase substrate p58/p53 and the insulin receptor are components of CNS synapses. – *J. Neurosci*., **19**, 1999, 7300-7308.
2. **Anastasia, L., N. Pipini, F. Colazzo, G. Palazzolo, C. Tringali, L. Dileo, M. Piccoli, E. Conforti, C. Sitzia, E. Monti, M. Sampaolesi, G. Tettamanti, B. Venerando**. NEU3 sialidase strictly modulates GM3 levels in skeletal myoblasts C2C12 thus favoring their differentiation and protecting them from apoptosis. – *J. Biol. Chem*., **283**, 2008, 36265-36271.
3. **Ariga, T., C. Wakade, R. K. Wu**. The pathological roles of ganglioside metabolism in *Alzheimer's* disease: effects of gangliosides on neurogenesis. – *Int. J. Alzheimer's Disease*, 2011, 193618.
4. **Barnes, S., Y. Sun, G. A. Grabowski**. Multi-system disorders of glycophospholipid and ganglioside metabolism. – *J. Lipid Res*., **51**, 2010, 1643-1675.
5. **Bosquet, P. A., J. A. Sandvik, N. F. J. Edin, U. Krengel**. Hypothesis: hypoxia induces *de novo* synthesis of NeuGc gangliosides in humans. – *Biochem. Biophys. Res. Commun*., **495**, 2018, 1562-1566.
6. **Brozinick, J. T., F. Hawkins, H. H. Bui, M.-S. Kuo, B. Tan, P. Krevit, K. Grove**. Plasma sphingolipids are biomarkers of metabolic syndrome in non-human primates maintained on Western-style diet. – *Internat. J. Obes*., **37**, 2013, 1064-1070.
7. **Canals, D., R. W. Jenkins, P. Roddy, M. J. Hernández-Corbacho, L. M. Obeid, Y. A. Hannun**. Differential effects of ceramide and sphingosine 1-phosphate on ERM phosphorylation. Probing sphingolipid signaling at the outer plasma membrane. – *J. Biol. Chem*., **285**, 2010, 32476-32485.

8. **Caughlin, S., J .D. Hepburn, D. H. Park, K. Jurcic, K. K. Yeung, D. F. Cechetto, S. N. Whitehead**. Increased expression of simple ganglioside species GM2 and GM3 detected by MALDI imaging mass spectrometry in a combined rat model of Aβ toxicity and stroke. – *PLoS One*, **10**, 2015, e0130364.
9. **de Chavez, J. A., M. M. Siddique, S. T. Wang, J. Ching, J. A. Shayman, S. A. Summers**. Ceramides and glycoceramides are independent antagonists in insulin signaling. – *J. Biol. Chem*., **289**, 2014, 723-734.
10. **de Chaves, E. P., S. Sipione**. Shingolipids and gangliosides of the nervous system in membrane function and dysfunction. – *FEBS Lett*., **584**, 2010, 1748-1759.
11. **Dotta, F., L. B. Peterson, M. Previty, J. Metzger, C. Tiberti, E. Anastasi, P. Zoppitelli, L. S. Wicker, U. Di Mario**. Pancreatic islet ganglioside expression in nonobese diabetic mice: comparison with C57BL/10 mice and changes after autoimmune beta-cell destruction. – *Endocrinol*., **130**, 1992, 37-42.
12. **Duchemin, A.-M., Q. Ren, L. Mo, N. H. Neff, M. Hadjiconstantinou**. GM1 ganglioside induces phosphorylation and activation of Trk and Erk in brain. – *J. Neurochem*., **81**, 2002, 696-707.
13. **Farwanah, H., T. Kolter**. Lipidomics of glycosphingolipids. – *Metabolites*, **2**, 2012, 134-164.
14. **Gillard, B. K., J. W. Thomas, L. J. Nell, D. M. Marcus**. Antibodies against ganglioside GT3 in the sera of patients with type I *Diabetes mellitus*. – *J. Immunol*., **142**, 1989, 3826-3832.
15. **Go, S., S. Go, L. Veillon, M. G. Ciampa, L. Mauri, C. Sato, K. Kitajima, A. Prinetti, S. Sonnino, J.-I. Inokuchi**. Altered expression of ganglioside GM3 molecular species and potential regulatory role during myoblast differentiation. – *J. Biol. Chem*., **292**(17), 2018, 7040-7051.
16. **Gracheva, E. V., N. N. Samovilova, G. F. Piksina, V. S. Shishkina, N. V. Prokazova**. Activation of ganglioside GM3 biosynthesis in human blood mononuclear cells in atherosclerosis. - *Biomed. Khim*., **59**, 2013, 459-468.
17. **Grimm, M. O. W., E. G. Zinser, S. Grosgen, B. Hundsdorfer, T. L. Rothhaar, V. K. Burg, L. Kaestner, T. A. Bayer, P. Lipp, U. Muller, H. S. Grimm, T. Hartmann**. Amyloid precursor protein (APP) mediated regulation of ganglioside homeostasis linking *Alzheimer's* disease pathology with ganglioside metabolism. – *PLoS One*, **7**, 2012, e34095.
18. **Gunasekaran, M., P. K. Chatterjee, A. Shih, G. H. Imperato, M. Addorisio, G. Kumar, A. Lee, J. F. Graf, D. Meyer, M. Marino, C. Puleo, J. Ashe, M. A. Cox, T. W. Mak, C. Bouton, B. Sherry, B. Diamond, U. Andersson, T. R. Coleman, C.N. Metz, K. J. Tracey, S. S. Chavan**. Immunization elicits antigen-specific antibody sequestration in dorsal root ganglia sensory neurons. – *Front. Immunol*., **9**, 2018, 638.
19. **Ichikawa, N., K. Iwabuchi, H. Kurihara, K. Ishii, T. Kobayashi, T. Sasaki, N. Hattori, Y. Mizuno, K. Hozumi, Y. Yamada, E. Hirasawa-Arikawa**. Binding of laminin-1 to monosialoganglioside GM1 in lipid rafts is crucial for neurite outgrowth. – *J. Cell. Sci*., **122**, 2008, 289-299.
20. **Inokuchi, J.-I.** GM3 and diabetes. – *Glycoconj. J*., **31**, 2014, 193-197.
21. **Janson, J., T. Laedtke, J. E. Parisi, P. O'Brien, R. C. Petersen, P. C. Butler**. Increased risk of type 2 diabetes in *Alzheimer* disease. – *Diabetes*, **53**, 2004, 474-481.
22. **Jirkovská, M., F. Majer, J. Šmídová, J. Stříteský, G. M. Shaik, P. Dráber, L. Vítek, Z. Mareček, F. Šmíd**. Changes in GM1 ganglioside content and localization in cholestatic rat liver. – *Glycoconj. J*., **24**, 2007, 231-241.
23. **Kabayama, K., T. Sato, K. Saito, N. Loberto, A. Prinetti, S. Sonnino, M. Kinjo, Y. Igarashi, J.-I. Inokuchi**. Dissociation of insulin receptor and calveolin-1 complex by ganglioside GM3 in the state of insulin resistance. – *Proc. Natl. Acad. Sci. U.S.A*., **104**, 2007, 13678-13683.
24. **Klehmet, J., S. Märschenz, K. Ruprehct, B. Wunderlich, T. Büttner, R. Heimann, D. Roggenbuck, A. Meisel**. Analysis of anti-ganglioside antibodies by a line immunoassay in patients with chronic-inflammatory demyelinating polyneuropathies (CIDP). – *Clin. Chem. Lab. Med*., **56**(6), 2018, 919-926.
25. **Krengel, U., L.-L. Olsson, C. Martinez, A. Talavera, G. Rojas, E. Mier, A. Ångstrom, E. Moreno**. Structure and molecular interactions of unique antitumor antibody specific for *N*-glycol GM3. – *J. Biol. Chem*., **279**, 2004, 5597-5603.
26. **Lipina, C., H. S. Hundal**. Ganglioside GM3 as a gatekeeper of obesity-associated insulin resistance: evidence and mechanisms. – *FEBS Lett*., **589**, 2015, 3221-3227.

27. **Lunn, M. P. T., L. A. Johnson, S. E. Fromholt, S. Itonori, J. Huang, A. A. Vyas, J. E. K. Hildreth, J. W. Griffin, R. L. Shnaar, K. A. Sheikh**. High-affinity anti-ganglioside IgG antibodies raised in complex ganglioside knockdown mice: reexamination of GD1a immunolocalization. – *J. Neurochem*., **75**, 2000, 404-412.
28. **Masson, E., L. Troncy, D. Russiero, N. Wiernsperger, M. Lagarde, S. El Balab**. a-Series gangliosides mediate the effects of advanced glycation end products on pericyte and mesangial cell proliferation. – *Diabetes*, **54**, 2005, 220-227.
29. **Meehan, G. R., R. McGonigal, M. E. Cunningham, Y. Wang, J. A. Barrie, S. K. Halstead, D. Gourlay, D. Yao, H.J. Willison**. Differential binding patterns of anti-sulfatide antibodies to glial membranes. – *J. Neuroimmunol*., **323**, 2018, 28-35.
30. **Menichella, D. M., N. D. Jayaraj, H. M. Wilson, D. Ren, K. Flood, X.-Q. Wang, A. Shum, R. J. Miller, A. S. Paller**. Ganglioside GM3 synthase depletion reverses neuropathic pain and small fiber neuropathy in died-induced diabetic mice. – *Molec. Pain*, **12**, 2016, 1-10.
31. **Misasi, R., S. Dionisi, L. Farilla, B. Carabba, L. Lenti, U. Di Maro, F. Dotta**. Gangliosides and autoimmune diabetes. – *Diab. Metab. Rev*., **13**, 1997, 163-179.
32. **Morano, S., C. Tiberti, G. Cristina, M. Sensi, R. Cipriani, L. Guidobaldi, P. Torresi, F. Medici, E. Anastasi, U. Di Mario**. Autoimmune markers and neurological complications in non-insulin-dependent *Diabetes mellitus*. – *Hum. Immunol*., **60**, 1999, 848-854.
33. **Mukherjee, P., A. Faber, L. Shelton, R. Baek, T. Chiles, T. Seyfried**. Ganglioside GM3 suppresses the proangiogenic effects of vascular endothelial growth factor and ganglioside GD1a. - *J. Lipid Res*., **49**, 2008, 929-938.
34. **Mutoh, T., A. Tokuda, T. Miyadai, M. Hamagushi, N. Fujiki**. Ganglioside GM1 binds to the Trk protein and regulates receptor function. – *Proc. Natl. Acad. Sci. U.S.A*., **92**, 1995, 5087-5091.
35. **Nagafuku, M., T. Sato, S. Sato, K. Shimizu, T. Taira, J.-I. Inokuchi**. Control of homeostatic and pathogenic balance in adipose tissue by ganglioside GM3. – *Glycobiol*., **25**, 2015, 303-318.
36. **Natalizio, A., D. Ruggiero, M. Lacomte, M. Lagarde, N. Wiernsperger**. Glycosphingolipid changes induced by advanced glycation end products. – *Biochem. Biophys. Res. Commun*., **281**, 2001, 78-83.
37. **Nematpour, F., F. Mahboudi, V. Khalaj, B. Vaziri, S. Ahmadi, S. Ebadat, F. Davami**. Optimization of monoclonal antibody expression in CHO cells by employing epigenetic gene regulation tools. – *Turk. J. Biol*., **41**, 2018, 622-628.
38. **Novak, A., M. N. Rezic, C. V. Cikes, J. Bozic, K. T. Ticinovic, L. Ferhatovic, L. Puljak, A. Markotic**. Renal distribution of ganglioside GM3 in rat models of types 1 and 2 diabetes. – *J. Physiol. Biochem*., **69**, 2013, 727-735.
39. **Özkök, E., S. Cengiz, B. Güvener**. Age dependent changes in liver ganglioside levels. – *J. Bas. Clin. Physiol. Pharmacol*., **10**, 2011, 337-344.
40. **Petr, T., V. Šmid, V. Kucerova, K. Vanova, M. Lenicek, L. Vitek, F. Šmid, L. Muchova**. The effect of Heme oxygenase on ganglioside distribution in hepatocytes in experimental estrogen-induced cholestasis. – *Physiol. Res*., **63**, 2014, 359-367.
41. **Randeria, P. S., M. A. Seeger, X.-Q. Wang, H. Wilson, D. Shipp, C. A. Mirkin, A. S. Paller**. siRNA-based spherical nucleic acids reverse impared wound healing in diabetic mice by ganglioside GM3 synthase knockdown. – *Proc. Natl. Acad. Sci. U.S.A*., **112**, 2015, 5573-5578.
42. **Riboni, L., D. Acquotti, R. Casellato, R. Ghidoni, G. Montagnolo, A. Benevento, F. Rubino, S. Sonnino**. Changes in the human liver GM3 ganglioside molecular species during aging. – *Eur. J. Biochem*., **203**, 1992, 107-113.
43. **Sánchez, S. S., A. V. Abregú, M. J. Aybar, R. A. N. Sánchez**. Changes in liver gangliosides in streptozotocin-induced diabetic rats. – *Cell. Viol. Int*., **24**, 2000, 897-904.
44. **Sasaki, N., Y. Itakura, M. Toyoda**. Ganglioside GM1 contributes to the state of insulin resistance in senescent human endothelial cells. – *J. Biol. Chem*., **290**, 2015, 25475-25486.
45. **Sato, T., Y. Nihei, M. Nagafuku, S. Tagami, R. Chin, M. Kawamura, S. Miyazaki, M. Suzuki, S. Sagahara, Y. Takahashi, A. Saito, Y. Igarashi, J.-I. Inokuchi**. Circulation levels of ganglioside GM3 in metabolic syndrome: a pilot study. – *Obes. Res. Clin. Pract*., **2**, 2008, I-II.
46. **Senn, H.-J., M. Orth, E. Fitzke, J. Schölmerich, W. Köster, H. Wieland, W. Gerok**. Altered concentrations, patterns and distribution in lipoproteins of serum gangliosides in liver diseases of different etiologies. – *J. Hepatol*., **11**, 1990, 290-296.

47. **Senn, H.-J., T. Gieser, E. Fitzke, U. Baumgartner, J. Schölmerich, W. Gerok**. Altered biosynthesis of gangliosides in developing biliary cirrhosis in the rat. – *J. Hepatol*., **13**, 1991, 152-160.
48. **Senn, H.-J., S. Sellin, E. Fitzke, T. Stehle, D. Haussinger, H. Wieland, W. Gerok**. Biosynthesis and excretion of gangliosides by the isolater perfused rat liver. - *FEBS J*., **205**, 1992, 809-814.
49. **Šmíd, V., T. Petr, K. Váňová, J. Jašprová, J. Šuk, L. Vítek, F. Šmíd, L. Muchová**. Changes in liver ganglioside metabolism in obstructive cholestasis – the role of oxidative stress. – *Folia Biol. (Praha)*, **62**, 2016, 148-159.
50. **Sohn, H., Y.-S. Kim, H.-T. Kim, C.-H. Kim, E.-W. Cho, H.-Y. Kang, N.-S. Kim, C.-H. Kim, S. E. Ryu, J.-H. Lee, J. H. Ko**. Ganglioside GM3 is involved in neuronal cell death. – *FASEB J*., **20**, 2006, 1248-1250.
51. **Tagami, S., J.-I. Inokuchi, K. Kabayama, H. Yoshimura, F. Kitamura, S. Uemura, C. Ogawa, A. Ishii, M. Saito, Y. Ohtsuka, S. Sakaue, Y. Igarashi**. Ganglioside GM3 participates in the pathological condition of insulline resestance. – *J. Biol. Chem*., **277**, 2002, 3085-3092.
52. **Tertov, V. V., E. Y. Nikonova, N. E. Nifant'ev, N. V. Bovin, A. N. Orekhov**. Human plasma *trans*-sialidase donor and acceptor specificity. – *Biochem. (Moscow)*, **67**, 2002, 908-913.
53. **Tessitore, A., M. P. Martin, R. Sano, Y. Ma, L. Mann, A. Ingrassia, E. D. Laywell, D. A. Steindler, L. M. Hendershot, A. d'Azzo**. GM1-ganglioside-mediated activation of unfolded protein response causes neuronal death in a neurodegenerative gangliosidosis. – *Molec. Cell*, **15**, 2004, 753-766.
54. **Tiberti, C., F. Dotta, E. Anastasi, P. Torresi, G. Multari, E. Vecci, D. Andreani, U. Di Maro**. Anti-ganglioside antibodies in new onset type 1 diabetic patients and high risk subjects. – *Autoimmunity*, **22**, 1995, 43-48.
55. **Veillon, L., S. Go, W. Matsuyama, A. Suzuki, M. Nagasaki, Y. Yatomi, J.-I. Inokuchi**. Identificantion of ganglioside GM3 molecular species in human serum associated with risk factors of metabolic syndrome. – *PLoS One*, **10**, 2015, e0129645.
56. **Vukovic, I., J. Bozic, A. Markotic, S. Ljubicic, T. T. Kurir**. The missing link-likely pathogenetic role of GM3 and other gangliosides in the development of diabetic nephropathy. – *Kidney Blood Press Res*., **40**, 2015, 306-314.
57. **Wang, X.-Q., S. Lee, H. Wilson, M. Seeger, H. Iordanov, N. Gatla, A. Whittington, D. Bach, J.-I. Lu, A. S. Paller**. Ganglioside GM3 depletion reverses impared wound healing in diabetic mice by activating IGF-1 and insulin receptors. – *J. Invest. Dermatol*., **134**, 2014, 1446-1455.
58. **Wentworth, J. M., G. Naselli, K. Ngui, G. K. Smyth, R. Liu, P. E. O'Brien, C. Bruce, J. Weir, M. Cinel, P. J. Meikle, L. C. Harrison**. GM3 ganglioside and phosphatidylethanolamine-containing lipids are adipose tissue markers of insulin resistance in obese women. – *Internat. J. Obes*., **40**, 2016, 706-713.
59. **Xu, Y.-H., S. Barnes, Y. Sun, G. A. Grabowski**. Multi-system disorders of glycophospholipid and ganglioside metabolism. – *J. Lipid Res*., **51**, 2010, 1643-1675.
60. **Yamashita, T., A. Hashiramoto, M. Haluzik, H. Mizukami, S. Beck, A. Norton, M. Kono, S. Tsuji, J. L. Daniotti, N. Werth, R. Sandhoff, K. Sandhoff, R. L. Proia.** Enhanced insulin sensitivity lacking ganglioside GM3. – *Proc. Natl. Acad. Sci. U.S.A*., **100**, 2003, 3445-3449.
61. **Yu, R. K., Y. Nakatani, M. Yanagisawa**. The role of glycosphingolipid metabolism in the developing brain. – *J. Lipid Res*., **50**, 2009, S440-S445.
62. **Yu, R. K., Y.-T. Tsai, T. Ariga, M. Yanagisawa**. Structures, biosynthesis, and functions of gangliosides – an overview. – *J. Oleo. Sci*., **60**, 2011, 537-544.
63. **Yuan, C., J. Furlong, P. Burgos, L. J. Johnston**. The size of lipid rafts: an atomic force microscopy study of ganglioside GM1 domains in sphingomyelin/DOPC/cholesterol membranes. – *Biophys. J*., **82**, 2002, 2526-2535.
64. **Yuan, C., L. J. Johnston**. Atomic force microscopy studies of ganglioside GM1 domains in phosphatidylcholine and L-α-dipalmitoylphosphatidylcholine/cholesterol bilayers. – *Biophys. J*., **61**, 2001, 1059-1069.
65. **Yuan, C., L. J. Johnston**. Distribution of ganglioside GM1 in L-α-dipalmitoylphosphatidylcholine/cholesterol monolayers: a model for lipid rafts. – *Biophys. J*., **79**, 2000, 2768-2781.
66. **Zador, I. Z., G. D. Deshmukh, R. Kunker, K. Johnson, N. S. Radin, J.A. Shayman**. A role for glycosphingolipid accumulation in the renal hypertrophy of streptizotocin-induced *Diabetes mellitus*. – *J. Clin. Invest*., **91**, 1993, 797-803.
67. **Zhao, H., M. Przybylska, I.-H. Wu, J. Zhang, C. Siegel, S. Komarnitsky, N. S. Yew, S. H. Cheng**. Inhibiting glycosphingolipid synthesis improves glycemic control and insulin sensitivity in animal models of type 2 diabetes. – *Diabetes*, **56**, 2007, 1210-1218.

Institute of Experimental Morphology, Pathology and Anthropology with Museum
Bulgarian Anatomical Society

Acta morphologica et anthropologica, 28 (1-2)
Sofia ● 2021

ANTHROPOLOGY AND ANATOMY 27 (2)

Original Articles

Anthropological Characteristic of Some Odontometric Dimensions between Certain Balkan Ethnicities

Zdravka Harizanova[1], Atanas Baltadjiev[1], Miroslava Yordanova[2], Ferihan Popova[1]*

[1] Department of Anatomy, Histology and Embryology, Faculty of Medicine, Medical University of Plovdiv, Bulgaria
[2] Department of Orthodontics, Faculty of Dental Medicine, Medical University of Plovdiv, Bulgaria

*Corresponding author e-mail: zarahar@abv.bg, Zdravka.Harizanova@mu-plovdiv.bg

The aim of the present study is to evaluate the variations of dental dimensions between Bulgarians and other populations. The study included 169 Bulgarians aged 20-40 years. Buccolingual and mesiodistal dimensions of teeth were measured by Dentistry Sliding Vernier Caliper and analyzed with SPSS 23.0. We found significant differences in mesiodistal dimensions of maxillary canines, premolars and molars and mandibular incisors and premolars between Bulgarians and Serbians. Similar significant differences were found in vestibulolingual and mesiodistal dimensions of upper canines and molars, vestibulolingual dimensions of upper incisors and mesiodistal dimensions of upper premolars, mesiodistal dimensions of mandibular incisors, premolars and second molars and vestibulolingual dimensions of mandibular lateral incisors, canines, premolars and molars between Bulgarians and Greeks. Our results showed that odontometric dimensions vary in different population and therefore it is necessary to determine specific population values in order to make identification possible.

Key words: dental dimensions, population specific values, Bulgarians

Introduction

Dental profile consists of specific individual characteristics related to the teeth and their size. They can help in estimation of age, sex, race, socio-economic status, personal habits, oral and systemic health, occupation and dietary status of the person [12, 18]. Variability observed in the human dentition provides a theoretical basis for

the individualization of human dentition [11]. Different dental traits, such as crown dimensions, tooth shape, cusp number, groove and fissure patterns can provide evidence about the nature and extent of diversity between human populations [13]. Examples of ethnic differences and geographic variability in tooth size have been documented [4]. Numerous factors can contribute to variation in tooth size but probably the combination between genetic factors and environmental influences leads to the differences between populations [3].

A synthesis of data on dental dimensions from different population worldwide has indicated that Western Eurasian population tend to have the smallest teeth while Australians, sub-Saharan Africans and Native Americans tend to have the largest teeth. East and Southeast Asian population were found to be intermediate in tooth size between these groups. Hanihara observed that this was due to the impact of agriculture [10]. Masticator forces, non-chewing parafunctional activities, use of teeth as tools, nature of the diet can also contribute to variations in dental size between different populations [2]. A tough fibrous and abrasive food requires prolonged mastication so populations relying on plant foot have larger teeth than those eating meat. Environmental influences can affect the dentition during prenatal and postnatal periods and depending on the time of the effect a variety of phenotypic variations may occur [16]. Environmental factors are local and systemic. Local factors usually produce localized defects [15] while systemic factors such as birth trauma, low birth weight, prematurity, drugs and chemicals, nutritional disorders, metabolic diseases lead to different changes in micromorphology of dental crowns as well as gross morphological changes such as tooth size [9]. In accordance with other researchers [5, 8] we think that variations in crown size between different populations are affected by interaction between genetic and environmental factors. Standards for skeletal identification vary among different populations and may not be applicable from one population to another. There are no odontometric standards for Bulgarian population.

The aim of this research is to assess the population specificity of some dental dimensions between Bulgarians and other Balkan populations.

Materials and Methods

The present study included 86 males and 83 females of Bulgarian origin living in South Bulgaria aged 20-40 (mean age 32,60± 4,30). Before starting the study, subjects were informed about the nature of the study and written informed consents were obtained. Patients were included based on the following criteria: presence of complete set of fully erupted and periodontally healthy teeth, presence of non-carious and non-worn teeth, no dental history of any crown restorations or bridges, normal occlusion. Patients with orthognathic surgery or trauma, history or clinical evidence of cleft palate, history or clinical features suggestive of endocranial disorders, metabolic disorders, developmental disorders and history of prolonged illness were excluded.

Buccolingual and mesiodistal dimensions of teeth were measured by Dentistry Sliding Vernier Caliper, Ridge Mapping Caliper Type A and Type B. We used the technique of Martin-Saller, 1957, modified by Yordanov et al. [19]. According to Yordanov et al. the mesiodistal dimension is the greatest mesiodistal distance between the contact points of teeth, usually it is in the upper or middle third of coronal height.

It is also termed the dental width. The buccolingual (vestibulolingual) dimension, also termed as the dental thickness is the greatest dimension between buccal and lingual surfaces of crown, taken at right angle to the plane in which mesiodistal diameter is taken. We used collected data about the dental dimensions of Serbians and Greeks reported by other authors [7, 20].

The measurements were analyzed with SPSS 23.0 using Student's t-test. The level of statistical significance was set at $P< 0.05$. The degree of significance was considered weak ($P<0,05$), moderate ($0,01>P>0,001$) or high ($P<0,001$). Only measurements which show significant differences were reported in the tables.

Results

Comparison of Bulgarian and Serbian samples (report results included in Tables 1-4)

We found statistically significant differences between the mesiodistal dimensions of maxillary canines and first molars of the Bulgarian and Serbian men with high degree of significance ($P<0,001$). The mean values in Bulgarians were higher than those in Serbians (**Table 1**).

Similar differences were found in the mesiodistal dimensions of mandibular incisors and premolars again with high degree of significance ($P<0,001$). This time mean values in Serbians were higher than those in Bulgarians (**Table 2**).

Mesiodistal dimensions of the maxillary premolars in Bulgarian women showed significantly lower values than those of Serbian women. For the first premolar the degree of significance was high ($P<0,001$) while for the second premolar the degree was weak ($P<0,05$). Similar differences with high degree of significance were found in the mesiodistal dimensions of maxillary canines in favor of Bulgarian women (**Table 3**).

We found statistically significant differences between the mesiodistal dimensions of mandibular incisors and premolars with high degree of significance ($P<0,001$). The mean values in Serbian women were higher than those in Bulgarian women (**Table 4**).

Comparison of Bulgarian and Greek samples (report results included in Tables 5-8)

Vestibulolingual dimensions of the maxillary incisors, canines and molars between Bulgarian and Greek men showed statistically significant differences in favor of Greeks. They were with high degree of significance in the molars. Similar statistically significant differences were found in the mesiodistal dimensions of the maxillary canines, premolars and molars. The degree of significance was high for the canines ($P<0,001$). Mean values in Greeks were higher except for the canines and molars (**Table 5**).

We found statistically significant differences in the mesiodistal dimensions of the mandibular incisors, premolars and second molars between Bulgarian and Greek men. Vestibulolingual dimensions in mandibular lateral incisors, canines, premolars and first molars showed statistically significant differences as well. The degree of significance was high ($P<0,001$) for the mesiodistal dimensions of the mandibular second premolars and second molars and for the vestibulolingual dimensions of the lateral incisors and premolars. Greeks showed higher mean values except for the vestibulolingual dimensions of premolars and first molars (**Table 6**).

Similar statistically significant differences were found in mesiodistal dimensions of the maxillary canines between Bulgarian and Greek women with high degree of

significance (P<0,001). Vestibulolingual dimensions of the maxillary premolars in Bulgarians were also significantly higher than those in Greeks (**Table 7**).

Mesiodistal dimensions of the mandibular second premolars between Bulgarian and Greek women were significantly higher in Greeks with weak degree of significance (P<0,05).Vestibulolingual dimensions in mandibular premolars and second molars showed statistically significant differences in favor of Bulgarian women. The degree of significance was high for the premolars (P<0,001) (**Table 8**).

Discussion

We found statistically significant differences in 6 odontometric dimensions between Bulgarian and Serbian men. Mesiodisital dimensions of maxillary canines and first molars were higher in Bulgarians than those in Serbians while mesiodistal dimensions in mandibular incisors and premolars in Serbians were higher than those in Bulgarians. We found statistically significant differences in 7 dimensions between Bulgarian and Serbian women and these were mesiodistal dimensions of upper canines, lower incisors and both upper and lower premolars. Similar results were reported by Filipopovic who measured dental size in Serbian population and found that Serbians were more similar to European than Asian populations [6, 7]. Although we found statistically significant differences between the two populations, a certain degree of similarity was present, and this can be explained by the fact that they have common elements in nutrition. Other authors such as Ates et al. also thought that environmental factors such as eating habits can influence the size of teeth [1]. Deepak et al. found that abrasive food required more continuous mastication hence dental size in these populations was smaller while populations relying more on plant food than meat had larger teeth [4]. Hanihara and Ishida proposed that the smaller tooth dimensions in Western Eurasians populations were related to the lower impact of natural selection on tooth size over the last few millennia, associated with cultural changes in food preparation practices following the adoption of agriculture [11]. On the other hand, the resemblance between the two populations can be explained with the geographical proximity of their countries. Both nations belong to the South – Slavic ethnic group and have common origin with other Balkan populations (Macedonians, Romanians).

Other authors suggested strong genetic contribution in tooth size as well [14, 17]. They have pointed the importance of the role of genetic influences on dental traits and dimensions [3]. This can also explain the fact that the statistically significant differences between Bulgarian and Serbian population were less than those we found between Bulgarians and Greeks [20].

Our results showed that there were 10 significant differences in the dimensions of the maxillary teeth between Bulgarian and Greek men - mesiodistal dimensions of canines, premolars and molars and vestibulolingual dimensions of incisors, canines and molars. Greeks have higher values than Bulgarians except for the mesiodistal sizes of canines and molars. Ten significant differences were found in the dimensions of the mandibular teeth as well between the two populations: mesiodistal dimensions of the incisors, premolars and second molars and vestibulolingual dimensions of lateral incisors, canines, premolars and first molars. The mean values in Greek men were significantly higher than in Bulgarian men except for the vestibulolingual dimensions

of premolars and first molars where Bulgarians showed higher values. Bulgarian and Greek women though showed statistically significant differences in considerably less odontometric dimensions. They were 3 for the maxillary teeth: mesiodistal dimensions of canines and vestibulolingual dimensions of premolars and 4 for the mandibular teeth: mesiodistal dimensions of second premolars and vestibulolingual dimensions of premolars and second molars. The more differences between Bulgarians and Greeks probably were due to the different origin between the two populations (ancient Greeks are Indo-European nation coming from Africa), so it can be concluded that genetic influence has an important role in the dental dimensions.

The fact that there were less differences between women than between men and that most of them were in the vestibulolingual dimensions for the women shows that not only odontometric dimensions are population-specific but the degree of sexual dimorphism as well shows variation among different nations.

Conclusion

The present study revealed that odontometric dimensions were population-specific. They can be used for establishing the phylogenetical and biological relationships between populations, for explaining historical, cultural and biological macro and micro-evolutionary processes and thus for understanding the origin, formation, contacts, migration pathways of the different populations leading to ethnic variation of humanity.

Table 1. Comparison of mesiodistal dimensions of maxillary teeth between Bulgarian and Serbian men with statistically significant differences

	Bulgarian - males			Serbian - males			
Tooth	N	Mean	SD	N	Mean	SD	P
C13MD	86	8,72	0,63	101	7,90	0,39	**<0,0001**
M16MD	86	10,70	0,67	101	10,11	0,66	**<0,0001**

Table 2. Comparison of mesiodistal dimensions of mandibular teeth between Bulgarian and Serbian men with statistically significant differences

	Bulgarian - males			Serbian - males			
Tooth	N	Mean	SD	N	Mean	SD	P
I41MD	86	5,16	0,43	101	5,50	0,31	**<0,0001**
I42MD	86	5,47	0,55	101	6,06	0,37	**<0,0001**
P44MD	86	6,47	0,74	101	6,94	0,41	**<0,0001**
P45MD	86	6,37	0,82	101	7,02	0,41	**<0,0001**

Table 3. Comparison of mesiodistal dimensions of maxillary teeth between Bulgarian and Serbian women with statistically significant differences

	Bulgarian - females			Serbian - females			
Tooth	N	Mean	SD	N	Mean	SD	P
C13MD	83	7,95	0,65	101	7,60	0,51	**<0,0001**
P14MD	83	6,49	0,67	101	6,85	0,53	**<0,0001**
P15MD	83	6,40	0,66	101	6,65	0,48	**<0,05**

Table 4. Comparison of mesiodistal dimensions of mandibular teeth between Bulgarian and Serbian women with statistically significant differences

	Bulgarian - females			Serbian - females			
Tooth	N	Mean	SD	N	Mean	SD	P
I41MD	83	5,14	0,35	101	5,47	0,31	**<0,0001**
I42MD	83	5,58	0,50	101	6,00	0,35	**<0,0001**
P44MD	83	6,47	0,63	101	6,84	0,46	**<0,0001**
P45MD	83	6,37	0,73	101	6,93	0,43	**<0,0001**

Table 5. Comparison of mesiodistal and vestibulolingual dimensions of maxillary teeth between Bulgarian and Greek men with statistically significant differences

	Bulgarian - males			Greek - males			
Tooth	N	Mean	SD	N	Mean	SD	P
I11VL	86	6.74	1.18	15	7,42	0,36	**<0.05**
I12VL	86	5.98	0.71	22	6.48	0,51	**<0,01**
C13MD	86	8.72	0,63	32	7.73	0,51	**<0,0001**
C13VL	86	8,02	0,89	32	8,55	0,63	**<0,01**
P14MD	86	6.72	0,59	32	7.03	0,67	**<0,05**
P15MD	86	6,40	0,62	32	6.73	0,43	**<0,01**
M16MD	86	10.70	0,67	32	10.38	0,63	**<0,05**
M16VL	86	10,84	0,53	31	11,34	0,52	**<0,0001**
M17MD	86	10.00	0.53	32	9.64	0.92	**0.010**
M17VL	86	10,47	0,55	33	11,44	0,71	**<0,0001**

Table 6. Comparison of mesiodistal and vestibulolingual dimensions of mandibular teeth between Bulgarian and Greek men with statistically significant differences

	Bulgarian - males			Greek - males			
Tooth	N	Mean	SD	N	Mean	SD	P
I41MD	86	5,16	0,43	32	5,35	0,41	**<0,05**
I42MD	86	5,47	0,55	32	5,92	0,56	**0,0002**
I42VL	86	5,63	0,69	30	6,24	0,46	**<0,0001**
C43VL	86	7,33	1,02	32	7,94	0,63	**<0,01**
P44MD	86	6,47	0,74	32	6,97	0,50	**<0,01**
P44VL	86	8,70	0,96	36	7,80	0,59	**<0,0001**
P45MD	86	6,37	0,82	32	7,06	0,56	**<0,0001**
P45VL	86	8,83	0,78	34	8,13	0,67	**<0,0001**
M46VL	86	10,65	0,72	29	10,35	0,38	**<0,05**
M47MD	86	10.05	0.62	32	10,75	0.65	**<0,0001**

Table 7. Comparison of mesiodistal and vestibulolingual dimensions of maxillary teeth between Bulgarian and Greek women with statistically significant differences

	Bulgarian - females			Greek - females			
Tooth	N	Mean	SD	N	Mean	SD	P
C13MD	83	7,95	0,65	15	7,26	0,42	**<0,0001**
P14VL	83	9,23	0.57	17	8,43	0,69	**<0,0001**
P15VL	83	9,28	0,50	20	8,73	0,63	**<0,0001**

Table 8. Comparison of mesiodistal and vestibulolingual dimensions of mandibular teeth between Bulgarian and Greek women with statistically significant differences

	Bulgarian - females			Greek - females			
Tooth	N	Mean	SD	N	Mean	SD	P
P45MD	83	6,47	0,74	22	6,88	0,52	**<0,05**
P44VL	83	8,51	0.74	24	7,20	0,71	**<0,0001**
P45VL	83	8,58	0,70	25	7,81	0,57	**<0,0001**
M47VL	83	9,98	0,46	28	9,59	0,54	**0,0003**

References

1. **Ates, M., F. Karaman, M. Y. Iscan, T. L. Erdem**, Sexual differences in Turkish dentition. – *Leg. Med. Tokyo*, **8**, 2006, 288-292.
2. **Brook, A. H**. A unifying aetiological explanation for anomalies of human tooth number and size. – *Arch. Oral Biol*. **29**(5), 1984, 373-378.
3. **Brook, A. H., J. Jernvall, R. N. Smith, T. E. Hughes, G. C. Townsend**. The dentition: the outcomes of morphogenesis leading to variations of tooth number, size and shape. – *Aust. Dent. J*., **59**, 2014, 131-42.
4. **Deepak, V., S. N. Goryawala, Y. Reddy, R. J. Chhabra, S. Nandaprasad, N. K. Shah**, Assessment of ethnicity in Indian population using tooth crown metric dental traits. – *JIOH*, **7**(9), 2015, 83-87.
5. **Dempsey, P. J., G. C. Townsend**. Genetic and environmental contributions to variation in human tooth size. - *Heredity*, **86**, 2001, 685-693.
6. **Filipović, G., J. Radojičić, M. Stošić, P. Janošević, Z. Ajduković**. Odontometric analysis of permanent canines in gender determination. - *Arch. Biol. Sci., Belgrade*, **65**(4), 2013, 1279-1283.
7. **Filipovic, G., T. Kanjevac, B. Cetenovic, Z. Ajdukovic, N. Petrovic**. Sexual dimorphism in the dimensions of teeth in Serbian population. - *Collegium Antropologicum*, **40**(1), 2016, 23-28.
8. **Garn, S. M, A. B. Lewis, D. R. Swindler, R. S. Kerewsky**. Genetic control of sexual dimorphism in tooth size. – *J. Dent. Res*., **46**(5), 1967, 963-972.
9. **Grainger, R. M., K. J. Paynter, L. Honey, D. Lewis**. Epidemiologic studies of tooth morphology. – *J. Dent. Res*, **45**(3), 1966, 693-702.
10. **Hanihara, K**., Distances between Australian aborigines and certain other populations based on dental measurements. – *J. Human Evolution*, **6**, 1977, 403-418.
11. **Hanihara, T., H. Ishida**. Metric dental variation of major human populations. – *Am. J. Phys. Anthropol.*, **128**(2), 2005, 287-298.
12. **Jensen, E., Y. P. Kai-Jen, C. F. Moorrees, S. O. Thomsen**. Mesiodistal crown diameters of the deciduous and permanent teeth in individuals. – *J. Dent. Res.,* **36**(1), 1957, 39-47.
13. **Moorrees, C.** The dentition of the growing child: A longitudinal study of dental development between 3 and 18 years of age. – *Harvard University Press, Cambridge*, **138**(4), 1959, 496-496.
14. **Nikolova, M.** Correlation between age of the individual and alterations in dental tissue. – *Biology, Univ. of Plovdiv "P. Hilendarski*", **15**(4), 1980; 209-219. [in Bulgarian]
15. **Seow, K. W.** Environmental, maternal, and child factors which contribute to early childhood caries: a unifying conceptual model. – *Int. J. Paediatr. Dent*., **22**(3), 2012, 157-168.
16. **Taji, S., T. Hughes, J. Rogers, G. Townsend**. Localised enamel hypoplasia of human deciduous canines: Genotype or environment? – *Australian Dental Journal*, **45**, 2000, 83-90.
17. **Townsend, G. C., N. G. Martin.** Fitting genetic models to carabelli trait data in south Australian twins. – *J. Dent. Res*., **71**(2), 1992, 403-409.
18. **Timonov P, A. Fusova.** Reconstruction of femur length from its proximal fragments in a Bulgarian modern population. – *Australian Journal of Forensic Sciences*; **50**, 2016, 1-11
19. **Yordanov, Y., K. Uzunov, H. Fakih**. *Manual in anatomy and anthropology for dentists*. 1st edition, Sofia, Artgraf, 2012, 248-258. [in Bulgarian]
20. **Zorba, E., K. Moraitis, S. K. Manolis**. Sexual dimorphism in permanent teeth of modern Greeks. – *Forensic Sci. Int.,* **210**(1-3), 2011, 74-81.

Institute of Experimental Morphology, Pathology and Anthropology with Museum
Bulgarian Anatomical Society

Acta morphologica et anthropologica, 28 (1-2)
Sofia ● 2021

Comparative Anthropological Characterization of few local Bulgarian Populations

Racho Stoev[1], Lukasz Macuga[2]*

[1] *Institute of Experimental Morphology, Pathology and Anthropology with Museum, Bulgarian Academy of Sciences, Sofia, Bulgaria*
[2] *Torun University, Torun, Poland*

* Corresponding author e-mail: rastesto@abv.bg

Anthropological data from 20 samples of adult Bulgarians from different local populations are processed statistically and analyzed with Michalski's methods and compared with each other by cluster and principal component analysis. The results show that they can be divided into two major groups (clusters), each of which with two subclusters. The first cluster includes populations with Centraleuropean characteristics – a combination of Nordic, Armenoid (Balkano-Caucasian) and Lapponoid (Uralo-Lapponoid) elements. The second cluster includes population with the typical Atlanto-Mediterranian (Atlanto-Pontic) combination of Nordic and Mediterranian elements. The subclusters of the first cluster differ on the basis of predominance of Armenoid or Lapponoid elements, the subclusters of the second cluster – on the more expressed Nordic or Mediterranian traits. The first group of population spreads mostly in Northern Bulgaria and the second – in South Bulgaria. Two samples (Melitopol Bulgarians and Crimean Bulgarians) remain outside the two main groups and the reason of this phenomenon is discussed.

Key words: Bulgarians, Michalski's methods, comparative anthropological analysis, Centraleuropean populations, Atlanto-Pontic populations

Introduction

Few national wide ethnoanthropological surveys have been conducted in Bulgaria: by Acad. Stefan Vatev around 1899, by Acad. Methody Popov in 1938-43, by Aris Poulianos in 1963 and the National Anthropological Program in 1989-93 [12, 13, 19, 20]. Their results show that the anthropological structure of the present Bulgarian population is very heterogeneous in territorial aspect. Unfortunately, the results from these studies are published only at national and regional level. Only few data are published on local level [12, 19]. The survey of Krum Dronchilov [2] perhaps the best exact and best known outside Bulgaria, presents anthropological data on local level, but does not cover the whole territory of Bulgaria. The materials of the extensive local anthropological studies of Peter Boev, Luchia Kavgazova and their collaborators, collected during the 1970s and 1980s are only partly published [4, 5, 6]. Resent review and analysis of some

incomplete data of Methody Popov's study also support the idea that more attention to the investigation of the anthropology of local Bulgarian populations should be paid [14].

That is why the authors of this paper in the last years processed statistically and analyzed data of few local populations from the rich collection of unpublished archive materials [15, 16, 17] and also published individual data of former anthropological studies when they are available [2, 8, 9].

Materials and Methods

Anthropological data from the archives of the former Department of Ethnic Anthropology of the former Institute of Morphology of BAS are processed statistically and analyzed. Also have been processed statistically and analyzed published individual data from the anthropological studies of Krum Dronchilov and Anatol Nosov [2,8, 9]. Thus the data of 20 local Bulgarian samples including individual data of 1641 adult men are analyzed in this paper.[1]

The analysis of the anthropological structure has been made according to the methodic of Michalski [3, 7, 10, 11]. In the methodic some minor modifications are made, which are described in previous article of the first author of this paper [15].

Next the samples have been compared between them by cluster analysis (unweighted pair group method of analysis has been used – UPGMA) and by principal component analysis.

Results and Discussion

The basic anthropological characteristics of these 20 local samples are presented in **Table 1.**

The phenotypic combinations of different anthropological elements after Michalski are presented in **Table 2.**

The Euclidean distances between the samples under study are presented in **Table 3.**

The cluster analysis and the principal component analysis on the base of this elementary anthropologic structure and the Euclidean distances between the samples are presented in **Fig. 1** and **Fig. 2.**

The results of our analysis show that the major part of Bulgarian local samples forms two clusters, each with two subclusters **(Fig.3)**

The first cluster includes Balkandjis from Razgrad district [17], Bulgarians from North Bulgaria [16], Turks from Middle North Bulgaria [16], Bulgarians from Pirdop county [2], from Orhanie county [2], from Sofia county – eastern part [2], Gagauzes from Kavarna [15], Bulgarians from Kjustendil county [2], and from Samokov county [2]. It includes populations with typical Centraleuropean characteristics – a combination of Nordic, Armenoid (Balkano-Caucasian) and Lapponoid (Uralo-Lapponoid) elements,

[1] The primary analysis of Dronchilov's individual data from Sofia county forced the author to divide it in two samples, so prominent was the anthropological differences between the eastern and the western part of this county.

first described by Cheboksarov [1]. These populations are brachycephalic, with mixed pigmentation and slight Mongoloid traits (mostly because of old, slightly differentiated Mongoloid anthropologic elements which have been presented in Europe long before the Great migration of peoples [1].

This cluster has two subclusters on the basis of predominance of Armenoid or Lapponoid element. In the first subcluster Armenoid element prevails over Lapponoid (Balkanjis, North Bulgarians, Turks, Pirdop county). On individual level here we find the highest presence of Dinaric type (AH) and of its characteristic traits on population level (greater body height, well expressed brachycephaly, darker pigmentation) – **Table 4.**

In the second subcluster Lapponoid element prevails over Armenoid, also the Nordic element is stronger – **Table 5**. Thus on individual level dominate the Subnordic type (AL) and its traits can be seen on population level (higher nasal index, lighter pigmentation, lower body height). It includes Bulgarians from Orhanie, Sofia-east, the Gagauzes, Bulgarians from Kjustendil and Samokov.

The second cluster includes samples from South Bulgaria (except one[2]) – from Tryn county [2], Pomaks from village Toros [16], mixed sample Bulgarians from South Bulgaria [16], from Panagjurishte county [2], Dupnica county [2], Caribrod county [2], Radomir county [2], Plovdiv county [2] and from the western part of Sofia county [2]. These populations present typical combination of Nordic and Mediterranean elements and the traits of these elements can be seen on population level (mesocephaly, mixed pigmentation). On individual level prevail the Atlanto-Pontic (Atlanto-Mediterranean or Northwestern) anthropological type AE, but also the so called Amoritic type (AK) can be found. This cluster can be also divided into two subclusters on the basis of the force of Nordic element.

The first subcluster includes the samples from Tryn, the Pomaks, from South Bulgaria and from Panagjurishte. Here the Nordic element is best expressed and thus the pigmentation is brighter. The second subcluster includes the samples from Dupnica, Caribrod, Radomir, Plovdiv and Sofia-west. Here the Nordic element is less expressed and consequently the pigmentation is darker.

Outside of these two clusters are the samples of Melitopol Bulgarians and Crimean Bulgarians, studied by Nosov [8, 9]. They are characterized by darker pigmentation, shorter nose with high nasal indexmore concave than convex nasal profiles. Mongoloid traits as prominent cheekbones and Mongolic eyelid fold are often. Thus in the elementary structure the Nordic complex is relatively low and the Eastern complex – high.

We have to say that there is some uncertainty in the individual data of Crimean and Melitopol Bulgarians. First, the pigmentation of the hair and of the eyes is given only in broad categories (dark-dark blond – blond, dark – mixed – light) and this makes the determination of the anthropological types and fractions problematic. Next, in 1939 Żejmo-Żejmis doubts in the proper measuring of the nose by the anthropologists of the Ukraine anthropological school [21], thinking that they underestimate the nasal height and thus overestimate nasal index. However, our analysis of individual anthropological data of the Ukranians from the village of Bondarova, measured by the Ukranian anthropologist Maksym Tkach [18] presents that they are almost identical with Ukranians measured in Buczacz county and analyzed without remarks by Michalski [7].

---

[2] This only Atlanto-Pontic sample in North Bulgaria are the Pomaks fron the village Toros. The historical reasons of their exclusivity are discussed in former publication of the first author of this paper [16].

This confirms the correctness of the anthropometry taken by the anthropologists of the Ukrainian school. Also we have to say, that high nasal index usually correlates with nasal concavity and in Europoids usually is a sign of Mongoloid admixture. Mongoloids also have darker hair than Europoids. Thus the combination of darker pigmentation, lower nasal index, nasal concavity, prominent cheekbones and often Mongolic eyelidfold can be real in these two local Bulgarian populations. We also do not know the exact place of their origin before the migration first in Bessarabia and then to Taurian province and what bottle neck and founder effects happened during their migrations. We only know that they originate from Eastern Bulgaria and all other samples except one, the Gagauzes, originate from more western regions. But exactly the Gagauzes are the second closest sample to Melitopol Bulgarians (after the Crimean Bulgarians). Thus the reasons of the specifity of these samples and if it is real remain unclear.

Conclusion

The results of the comparative anthropological characterization of 20 local Bulgarian samples show that they can be divided into two major groups (clusters), each of which with two subclusters. The first cluster includes populations with Centraleuropean characteristics – a combination of Nordic, Armenoid (Balkano-Caucasian) and Lapponoid (Uralo-Lapponoid) elements. The second cluster includes population with the typical Atlanto-Mediterranian (Atlanto-Pontic) combination of Nordic and Mediterranian elements. The subclusters of the first cluster differ on the basis of predominance of Armenoid or Lapponoid elements, the subclusters of the second cluster – on the more expressed Nordic or Mediterranian traits. The first group of population spreads mostly in Northern Bulgaria and the second – in South Bulgaria. Two samples (Melitopol Bulgarians and Crimean Bulgarians) remain outside the two main groups but the reason of this is unclear.

Acknowledgements: To Ivayla Ivanova-Pandourska for discussion when working on these materials.

R e f e r e n c e s:

1. **Cheboksarov, N. N.** The anthropological structure of recent Germans. – *Uchenye Zapiski MGU*, LVIII, 1941, 271-308 [in Russian].
2. **Dronchilov, K.** *Contribution to the anthropology of Bulgarians*. Braunschweig, Friedr. Vieweg @ Sohn, , 1914, 1-80 [in German].
3. **Henzel, T., I. Michalski.** Principles of human classification after Tadeusz Henzel and Ireneusz Michalski. – *Przegl. Antropol*., tom XXI, zeszyt **2**, 1955, 537-662 [in Polish].
4. **Kavgazova, L., P. Boev, A. I. Hadjioloff.** Morphological characteristics of highland population in Central Rhodopes. – *C. R. Acad. Bulg. Sci.,* **37**, 1984, 5, 657-659.
5. **Kavgazova, L., P. Boev.** Anthropological characteristics of Rhodope variant of Dinaric race – *C. R. Acad. Bulg. Sci.,* **37**, 1984, 5, 665-667.
6. **Kavgazova, L., Zl. Filcheva, R. Stoev.** Anthropological characteristics of the population in the western part of Smolyan region. – *Acta morphol. anthropol*, **6**, 1987, 58-64.
7. **Michalski, I.** Anthropological structure of Poland. – *Acta anthropologica universitatis Lodziensis*, **1**, 1949, 1-236 [in Polish].
8. **Nosov, A.** To the anthropology of Bulgarians – the Crimean Bulgarians. – *Antropolohia, Kyiv*, 1929, **III**, 1-52 [in Ukrainian].

9. **Nosov, A.** To the anthropology of Bulgarians – the Melitopol Bulgarians. – *Antropolohia, Kyiv*, 1930, IV, 1-76 [in Ukrainian]
10. **Orczykovska, Z.** An attempt of constructing an anthropological key on the base of classification of Michalski. – *Przegl. Antropol.,* **22**(1), 1959, 212-229 [in Polish].
11. **Orczykowska, Z.** Anthropological analysis of Tajiks from Pamir. – *Mat. Pr. Antropol*., **46**, 1959, 5-51 [in Polish].
12. **Popov, M., G. Markov.** *Anthropology of Bulgarian people*. Sofia, BAS Publ. House, 1959, 1-296 [in Bulgarian]
13. **Poulianos, A. N.** *Anthropological studies on the Balkans (Bulgaria-Greece-Yugoslavia)*, Athens, 1967, 1-157 [in Greek].
14. **Stoev, R.** Anthropological types in Bulgarian population around 1940 – regional and local level. – *Acta morphol. anthropol*., **23**, 2016, 93-101.
15. **Stoev, R.** Anthropological characteristics of Gagauzes from Kavarna. – *Acta morphol. anthropol.*, **26** (1-2), 2019, 79-83.
16. **Stoev, R.** Anthropological characterization of few local populations of middle-north Bulgaria after archive materials from 1943/44. – *Acta morphol. anthropol*., **26** (3-4), 2019, 94-101.
17. **Stoev, R.** Anthropological characterisation of Balkanjis from Razgrad District. – *Acta morphol. anthropol*., **27** (3-4), 2020, 94-100.
18. **Tkach, M.** Anthropological measurements of the population of the village Bondarova in Shevchenkivshchyna. – *Antropolohia, Kyiv*, 1928, **II**, 70-105 [in Ukrainian].
19. **Vatev, St.** *Anthropology of Bulgarians*. Sofia, 1939, 1-80 [in Bulgarian].
20. **Yordanov, Y., A. Nacheva, S. Tornyova-Randelova, N. Kondova, B. Dimitrova, D. Paskova-Topalova.** *Anthropology of the population of Bulgaria in the end of 20th century*, Sofia, Academic publishing house "Marin Drinov", 2006, 1-432 [in Bulgarian].
21. **Żejmo-Żejmis, St.** From the anthropology of the Black sea region. – *Przeglad Antropologiczny*, 1939, XIII, 12-49 [in Polish].

Table 1. Basic anthropological traits in Bulgarian populations

Sample	N	Height, cm	Head length, mm	Head breadth, mm	Cephalic index, %		Face breadth, mm	Face height, mm	Facial index, %	Nose height, mm	Nose breadth, mm	Nasal index, %	Eye color	Hair color	Nasal profile
					mean	SD									
Balkandzhis	126	168,5	186,0	157,0	84,5	3,5	139,8	126,0	86,7	57,8	33,7	64,3	6,5	49,8	68,5
North Bulgaria	226	172,6	183,8	156,1	85,0	3,9	142,0	123,0	86,7	58,3	36,2	62,3	6,7	51,3	60,5
Turks (Midle North Bulg.)	23	165,0	180,1	151,7	84,3	4,2	137,6	124,4	90,5	58,1	35,7	61,7	7,6	52,6	67,4
Pirdop	38	170,5	187,3	152,0	81,2	3,4	141,6	122,4	86,5	56,6	36,4	64,7	7,9	46,2	-
Orhanie	37	170,7	187,5	155,0	82,7	3,5	141,8	120,8	85,3	55,8	36,5	65,8	7,7	45,7	-
Sofia-east	62	169,6	184,5	153,1	83,1	3,9	142,1	121,1	85,3	55,3	36,6	66,4	7,4	45,3	-
Gagauzes	112	167,3	185,0	153,4	82,9	3,4	140,8	123,5	87,8	55,2	36,5	66,6	7,3	51,3	67,5
Kjustendil	64	169,6	187,8	152,9	81,5	3,3	139,5	120,0	86,1	55,0	35,5	64,8	8,2	43,4	-
Samokov	49	171,0	184,1	152,3	83,0	3,3	140,6	118,5	84,3	54,0	35,7	66,5	7,9	43,3	-
Tryn	53	170,4	191,6	149,5	78,1	3,1	139,3	123,2	88,6	55,9	36,2	65,0	7,3	45,8	-
Pomaks (North Bulg.)	23	167,4	184,1	147,9	80,4	3,2	139,5	124,0	88,9	59,6	38,1	64,3	9,2	47,2	73,3
South Bulgaria	12	171,1	186,0	150,9	81,2	2,6	138,0	122,3	88,7	56,1	36,7	65,9	7,8	48,3	54,6
Panagjurishte	19	168,2	190	148,7	78,4	3,6	137,0	118,8	86,8	55,1	35,6	65,0	8,3	41,1	-
Dupnica	60	168,8	189,7	148,7	78,4	2,9	138,1	118,6	85,9	53,8	35,3	66,0	7,3	43,7	-
Caribrod	67	168,7	190,1	149,8	78,9	3,1	138,9	121,5	87,5	55,4	35,7	64,8	8,0	43,8	-
Radomir	52	171,1	191,3	151,0	79,0	2,9	140,0	122,9	87,9	55,8	36,2	65,1	7,2	48,3	-
Plovdiv	74	168,6	188,7	147,0	78,0	3,7	135,8	119,3	87,9	54,1	35,1	65,2	7,0	46,3	-
Sofia-west	26	170,4	191,1	149,1	78,1	3,7	139,0	122,1	87,9	55,9	36,6	65,8	7,1	48,5	-
Melitopol Bulgarians	356	168,6	189,0	152,8	81,0	3,3	142,0	123,8	87,2	52,2	35,9	69,4	5,7	51,3	52,9
Crimean Bulgarians	162	168,8	192,2	150,0	78,1	3,3	140,0	121,7	87,0	51,0	37,4	73,7	5,6	54,9	48,7

Remarks: Eye color has been given after Martin, hair color - after Michalski (10-light blond, 20-blond, 30-dark blond, 40-blond-chatain (light brown), 50 – chatain (brown), 60 – dark brown (brown-black), 70 black, nasal profile also after Michalski (10 strongly concaved, 20 – concaved, 30 slightly concaved, 40 cancave-wavy, 50 – wavy, 60- straight, 70 wavy-convex, 80 – slightly convex, 90 – convex, 100 – strongly convex.

Table 2. Elementary anthropological structure after Michalski (in %)

	Anthropological element, %										Eastern complex, %	Southern complex, %	formula
Sample	a	y	b	e	u	h	l	m	z	q			
Balkandzhis	29,8	3,0	0,6	11,3	3,2	27,4	22,0	1,2	0,2	1,4	24,8	56,5	ahl(e)
North Bulgaria	31,2	0,6	0,9	6,1	6,7	27,3	14,2	8,1	3,3	2,0	27,6	56,6	ah(l)
Turks (Midle North Bulg.)	27,2	-	-	10,9	5,4	23,9	12,0	6,5	3,3	10,9	32,7	59,7	ah(le=q)
Pirdop	30,9	9,2	1,3	15,8	7,9	21,7	9,9	-	-	3,3	13,2	69,0	ah(e)
Orhanie	41,2	0,7	5,4	12,8	-	16,9	21,6	-	-	1,4	23,0	45,6	al(he)
Sofia-east	36,7	6,0	2,4	10,5	4,8	13,3	22,6	0,8	-	2,8	26,2	42,0	al(he)
Gagauzes	31,9	2,5	2,3	10,3	6,9	18,8	21,6	0,7	0,9	4,1	27,3	52,7	al(he)
Kjustendil	42,2	8,2	1,2	16,0	3,1	11,7	16,0	-	-	1,6	17,6	38,8	a(l=eh)
Samokov	39,3	4,1	1,0	13,3	3,6	7,1	29,6	-	-	2,0	31,6	36,5	al(e)
Tryn	38,2	7,1	2,8	20,8	12,3	4,7	4,7	-	-	9,4	14,1	47,3	ae(k)
Pomaks (North Bulg.)	44,6	1,1	3,3	16,3	8,7	5,4	8,7	-	3,3	8,7	20,7	42,5	a(e0
South Bulgaria	35,4	-	-	14,6	12,5	6,2	8,3	8,3	8,3	6,2	31,1	48,3	a(ek)
Panagjurishte	39,5	15,8	-	17,1	6,6	2,6	10,5	-	3,9	3,9	18,3	32,2	a(eyl)
Dupnica	35,4	8,8	8,3	27,1	4,6	4,2	9,6	-	-	2,1	11,7	50,1	ae
Caribrod	37,3	7,5	4,1	25,0	11,6	5,2	8,2	-	-	1,1	9,3	50,6	ae(k)
Radomir	27,4	4,8	5,3	29,8	11,5	13,5	4,8	-	-	2,9	7,7	59,4	ea(hk)
Plovdiv	29,7	4,7	2,4	28,4	15,5	5,4	12,2	-	-	1,7	13,9	60,0	ae(kl)
Sofia-west	29,8	1,0	12,5	21,2	13,5	4,8	9,6	-	-	7,7	17,3	62,9	ae(kb)
Melitopol Bulgarians	18,3	4,1	0,6	18,3	13,2	13,0	22,3	2,0	1,8	6,5	32,6	66,9	l(a=ekh)
Crimean Bulgarians	13,3	6,2	4,9	20,4	12,2	4,0	17,4	3,2	0,8	17,6	39,0	68,0	e(qlak)

Remarks: The anthropological elements after Michalski (in brackets – synonyms, used by other anthropologists) – a – Nordic (Atlanto-Baltic), y – Cromagnoid (Dalish, Falish), b – berberic (Mediterranoid), e – Mediterranean (Ibero-Insular), k – Oriental (Eastern Mediterranean, Indo-Afgan), h – Armenoid (Balkano-Caucasian), l – Lapponoid, m – Mongolian, z – Pacific, q – Highland (Uralic, Sudetic, Tibetan).

Table 3. Euclidean distances between the samples under study (matrix of Czekanowski)

	Sample	1	2	3	4	5	6	7	8	9	10	11	12	13	14	15	16	17	18	19	20
1	Balkandzhis	**0**																			
2	North Bulgaria	**12,9**	**0**																		
3	Turks (Midle North Bulg.)	**16,2**	**11,8**	**0**																	
4	Pirdop	**16,3**	**17,3**	**15,8**	**0**																
5	Orhanie	**16,8**	21,2	23,3	20,7	**0**															
6	Sofia-east	**16,3**	20,4	21,6	**17,8**	**10,1**	**0**														
7	Gagauzes	**10,2**	**14,7**	**15,5**	**15,0**	**12,9**	**8,6**	**0**													
8	Kjustendil	22,1	24,8	25,1	**17,1**	**12,4**	**10,9**	**16,6**	**0**												
9	Samokov	23,8	29,3	30,0	26,9	**14,4**	**10,5**	**16,9**	**15,5**	0											
10	Tryn	33,8	32,8	28,3	21,4	27,8	24,6	26,7	**19,1**	28,7	**0**										
11	Pomaks (North Bulg.)	31,8	30,2	27,5	23,8	21,6	20,9	24,0	**15,7**	23,9	**11,8**	**0**									
12	South Bulgaria	30,2	25,4	22,6	22,8	26,0	22,6	22,9	21,3	26,9	**16,4**	**14,7**	0								
13	Panagjurishte	32,7	33,4	31,4	22,4	25,9	20,8	26,1	14,6	23,8	**14,7**	**17,1**	20,5	**0**							
14	Dupnica	32,7	34,9	31,6	22,7	25,3	23,9	27,2	17,9	26,3	**14,8**	**19,0**	22,9	**16,1**	**0**						
15	Caribrod	32,1	32,8	30,4	20,7	25,8	23,2	25,9	17,0	26,2	**10,1**	**15,8**	**18,7**	**14,6**	**9,0**	**0**					
16	Radomir	30,6	31,5	26,9	18,7	30,4	28,8	27,4	25,3	33,9	**18,2**	25,1	23,7	25,5	**15,9**	**14,6**	**0**				
17	Plovdiv	32,1	34,0	30,4	22,6	29,4	25,6	26,2	23,1	27,8	**16,2**	22,4	20,8	21,5	**14,6**	**10,6**	**12,4**	**0**			
18	Sofia-west	32,5	32,4	27,7	23,6	27,6	25,1	25,0	24,4	28,8	**15,2**	**19,1**	**19,4**	23,9	**16,0**	**15,3**	**16,5**	**14,6**	0		
19	Melitopol Bulgarians	22,8	26,4	21,9	21,6	28,5	22,3	**18,3**	27,7	26,0	28,5	31,4	25,5	29,9	28,1	27,0	23,8	20,8	23,0	0	
20	Crimean Bulgarians	36,1	37,8	29,6	30,9	38,4	32,3	30,4	35,8	35,1	29,4	34,8	29,7	33,2	30,4	31,1	27,7	25,4	23,0	**16,8**	0

Remarks: Small distances (under 20) are marked in bold.

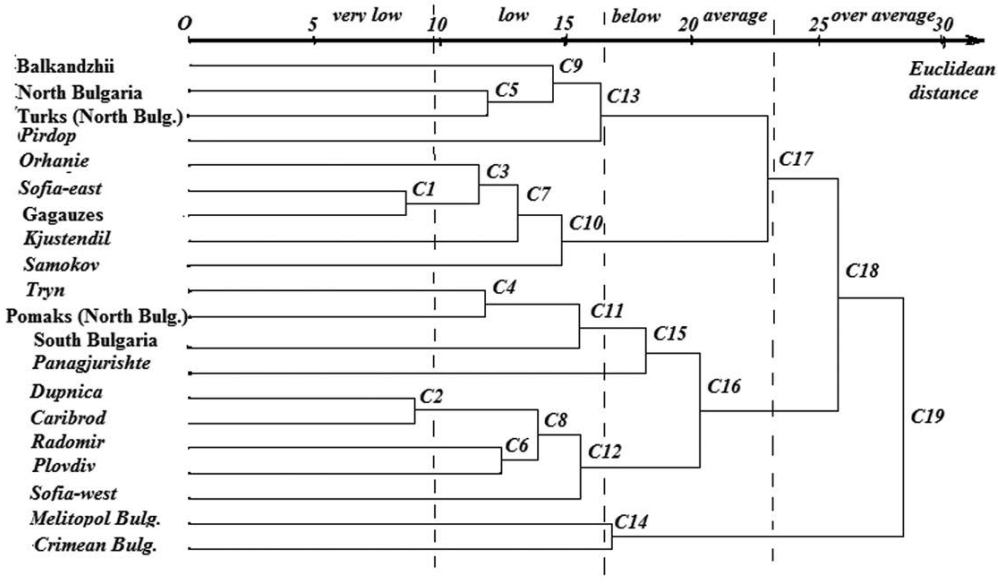

Fig. 1. Cluster analysis of the subsamples under study – Euclidean distances, unweighted pair group method of analysis (UPGMA)

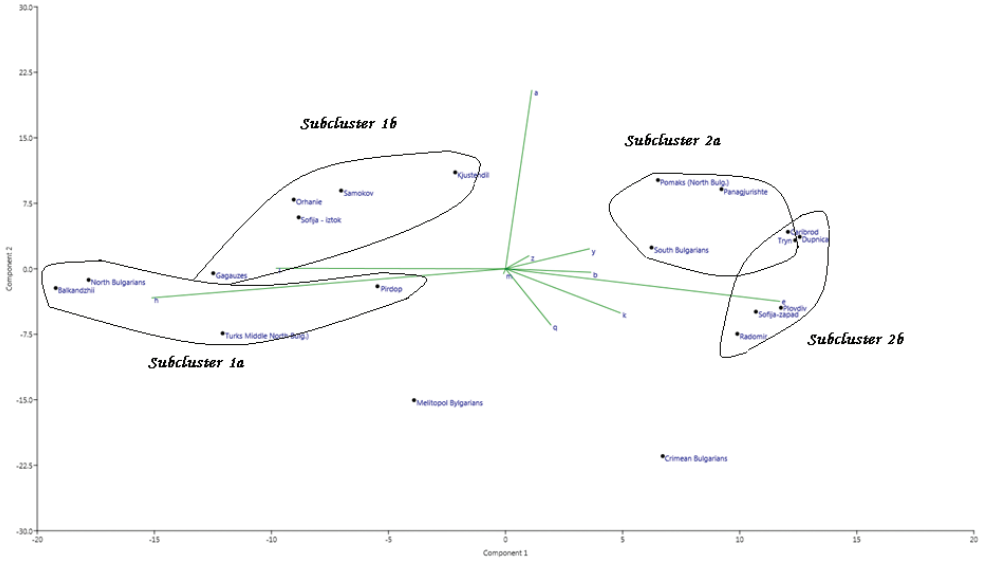

Fig. 2. Principal component analysis on the samples under study

Table 4. Basic anthropological traits in Bulgarian populations by clusters

Cluster/sample	N	Height, cm	Head length, mm	Head breadth, mm	Cephalic index, %		Face breadth, mm	Face height, mm	Facial index, %	Nose height, mm	Nose breadth, mm	Nasal index, %	Eye color	Hair color	Nasal profile
					mean	SD									
1a	413	170,7	184,6	155,8	84,5	3,9	141,0	123,9	86,9	58,0	35,4	63,1	6,8	50,4	(63,6)
1b	324	169,1	185,6	153,3	82,7	3,5	140,9	121,3	86,2	55,1	36,2	66,1	7,6	46,7	(67,5)
2a	107	169,4	189,1	149,2	79,0	3,3	138,8	122,5	88,4	56,6	36,6	65,0	7,9	45,5	(66,9)
2b	279	169,3	190,0	149,0	78,5	3,3	138,1	120,6	87,4	54,8	35,6	65,3	7,4	45,7	-
Melitopol Bulgarians	356	168,6	189,0	152,8	81,0	3,3	142,0	123,8	87,2	52,2	35,9	69,4	5,7	51,3	52,9
Crimean Bulgarians	162	168,8	192,2	150,0	78,1	3,3	140,0	121,7	87,0	51,0	37,4	73,7	5,6	54,9	48,7

Table 5. Elementary anthropological structure after Michalski by clusters (in %)

	Anthropological element, %										Eastern complex, %	Southern complex, %	formula
Sample	a	y	b	e	k	h	l	m	z	q			
1a	30,5	2,1	0,8	8,8	5,7	26,6	16,1	5,2	2,1	2,4	25,8	56,5	ah(l)
1b	37,0	4,3	2,3	12,2	4,5	14,4	21,9	0,4	0,3	2,7	25,3	44,7	al(he)
2a	39,5	6,6	2,1	18,5	10,5	4,6	7,0	0,9	2,3	7,9	18,1	43,6	a(ek)
2b	32,3	5,9	5,6	26,9	11,3	6,5	9,1	-	-	2,4	11,5	56,8	ae(k)
Melitopol Bulgarians	18,3	4,1	0,6	18,3	13,2	13,0	22,3	2,0	1,8	6,5	32,6	66,9	l(a=ekh)
Crimean Bulgarians	13,3	6,2	4,9	20,4	12,2	4,0	17,4	3,2	0,8	17,6	39,0	68,0	e(qlak)

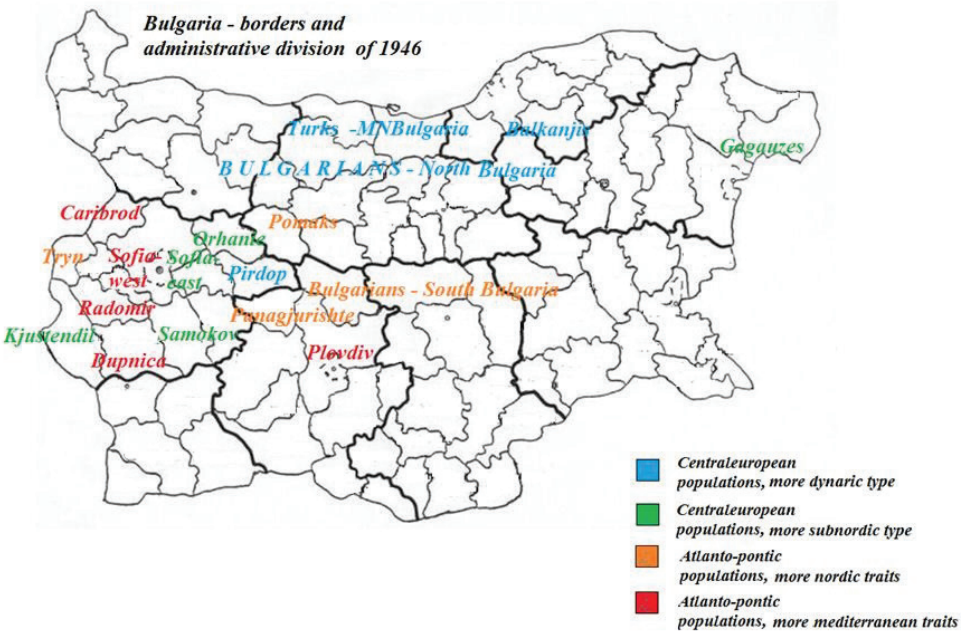

Fig. 3. Geographic distribution of the analysed samples (Melitopol Bulgarians and Crimean Bulgarians excluded)

Institute of Experimental Morphology, Pathology and Anthropology with Museum
Bulgarian Anatomical Society

Acta morphologica et anthropologica, 28 (1-2)
Sofia ● 2021

Comparative Dermatoglyphic Study of Patients with Bipolar Affective Disorder type I and Healthy Controls

Ferihan Ahmed-Popova

Department of Anatomy, Histology and Embryology, Medical University – Plovdiv

* Corresponding author: ferylin@abv.bg; Ferihan.Popova@mu-plovdiv.bg

The aim of this study was to compare the fingerprint patterns and finger ridge count in patients with bipolar I disorder (BPI) and healthy controls. The study included 61 BPI patients and 100 mentally healthy subjects. Rolled palmprints were obtained using an ink method and were read with light (6D) magnification. We found an increased incidence of loops and reduced finger ridge count in male BPI patients, and an increased finger ridge count and higher incidence of whorls in female BPI patients in comparison with their same-sex controls. For both genders we observed increased fluctuating asymmetry in the fingerprint images. Within the context of neurodevelopmental hypothesis of mental disorders dermatoglyphic traits may become reliable biological markers of the timing of prenatal damage and the pathogenetic mechanisms behind it.

Key words: dermatoglyphics, bipolar I disorder, fingerprint patterns, finger ridge count, fluctuating asymmetry.

Introduction

In contrast to schizophrenia, studies on dermatoglyphics in bipolar I disorder (BPI) are insufficient and dermatoglyphic traits have rarely been examined [17, 19]. Schizophrenia and bipolar affective disorder are similar in some epidemiological and pathophysiological characteristics, suggesting that the causes for both disorders can be found in the perinatal or early postnatal period, which is one of the basic principles of neurodevelopmental hypothesis of mental illness. Several neuroimaging dissimilarities between the two disorders have been observed together with the clinical characteristics, which are probably due to differences in the affected hemisphere and a specific brain area, as well as to the predisposing genes of the individual [7, 17, 19]. Subtle dermatoglyphic alterations have been found in patients with severe bipolar disorder suggesting connection between early prenatal insults and later onset of the disease [4, 10].

The importance of dermatoglyphics as biological markers of abnormal neurodevelopment is associated with the common ectodermal origin of the brain and dermal patterns and the strictly defined periods of embryonic formation of papillary ridges that defines them as potential chronomarkers in determining the time of exposure

to prenatal insults. This applies primarily to the degree of fluctuating asymmetry, which is a random deviation from symmetry typical for the individuals, and is a sign of ontogenetic stability in different organisms, including humans [8, 9].

The formation of papillary ridges takes place during the III-V months of embryogenesis and the main differentiation of ridge patterns ends at the end of the IV month of prenatal development. Ridge patterns appear first on the pads of the fingers, and later on the palms and then on the soles [14]. The critical period in differentiation is the III month, which is before the appearance of fingers on the limb germ. Harmful agents of different origin may interfere during the formation of the ridges and disrupt their normal development.

The aim of this study was to compare the fingerprint patterns and finger ridge count in patients with bipolar I disorder (BPI) and healthy controls in order to find evidence suggestive of prenatal factors in the etiology of the disease.

Material and Methods

Subjects

The study included 61 BPI patients (24 males, 37 females) with a mean age of 38.15±14.81 years, consecutively admitted to the Clinic of Psychiatry in Plovdiv and the District Psychiatry Dispensary in Plovdiv. All patients met DSM-IV criteria for a diagnosis of bipolar I disorder (1) on the basis of case records review, a semi-structured interview based on a checklist of DSM-IV items and information obtained from relatives to enhance the validity of the diagnosis. Potential subjects were excluded if they had a history of drug or alcohol abuse, an identifiable neurological disorder, any signs of mental retardation or a somatic disorder with neurological components. Potential patients were excluded if there were evidences of pathological conditions known to be associated with variation of dermatoglyphic characters, e.g., psoriasis, congenital abnormalities such as polydactylia and spina bifida, congenital heart disorders, diabetes mellitus, certain diseases with abnormal caryotype, etc.

The normal comparison group comprised 100 mentally healthy subjects (47 males and 53 females) with a mean age of 39.65 ± 10.68 years. Normality was defined as the absence of a major axis I or axis II disorder according to DSM-IV. Normal controls satisfied exclusion criteria similar to those applied to patients. In addition, to separate the two groups better, potential controls were excluded if they had a first-degree relative with a history of a psychotic disorder, major affective disorder or suicide.

All patients and control subjects were of Bulgarian origin in order to avoid the potential confounding effects of racial and ethnic variation in the expression of dermatoglyphics. Individuals were excluded if their parental or grandparental ethnic group was other than Bulgarian.

The study was approved by the local Ethics Committee at St. George University Hospital. All subjects gave written informed consent to participate.

Assessment of dermatoglyphic patterns

A set of dermatoglyphic configurations with low racial instability and high diagnostic value was examined [5, 6]. Rolled palmprints were obtained using an ink method and

were read with light magnification (6D). Fingerprinting was carried out in a passive manner, using a rotary cone sample divider method. For a greater reliability the scoring of the palmprints was done separately by two persons according to the rules in Memorandum on dermatoglyphic nomenclature [13].

Finger ridge patterns were analyzed in accordance with the methods given by Cummins, Midlo [2]. Dermatoglyphic patterns are classified as arches, loops and whorls according to the number of deltas [3].

Several quantitative variables were measured: the sum of each individual finger ridge count, the finger ridge count of each hand and the total ridge count (TFRC), the sum of the ridge counts for all 10 fingers. Ridge count was calculated from the number of ridges that intersected or touched the line of Galton, which connects the triradius with the core of the pattern. Ridge count of whorl patterns was analyzed by using the higher of the two counts.

Fluctuating asymmetry is defined as small random deviations from perfect symmetry in bilateral traits. It is commonly used as an index of developmental stability: i.e. the ability of an organism to neutralize harmful insults during the prenatal period [11, 18].

Statistical analysis

The data were analyzed with SPSS 17.0. (Statistical Package for the Social Sciences 17.0), using descriptive statistics, nonparametric analysis: c^2- test, Fisher's Exact Test, parametric analysis: Student's t–test.

The level of statistical significance was set at $P < 0.05$.

Results and Discussion

The distribution of the main types of fingerprint images in patients with BPI and controls is presented in **Table 1**. BPI patients showed increased incidence of loops, followed by whorls and arches. BPI males had a higher incidence of loops, and BPI females showed a higher incidence of whorls compared with their same-sex controls, the latter difference falling just short of statistical significance.

Table 1. Comparison of mean number of fingerprint patterns in BPI patients and healthy controls distributed by gender.

	Males						**Females**					
	Controls (n=47)		Bipolar I disorder (n=24)		Statistical significance		Controls (n=53)		Bipolar I disorder (n=37)		Statistical significance	
	Mean	SD	Mean	SD	t	p	Mean	SD	Mean	SD	t	p
Arches	0,36	1,09	0,58	1,55	-0,697	0,488	0,57	1,29	0,32	0,67	1,157	0,251
Loops	5,66	2,78	5,96	3,04	-0,414	0,680	6,91	2,31	6,16	2,68	1,404	0,164
Whorls	3,89	2,85	3,46	3,31	0,577	0,566	2,53	2,36	3,51	2,91	-1,769	0,080

The results of our study showed lower finger ridge count in BPI males compared with controls of the same gender, for the right and the left hand, as well as for both hands (**Table 2**). In BPI female patients finger ridge count was increased for the right and the left hand as well as for both hands.

Table 2. Finger ridge count in BPI patients and healthy controls distributed by gender.

	Males				**Females**			
	Controls (n=47)		Bipolar I disorder (n=24)		Controls (n=53)		Bipolar I disorder (n=37)	
	Mean	SD	Mean	SD	Mean	SD	Mean	SD
Right hand	74,43	22,43	69,50	28,13	67,36	24,50	70,76	20,87
Left hand	69,42	24,41	67,61	27,31	66,33	23,77	67,39	24,96
Total	142,68	46,05	136,17	54,88	133,88	47,61	137,42	44,56

Figure 1 shows the level of matching in fingerprint patterns between BPI patients and healthy subjects. The results showed a high degree of discordance in the second fingers, followed by the first, fourth, third and fifth fingers, which determined increased fluctuating asymmetry in the homologous structures between patients and controls. The high level of fluctuating asymmetry is considered a sign of impaired neurodevelopment occurring during the formation of papillary ridges, which is during the 3rd to 5th month of gestation. The main differentiation of the papillary ridges ends at the end of the 4th month of prenatal development, but the ridges do not rise above the skin surface before the 18th week of gestation. It is obvious that deviations from the normal configuration of the papillary ridges can result from genetic or exogenous factors acting during the period of embryogenesis. Harmful agents of different origin may interfere during the formation of the ridges and disrupt their normal formation which might be combined not only with development of psychiatric disorders later in life, but also with other diseases like chromosomal aberrations and visual impairment [16]. In the scientific research of Tornjova-Randelova S. et al. [16] the authors applied a new approach to the examination of dermatoglyphic patterns according to the topical innervation of the volar surface of the fingers and palms and established deviations in the dermatoglyphic traits affecting structures of visual apparatus in children of both ectodermal and mesodermal origin.

However, our study has several limitations. Larger sample size is probably necessary to find statistical significant differences between the groups when comparing the fingerprint patterns. Further research and statistical analysis is indispensable for evaluation of the specific differences in dermatoglyphic patterns comparing both subject groups in order to contribute to the differentiation between health and disease.

Conclusions

Our findings are suggestive of prenatally acting exogenous factors that affect the normal morphogenesis of ectodermal derivatives. The common ectodermal origin of dermal ridges and nervous system renders the observed dermatoglyphic traits relevant to the body of morphological, histological and brain-imaging research in support of the neurodevelopmental hypothesis of bipolar disorder [12, 15].

Within the context of this hypothesis dermatoglyphic traits may become reliable biological markers of the timing of prenatal damage and its underlying pathogenetic mechanisms.

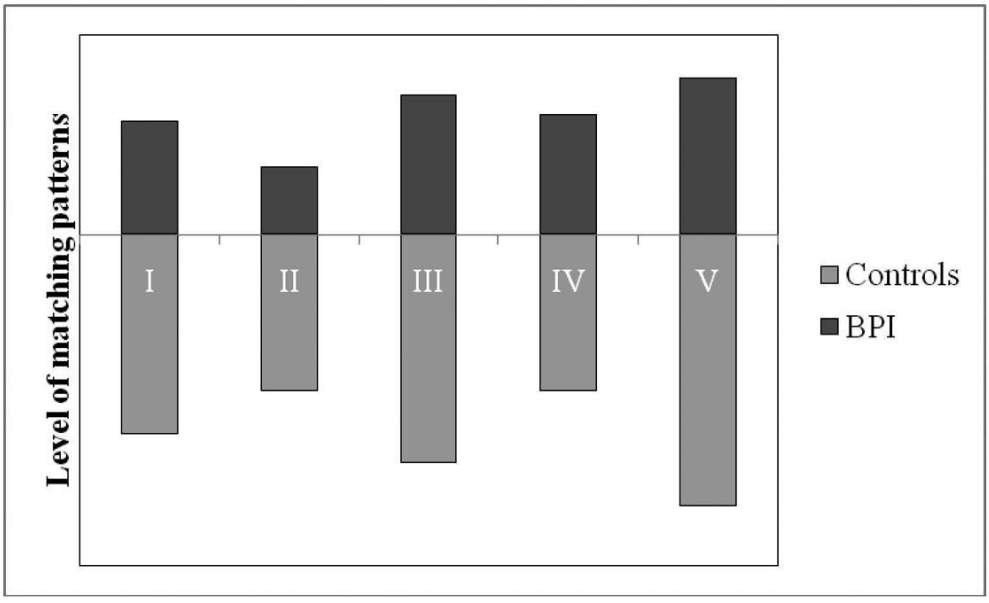

Fig. 1. Fluctuating asymmetry in fingerprint patterns in BPI patients and healthy controls.

References

1. **American Psychiatric Association.** *Diagnostic and statistical manual of mental disorders*, ed. 4, Washington, DC, APA, 1994.
2. **Cummins, H., C. Midlo**. *Fingerprints, palms and soles*. New York: Dover Publications, 1961.
3. **Galton F.** *Fingerprints. London: Macmillan*, 1892, reprinted, New York, 1965.
4. **Gutiérrez, B., J. Van OS, V. Vallés, R. Guillamat, M. Campillo, L. Fañanás.** Congenital dermatoglyphic malformations in severe bipolar disorder. – *Psychiatry Res.,* **78**, 1998, 133–140.
5. **Hit, G. L., I. G. Shirobokov, I. A. Slavolyubova.** *Dermatoglyphics in anthropology*. Nestor-History, 2013. [in Russian].
6. **Hit, G., N. Dolinova.** *Racial differentiation of humanity (Dermatoglyphic data)*. Moscow: Science, 1990 [in Russian].
7. **Jelovac, N., J. Milicić, M. Milas, G. Dodig, S. Turek, Z. Ugrenović.** Dermatoglyphic analysis in bipolar affective disorder and schizophrenia: "continuum of psychosis" hypothesis corroborated? – *Coll. Antropol*., **23**, 1999, 589-595.
8. **Markow, T., I. Gottesman.** Fluctuating dermatoglyphic asymmetry in psychotic twins. - *Psychiatry Res*., **29**, 1989, 37-43.
9. **Markow, T., K. Wandler.** Fluctuating dermatoglyphic asymmetry and the genetics of liability to schizophrenia. – *Psychiatry Res.,* **19**, 1986, 323-328.
10. **McTigue, O., M. Clarke, M. Gervin, M. Kamali, S. Browne, P. Whitty, A. Kinsella, A. Lane, C. Larkin, E. O`Callaghan.** Dermatoglyphics: A comparison of schizophrenia and bipolar disorder. – *International Congress on Schizophrenia Research,* 2003.
11. **Mellor, C. S.** Dermatoglyphic evidence of fluctuating asymmetry in schizophrenia. – *Br. J. Psychiatry*, **160**, 1992, 467-472.

12. **Nasrallah, H. A.** Neurodevelopmental aspects of bipolar affective disorder. – *Biol. Psychiatry*, **29**, 1991, 1–2.
13. **Penrose, L.** Memorandum on dermatoglyphic nomenclature. *Birth Defects: Original Article Series*, **4** (3), 1968, 1-12.
14. **Penrose, L. S., P. T. Ohara.** The Development of the Epidermal Ridges. – *J. Med. Genet.*, **10**, 1973, 201.
15. **Sanches, M., M. Keshavan, P. Brambilla, J. C. Soares.** Neurodevelopmental basis of bipolar disorder: A critical appraisal. *Prog. Neuropsychopharmacol. Biol. Psychiatry,* **32**, 2008, 1617-1627.
16. **Tornjova-Randelova, S., D. Paskova-Topalova, Y. Yordanov.** *Dermatoglyphics in anthropology and medicine.* Sofia: Professor Marin Drinov Academic Publishing House, 2011. [in Bulgarian].
17. **Torrey, E. F.** Epidemiological comparison of schizophrenia and bipolar disorder. – *Schizophr. Res.*, **39**, 1999, 101–106.
18. **Weinsten, D., D. Diforio, E. Schiffman, R. Bonsall.** Minor physical anomalies, dermatoglyphic asymmetries, and cortisol levels in adolescents with schizotypal personality disorder. – *Am. J. Psychiatry*, **156** (4), 1999, 617-623.19.
19. **Yousefi-Nooraie, R., S. Mortaz-Hedjri.** Dermatoglyphic asymmetry and hair whorl patterns in schizophrenic and bipolar patients. – *Psychiatry Res.*, **157**, 2008, 247-250.

Institute of Experimental Morphology, Pathology and Anthropology with Museum
Bulgarian Anatomical Society

Acta morphologica et anthropologica, 28 (1-2)
Sofia ● 2021

Craniological Series from the Necropolis, Excavated in the North Suburb of the Capital Town Tarnovgrad (Assenov Quarter of Contemporary Town) in Relation to the Results from the Population from "Holy Forty Martyrs" Church, Late Middle Ages, Veliko Tarnovo

V. Russeva, L. Manoilova*

Institute of Experimental Morphology, Pathology and Anthropology with Museum, Bulgarian Academy of Sciences

* Corresponding author e-mail: victoria_russeva@yahoo.com

Craniological study retains its values concerning variation in smaller groups and the appearance of the inhabitants of ancient sites. The very scarce and fragmented material for craniological study from our archeological excavations makes such finds highly valuable. The studied craniological series is provided from the necropolis, excavated in the Assenov quarter in Veliko Tarnovo (13th -14th c.). It is analyzed in comparison with the results from the series from the "Holy Forty Martyrs" church. Classical methods are used, combined with specially developed for the aims of the research. The studied series presents similar features to the relatively small dolychocranian group from the series from the "Holly Forty Martyrs" church. Differences from the latter series appear mostly in the facial part – broader and more prognatic faces in the necropolis from Assenov quarter. Some features ~~of~~ in the studied series are closer to the observed in the series from previous period.

Key words: craniometry, Middle Ages, Veliko Tarnovo

Introduction

Even if in contemporary science craniological data do not preserve the leading position in answering questions about genetic connections between paleo-populations, craniological study retains its values concerning variation in smaller groups and the appearance of the inhabitants of ancient sites. The very scarce and fragmented material for craniological study from our archeological excavations makes such finds highly valuable, even more so because in many cases they remain singular.

The studied craniological series is provided from the necropolis, excavated in the "Assenov quarter" in Veliko Tarnovo, dated in the last quarter of 13th – end of the 14th c. [12, 13]. The necropolis was in use in the period in which the medieval town was the capital of the Second Bulgarian Kingdom and was situated in its suburb

area [12, 13]. The studied series originates from the excavated section of its territory, most of which remains uninvestigated. The craniological series adds to our knowledge about the variable population of the capital of the second Bulgarian Kingdom, which until now was only represented by the series from the necropolis around the church of the "Holy Forty Martyrs" [19]. The comparison with the latter is the main aim of this study, in order to establish similarities to some of the groups defined there and expand our knowledge about the anthropological groups, which inhabited the capital in the period. Eventually such an approach would contribute to the identification of different ethnical and social groups in the capital with their specific anthropological appearance and different origin.

Material and Methods

The craniometrical study is performed based on the methods of Martin-Saller [17]. The horizontal profile of the face is evaluated after the frontomalar and the zygomaxilar angles and depth of the canine fossa after the Alekseev and Debets methods [2]. In addition to the angles of the vertical profile, used in classical methods [17], the feature is also assessed based on the angle between the length of the face and the upper face height, derived from the cosine theorem applied to the linear measurements between the length of the cranial base (basion-nasion), length of the facial section (basion-prostion) and upper face height (prostion-nasion). This measurement is included in the investigation of this series in order to include some of the more fragmented material and to make possible a comparison with the results from the investigation of the series from the "Holy Forty Martyrs" church necropolis. Again in order to be used for correlation with the results from the craniometrical data from "Holy Forty Martyrs" and to include some of the more fragmented material, the length of the hard palate is assessed following the classical methods and additionally as a linear distance between point orale and the palatine suture in the saggital plane.

Sex identification of individuals is achieved based on the available material from skeletons, using macroscopic methods as summarized in: Acsadi and Nemeskeri [1], White and Folkens [24], Walrath et al. [23] with priority placed on the results obtained from pelvic bones. The age of the adults is ascertained by using methods of assessment of the pubic bone's symphyseal surface relief based on Todd's scale in: Schwartz [21)]; the iliac auricular surface relief based on Ubelaker [21] and the cranial sutures' obliteration according to the scale in Olivier and Simpson in: Alekseev and Debets [2], compared to the scales of Meindl and Lovejoy [18]. Metrical data are compared to the standard tables of Dwight, Krongman, Thieme and Pearson for diameters of femoral, humeral and radial heads, femoral and humeral bicondylar breadth as summarized in Bass [3] and used in Kühl [16)]. Reconstructed pelvic girdle is used in sex identification of 22.73 % of the studied males and 18.18 % of the females, while in rest of the population only pelvic fragments are used [20].

Results and Discussion

The small number of studied skulls does not allow statistical analysis (**Tables 1-7**).

Nevertheless, it could be pointed out that in some features the studied group represents a relatively uniform population. This conclusion is supported especially in the obtained distribution of categories of some indices: the skull index, which shows a predominance of dolychocranian skulls; the height-length index, with height measured between porion-bregma points, which shows a predominance of skulls with no prevalence of length or height in the proportion; the height-breadth index, measured again between porion-bregma points, which shows a lack of high skulls; the occipito-parietal index, based on which most of the skulls fall into the medium category (**Table 5**). Based on the indexes for the facial area most of the skulls represent broad faces; based on the jaw index the vertical profile is described as prognath; based on the alveolar process of the maxilla and the length-breadth index of the mandible jaws are long-shaped as dolyhouranian and dolyhostenomandibular (**Table 6, Figs. 1-2**). The face profile presents mostly mesognath skulls, but the small values of the alveolar angle point to the development of prognath alveolar form (**Table 7, Figs. 1-2**). Horizontal profile of the nasomalar angle highly varies, but the zygo-maxilar region presents well-profiled faces (**Table 8**).

In comparison to the series from "Holy Forty Martyrs" the studied group shows close similarity in the proportions of the neurocranium, described in the skull index and indices of height with porion-bregma measurement with the relatively small group of dolychocranean skulls in the King's court church. The prevalence of broad faces places the series near to the first mesocranean group from "Holy Forty Martyrs", while all other groups in the latter series present higher faces. In relation to the found broader faces appears the higher incidence of prognath profile of faces in studied series, compared to the one from "Holly Forty Martyrs". The feature is observed in the values of jaw index and vertical facial angles (facial angle and alveolar angle) and their distribution. From four skulls, which provide data for measurement of the angle between facial length and height only the one from grave N 14 presents values close to the obtained in the "Holly Forty Martyrs", the other three skulls present significantly lower values. The same situation is observed in jaw index, after which the skull from grave N 14 again approaches to the series from "Holly Forty Martyrs", while the remaining three skulls present significantly higher values as related to the mean values found in the "Holly Forty Martyrs". As the dolihocranean group in the series from "Holy Forty Martyrs" the studied one presents close value for orbital index in two cases (males), which stay near to the lower limits of the mesoconh category. Two other skulls (from a male and a female), with relatively low orbits, fall into the chamaeconch category, characteristic for the cited group of skulls in the "Holy Forty Martyrs", most of the skulls from the other groups in this series show higher orbits.

Craniometrical series with close dating from Bojenishki Urvich [5, 6], North-West Bulgaria, Kavarna – Chirakman [7], North-East Bulgaria, Pernik – Fortress [9], South-West Bulgaria and Kabile - North-West Gate necropolis [11], Perperikon [14] and Tatul [8], in the Thracian region as most widespread are mesocranian skulls like in the series from "Holy Forty Martyrs" unlike the studied series from the "Assenov quarter". The series from Bojenishki Urvich and the 14^{th} – 15^{th} century necropolises from Chirakman, Kavarna, Kabile and Pernik show similarities with the cranial series from "Holy Forty

Martyrs" also in regards to the predominance of orthognath vertical face profiles in contrast to the relatively prognath forms in the studied population. Bojenishki Urvich and Kabile present low values of the zygo-maxillar angle of the horizontal profile, as established for both series from Veliko Tarnovo. Results, obtained for craniometrical series from the earlier period, 11th – 12th century CE – from Kovachevo [10] and Pliska [4] (male population) present closer values to the dolihocranial group from the "Holly Forty Martyrs" and the one from the "Assenov quarter". The distribution of cranial index in Odartsi 1 and 2 [15, 25] also presents bigger portions of dolichocranial and brachycranial skulls, while the relative number of mesocranian skulls remains significantly lower as presented in "Assenov quarter" as opposed to the ones from "Holy Forty Martyrs".

Conclusions

The studied series presents features that are more similar to the relatively small dolichocranial group from the series from the "Holy Forty Martyrs" necropolis. Differences from the latter series appear mostly in the facial part – with broader and more prognath faces in the necropolis from the "Assenov quarter". Some features of the studied series are closer to the ones observed in the series from the earlier period. It could be supposed that the series from King's court church presents more variation in types of features obtained by the population after intense mobility with political, social and clerical duty. In contrast, the group, which buried its dead in the necropolis in the "Assenov quarter" retained features, characteristic for the earlier period and possibly was more static, having less contacts with other populations.

References

1. **Acsádi, G., J. Nemeskéri.** *History of Human Life Span and Mortality*. Budapest, Akademiai Kiado, 1970, 333 p.
2. **Alekseev, V., G. Debets.** *Craniometry, Methods of Anthropological Study*. Moscow, Nauka, 1964, 228 p. (Алексеев, В., Г. Дебец. *Краниометрия, методика антропологических исследований*.) [in Russian].
3. **Bass, W.** *Human osteology: a laboratory and field manual of the human skeleton*. University of Missoury, 1971, p. 281.
4. **Boev, P., S. Cholakov.** Anthropological and paleo-pathological investigation of skeletons from the necropolis in the North area of the West fortress wall of Pliska. – *Pliska-Preslav* 5, 1992, p. 302-311. (Боев, П., Сл. Чолаков, Антропологично и палеопатологично проучване на скелетите от некропол в Северния сектор на Западната крепостна стена на Плиска. – *Плиска-Преслав*) [in Bulgarian].
5. **Boev, P., S. Cholakov.** Anthropological investigation. *In: Bozhenishki Urvich.* Sofia, 1979 (Боев, П., Сл. Чолаков, Антропологично проучване. *В: Боженишки Урвич*) [in Bulgarian].
6. **Boev, P., N. Kondova, S. Cholakov.** Anthropological investigation of the skeletons from the necropolis by the fortress "Bozhenishki Urvich". Interdisc. Invest. *III-IV,* 1979, p. 139-148. (Боев, П., Н. Кондова, С. Чолаков, Антропологично проучване на скелетите от некропола при крепостта "Боженишки Урвич". – *ИИ*) [in Bulgarian].
7. **Boev, P., N. Kondova, S. Cholakov.** Anthropological investigation of medieval necropolisses. *In: Chirakman, Karvuna-Kavarna, Sofia,* 1982, p. 62-65. (Боев, П., Н. Кондова, Сл. Чолаков. Антропологично проучване на средновековни некрополи. В: *Чиракман-Карвуна-Каварна*) [in Bulgarian].

8. **Boev, P., N. Kondova, S. Cholakov.** Anthropological investigation of medieval necropolis by the village Tatul. *In: Ahrid, Kardzhali*, 1978, p. 87-121. (Боев, П., С. Чолаков, Н. Кондова, Антропологично проучване на средновековния некропол при с. Татул. В: *Ахридъ*.) [in Bulgarian].
9. **Boev, P., N. Kondova, S. Cholakov.** Medieval necropolis. Anthropological data. In: *Pernik II,* 1983, p. 177-212. (Боев, П., Н. Кондова, С. Чолаков. Средновековният некропол. Антропологични данни. В: *Перник*) [in Bulgarian].
10. **Boev, P., Sl. Tscholakov, N. Kondova, Zv. Minkov, A. Natscheva, D. Piperkova.** Anthropological investigation of the medieval necropolis by the village Kovachevo, Pazardzhik distr. - *Anatomische Anzeiger,* **1**, 1977, 58-66. (Anthropologische Untersuchung einer mittelarterlichen Nekropole bei dem Dorf Kovatschevo, Bezirk Pazardzik) [in German].
11. **Cholakov, S., N. Kondova, P. Boev.** Biological reconstruction of the medieval population of Kabyle. *K, II,* 1991, p. 137-155. (Боев, П., Сл. Чолаков 1991. Антропологично проучване на средновековни погребения върху надгробна могила от елинистическата епоха при Кабиле. – *Кабиле***)** [in Bulgarian].
12. **Dermendzhiev, E., M. Tomanova.** Necropolis in the North suburb of the metropolis Tarnovgrad. – *Izvestia na RIM- Veliko Tarnovo, XXXIV,* 2020, p. 41-98. (Дерменджиев, Е., М. Томанова, Некропол в северното подградие на столичния Търновград. – *Известия на РИМ-Велико Търново*) [in Bulgarian].
13. **Dermendzhiev, E., M. Tomanova.** Rescue archaeological excavations of the site "Necropolis in Assenov quarter in Veliko Tarnovo (UPI XIV, sq. 223 PUP, Veliko Tarnovo*)". Archaeological excavations and finds in the 2018, Sofia,* 2019, p. 486-489. (Дерменджиев, Е., М. Томанова, Спасително археологическо проучване на обект „Некропол в квартал „Асенов" във Велико Търново (УПИ XIV, кв. 223 по ПУП на Велико Търново)". – *АОР за 2018*) [in Bulgarian].
14. **Kavgazova, L., R. Stoev, P. Boev.** Anthropological study of medieval necropolis of Perperakion fortress near Gorna Krepost, Kurdjali District. – *Comp. Rend. Acad. Bulg. Sci.,* **38**, 1985, 6, 779-781.
15. **Kondova, N., S. Cholakov.** Anthropological data for the physical type, life span and epidemiology of a medieval population from Dobrudzha. - *Bulg. Ethnograpy*, **3**, 1993, 45-54. (Кондова, Н., С. Чолаков. Антропологични данни за физическия тип, продължителността на живота и заболеваемостта на една средновековна популация от Добруджа. – *Българска етнография*) [in Bulgarian].
16. **Kühl, R.** Skeletal remains from praehistorical cremations and their possibilities for interpretation with with attention to the special problems in Schleswig-Holstein. – *Communications of the Anthropological Society in Wien (MAGW),* **115**, 1985, 113-137 (Kühl, R., Skelettreste aus prähistorische Brandbestattungen und ihre Aussagemöglichkeiten, mit Hinweisen auf spezielle Fragestellungen in Schleswig-Holstein. – *MAGW*) [in German].
17. **Martin, R., K. Saller.** *Textbook of Anthropology*, Stuttgart, Gustav Fischer Verlag, Band 2, 1959. (Lehrbuch der Anthropologie) [in German].
18. **Meindl, R. S., C. O. Lovejoy**., Ectocranial suture closure: A revised method for determination of skeletal age at death based on the lateral-anterior sutures. – *Am. J. Phys. Anthropol.,* **68**, 1985, 57-66.
19. **Russeva, V.** Craniological series from the graveyard around the "40 Holy martyrs" church. – *Anthropological Researches and Studies*, **7**, 2016, 88-104.
20. **Russeva, V., L. Manoilova.** Demographic characteristics, physical development, and pathological changes of population, presented in the medieval necropolis in the North suburb of the capital Tarnovgrad. – *Izvestia na RIM- Veliko Tarnovo,* XXXIV, 2020, 99-120. (Русева, В., Маноилова, Л. Демографски характеристики, физическо развитие и патологични изменения на популацията, представена в средновековния некропол в северното подградие на столичния Търновград. – *Известия на РИМ-Велико Търново*) [in Bulgarian].
21. **Schwartz, J. H.** *Skelleton keys (an introduction to human skelletal morphology, development and analysis)*. New York, Oxford Press, 1995.
22. **Ubelaker, D.** *Human skeletal remains: excavation, analysis, interpretation*. 2nd ed. Washington, D.C., Taraxacum, 1989
23. **Walrath, D., P. Turner, J. Bruzek.** Reliability test of the visual assessment of cranial traits for sex determination. – *Am. J. Phys. Anthropol.*, **125**, 2004, 132-137.
24. **White, T., P. Folkens.** *The human bone manual.* Elsevier, 2005, 464 p.
25. **Yordanov, Y., B. Dimitrova,** Data from the anthropological investigation of the buried in the medieval necropolis N **2** by the village Odartsi, Dobrich distr. – *In: Doncheva-Petkova, L. Odartsi – necropolises from XI s., 2.* Sofia, "Marin Drinov , 2005, p. 415-460. [in Bulgarian].

Table 1. Basic skull linear measurements and corresponding indices, neurocranium, males and females, Assenov quarter, Veliko Tarnovo. Gr. N – grave number; No – number by Martin-Saler [17]; *8:1* – correlated measurements in the index by Martin, Saller [17]

	Measurements and indices	No		Males, Gr N						Females, Gr N			
				11	14	16	22	27	35	9	10	33	37
Measurements	Cranial length	1	gl-op	200	176	-	182	182	-	189	176	186	169
	Cranial breadth	8	eu-eu	149	147	-	136	128	-	133	150	134	141
	Cranial height	17	ba-br	151	127	-	137	-	-	140	123	126	
	Cranial height (po)	20	po-v	-	107	-	-	-	-	120	-	111	116
	Cranial height (po-br)	-	po-br	116.5	105.5	-	-	107	109	119	108	-	-
	Smallest frontal breadth	9	ft-ft	103	89	93	97	83	100	98	98	96	100
	Occipital breadth	12	ast-ast	120	112	-	108	101	-	110	115	105	107
	Cranial base length	5	ba-n	110	98	-	96	127	-	103	-	100	-
Indices	Cranial index	1:8	-	74.5	83.52	-	74.73	70.33	-	70.37	85.23	72.04	83.43
	Hight-length index	17:1	-	75.55	72.16	-	75.27	-	-	74.07	69.89	67.74	-
	Hight-breadth index	17:8	-	101.41	86.39	-	100.74	-	-	105.26	82	94.03	-
	Hight-length index (po)	20:1	-	-	60.8	-	62.64	-	-	62.96	-	59.68	-
	Hight-breadth index (po)	20:8	-	-	72.79	-	83.82	-	-	89.47	-	82.84	-
	Hight-length index (po-br)	-	-	58.25	59.94	-	59.62	58.79	-	63.49	61.36	59.41	68.64
	Hight-breadth index(po-br)	-	-	78.19	71.77	-	79.78	83.59	-	90.23	72	82.46	82.27
	Fronto-parietal index	9:8	-	69.13	60.54	-	71.32	64.84	-	73.68	65.33	71.64	70.92
	Occipito-parietal index	12:8	-	80.54	76.19	-	79.41	78.91	-	82.71	76.67	78.36	75.89

Table 2. Basic skull linear measurements and corresponding indices, facial part, males and females, Assenov quarter, Veliko Tarnovo. Gr. N – grave number; No – number by Martin-Saler [17]; *8:1* – correlated measurements in the index by Martin, Saller [17]

	Measurements and indices	No		Males, Gr N							Females, Gr N		
				8	11	14	16	22	27	35	9	33	37
Face	Facial length	40	ba-pr	-	-	90	-	99	-	-	103	101	-
	Facial breadth	45	zg-zg	-	-	133	-	-	122	-	121	123	-
	Upper face breadth	43	fmt-fmt	-	116	103	104	96.5	104	104	103	105	104
	Zygomaxilar breadth	46	zm-zm	92	-	98	84	88	98	98	91	98	95.5
	Facial height	47	n-gn	-	-	111.2	-	110	-	-	106	100.5	109
	Upper face height	48	n-pr	-	-	63.4	-	67.2	66.8	-	67	63	61
	Face index	47:45	-	-	-	83.61	-		104.1	-	86.6	81.71	-
	Upperface index	48:45	-	-	-	47.67	-		54.75	-	55.37	51.22	-
	Face index(Virhov)	47:46	-	-	-	113.47	-	125	129.57	-	116.48	102.55	114.14
	Upperface index (Virhov)	48:46	-	-	-	64.69	-	76.36	68.16	66.12	73.63	64.29	63.87
	Jaw index	40:5	-	-	-	91.84	-	103.12	-	-	100	101	-
Orbital	Orbital breadth	51	mf-ek	-	-	40	45	41	41	42.7	39.1	41	40
	Orbital height	52	-	-	-	34.5	34.4	42	31.2	29.5	35.5	28.5	32
	Orbital index	52:51	-	-	-	86.25	76.44	-	76.1	69.09	90.79	69.51	80
Nasal	Nasal height	55	n-ns	-	-	46	54.3	51	50	51	49	49	51
	Piriform aperture breadth	54	lt-lt	22	-	23	24	24	26.4	26	26.5	27.5	22.4
	Nasal index	54:55	-	-	-	50	44.2	47.06	52.8	50.98	54.08	56.12	43.92
	Nasal bones breadth	57	-	-	13	9	10	10	9	9	12	10	11
	Nasal bones height		-	-	4.5	6	5.5	5	5	5.5	6	3	5.5
	Nasal bones length	56	n-rhi	-	-	-	-	-	21.5	-	23	-	-
	FC		-	-	-	5.5	4.6	3	4.5	4	2.5	4	7
Maxilar	Alveolar process height	48.1	ns-pr	19.5	-	18.2	-	-	-	14	19	-	10
	Palatine length	62	-	49	-	45	-	53	45	-	-	52.1	45.5
	Palatine breadth	63	enm-enm	35	-	35.5	-	40	35.5	39	37	59.5	37
	Palatine, anterior length	AL	-	37	-	35	-	37	38	41	-	43	39
	Palatine index	62:63	-	-	-	-	-	75.47	78.89	-	-	114.2	-
	Palatine index (anterior)	62:AL	-	-	-	-	-	108.11	93.42	112.97	-	138.37	-
	Maxilla, alveolar process lenght	60	-	52.5	-	54.5	-	50	5	44.7	52.5	47	45
	Maxilla, alveolar process breadth	61	-	57	-	59.5	-	59.5	56.2	63.6	59	35.5	63
	Maxillar index	61:60	-	-	-	109.17	-	119	112.4	142.28	88.98	75.53	140.0

Table 3. Basic skull facial angle measurements in degrees, horizontal and vertical profile, males and females, Assenov quarter, Veliko Tarnovo. Gr. N – grave number; No – number by Martin-Saler [17]

Measurements	No	Males, Gr N							Females, Gr N			
		8	11	14	16	22	27	35	9	10	33	37
Nasomalar angle	77	-	162	135	148	-	145.5	136	141	135	141	152.5
Zygomaxilar angle	-	125	-	140	127	122	126.5	131	122	-	129	128
Face Angle	72	-	-	83	-	75	84	-	81	-	82	-
Ba-n-pr angle	-	-	-	77.27	-	67.46	-	-	70.31	-	70.87	-
Nose angle	75	-	-	60	-	42	59	-	46	-		-
Alveolar angle	74	-		68	-	65	69	-	71	-	77	-

Table 4. Basic skull measurements, in *mm* and indices, mandible, males and females, Assenov quarter, Veliko Tarnovo. Gr. N – grave number; *8:1* – correlated measurements in the index by Martin, Saller [17]

Measurement and indices	Males, Gr N									Females, Gr N				
	6	8	11	14	16	22	24	27	35	9	10	31	33	37
Symphiseal height	23.5	32	35.5	25.5	29	33	29	32	29	30.5	29.5	32	26	29.1
Breadth at mental foramen	10.8	11	11.1	10	10	10	19	10	11.5	-	10	9.5	13	11.1
Bigonial breadth	106	112	118	105	106	100	113	81	-	94	93	96	91	105
Mental breadth	44	41.5	49.2	41.5	42	-	48	41	43.5	40.5	47	42.5	47.2	-
Projection length	81	78	85	72	75	72	83	80	75	82	77	71	74	72
Branch height	65	-	74	56	56	49	64	62	62	61	57	57	57	55
Branch smallest breadth	32	32	33.4	27	25*	29*	-	34	34.6	32	31	22.5	31	26.8
Mandible angle (in degrees)	120.5	132	115	127	124	141*	131	115	133	111	120	119	122.5	127
Coronial breadth	-	100	139	91	106	95	-	91	-	96	98	95	10	100
Condilar breadth	-	-	-	-	-	-	-	111	-	119	-	115	113	-
Length-breadth index	-	-	-	-	-	-	-	72.07	-	68.91	-	61.74	65.14	-
Breadth index	-	-	-	-	-	-	-	72.97	-	78.99	-	83.48	80.53	-

Table 5. Distribution of studied skulls after main indices of cerebral section of skull, males and females, Assenov quarter, Veliko Tarnovo; N – number of measured skulls

		Skull index, 8:1			Height-length index					Height-breadth index					Fronto-parietal index 9:8				Occipito-parietal* index 12:8			
	N	Dolicho-cranian	Brachy-cranian	Hyperbrachy-cranian		N	chamae-cranian	ortho-cranian	Chypsi-cranian		N	tapeino-cranian	Metrio-cranian	Acrocra-nian	N	Stenome-top	Metriome-top	Euryme-top	N	Medium	High	Very high
M	4	3	1	-	ba, 17:1	3	-	1	2	ba, 17:8	3	1	-	2	4	1	1	2	4	2	2	-
F	4	2	1	1		3	1	2	-		3	1	1	1	-	-	-	-	4	3	-	1
Tt	8	5	2	1		6	1	3	2		6	2	1	3	4	1	1	2	8	5	2	1
M					po, 20:1	4	-	4	-	po, 20:8	4	3	1	-								
F						4	-	2	2		4	1	2	1								
Tt						8	-	6	2		8	4	3	1								

Table 6. Distribution of values and means of main indices of facial section of skull, males and females, Assenov quarter, Veliko Tarnovo; N – number of measured skulls

	Upperface, 47:45				Upperface, 48:46 Virhow				Jaw, 40:5			Orbtal, 52:51				Nasal, 54:55				Palatin, 63:62			Upper jaw 61:60			Lower jaw 68:65	
	N	eurien	mesen	lepten	N	hyperchamaeprosop	chamaeprosop	orthoprosop	N	orthognath	prognath	N	chamaeconch	mesoconch	hypsiconch	N	leptorhinian	mesorhinisn	chamaerhinian	N	leptostaphylin	brachystaphylin	N	dolihouran	brahyuran	N	Dolichostenomandi-bular
M	2	1	1	-	4	1	2	1	4	1	3	3	1	2	1	5	1	3	1	3	3	-	3	3	-	2	2
F	2	-	1	1	3	2	1	-	2		2	3	1	1	1	3	1	-	2	1	-	1	3	2	1	2	2
Tt	4	1	2	1	7	3	3	1	6	1	5	6	2	3	2	8	2	3	3	4	3	1	3	5	1	4	4

Table 7. Distribution of values of angle measurements, males and females, Assenov quarter, Veliko Tarnovo; N – number of measured skulls

	Face			Alveolar				Nasomalar angle							Zygomaxilar angle			
	N	prognath	mesognath	N	small	medium	big	N	very small	small	medium	big	very big	over very big	N	very small	small	medium
M	3	1	2	3	3	-	-	5	1	1	-	2	-	1	6	1	3	2
F	2	-	2	2	-	1	1	4	1	-	2	-	1	-	3	1	2	-
Tt	5	1	4	5	3	1	1	9	2	1	2	2	1	1	9	2	5	2

Fig. 1. Skull, frontal, right lateral, occipital and vertical view, grave N 27. Male, 60-65 years at death

Fig. 2. Skull, frontal, left lateral, occipital and vertical view, grave N 33. Female, 40-50 years at death

Institute of Experimental Morphology, Pathology and Anthropology with Museum
Bulgarian Anatomical Society

Acta morphologica et anthropologica, 28 (1-2)
Sofia ● 2021

Occupational Dental Abrasion from Medieval Plovdiv

Georgi Tomov[1], Stefan Zlatev[2], Rumen Ivanov[3], Rada Kazakova[4], Nadezhda Atanassova[5]

[1] *Oral Pathology Department, Faculty of Dental Medicine, Medical University, Plovdiv, Bulgaria*
[2] *Research Institute at Medical University of Plovdiv, Division - Innovative technologies in dental medicine, Center for CAD/CAM dentistry, Medical University, Plovdiv, Bulgaria*
[3] *Medical History Museum, Medical University, Plovdiv, Bulgaria*
[4] *Prosthetic Dentistry Department, Faculty of Dental Medicine, Medical University, Plovdiv, Bulgaria*
[5] *Institute of Experimental Morphology, Pathology and Anthropology with Museum, Bulgarian Academy of Sciences, Sofia, Bulgaria*

* Corresponding author e-mail: Georgi.Tomov@mu-plovdiv.bg

Dental abrasion is a natural phenomenon with universal occurrence that has existed from the origin of humankind and depends on the lifestyle, diet and occupation. Dental abrasion was very serious in ancient populations up to the late medieval period. The paper presents a male skeleton from medieval Plovdiv with marked dental abrasion which is considered to be occupational, possibly related to carpentry or shoemaking. The hypothesis of occupational abrasion is tested in archeological experiment.

Key words: dental abrasion, nails, occupation,medieval

Introduction

In anthropology and archaeology, it has been assumed for several decades that teeth provide interesting material for observation because of their high mineral content, which gives them strong resistance to post mortem taphonomic processes [4]. The paleopathological findings reveal the prevalence and evolution of a number of pathological processes than the morphological changes in teeth are relevant to living conditions, mostly with occupational and environmental factors, which allows to draw conclusions about the life and the socio-economic situation of the studied population [9]. Tooth wear is of particular interest in the study of relationships between man, his environment and his pattern of subsistence.

From the point of view of palaeopathology, the Middle Ages constitute an interesting period because of the numerous collections available and the fact that many authors have confirmed the existence of notable tooth wear on the populations studied. Brabant [1], one of the pioneers of dental anthropology in Europe, wrote that “tooth wear in the Middle Ages was much more accentuated than today”. In the medieval

population of Valjevo (Serbia, 15th century), Djuric-Srejic[3] estimated that "tooth wear was the most common finding". Caglar et al. [2] wrote, about a Byzantine medieval sample (12th century), that "in contrast with dental caries, tooth wear was remarkable in our sample". More recently, Meinl et al. [6] found "a very pronounced attrition" in an Austrian sample from Avar (11th century).

In these anthropological and historical contexts, the aim of the paper is to present a medieval male dentition that displays marked dental abrasion which is considered to be occupational, possibly related to carpentry or shoemaking. The examined skeleton originates from the medieval necropolis at the archeological site "Bishop's Basilica of ancient Philippopolis" in Plovdiv, Bulgaria [8].

Materials and Methods

During the anthropological examination of 216 dentitions from a medieval necropolis (10th - 12th century) at the archeological site "Bishop's Basilica of ancient Philippopolis" in Plovdiv, Bulgaria, one case (grave #28) of marked dental abrasion in a 35–40 year old male individual was found. The most severe changes involve the anterior left maxillary incisor and its antagonist – mandible left central incisor. In central occlusion the affected teeth display loss of enamel and dentine that frames a triangular-shaped defect (**Fig. 1**). These unusual findings were the reason for more detailed anthropological study including use of X-ray examination and computerized evaluation of the occlusion and tooth wear pattern.

Fig. 1. Marked dental abrasion of both anterior left maxillary incisor and its antagonist. In central occlusion the affected teeth display loss of enamel and dentine that frames a triangular-shaped defect.

Results

Except the maxillary right central incisor and the mandible left canine which are lost post mortem and were not found at the excavation site, the other teeth are present and intact. The occlusal view of the maxillary first left incisor (**Fig. 2A**) and segmented X-ray of the same tooth (**Fig. 2B**) revealed irregular loss of tooth substance with larger distal defect and root resorption. There is no evidence for communication between the defect and the pulp chamber but the consequences from pulpal necrosis are beyond any doubt. Both the bone defect and root resorption could be attributed to chronic occlusal trauma. The incisal aspect of the left mandible central incisor displays a wide plane abrasion extended in a buccal aspect with loss of enamel and substantial loss of dentine but not exposing the pulp. The deposition of calculus at the mandible frontal area is significant.

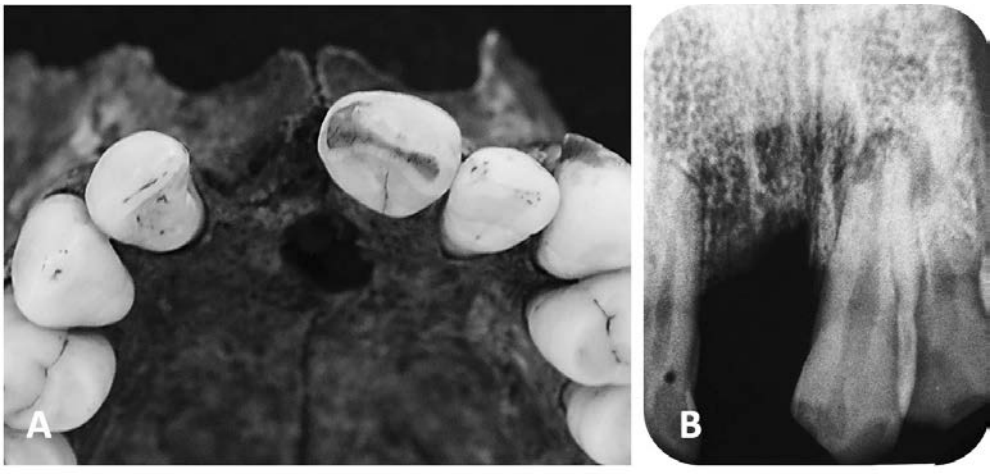

Fig. 2. Occlusal view of the maxillary first left incisor (**A**) and segmented x-ray of the same tooth (**B**) revealed irregular loss of tooth substance with larger distal defect and root resorption.

In order to evaluate the occlusion and the tooth wear pattern a digital impressions from the lower and upper jaws were taken with a Trios 3® (3Shape, Copenhagen) intraoral scanner (**Fig. 3A**). The software and hardware of Trios 3® have the capability to capture fully colored model. This scanner is a powder-free scanner which operates on the confocal principle with the video-recording method. The software version 3Shape Trios Classic 1.3.4.6 was used. Scanning procedures were performed according to the manufacturer's instructions. It was started with the upper jaw, followed by the lower one. Scanning was started on the right third molar and ended on the left third molar. The scanning strategy on the upper arch is the following: occlusal surface followed by buccal surface and, nally, palatal surface. Scanning strategy on the lower jaw starts with the occlusal surface, then the lingual surface and, nally, the buccal surface. The next step was bite registration in intercuspidal position on both sides. During bite scan the scanner tip was positioned at molar region, the buccal side of the teeth and slowly moved in mesial direction. After the scanning of the upper and lower arches, the virtual cast appeared on the screen (**Fig. 3B**). The virtual casts of upper and lower arches were found acceptable if included accurate scans of all the surfaces of every teeth with 3-4 mm of alveolar bone and no crack lines were found. The quality of the scans was satisfactory if the software could attach the arches to each other based on bite registration scan (**Fig. 3C**). The evaluation of the occlusion and the attrition pattern revealed that the attrition follows the normal pattern and a clear reversed or anti-curve of Monson has been established i.e. the greatest wear occurs on the buccal aspect of the lower molar and the palatal aspect of the upper molar crowns (**Fig. 3D**). The lack of evidence for contacts between the upper central left incisor and its antagonist raised the question about the ethiology of this defect.

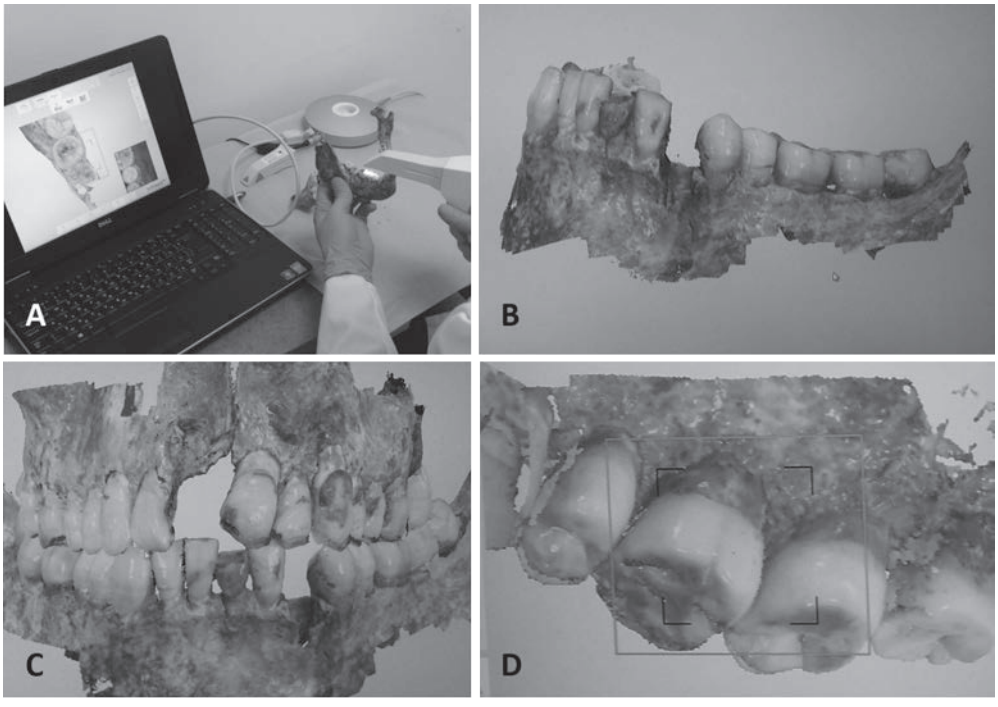

Fig. 3. Digital impressions of the lower and upper jaws were taken with a Trios 3® intraoral scanner (**A**). The virtual after complete scanning (**B**). Software attaches the arches to each other based on bite registration scan (**C**). Evaluation of the tooth wear patterns (**D**).

Discussion

Marked attrition, reaching the dentin and pulp chamber is not unusual in archaeological material [1, 2, 3, 4, 6, 9]. The chewing of hard objects and the mastication of materials such as leather or rope would result in marked regular attrition of the tooth crowns, possibly with linear grooves occlusally [5]. However, this is quite dissimilar to the present case with irregular, sharp abrasions only of two antagonist teeth. Nor does the overall appearance, varying degrees of involvement and asymmetrical presentation support deliberate mutilation. Such dental mutilations appear to be largely confined to Africa, North and South America [7] but are not relevant to cultural tradition of the medieval Europe.

Our hypothesis is that the dental abrasion is related to occupational activity as it was already reported once by Turner G. and Anderson T. [9]. In their publication they reported for marked occupational dental abrasion from medieval Kent. In experimental study done with nails found at the archeological site they confirmed the relation between the dental loss and the use of frontal teeth as a tool for holding nails during work. Considering the possibility to deal with a carpenter or a shoemaker who repeatedly held nails between his teeth we reconstructed the situation with nail found at the same site. The results revealed that the example of iron nail known to date from the medieval period appears to fit very accurately into the abrasion defect (**Fig. 4A, 4B, 4C**).

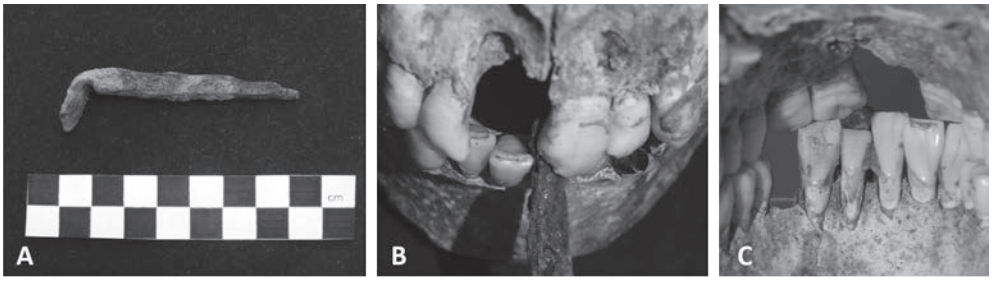

Fig. 4. Medieval iron carpentry nail recovered from the same archeological site (lengths: 72 mm; rectangular in cross-section and tapering to a 2 mm point); (**A**). Vestibular (**B**) and palatal (**C**) view of the dentition in occlusion with the nail fitting accurately into the anterior incisal abrasion.

Conclusions

A medieval male skeleton from Plovdiv displays marked dental abrasion of the anterior teeth, which appears to be occupational. The evaluation of the occlusion and the tooth wear pattern revealed normal distribution of the occlusal forces and attrition relevant to the sex and age with only one exception – the upper central left incisor and its antagonist. Although we cannot be certain of the etiology, medieval iron nail appears to fit into the incisal abrasion very precisely. This suggests that the individual may have followed the occupation of carpenter or shoemaking for many years. The hypothesis of occupational abrasion is confirmed in archeological experiment and the skeletal remains are exhibited at the Museum of medical history in Medical University of Plovdiv, Bulgaria.

References

1. **Brabant, H.** Evaluation of 20 years' experience in scientific dental research. – *Rev. Belg. Med. Dent*., **28,** 1973, 179-186.
2. **Caglar, E., O. Kuscu, N. Sandallia, I. Arib.** Prevalence of dental caries and tooth wear in a Byzantine population (13th c. AD.) from Northwest Turkey. – *Arch. Oral. Biol.,* **52**, 2007, 136-1145.
3. **Djuric-Srejic, M. S.** Dental paleopathology in a Serbian Medieval population. – *Anthropol. Anz.,* **59**, 2001, 113-122.
4. **Esclassan, R., D. Hadjouis, R. Donat, O. Passarrius, D. Maret, F. Vaysse, E. Crubézy**. A panorama of tooth wear during the medieval period. – *Anthropol. Anz.,* **72**(2), 2015, 185-199.
5. **Larsen, C. S.** Dental modifications and tool use in the western Great Basin. – *Am. J. Phys. Anthropol.*, **67**, 1985, 393-402.
6. **Meinl, A., G. M. Rottensteiner, C. D. Huber, S. Tangl, G. Watzak, G. Watzek.** Caries frequency and distribution in an early medieval Avar population from Austria. – *Oral. Dis.,* **16**, 2010, 108-116.
7. **Milner, G. R., C. S. Larsen.** Teeth as artifacts of human behavior: intentional mutilation and accidental modification. In: *Advances in dental anthropology*, (Eds. M. A. Kelley, C. S. Larsen), New York, Wiley-Liss, 1991, 357-378.
8. **Tomov, G.** Paleopathological data for the medieval population of Plovdiv according to necropolis findings at archeological site „Bishop's basilica". *Plovdivski istoricheski forum*, **1**, 2017, 82-90. [in Bulgarian, with English summary]
9. **Turner, G., T. Anderson**. Marked Occupational Dental Abrasion from Medieval Kent. – *Int. J. Osteoarchaeol*., **13**, 2003, 168-172.

Institute of Experimental Morphology, Pathology and Anthropology with Museum
Bulgarian Anatomical Society

Acta morphologica et anthropologica, 28 (1-2)
Sofia ● 2021

Analysis of the Sick Leaves among Employee in the Laser Cutting Company

Vlayko Vodenicharov[1], Konstantin Tachkov[2], Konstantin Mitov[2]

[1] *Department of Epidemiology and Hygiene, Faculty of Medicine, Medical University of Sofia*
[2] *Department of Organization and Economy of Pharmacy, Faculty of Pharmacy, Medical University of Sofia*

* Corresponding author e-mail: vlayko_vodenicharov@abv.bg

We aimed to explore all registered sick leaves in the company for laser cutting stratified by the reasons, length of absence from work and their relation to the gender, occupation, and age.

This is a one-year, retrospective study of all claims of sick leave by employees working at the biggest Bulgarian company for laser cutting. All health claims for sick leaves after the end of 2017 were collected and systematized by the reason, according to the international classification of diseases (ICD) 10th edition; employee occupation position; length of sick leave; gender, and age. The productivity loses were calculated and analysed and statistical analysis was performed through $\chi 2$ method and correlation analysis. In the production company for laser cutting most prevalent were the sick leaves due to respiratory and infectious disease, with a prevailing share of younger employees – approximately 46 years of age. Production loses are significant for the employer and country economy.

Key words: sick leaves, laser cutting, productivity loses, temporary disability

Introduction

Metallurgy and mechanical engineering companies are often considered as having highly polluted environments [2]. The nature of the work done in such companies produces conditions (i.e., microclimate changes), which adversely affect the employees' health, leading to reduced productive capacity, and increased absence from work due to sickness [6]. Environmental risk factors in the production area might include heating conditions, pollutants, air quality, humidity, air velocity;otherwise known as thermal factors [12]. There are many ways in which these factors interact in order to produce an adverse health effect. For instance, heating and melting of metals requires extreme temperatures, which puts employees at risk of having a heat stroke, additionally, the subsequent rapid cooling procedures greatly raise the humidity, which increases air pollutant concentrations, due to the formation of fine spherical particles of dust and sod, all suspended in a stale air environment [21]. In such conditions, workers are frequently exposed to drastic temperature fluctuations and are at risk of cough and flu infections, which later could progress to chronic conditions. Improvements in

workplace microclimate in production facilities are aimed at ensuring better working conditions, improving production capacity, and decreasing the incidence of accidents, adverse health effects, as well as employee morbidity [22].

Companies often time monitor closely the sick days of employees as well as the reasons for them in order to identify patterns and address health issues pre-emptively [24]. Appropriate action, whether that of an incapacity investigation or taking preventive measures, should always be undertaken and conducted within the stipulations laid down by applicable legislation. In addition, the sick leaves have probable impact of the production of the companies. Sick leave can be defined as the absence from work due to illness or injury [30]. Little is known about temporary disability due to sick leaves in the laser cutting companies and its influence on the employee and employer [10]. This provoked our interest towards exploring the sick leaves due to short- and long-term morbidity in a Bulgarian company for laser cutting.

We aimed to explore all registered sick leaves in the company for laser cutting stratified by the reasons, length of absence from work and their relation to the gender, occupation, and age.

Materials and Methods

This is a one-year, retrospective study of all claims of sick leave by employees working at the biggest Bulgarian company for laser cutting. All health claims for sick leaves after the end of 2017 were collected and systematized by the following characteristics:

– Reason, according to the international classification of diseases (ICD) 10th edition;
– Employee occupation position;
– Length of sick leave;
– Gender, and
– Age.

The productivity loses were analysed by multiplying the number of days out of work with average wage for the country and classified according to payer. The average national wage was taken from the National statistical institute for 2017 year, estimated to be 570 euro [18].The average monthly wage in the production companies in 2017 was 570 euro. Therefore, we estimated the average daily wage to be 27 euro. According to the national legislation, the first 3 days of sick leaves are paid by the employer with the rate being the individual employee's daily salary, however since that information is private, our results are for the average national wage. The repeated sick leaves claimed by a single person were counted separately.

Statistical analysiswas performed through χ^2 method and correlation analysis.

Results

Sick leave analysis

The share of males in the company was 78% out of all 265 permanent employees at the end of 2017. 79% of them had applied for a sick leave, although the majority of them were absent from work for no more than 3 days (n=220). Absences longer than 3 days were recorded for n=9 people, while only 21% stated that they had more than one

reason for sick leave. Long-term absences of up to 30 days and more were registered for 18% of the employees (**Table 1**).1.2% reported having work-related injuries. Due to separated counting of the repeated sick leaves claimed by a single person the number of employees with ≤3 days sick leave days + number of workers with >3 days sums up to 276, more than the total employees in 2017.

Table 1. General characteristics of the observed group

Indicator	Value
Total number of employees at the end of 2017	265
Male	208
Female	57
Number of people with sick leave days	211
Number of cases with 3 days sick leave	220
Number of people with more than 4 reasons for sick leave	56
Number of people with 30 or more sick days	48
Share of people with sick leave days (%)	61.3%
Average length of temporarily incapacity for work (days)	7 (SD 8.6)
Average share of long-lastingwork incapacity (%)	30.2%
Average share of short-lasting work incapacity (%)	35.7%
Frequency of working people with work injuries (%)	1.2%

Table 2. Registered cases and days of sick leaves according to ICD code of the disease

Disease group	ICD code	N days	N cases	Average length (days)
Infectious diseases	A00-B99	391	100	3.91
Malignancies	C00-D48	2	1	2
Endocrine disorders	E00-E90	10	2	5
Psychotic and anxiety disorders	F00-F99	108	3	36
Nervous system disorders	G00-G99	315	43	7.3
Eye diseases	H00-H59	110	16	6.9
Ear diseases	H60-H95	63	13	4.8
Blood system disorders	I00-I99	239	19	12.6
Respiratory system disorders	J00-J99	938	193	4.9
Digestive system disorders	K00-K93	215	29	7.4
Skin and subcutaneous tissues	L00-L99	75	9	8.3
Bones and muscles system	M00-M99	706	96	7.4

Urinary tract system disorders	N00-N99	87	21	4.1
Pregnancy, delivery and maternal period	O00-099	132	5	26.4
Laboratory tested symptoms	R00-R99	12	5	2.4
Injuries, poisoning and external factors influence	S00-T98	717	56	12.8
External factors morbidity and mortality	V01-V98	1	1	1.0
Health system general factors and contacts	Z00-Z99	197	4	49.3
Total		4318	616	7

According to the causes of sick leave, respiratory system disorders prevailed with 193 observed cases, lasting approximately 5 days on average, followed by musculoskeletal diseases (n=706 for 7.4 days), and infectious diseases (n=391 for 4 days on average) – (Table 2). The high number of cases is because people stated that they had more than one reason for sick leave. Infectious diseases and respiratory system disorders are typical for the winter season and we can suppose that they are probably less connected with the working environmental factors, while the diseases of bones and muscles could be influenced by the working conditions. The long-lasting absences are due to psychotic and anxiety disorders of 3 people which were out of work for 36 days per person on average. Relatively high was the share of injuries and metal poisoning, and it can be argued that nervous system disorders, eyes and ears diseases could also be attributed to the working environment.

According to the employee occupation the highestgroup at risk were the mechanics which comprised a total of 314 cases of sick leaves – (**Table 3).**

Mechanics suffer mostly from respiratory system, bones and muscles, and infection diseases, but injures and poisoning are also observed at a very high rate with a share of 9% sick leaves.

The total number of sick days recorded for the year was 4318 and almost half of them are attributed to mechanics (n=2078) – (**Table 4**), 3267cases are attributed to males and the rest to female employees.

Stratification by age group revealed that young to middle aged workers (median 46 years) accounted for most of the sick days – (**Table 5)**.However, the most common reason given was infectious disease, due to which we can assume that these were seasonal diseases, owing to the higher frequency of respiratory andinfectious diseases in the winter season.

Productivity loses

The average monthly wage in the production companies in 2017 was 570 euro. Therefore,we estimated the average daily wage to be 27 euro. According to the national legislation, the first 3 days of sick leaves are paid by the employer [15] with the rate being the individual employee's daily salary, however since that information is private,

Table 3. Registered number of cases of sick leaves per occupation and reason

Disease group	ICD code	laser cutting	powder coating	welder	mechanics	ware-houses	Adminis-tration	Insta-leers	Total
Infectious diseases	A00-B99	2	4	5	51	11	21	4	100
Malignancies	C00-D48							1	1
Endocrine disorders	E00-E90				1			1	2
Psychotic and anxiety disorders	F00-F99				1	2			3
Nervous system disorders	G00-G99		1	1	24	11	6		43
Eye diseases	H00-H59			3	8		5		16
Ear diseases	H60-H95			3	6		3	1	13
Blood system disorders	I00-I99			1	15		1	2	19
Respiratory system disorders	J00-J99	4	11	21	87	15	38	17	193
Digestive system disorders	K00-K93			6	19	1	3		29
Skin and subcutaneous tissues	L00-L99		1		5	2		1	9
Bones and muscle system	M00-M99	3	3	8	57	12	7	6	96
Urinary tract system disorders	N00-N99		2	2	9	1	1	6	21
Pregnancy, delivery and maternal period	O00-099						5		5
Laboratory tested symptoms	R00-R99			1	1			3	5
Injuries, poisoning and external factors influence	S00-T98	2	1	9	29	1	9	5	56
External factors morbidity and mortality	V01-V98						1		1
Health system general factors and contacts	Z00-Z99				1		3		4
Total		11	23	60	314	56	105	47	616

Table 4. Number of days of sick leaves per occupation

Disease group	ICD code	laser cutting	powder coating	welder	Mech-anics	Ware-Houser	Admini-stration	installers	Total
Infectious diseases	A00-B99	4	14	58	181	36	88	10	391
Malignancies	C00-D48							2	2
Endocrine disorders	E00-E90				9			1	10
Psychotic and anxiety disorders	F00-F99				44	64			108
Nervous system disorders	G00-G99		3	7	148	64	93		315
Eye diseases	H00-H59			19	73		18		110
Ear diseases	H60-H95			24	20		12	7	63
Blood system disorders	I00-I99			3	225		2	9	239
Respiratory system disorders	J00-J99	19	39	162	410	66	159	83	938
Digestive system disorders	K00-K93			20	140	13	42		215
Skin and subcutaneous tissues	L00-L99		1		51	14		9	75
Bones and muscle system	M00-M99	21	17	81	405	63	50	69	706
Urinary tract system disorders	N00-N99		12	5	28	2	3	37	87
Pregnancy, delivery and maternal period	O00-099						132		132
Laboratory tested symptoms	R00-R99			2	1			9	12
Injuries, poisoning and external factors influence	S00-T98	34	7	114	335	14	128	85	717
External factors morbidity and mortality	V01-V98						1		1
Health system general factors and contacts	Z00-Z99				8		189		197
Total		78	93	495	2078	336	917	321	4318

Table 5. Age distribution of sick leave days

Age group	laser cutting	powder coating	Welder	mechanics	warehousers	administration	installers	Total
to 25	11	46	140	581	62	100	5	945,0
26-35	48	30	166	859	103	473	103	1782
36-45	19	17	136	584	28	220	67	1071
46-55			53	52	120	121	143	488
above 55				2	23	3	4	32
Total	78	93	495	2078	336	917	321	4318

our results are for the average national wage. For the registered 616 cases,the number of days that the employer covered was 1848 days amounting to 49 896 euro. The other 2470 days are covered by the Social insurance fund but only at the rate of 75% the monthly wage.We calculated the cost covered by the social insurance fund to be 50 018 euro and the total amount of sick days cost was 99 914 euro. Thus, the total amount of productivity loses sums up to 149 819 euro and out of them 67% is paid by society in the form of insurance coverage or out-of-pocket expense.

Statistical analysis

There is a statistically significant difference (p=0.0104) between the average number of cases of sick leaves for male (n=6.6) and female (n=8.7) employees. No statistically significant difference (p=0.5271) was found between the average number of days (p=0.2962) of sick leaves for male (15.7) and female (18.4).

A strong correlation was observed between the number of days and cases of sick leaves regardless of occupation, age group or gender with correlation coefficients varying between 0.995 and 0.982 (**Fig.1**).

Discussion

The current study explores for the first time the temporary disability in the laser cutting company in Bulgaria focusing on the medical reasonsfor diseases, age and gender distribution [25,26]. For the purposes of the analysis, temporary disability was defined asa condition that workers face as a result of illnessor accident, because of which they temporarily could not perform their work and required health care services [13]. The regulatory framework in the country follows that of the European directives and its primary objective is to defend the interest of workers [8]. No cap on the number of sick days per year exist, but if the employee is out of work for 6 months, local legislation requires him to be examined by a medical committeewhich could decide that he is incapable of working and be diagnosed with a workplace related disability. To receive a

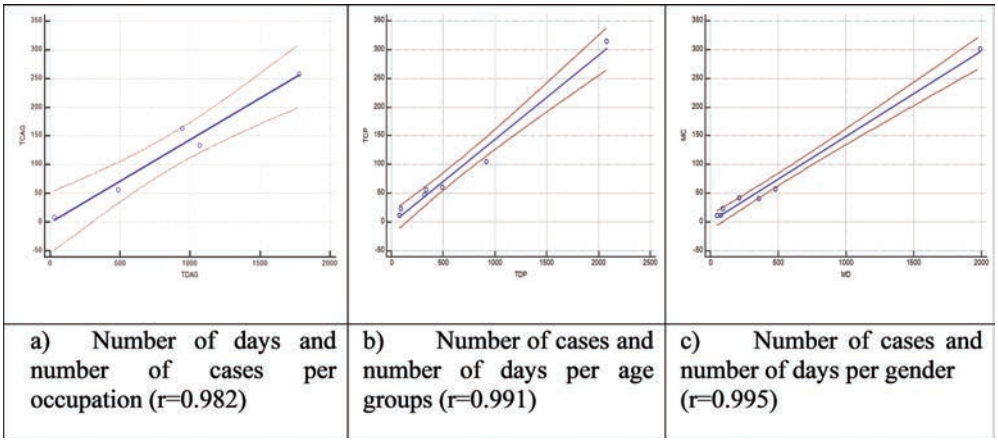

a) Number of days and number of cases per occupation (r=0.982)

b) Number of cases and number of days per age groups (r=0.991)

c) Number of cases and number of days per gender (r=0.995)

*Average line is the mean calculate value and upper and lower bands are for 95%CI
Fig.1. Correlation analysis

sick day, an employee has to document it through a health claim after which it is covered either by the employeror by the National Insurance Fund. Therefore,the data regarding all documented sick leaves in the company is valid and all days were consumed and correspond to the actual absences of the workers due to health reasons.

The temporary disability of 7 days per case in theobserved company is close to number of sick leave daysreported from other countries. The average number of sick days is 5.9 in UK [29]. Norway and Finland had the highest number of sickness absences per year per employee (Norway: women = 9.5, men = 8.0; Finland: women = 9.5, men = 6.2). Denmark and Sweden had the lowest number of sickness absence days (Denmark: women = 6.8, men =5.3; Sweden: women = 7.1, men = 4.8) [23]. In Greece, in the private sector, the number of sick leave days was reported to be between 4.6 and 8.7 [1]. In the private sector of Singapore 3.2 days of medical leave per person per year were reported [5]. We can assume that industry and country specific characteristics have more influence on sickness absence than establishment size, employee's gender and occupation.

Studies thatanalyse the gender differences reported that women on average have more sick leaves than men [9,19]. Health differences and family reasons appear to be the best explanation for the gender difference in sickness absence [11]. In our study men comprised the majority of employees in the company which is why our results differ and a larger share of absences for males. Only 5 females were registered to have pregnancy and/or maternal leave for 132 days during the year.

In contrast with other authors, our study shows that younger ages consume more sick days, than older ones [17]. A reason for this could be the prevailinacute nature of the diseases for which employees applied for sick leave. Nonetheless, prophylactic measures should be taken more seriously among the observed workers and medical reasons should be explored in more detailin order to prevent chronic disease development [4,20]. Some authors also recommend ensuring zones for physical activities to reduce the likelihood of absence [27]. This is especially important for workers in production companies due to the high risk of musculoskeletal diseases [28]. Our study found a high prevalence of such diseases in comparison to other physiological systems that support such a proposal [7].

Sick leaves are causing significant production loses. Health-related productivity loss is estimated to cost the UK economy more than $100 billion (£77.5 billion)[16]. In Spain per person cost due to productivity loss is reported to be from 2.589 euros to 1941 euros [3]. It is argued that costs could be reduced significantly if companies invested in adequate health and wellbeing programs for their employees [31]. In Bulgaria the average wage is the lowest one in EU and productivity loses are relatively lower in comparison to other countries but for the country itself they are not at all insignificant. Companies also experience a large burden due to sick leaves, evidence by the high productivity loses for the employer and employee in the observed company.

Limitation of our study is that we analysed only the officially registered health claims due to temporary disability and not the productivity loses due to presenteeism, although it also might have significant impact on the workforce's performance [14]. In addition, we recognize that the study might be mostly of interest of local authorities but international comparison shows that similar problems exist in many other countries and their comparison is important in order to reshape the national and international labour legislation.

Conclusion

In the production company for laser cutting most prevalent were the sick leaves due to respiratory and infectious disease, with a prevailing share of younger employees – approximately 46 years of age. Production loses are significant for the employer and country economy. There is a need of prophylactic and disease prevention programs to reduce the number of sick days leave and economic loses.

References

1. **Alexopoulos, E. C., G. Merekoulias, D. Tanagra, E. C. Konstantinou, E. Mikelatou, E. Jelastopulu.** Sickness absence in the private sector of Greece: comparing shipyard industry and national insurance data. – *Int. J. Environ. Res. Public Health,* **9**(4), 2012, 1171-1181.
2. **Allebeck, P., A. Mastekaasa.** Risk factors for sick leave - general studies. – *Scandinavian Journal of Public Health*, **32**, 2004, 49-108.
3. **Ballesteros, P. M., C. S. Pujadas, J. M. Martínez, M. P. Almuni, G. L. Delclos, F. G. Benavides.** Cost comparison of temporary sickness absence in 2006 between Barcelona and Madrid provinces Spain. – *Rev. Esp. Salud Publica*, **83**(3), 2009, 453-461.
4. **Breucker G., A. Schroër.** Concept and principles of workplace health promotion. – *Promot. Educ.,* 6(3), 1999, 3-8.
5. **Chan, O. Y. , S. L. Gan, S. E. Chia.** Sickness absence in private sector establishments in Singapore. – *Singapore Med. J*., **38**(9), 1997, 379-383.
6. **Christensen, K. B., T. Lund, M. Labriola, E. Villadsen, U. Bultmann.** The fraction oflong-term sickness absence attributable to work environmental factors: prospectiveresults from the Danish Work Environment Cohort Study. – *Occup. Environ. Med.,* **64**(7), 2007, 487-489.
7. **de Vries H. J., M. F. Reneman, J. W. Groothoff, J. H. Geertzen, S. Brouwer.** Self-reported work ability and work performance in workers with chronic nonspecific musculoskeletal pain. – *J. Occup.Rehabil.,* **23**(1), 2013,1-10.
8. **European commission.** Employment, social questions and inclusion. Available at https://ec.europa.eu/social/main.jsp?catId=1103&langId=bg&intPageId=4435.
9. **European Foundation for the Improvement of Living and Working Conditions.** Absence from work. 2010. Dublin, European Foundation for the Improvement of Living and Working Conditions.
10. **Høverstad, T., G. Koefoed, I. H. Gudding.** Interventionagainst sick-leave in an industrial company. – *Tidsskr. Nor. Laegeforen*.,**114**(11), 1994,1317-1320.

11. **Laaksonen, M, P. Martikainen, O. Rahkonen, E. Lahelma.** Explanations for genderdifferences in sicknessabsence: evidence from middle-aged municipal employeesfrom Finland. – *Occupational and Environmental Medicine*, **65**(5), 2008,325-330.
12. **Lund, T, M. Labriola, K. B. Christensen, U. Bultmann, E. Villadsen.** Physical workenvironment risk factors for long term sickness absence: prospective findingsamong a cohort of 5357 employees in Denmark. – *BMJ*, **332**, 2006, 449-452.
13. **Martin-Fumadó, C., G. Martí-Amengual, L. P. Bausili, J. Arimany-Manso.** Temporary disability and its legal implications. – *Med. Clin. (Barc.)*, **142**, 2014, 37-42.
14. **Middaugh, D. J.** Presenteeism: sick and tired at work. – *Medsurg. Nurs.*,**15**(2), 2006, 103-105.
15. **Ministry Council.** Decree 364 on regulation on calculation and payment of monetary compensations and support from the public insurance. Governmental Newspaper 2006, last amended Gov. Newspaper 57, 2016.
16. **Mitchell R. J., P. Bates.**Measuring health-related productivity loss. – *Popul. Health Manag*., **14**(2), 2011,93-98.
17. **Molarius A., S. Janson.** Self-rated health, chronic diseases, and symptoms among middle-aged and elderly men and women. – *J Clin Epidemiol*, 55(4), 2002, 364-70.
18. **National Statistical Institute.** Available athttps://www.nsi.bg/bg/content/3927/%D1%81%D1%80%D0%B5%D0%B4%D0%BD%D0%B0-%D1%80%D0%B0%D0%B1%D0%BE%D1%82%D0%BD%D0%B0-%D0%B7%D0%B0%D0%BF%D0%BB%D0%B0%D1%82%D0%B0
19. **Nyman, K., E. Palmer, S. Bergendorff.** The Swedish disease (In Swedish). 2002. Stockholm, ESO.
20. **Olsen, G. W., J. M. Burris, M. M. Burlew, M. E. Steinberg, N.V. Patz, J.A. Stoltzfus, J. H. Mandel.** Absenteeism among employees who participated in a workplace influenza immunization program. – *J. Occup. Environ. Med*., **40**(4), 1998, 311-316.
21. **Oude, Hengel K. M., J. E. Bosmans, J. M. Van Dongen, P. M. Bongers, A. J. Van der Beek, B. M. Blatter.** Prevention program at construction worksites aimed at improving health and work ability is cost-saving to the employer: results from an RCT. – *Am. J. Ind. Med.*, **57**(1), 2014, 56-68.
22. **Parent-Thirion, A., E. F. Macias, J. Hurley, G. Vermeylen.** Fourth European working condition survey, 2007. European foundation for the Improvement of Living and Working Condition.
23. **Thorsen, S. V., C. Friborg, B. Lundstrøm, J. Kausto,K. Örnelius, T. Sundell, Å. M. Kalstø, O. Thune, B. O. Gross,H. Petersen, Ö. Haram**. Sickness absence in the Nordic countries. Nordic Social Statistical Committee, Copenhagen 2015.
24. **Sjöberg. O.** Positive welfare state dynamics? Sickness benefits and sickness absence in Europe 1997-2011. – *Soc. Sci. Med*., **177**, 2017, 158-168.
25. **Toseva, E., T. Turnovska.** Frequency and burden of diseases with temporary disability among waste water treatment plants workers. *Scientific works of the Union of Scientists in Bulgaria-Plovdiv, series G. Medicine, pharmacy and dental medicine*, XX, 2017.
26. **Tsacheva, N.** Working-hygienic aspects in examining the morbidity with temporary disability. *PhD Thesis*, National center for hygiene and epidemiology, 1987.
27. **van Amelsvoort, L. G., M. G. Spigt, G. M. Swaen, I. Kant.**Leisure time physical activity and sickness absenteeism; a prospective study. – *Occup. Med. (Lond).*,**56**(3), 2006, 210-212.
28. **Viester, L, E. A. Verhagen, K. I. Proper, J. M. van Dongen, P. M. Bongers, A. J. van der Beek.** VIP in construction: systematic development and evaluation of a multifaceted health programme aiming to improve physical activity levels and dietary patterns among construction workers. – *BMC Public Health*, 2012, 12-89.
29. **Walsh, I. A., S. Corral, R. N. Franco, E. E. Canetti, M. E. Alem, H. J. Coury.** Work ability of subjects with chronic musculoskeletal disorders. – *Rev. Saude Publica*, **38**(2), 2004, 149-156.
30. **Wendt, J. K., S. P. Tsai, F. A. Bhojani, D. L. Cameron.**The Shell Disability Management Program: a five-year evaluation of the impact on absenteeism and return-on-investment. – *J. Occup. Environ. Med*., **52**(5), 2010, 544-550.
31. **World economic forum.** Working when sick is rising and harms you and your employer. Available at https://www.weforum.org/agenda/2019/05/working-when-sick-is-rising-and-harms-you-and-your-employer-this-is-why/.
32. **Holtermann, A, J. V. Hansen, H. Burr, K. Søgaard.** Prognostic factors for long-term sickness absence among employees with neck-shoulder and low-back pain. – *Scand. J. Work Environ. Health*, **36**(1), 2010, 34-41.

Institute of Experimental Morphology, Pathology and Anthropology with Museum
Bulgarian Anatomical Society

Acta morphologica et anthropologica, 28 (1-2)
Sofia ● 2021

Prosthetic Treatment Methodology of Edentulous Patients with Maxillary Resection

Ivan Gerdzhikov

Department of Prosthetic Dentistry, Faculty of Dental Medicine, Medical University, Sofia

* Corresponding author e-mail: ivan_ger1971@abv.bg

Prosthetic treatment methods are main treatment techniques for rehabilitation of speech and feeding in patients with maxillary resection. The presented clinical case introduces a hollow-bulb obturator treatment methodology of a patient with a unilateral defect and complete edentulism. The preliminary impressions have been taken with alginate and the defect has been tamponaded with gauze. The final impression of the mandible has been taken with a custom tray and creamy-consistency silicon impression material. After the trial denture, the maxillary occlusal rim has been used for taking functional impression to ensure good retention and stability. A hollow-bulb obturator for upper jaw and complete denture for lower jaw have been fabricated and then adjusted into the patient's mouth. Treatment results have demonstrated good retention and stability of the obturator and mandible denture. The examination with the "Oronasopneumotest" device has registered good defect hermetization, which contributed to successful speaking rehabilitation.

Key words: denture, maxillary resection, maxillary defect, obturator.

Introduction

Nowadays, there is a significant increasing in the number of oncological diseases in the maxillo-facial area, which leads to growth in the cases of maxillary resection [3]. Treatment options of these cases include defect coverage by tissue transplantation or obturating prostheses. There isn't a consensus view regarding the method for the most optimal restoration of the damaged functions [2]. In most cases, the size and localization of the defect, as well as the presence of teeth, determine the stage of speaking and feeding rehabilitation [4, 5]. Previous studies suggest that treatment results are significantly better among patients with small defects [16].

Research findings indicate the highest prevalence of the resection of the half maxilla [20]. In rare instances, it is combined with a complete teeth loss which makes the treatment extremely difficult. The main issues, which exist in the cases of total edentulism, are related to the achievement of retention and stability of the obturator [6]. This necessitates the application of specific techniques and materials for taking impressions and fabricating dentures [18]. Most researchers consider acrylic resins as

appropriate for achieving stable support and retention of the obturator [1, 15]. Obturator's type and shape remain important factors for determining the quality of speaking and feeding processes. It is suggested that the light construction of the open obturators delivers improved phonetic and speech intelligibility properties [13]. This is shown by examining patients with I and II class defects of Armani. They have experienced insignificant changes in articulation and nasal speech six weeks after treatment with such types of obturators [8].

Research findings indicate the height of the obturating part and the right placement of the defect as factors affecting treatment result, as well. Some researchers suggest that high lateral and short medial sides provide optimal speech recovery, whereas others recommend maximum height of the lateral sides for reduction of nasal speaking [9, 12]. Some studies however, suggest that speaking and feeding normalization is possible only when the obturator has short walls [7, 11]. In a comparative study, Turkaslan et al. [17] report 94.24% speech intelligibility in 10 mm wall's height, 91.2% in 5 mm and 90.5% in 15 mm. These similar results and the comparison with the pre-treatment values of 45.04% ± 5.86% demonstrate the efficiency of open obturators regardless of their height.

There is a prevailing opinion that obturators provide a successful recovery of the damaged functions, despite the mixed evidence regarding most optimal treatment method after maxillary resection [14]. This is confirmed from a study with 188 patients, who have been treated with different types of obturators and successful rehabilitation of speaking and feeding has been achieved [10]. There is an interesting positive relationship between the rate of speaking recovery and patient's individual intellectual level and will. These findings coincide with the concept that treatment methods should align not only with the main prosthetic principles, but also with the individual specifics of each case [19].

Materials and Methods

The reported clinical case presents the prosthetic treatment of 65-year-old patient, who has been operated from maxillary cancer. There was a defect in the left half of the jaw as a result of maxillary resection. The examination has shown that the defect is localized in the region of the hard palate, on the border between the midline and soft palate. The alveolar bone has been partially preserved, but edentulous. The mandible has been edentulous, as well, and the alveolar bone had reduced height and volume, due to atrophy. The patient was able to open his mouth to a limited extent, because of the earlier conducted radiation therapy; hence, making the treatment process even more difficult. The treatment plan has included a fabrication of hollow-bulb obturator and complete denture of the mandible. The impressions of both jaws have been taken with standard metal trays and alginate, whereas the maxillary defect has been preliminary tamponaded with gauze. The mandible's final impression has been taken with custom tray and creamy-consistency silicone material. The occlusal height and the jaw relationships have been registered in the next appointment by using occlusal rims. After the trial denture, the maxillary occlusal rim has been used as a custom tray and the final impression has been taken with creamy-consistency silicone material. The primary gauze tamponde and the functional design of the impression facilitated the casting of

a precise master model, which is important to the fabrication of hollow-bulb obturator. Both dentures had been made of acrylic resin (Figs. 1, 2). The "Oronasopneumotest" device was used for assessing defect hermetization and treatment efficiency. This methodology has been developed by Prof. Trifon Mihailov and provides the opportunity to registrate the pressure in the oral and nasal cavity during expiration. Its application shows the luck or the present of prosthesis' hermetization, on which depends the state of chewing and swallowing rehabilitation. The application of this methodology allows precise and objective evaluation of the achieved defect hermetization after the treatment. The results from the control examinations have indicated some decubital ulcers, which required insignificant corrections.

a b

Fig. 1. Completed dentures – occlusal (a) and palate (b) point of view

Results

Treatment results have demonstrated good retention and stability of the obturator and mandible complete denture. The designed hollow-bulb part of the obturator has provided easy denture insertion into the defect, which has significant importance, due to the occurred radial trismus. The examination with the "Oronasopneumotest" device has registered good defect hermetization, which contributed to successful speaking rehabilitation. The hollow-bulb design of the obturator provided the necessary retention, reduced the snuffle and normalized the occlusion relations (Fig. 3). Normalization of the feeding and drinking functions was achieved, as well. The results from the recalls have indicated easy adaptation to the dentures. Some typical corrections for such type of treatment, which were related to the decubital trauma of the soft tissue, were performed accordingly. Improvements in the patient's overall life quality, social activity and self-esteem were consequently reported.

Discussion

The main difficulties, in treatment of patients with large maxillary defects and complete edentulism, are related to taking an accurate functional impression from the defect. Additional problems, due to radiotherapy-induced trismus, are common and required specific treatment methods. The presented methodology of taking a functional impression

Fig. 2. Finished obturator

Fig. 3. Restored occlusal relations

after the trial denture, facilitated the correct insertion of the obturator into the defect. The preliminary gauze tamponation and the application of creamy-consistency silicone material allow the design of the substitution part with the desired height and volume. The height of the obturator's walls was 10 mm according to the design specifications. It enhanced obturator's easy and effortless placement into the defect, despite the limited mouth opening. The application of acrylic resin provided good retention and stability, similarly to results from other studies [1, 15]. The design of open substitution part with mid-height walls facilitated successful speech rehabilitation; thereby, confirming previous findings by Turkaslan et al. [17]. The achieved correct articulation and luck of snuffle demonstrated the open obturators' actual ability to provide good phonetic and speech intelligibility [8, 13]. Findings did not confirm other hypothesis, suggesting that such results are possible only when high lateral and short medial walls or maximum obturator's height, are designed [9, 12]. Research outcomes suggest that speech and feeding restoration are possible even in instances of complete edentulism; hence, challenging the opinion that the presence of teeth is a main determinant for treatment [4, 5]. Thus, it was possible to confirm the general opinion regarding the effective role of specific prosthetic treatment methods for successfully rehabilitation of damaged functions [10, 14].

Conclusions

Prosthetic treatment of patients with maxillary resection is accompanied by numerous difficulties and issues, especially in cases with complete edentulism. This requires the application of specific treatment methods reflecting the individual specific characteristics. The effective planning, designing and fabricating of prostheses determines the successful recovery of speaking and feeding functions; thereby, contributing to life quality improvement .

References

1. **Ali, R., A. Altaie, B. Nattress.** Rehabilitation of oncology patients with hard palate defects Part 3: Construction of an acrylic hollow box obturator. – *Dent. Update.*, **42**, 2015, 612-624.
2. **Brandão, T. B., A. J. Filho, V. E. de Souza Batista, M. C. Q. de Oliveira, A. R. Santos-Silva.** Obturator prostheses versus free tissue transfers: A systematic review of the optimal approach to improving the quality of life for patients with maxillary defects. – *J. Prosthet. Dent.*, **115**, 2016, 247-253.

3. **Cohen, N., S. Fedewa, A. Chen.** Epidemiology and demographics of the head and neck cancer population. – *Oral. Maxillofac. Surg. Clin. North. Am.*, **30**, 2018, 381-395.
4. **Dalkiz, M., A. S. Dalkiz.** The effect of immediate obturator reconstruction after radical maxillary resections on speech and other functions. – *Dent. J. (Basel)*, **6**, 2018, 22.
5. **Dholam, K., G. Bachher, S. Gurav.** Changes in the quality of life and acoustic speech parameters of patients in various stages of prosthetic rehabilitation with an obturator after maxillectomy. – *J. Prosthet. Dent.,* **123**, 2020, 355-363.
6. **Dos Santos, D. M., F. P. de Caxias, S. B. Bitencourt, K. H. Turcio, A. A. Pesqueira, M. C. Goiato.** Oral rehabilitation of patients after maxillectomy. A systematic review. – *Br. J. Oral. Maxillofac. Surg.*, **56**, 2018, 256-266.
7. **Kobayashi, M., M. Oki, S. Ozawa, T. Inoue, H. Mukohyama, T. Takato, T. Ohyama, H. Taniguchi.** Vibration analysis of obturator prostheses with different bulb height designs. – *J. Med. Dent. Sci.,* **49**, 2002, 121-128.
8. **Kumar, P., V. Jain, A. Thakar.** Speech rehabilitation of maxillectomy patients with hollow bulb obturator. – *Indian. J. Palliat. Care*., **18**, 2012, 207-212.
9. **Kwon, H. B., S. Chang, S. Lee.** The effect of obturator bulb height on speech in maxillectomy patients. – *J. Oral. Rehabil.,* **38,** 2011, 185-195.
10. **Matiakin, E. G., V. Chuchkov, A. Akhundov, R. Azizian, I. Romanov, M. Chuchkov, V. Agapov.** Restoration of speech function in oncological patients with maxillary defects. – *Vestn. Otorinolaringol.,* **5,** 2009, 43-46.
11. **Murase, I.** In-vivo modal analysis of maxillary dentition in a maxillectomy patient wearing buccal flange obturator prostheses with different bulb height designs. – *Nihon Hotetsu Shika Gakkai Zasshi*, **52**, 2008, 150-159.
12. **Oki, M., T. Iida, H. Mukohyama, K. Tomizuka, T. Takato, H. Taniguchi.** The vibratory characteristics of obturators with different bulb height and form designs. – *J. Oral. Rehabil.,* **33**, 2006, 43-51.
13. **Patil, P. G., P. S. Patil.** A hollow definitive obturator fabrication technique for management of partial maxillectomy. – *J. Adv. Prosthodont*., **4**, 2012, 248-253.
14. **Sahoo, N. K., A. P. Desai, I. D. Roy, V. Kulkarni.** Oro-nasal communication. – *J. Craniofac. Surg.,* **27**, 2016, 529-533.
15. **Singh, M., I. K. Limbu, P. K. Parajuli, R. K. Singh.** Definitive obturator fabrication for partial maxillectomy patient. – *Case Rep. Dent.,* **21**, 2020, 6513210.
16. **Tripathi, A., A. Gupta, V. Arora.** Effect of prosthodontic rehabilitation of maxillary defects on hypernasality of speech. – *J. Prosthodont.,* **25**, 2016, 202-206.
17. **Turkaslan, S., T. Baykul, M. Aydin, M. Ozarslan.** Articulation performance of patients wearing obturators with different buccal extension designs. – *Eur. J. Dent.,* **3**, 2009, 185-190.
18. **Wang, Y., X. Yang, R. Gan, H. Liu, G. Wu, Q. Yu, Z. Wang, X. Lu, J. Jing, W. Ma, Y. Quan, Z. Sun, L. Fan, Y. Wang.** Digital planning workflow for partial maxillectomy using an osteotomy template and immediate rehabilitation of maxillary brown II defects with prosthesis. – *J. Oral. Rehabil.,* **46**, 2019, 1133-1141.
19. **Youny Lee, S. K., L. D. Baier, A. H. Douglas, S. M. Munz.** Application of the basic tenants of restorative dentistry in the management of a patient post-maxillectomy – *J. Mich. Dent. Assoc*., **97**, 2015, 66-70.
20. **Yu, S., Y. Wang, C. Mao, C. B. Guo, G. Y. Yu, X. Peng.** Classification and reconstruction of 1,107 cases of maxillary defects. – *Beijing Da Xue Xue Bao Yi Xue Ban.*, **47**, 2015, 509-513.

Institute of Experimental Morphology, Pathology and Anthropology with Museum
Bulgarian Anatomical Society

Acta morphologica et anthropologica, 28 (1-2)
Sofia ● 2021

Rare Anatomic Variation of the Upper Limb Blood Supply: Case Report and Literature Review

Viktor Stoykov[1], Atanas Mitev[1], Ivan Maslarski[1]*

Department of Anatomy, Histology, Pathology and Forensic Medicine, Faculty of Medicine, SU "St. Kliment Ohridski", Sofia, Bulgaria

* Corresponding author e-mail: atanas.vl.mitev@abv.bg

Variations in vasculature of the upper extremity are fairly common and have been extensively studied throughout the years. During standard anatomical dissection of an upper extremity, multiple variations of vasculature were noted. Presence of a brachial artery (BA) with two main arterial stems was noted, with the superficial branch giving two main forearm arteries - a. radialis and a. medioulnaris – and the deep branch continuing in the forearm as the common interosseous artery. Furthermore, an open superficial palmar arch was discovered, with two common palmar digital arteries originating from a. radialis, and the other two from a. ulnaris (a. medioulnaris). To our knowledge, this is the first case report presenting these exact variations simultaneously in a single limb. Larger scale trials are still needed to determine the frequency of similar, multiple variations and to revise and improve existing classifications and terminology.

Key words: deep proper brachial artery (DPBA), superficial brachial artery (SBA), superficial brachioulnoradial artery (SBURA), incomplete arcus palmaris superficialis

Introduction

Variations of the arterial patterns in the upper limb have been the subject of many anatomical studies due to their high incidence. Knowing all the normal anatomical variations and their prevalence is important in clinical practice and crucial for numerous medical procedures like arterial and venous catheterization, creating skin flaps with a consistent vascular pedicle for resurfacing defects, used commonly in reconstructive surgery, surgical management of fractures, compartment syndrome, etc. The presence of a rare vascular pattern can increase the risk of an injury to the blood supply of a superficially located variant artery, or of an accidental injection.

In the course of a routine dissection of upper limb, according to the guidelines prescribed in *"Gray's Clinical Photographic Dissector of the Human Body"* [10], a rare variant of the vasculature pattern was discovered and carefully studied. A presence of a brachial artery (BA) with two main arterial stems was found, with the superficial branch artery giving two main forearm arteries - a. radialis and a. medioulnaris – and the deep

branch continuing in the forearm as the common interosseous artery. Furthermore, an open superficial palmar arch was discovered, with the two common palmar digital arteries originating from a. radialis, and the other two from a. ulnaris (a. medioulnaris).

Materials and Methods

In the past ten years 33 embalmed human bodies were assessed, that included 19 males and 14 females. The variation has been discovered in a routine dissection of a female, right upper limb with medical students in the Medical Faculty of University of Sofia "St. Kliment Ohridski". The cadaver has been fixed with standard solution containing formalin. Three anatomical significant arterial variations were noted. The purpose of this case report is to describe them as a rare, simultaneously occurring variation.

Results

The blood supply of the brachium region begins in a normal fashion, with the axillary artery giving rise to the brachial artery at the distal border of the teres major muscle. The brachial artery then traverses distally in its normal anatomical location and, as noted during performed measurements, has a diameter of around 0,8 cm. As seen in **Fig. 1**, the artery first gives rise to the profunda brachii artery, 4 cm after its emergence. This branch, as noted during examination, has no notable variability, traverses backwards to the posterior region of the brachium where it gives non-variable branches and is accompanied by the radial nerve. After this initial branching, the brachial artery soon bifurcates at the 7,5 cm mark, around the level of origination of the brachialis muscle, into two large vessels of similar size and caliber. Their relation regarding the median nerve was noted, with the anterior branch positioned in front, and the posterior branch positioned behind the nerve.

The superficial brachial artery (SBA) was found to have a fairly convoluted course through the brachium and was positioned similarly to a normal brachial artery regarding surrounding structures. It was found to give muscular branches before entering the cubital fossa at the level of a normal, non-variable brachial artery. Around the elbow the artery was found to pass through the medial portion of the cubital fossa after which it branched into two large vessels – the radial artery (RA) laterally, and a very superficially positioned branch medially, which was later named as the medioulnar (MU) or superficial ulnar (SU) [1, 3] artery of the forearm.

Fig. 1. Demonstration of the origin of the deep brachial artery and the division of the brachial artery into superficial brachial artery and deep proper brachial artery.

The deep proper brachial artery (DPBA) traverses distally behind the median nerve and gives four

branches, all arising from its medial aspect. The two larger branches were identified as the superior collateral ulnar and the inferior collateral ulnar arteries (**Fig. 2**). The smaller ones were muscular branches. The artery then passes immediately under the superficial brachial artery in the cubital fossa at the level of the elbow, after which it leaves the elbow region and angles posteriorly where it lies deep between the forearm muscles and gives rise to the common interosseous artery, which terminates into its two main branches: the anterior and posterior interosseous arteries.

Fig. 2. The brachial artery divides into two main stems, one running behind and the other in front of the median nerve: superficial brachial artery and the deep proper brachial artery

At the level of the forearm (antebrachium), the radial artery was found to have a non-variable course, structure and branching. It travels down from the medial aspect of the neck of the radius to the styloid process of the anterior surface of the radius. In its proximal part it lays deep to the brachioradialis muscle, while distally it was covered only by fascia and skin. During its course in the forearm it was found to give off standard arterial branches as follows: the recurrent radial artery, palmar carpal branches and the superficial carpal branch. The medioulnar artery branches off from the superficial brachial artery at the lower border of the cubital fossa (**Fig. 3**). From its beginning it travels distally in an oblique fashion and is positioned above the muscles of the anterior group of the forearm. In the proximal half of the forearm the artery crosses above the muscle bodies of the pronator teres and flexor carpi radialis muscle. In the distal part of the forearm the artery navigates to the typical anatomical position of the ulnar artery (UA), and lays between the flexor carpi ulnaris and flexor digitorum superficialis. In the wrist it is situated in a similar fashion to the non-variable ulnar artery and passes through Guyon's channel. After passing the lower border of the cubital fossa, the deep proper brachial travels distally and posteriorly between the muscles of the anterior compartment of the hand where it gives of several arterial branches. Here we identified the anterior and posterior ulnar recurrent branches, after which the deep proper brachial artery continues as the common interosseous artery. This artery then gives its two main terminal branches in the anterior and posterior interosseous arteries, which on the cadaver showed no variations.

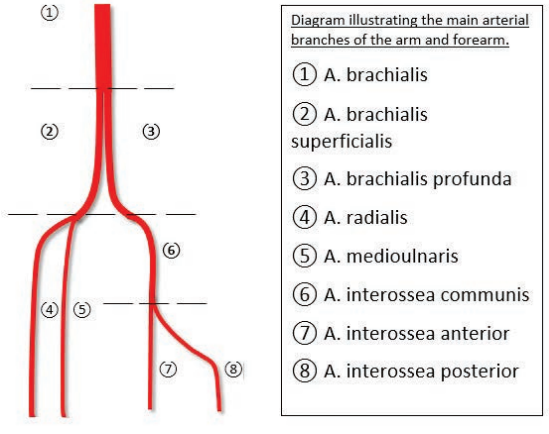

Fig. 3. Illustration of the main arterial branches of the arm and forearm by Stoykov V., Mitev A., Maslarski I.

In the palmar region, an incomplete SPA was visualized. The superficial palmar branch of the radial artery entered the hand deep to the abductor pollicis brevis muscle, giving off two common digital arteries and a digital artery to the thumb. The first common digital artery gave two proper digital arteries for the blood supply of the thumb and index finger, and the second common digital artery gave two proper digital arteries for the blood supply of the ulnar side of index finger and radial side of the middle finger. On the ulnar side, we found a superficial branch of ulnar artery entering the hand, superficial to the flexor retinaculum. After giving off a deep palmar branch (*r. palmaris profundus*), two common palmar digital arteries and a proper palmar digital artery for the ulnar side of the little finger were observed. The two common palmar digital arteries gave off two proper digital arteries each. One for the radial side of the little finger and the ulnar side of the ring finger, and the other for the radial side of ring finger and ulnar side of middle finger.

Discussion

To understand the different patterns of blood supply of the upper extremity, a complete knowledge of the embryological development of the vascular system is required. As a detailed description of the embryological development is beyond the scope of this article, this chapter is restricted only to a brief explanation and illustration of the embryology of the arteries of the upper extremity.

According to *Senior* [14], in the embryonic development of the arteries of the upper limb, five stages can be recognized **(Fig. 4).**

Stage I: The axial artery of the arm develops from the sixth cervical segmental artery, recognized for the first time in an embryo of 4-7 mm. The proximal part of the axial artery becomes the brachial artery (BA) and the distal portion becomes the interosseous artery.

Stage II: At this stage, a median artery develops as a main artery which runs with the median nerve. The interosseous artery subsequently undergoes atrophy.

Stage III: Observed in human embryos of approximately 18 mm in length. The ulnar artery arises from the BA, which anastomoses with the median artery to form the superficial palmar arch, which supplies the arteries of the fingers.

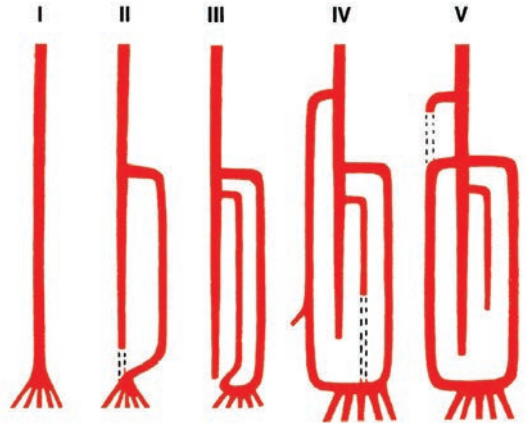

Stage IV: Observed in human embryos of app. 21 mm in length. The key point of the stage is the development of a superficial brachial artery (SBA).

Stage V: Three consecutive changes occur: the median artery undergoes atrophy, the SBA gives off

Fig. 4. Diagram illustrating the five stages of development of the arteries of the arm by Stoykov V., Mitev A., Maslarski I.

a distal branch anastomosing with the superficial arch, and, at the level of the elbow, an anastomotic branch between the BA and the SBA hypertrophies, becoming the radial artery.

After performing a literature review, such variation was noted in a number of sources [1, 5, 6], and the arteries were deemed to be the superficial brachial artery and the deep brachial artery. This posed a problem, because in Anglo-Saxon literature this artery is also called the "deep brachial artery". To avoid confusion, for the purpose of this article, we will refer to the deep laying branch relative to the median nerve as the deep proper brachial artery. A frequency of up to 14% of this variation was described in cited literature [1, 9, 11]. Both arteries continued distally in the anterior region of the brachium and medially regarding the long head of the biceps. The diameter of the arteries after the point of bifurcation was noted to be 0,6 cm (SBA) and 0,5 cm (DPBA).

Singular arterial variations of the upper extremity are frequent occurrences that have been extensively researched through the years. A widely accepted general classification still doesn't exist, which makes comparing data and individual cases difficult. That is particularly true in cases where multiple, concurrent variations exist. Regarding the currently presented case, a literature review was performed, which aimed to establish the novelty (or lack thereof) of the observed multiple variations, and to try to classify them as accurately as possible.

The presence of a superficial brachial artery has been frequently described [1, 5]. Extensive studies on the topic have been performed in the past using a large number of cadavers, which have reported a very variable frequency ranging from 3% to 22%. Some of these authors [3, 4, 12] have proposed terminology (mostly based on the topographical approach) which is still widely accepted today. The term superficial brachial artery stems from the position of the structure regarding the median nerve. As per McCormack et al. [11] the superficial brachial artery "lies superficial to the median nerve in an abnormal site and forms a common stem of origin for the radial and ulnar arteries". This explanation could lead to oversimplification and confusion because of different reasons. For example the superficial brachial artery can be a singular large arterial entity arising in the arm, and continuing in forearm, but it can also be an accessory artery, accompanied by another large arterial vessel following bifurcation at some point in the arm (as in this case report).

Furthermore, during the literature review, it was noted that not only structures that continue in the forearm as the radial and ulnar arteries were named as the *SBA*, but also structures which had a variable course in the forearm (i.e. SBA continuing as only the radial orulnar arteries) [9, 11, 13]. For these reasons, authors of newer studies have attempted to propose a different approach regarding terminology **(Fig. 5)**. For example Rodríguez-Niedenführ et al. [13, 15] have proposed different terms for an accessory artery situated in front of the median nerve, based on its continuation in the forearm, which are as follows:

Fig. 5. A. *brachialis superficialis* (SBA) dividing into *a. radialis* and *a. medioulnaris* (MUA).

- brachioradial artery – when it continues as the radial artery in the forearm
- superficial ulnar artery – for ulnar artery with a high origin, which courses over the superficial forearm flexor muscles
- superficial brachioulnoradial artery (SBURA) – for an accessory, superficial brachial artery dividing at elbow level into radial and ulnar arteries and coexisting with a "normal" brachial artery that continues as the common interosseous trunk in the forearm

In accordance to the described classification, the authors have revised the previously described definition of a superficial brachial artery given by McCormack et al., [9] to become the following "The superficial brachial artery represents a brachial artery, which instead of coursing deep to the median nerve runs in front of it after adopting its superficial course. This variation does not present any further deviation from the norm and at the elbow it branches into the forearm arteries". In such, they have attempted to preserve the specificity of the term and to give further, more complex description of different variations. For the purpose of this case report we find the term superficial brachioulnoradial artery appropriate, as it describes fully the observed variation on our cadaver.

Following the bifurcation at the arm, the deep artery, relative to the median nerve, passes through the cubital fossa to enter the forearm and continue as the common interosseous branch. A frequency of occurrence was difficult to determine, as most articles focused on examining the superficial branch, but incidence of two main arterial stems was noted as around 8-14% [13, 14]. In existing literature this vessel was named as the brachial artery [1, 7, 11]. This seemed to imply a logic that the structure is a direct continuation of the brachial artery before the point of bifurcation, with which in this presented case we don't agree, because the distal course of the artery does not follow the path of a non-variable brachial artery, and continues as the common interosseous artery in the forearm **(Fig. 6)**. As stated previously in the article, we propose the secondary brachial branch, positioned deep to the median nerve to be called the deep proper brachial artery, which in our opinion is an accurate topographic description that avoids confusion with the brachial artery (*a.brachialis*) before the point of bifurcation,the deep brachialartery (*a.profunda brachii).*

At the level of the proximal forearm the SBA bifurcates into two branches: the radial artery (RA) and the medioulnar (MUA) or superficial artery (SUA). The term MUA was found in one source [2], while SUA was more frequently noted [1, 11, 13]**.** The frequency of this variation was found to be between 0.7% and 7% [1, 5]. The artery was found to give only muscular branches on its course through the forearm. Only one more such case was noted during the literature review [13, 16]. This particular variation presents an interesting clinical significance because of its superficial position in the proximal and middle third of the

Fig. 6. Incomplete (open) superficial palmar arch, first two common palmar digital arteries originate from *a. radialis*, the other to originate form a. ulnaris (*a. medioulnaris*, MUA).

forearm, which makes it vulnerable to trauma, accidental intra-arterial injections and accidental intraoperative lacerations.

According to a meta-analysis performed by Zarzecki et al. [16] an incomplete SPA was observed in 18.7% of all cases. The most common pattern observed was a complete arch with radio-ulnar anastomosis (72%), the variant included in most anatomical textbooks or atlases. As reported by Janevski [5], this variant is classified as type D and is seen as a very uncommon pattern, observed in only 2% of the cases. According to Coleman's classification [4], based on a study on 650 specimens, the variation observed in our cadaver is described as type A incomplete SPA, with a frequency of 3.2%.

Plenty of medical procedures are affected by the above mentioned arterial variations. Some of them include RA harvesting for coronary artery bypass grafting, RA cannulation and RA arterio-venous fistulas used for hemodialysis. The RA graft, in particular, is seen as a reliable source because of the diameter of the artery, its thickness and resistance are all appropriate for myocardial revascularization. RA cannulation is also performed for continuous monitoring of blood pressure and arterial blood gas analysis in major surgeries and intensive care units. There is increased risk of ischemia of the hand in incomplete SPA, therefore it should be checked if possible prior to any major procedures.

Conclusion

To the best of our knowledge, this is the first case report describing simultaneously occurring double brachial arteries, medioulnar artery and an incomplete superficial palmar arch in a cadaver. Although this, most likely, is a very rare multiple variation in a single limb, it again emphasizes the need for clinicians to be vigilant of possible typical and atypical vascular variations. This report should be of great interest to reconstructive hand surgeons, where the described variation of a very superficially lying MU artery continues into an incomplete SPA. The MU artery in this case, which is of similar caliber as the RA, can be easily injured during various surgical approaches to the forearm. Potential injury to this artery could lead to tissue ischemia of the ulnar side of the hand and the fourth and fifth digit.

Although this is not the target of this case report, we feel that it is important to research multiple simultaneously occurring vascular variations and their possible clinical consequences. There is a need for large scale population studies which examine the incidence rates of concomitant variations and the correlation between them. We feel that a byproduct of such research could be the creation of a new, improved and unified classification system, which would better suit further research and clinical needs.

References

1. **Adachi, B.** *The artery system of Japanese*. Kyoto, Maruzen Press, **1**, 1928, 285-356. [In German].
2. **Al-Fayez, M., Z. KaimkhanI, M. Zafar, H. Darwish, A. Aldahmash, A. Al-Ahaideb**. Multiple arterial variations in the right upper limb of a Caucasian male cadaver. – *Int. J. Morphol.* **28**, 2010, 659-665.
3. **Chin, K., K. Sing**. The superficial ulnar artery - a potential hazard in patients with difficult venous access. – *British Journal of Anaesthesia,* **94**, 2005, 692-693.
4. **Coleman, S., B. Anson**. Arterial patterns in the hand based upon a study of 650 specimens. – *Plastic and Reconstructive Surgery*, **29**, 1961, 85-86.

5. **Janevski, B.** Anatomy of the arterial system of the upper extremities. Angiography of the upper extremity. – *Series in Radiology*, **7**, 1982, 41-122.
6. **Kachlic D. V. Musil, V. Baca.** Contribution to the anatomical nomenclature concerning upper limb anatomy. – *Surg. Radiol. Anat*., **4,** 2017, 405-417.
7. **Keen, J**. A study of the arterial variations in the limbs with special reference to symmetry of vascular patterns. – *Am. J. Anat.,* **61**, 1961, 245-261.
8. **Konarik M, V. Musil, V. Baca, D. Kachlik.** Upper limb principal arteries variations: A cadaveric study with terminological implication. – *Bosn. J. Basic. Med. Sci*., **4**, 2020, 502-513.
9. **Lippert, H., R. Pabst**. *Arterial variations in man*, J.F.Bergmann-Verlag 2011, pp.128.
10. **Loukas, M., B. Benninger, R. Tubbs**. *Gray's clinical photographic dissector of the human body*. 2nd edition, 2018, pp.480.
11. **McCormack, L., E. Cauldwell. B. Anson**. Brachial and antebrachial arterial patterns. – *Surg. Gynae. Obs*., **96**, 1953, 43–44.
12. **Miller, E.** Observations upon the arrangement of the axillary artery and brachial plexus. – *American Journal of Anatomy*, 64, 1939, 143-163.
13. **Rodriguez-Niedenfuhr M., T. Vazquez, L. Nearn, B. Ferreira, I. Parkin, J. Sanudo.** Variations of the arterial pattern in the upper limb revisited: a morphological and statistical study, with a review of the literature. – *J. Anat.,* **199**(5), 2001, 547-566.
14. **Senior, H.** A note on the development of the radial artery. - *Anat. Rec*., **32**, 1926, 214-220.
15. **Sharma, T., R. Singla, K. Sachdeva.** Bilateral superficial brachial artery. – *Kathmandu University Medical Journal*, **7**, 1970, 426-428.
16. **Zarzecki, M., P. Popieluszko, A. Zayachkowski, P. Pekala, B. Henry, K. Tomaszewski.** The surgical anatomy of the superficial and deep palmar arches: a meta-analysis. – *J. Plast. Reconstr. Aesthet. Surg*., **71**, 2018, 1577-1592.

Author Guidelines

Acta morphologica et anthropologica is an open access peer review journal published by Bulgarian Academy of Sciences, Prof. Marin Drinov Publishing House.
Corporate contributors are Bulgarian Academy of Sciences, Institute of Experimental Morphology, Pathology with Museum and Bulgarian Anatomical Society.

Acta morphologica et anthropologica is published in English, 4 issues per year.
The journal accepts manuscripts in the following **fields**: experimental morphology, cell biology and pathology, anatomy and anthropology.

Publication types: original articles, short communications, case reports, reviews, Editorial, letters to the Editors.

Acta morphologica et anthropologica is the continuation of Acta cytobiologica et morphologica

The **aim** of the Journal is to disseminate current interdisciplinary biomedical research and to provide a forum for sharing new scientific knowledge and methodology. The general editorial policy is to optimize the process of issuing and distribution of *Acta morphologica et anthropologica* in line with modern standards for scientific periodicals focusing on content, form, and function.

Scope – experimental morphology, cell biology and pathology (neurobiology, immunobiology, tumor biology, environmental biology, reproductive biology, etc.), new methods, anatomy and pathological anatomy, anthropology and paleoanthropology, medical anthropology and physical development.

Acta morphologica et anthropologica is published twice a year as one volume with 4 issues. For the first two issues (1-2) the deadline for manuscript submission is March 15th and for the next two issues (3-4), the deadline is September 15th. Electronic version for issues 1-2 is uploaded on the website till June 30th and for issues 3-4 – till December 30th.

Contact details and submission

Manuscript submission is electronical only. The manuscripts should be sent to the Managing Editor's e-mail address ygluhcheva@hotmail.com with copy to iempam@bas.bg
All correspondence, including notification for Editor's decision, requests for revision, is sent by e-mail.

Article structure

Manuscripts should be in English with total length not exceeding 10 standard pages, line-spacing 1.5, justified with 2.5 cm margins. The authors are advised to use Microsoft Word 97-2003, Times New Roman, 12 pt throughout the text. Pages should be numbered at the bottom right corner of the page.

The article should be arranged under the following headings: Introduction, Material and Methods, Results, Discussion, Conclusion, Acknowledgements and References.

Title page – includes:

- **Title** – concise and informative;
- **Author(s)' names and affiliations** – indicate the given name(s) and family name(s) of all authors. Present the authors' affiliation addresses below the names. Indicate all affiliations with a lower-case superscript after the author's name and in front of the appropriate address. Provide the full postal address information for each affiliation, including the country name.
- **Corresponding author** – clearly indicate who will handle the correspondence for refereeing, publication and post-publication. An e-mail should be provided.
- **Abstract** – state briefly the aim of the work, the principal results and major conclusions and should not exceed 150 words. References and uncommon, or non-standard abbreviations should be avoided.
- **Key words** – provide up to 5 key words. Avoid general, plural and multiple concepts. The key words will be used for indexing purposes.

Introduction – state the objectives of the work and provide an adequate background, avoiding a detailed literature survey or summary of the results.

Material and Methods – provide sufficient detail to allow the work to be reproduced. Methods already published should be indicated as a reference: only relevant modifications should be described.

Results – results should be clear and concise.

Discussion – should explore the significance of the results in the work, not repeat them. A combined *Results and Discussion* section is often appropriate. Avoid extensive citation and discussion of published literature.

Conclusions – the main conclusions of the study should be presented in a short section.

Acknowledgements – list here those individuals who provided help during the research and the funding sources.

Units – please use the International System of Units (SI).

Math formulae – please submit math equations as editable text, not as images.

Electronic artwork – number the tables and illustrations according to their sequence in the text. Provide captions for them on a separate page at the end of the manuscript. The proper place of each figure in the text should be indicated in the left margin of the corresponding page. **All illustrations (photos, graphs and diagrams)** should be referred to as "figures" and given in abbreviation "Fig.", and numbered in Arabic numerals in order of its mentioning in the manuscript. They should be provided in grayscale as JPEG or TIFF format, minimum 300 dpi. The illustrations should be submitted as separate files.

References – they should be listed in alphabetical order, indicated in the text by giving the corresponding numbers in parentheses. The "References" should be typed on a

separate sheet. The names of authors should be arranged alphabetically according to family names. In the reference list titles of works, published in languages other than English, should be translated, original language must be indicated at the end of reference (e.g., [in Bulgarian]). Articles should include the name(s) of author(s), followed by the full title of the article or book cited, the standard abbreviation of the journal (according to British Union Catalogue), the volume number, the year of publication and the pages cited, for books - the city of publication and publisher. In case of more than one author, the initials of the second, third, etc. authors precede their family names. The names of all authors should be provided. In case of more that five authors, usage of "et al" after the fifth author in long author lists is allowed.

For articles: **Davidoff, M. S., R. Middendorff, G. Enikolopov, D. Riethmacher, A. F. Holstein, D. Muller**. Progenitor cells of the testosterone-producing Leydig cells revealed. – *J. Cell Biol.,* **167**, 2004, 935-944.

Book article or chapter: **Rodriguez, C. M., J. L. Kirby, B. T. Hinton. The development of the epididymis.** – In: *The Epididymis - from molecules to clinical practice* (Eds. B. Robaire, B. T. Hinton), New York, Kluwer Academic Plenum Publisher, 2002, 251-269.

Electronic books: **Gray, H.** *Anatomy of the human body* (Ed. W.H.Lewis), 20th edition, NY, 2000. Available at http://www.Bartleby.com.

PhD thesis: **Padberg, G**. Facioscapulohumeral diseases. *PhD thesis*, Leiden University, 1982, 130 p.
Website: National survey schoolchildren report. National Centre of Public Health and Analyses, 2014. Available at http://ncphp.government.bg/files

Page charges

Manuscript publication is free of charges.

Ethics in publishing

Before sending the manuscript the authors must make sure that it meets the Ethical guidelines for journal publication of Acta morphologica et anthropologica.

Human and animal rights

If the work involves the use of human subjects, the authors should ensure that work has been carried out in accordance with *The Code of Ethics of the World Medical Association* (Declaration of Helsinski). The authors should include a statement in the manuscript that informed consent was obtained for experimentation with human subjects. The privacy rights of human subjects must always be observed.
All animal experiments should comply with the *ARRIVE guidelines* and should be carried out in accordance with the U.K. Animals (Scientific procedures) Act, 1986 and the associated guidelines *EU Directive 2010/63/EU* for animal experiments, or the National Institutes of Health guide for the care and use of Laboratory animals (NIH Publications No. 8023, revised 1978) and the authors should clearly indicate in the manuscript that such guidelines have been followed.

Submission Details

Acta morphologica et anthropologica is published twice a year as one volume with 4 issues. For the first two issues (1-2) the deadline for manuscript submission is March

15th and for the next two issues (3-4), the deadline is September 15th. Electronic version for issues 1-2 is uploaded on the website till June 30th and for issues 3-4 – till December 30th.

Manuscript submission is electronical only.

The manuscripts should be sent to the Managing Editor email address ygluhcheva@hotmail.com with copy to iempam@bas.bg
All correspondence, including notification for Editor's decision, requests for revision, is sent by e-mail.

Submission declaration

Submission of the manuscript implies that the work described has not been published previously, is not considered under publication elsewhere, that its publication is approved by all authors, and that if accepted, it will not be published elsewhere in the same form, in English or in any other language, including electronically, without the informed consent of the copyright-holder.

Contributors
The statement that all authors approve the final article should be included in the disclosure.

Copyright
http://www.iempam.bas.bg/journals/acta/Author%20Copyright%20Agreement_last.pdf

Upon acceptance of an article, the authors will be asked to complete a "**Copyright Transfer Agreement**".
http://www.iempam.bas.bg/journals/acta/Copyright_Transfer_Agreement_Form_AMA.doc

Peer review
Once a manuscript is submitted, the Managing Editor (or the Editor-in-Chief) briefly checks the manuscript for conformance with the journal's Focus, Scope, Policies and style requirements and decide whether it is potentially suitable for publication and can be processed for review, or rejected immediately, or returned to the author for improvement and re-submission.
Manuscripts are peer-reviewed by the Editors, Editorial Board members, and/or external experts before final decisions regarding publication are made. The entire editorial workflow is performed in the following steps:

1. The submitted manuscript is checked in the editorial office whether it is suitable to go through the normal peer review process.
2. If deemed suitable, the manuscript is sent to 2 reviewers for peer-review. The choice of reviewers depends on the subject of the manuscript, the areas of expertise of the reviewers, and their availability.
3. Each reviewer will have 2 weeks to provide evaluation of the manuscript. The Editor may recommend publication, request minor, moderate or major revision, or provide a written critique of why the manuscript should not be published (rejected).

4. In case only one reviewer suggests rejection of the manuscript, the latter is subjected to additional evaluation by a third reviewer.
5. The manuscript will be published in a revised form provided that the authors successfully answer the critics received. The Editor-in-Chief is the final authority on all editorial decisions.

Open Access

This journal provides immediate open access to its content on the principle that making research freely available to the public supports a greater global exchange of knowledge.

After acceptance

Proof correction

The corresponding author will receive proofs by e-mail in PDF format and will be requested to return it with any corrections within two weeks.

ISSN 1311-8773 (print)
ISSN 2535-0811 (online)